The Role of NagC in *Yersinia pestis* and *Yersinia pseudotuberculosis* Biofilm Development and Insect Transmission

---

Thesis submitted to The University of Nottingham for the degree of Doctor of Philosophy

Linzy Elton, BSc (Hons), MSc

September 2018

Declaration

Unless otherwise acknowledged, the work presented in this thesis is entirely my own. No part has been submitted for another degree in The University of Nottingham or any other institute of learning.

Linzy Elton
September 2018

Abstract

There are three species of human-pathogenic *Yersiniae*; two of which cause gastrointestinal disease (*Yersinia pseudotuberculosis* and *Yersinia enterocolitica*) and one which causes plague (*Yersinia pestis*), one of the deadliest diseases in human history. Whilst *Y. pseudotuberculosis* and *Y. enterocolitica* are transmitted faeco-orally, *Y. pestis* is transmitted by insects, classically the Oriental rat flea, *Xenopsylla cheopis*. All *Yersiniae* are capable of a method of bacterial messaging known as quorum sensing (QS), which allows individual cells to communicate in a density dependent manner using signalling molecules such as *N*-acyl-homoserine lactones (AHLs). QS regulates several virulence phenotypes, including the production of *Yersinia* virulence factors (YOPs), secreted by the type three secretion system (T3SS) into mammalian host cells, auto-aggregation and biofilm formation.

Biofilms are aggregates of bacteria within a protective exopolysaccharide matrix and are especially important for *Y. pestis*, as transmission of plague relies on the biofilm-mediated blockage of the proventriculus within the digestive system of a flea. Understanding the mechanisms of biofilm development are therefore potentially important for developing methods to prevent or control plague transmission. Recent research has also suggested a more prominent role in the spread of plague for other insect vectors, such as body lice (*Pediculus corporis*). In the *Yersiniae*, the extracellular polymeric substance (EPS) matrix is composed primarily of the polysaccharide *N*-acetyl-D-glucosamine (poly-GlcNAc) and extracellular DNA. The production of GlcNAc but not poly-GlcNAc is known to be regulated by NagC, a DNA binding

protein responsible for the repression of *nagE-nagBACD* (GlcNAc catabolic operon) and activation of *glmUS* (GlcNAc biosynthesis operon) in *Escherichia coli*, but there is little information on the NagC-dependent regulation of GlcNAc metabolism or on poly-GlcNAc biosynthesis *via* the *hmsHFRS* operon in the *Yersiniae*.

This study set out to investigate the contribution of NagC in *Y. pseudotuberculosis* and *Y. pestis* to QS, poly-GlcNAc production and biofilm formation *in vitro* and *in vivo* on and within the established *C. elegans* and insect vectors. Artificially fed colonies of *X. cheopis* and *P. corporis* were investigated for use in experimental infection models. For both insect species, defibrinated human blood fed through a collagen membrane was the most successful combination for feeding, although problems with reproducible control of environmental conditions, such as humidity, prevented the insect colonies from becoming established.

To investigate the contribution of NagC to QS, YOP production, auto-aggregation, poly-GlcNAc biosynthesis and biofilm formation, a Δ*nagC* mutant was constructed in *Y. pestis* and compared with a *Y. pseudotuberculosis* Δ*nagC* mutant as well as with the corresponding wild type strains. NagC did appear to influence AHL and YOP production in both *Y. pseudotuberculosis* and *Y. pestis*. NagC did not influence auto-aggregation in *Y. pestis*, although the rate of auto-aggregation was slower for the *Y. pseudotuberculosis* Δ*nagC* mutant.

NagC was however required for the production of poly-GlcNAc (*Y. pseudotuberculosis*) and biofilm formation (both *Y. pseudotuberculosis* and *Y. pestis*). To determine whether NagC directly regulates poly-GlcNAc

biosynthesis, the *Y. pestis nagC* was expressed in *E. coli*, the recombinant protein purified and subjected to electrophoretic mobility shift assays. The data obtained show that NagC binds to the promoter regions of the GlcNAc metabolic operons *nagE-nagBACD* and *glmUS*, as well as *hmsHFRS* in *Y. pestis* and hence directly regulates the production of poly-GlcNAc.

Using *in vitro* (glass) and *in vivo* (nematode and insect) models, both *Y. pestis* and *Y. pseudotuberculosis* Δ*nagC* mutants were evaluated for biofilm formation. In addition, a 'fake flea' proventriculus model was developed to investigate attachment and biofilm formation on a chitin substrate. The *Y. pseudotuberculosis* Δ*nagC* mutant showed reduced biofilm formation on the chitin surface, compared with the parental strain. On the nematode *C. elegans*, the *Y. pestis* Δ*nagC* mutant produced substantially less biofilm formation than the parent. When *Y. pseudotuberculosis* was fed to *P. corporis*, the Δ*nagC* mutant showed an increased ability to clear the infection and increased survival rates compared with insects fed the parent strain.

Taken together, these results indicate that NagC plays a central role in biofilm formation and in the ability of the *Yersiniae* to be transmitted by insect vectors.

Acknowledgements

I would like to thank Paul Williams, Steve Atkinson and Alan Cockayne, for the opportunity to work in the Quorum Sensing lab and thanks also to the *Yersinia* group postdocs Vanina Garcia and Jo Purves, whose help has been invaluable. The *Yersinia* lab family have made my time at Nottingham special; Amy Slater, Natalie Barratt, Clair Brooks and Carol Paiva (who will always count as a *Yersinia*), we will see each other in Georgia one day! Thanks also to all the other members of C69/C72/C81; Jeni Luckett, for fake flea advice and mouse skins, Carmen Tong, Ewan Murray, Phil Barderlang, who helped me to purify my protein, Nigel Halliday, who ran my samples through the mass spec and Manuel Romero, who helped me get my head around EMSAs, who have helped me with valuable advice, even when what I asked of them perhaps sounded crazy.

My friends in the DTP cohort have provided me with laughter and support throughout my PhD. I would also like to thank all of my wonderful blood donors, who very kindly (and bravely!) donated their blood to the cause. Without you, a lot of this would have been impossible. Thanks must also go to Andy Bennett and Vince Wilson; without your help, support and guidance, I may never have had the courage to finish at all.

Finally, to my family, who have been ready and willing to support me in every way possible. I'm sorry about the endless conversations about parasites and bacteria! I have literally put my blood, sweat and tears into this project and although at times it was extremely psychologically challenging, I am immensely proud of what I have achieved.

All of this work is dedicated to my incredible dad, who believed in me always. You dropped everything to help me whenever I needed you and shared my love for weird and wonderful bugs. You even let me take your blood for my research, even though you were scared of needles. You and mum made me the person I am today and I hope that you will always be proud of me.

Abbreviations

Abbreviation	Description
µF	Microfarad
µg	Microgram
µl	Microlitre
µM	Micromolar concentration
∞	Infinite/infinity
AHL	*N*-acyl-homoserine lactone
AI-2	Autoinducer-2
Amp	Ampicillin
APS	Ammonium persulfate
BHI	Brain heart infusion media
bp	Base pair
BSA	Bovine serum albumin
BSI	Biofilm severity index
Ca^{2+}	Calcium
CL2	Containment level 2 laboratory
CL3	Containment level 3 laboratory
Cm	Chloramphenicol
CO92	Colorado (1992) *Y. pestis* strain
CR-MOX	Congo red Magnesium Oxalate agar
dH_2O	Distilled water
DMSO	Dimethyl sulfoxide
DNA	Deoxyribonucleic acid
dNTP	Deoxynucleotide
DTT	DL-Dithiothreitol
ECM	Extracellular matrix
EDTA	Ethylenediaminetetraacetic acid
EMSA	Electrophoretic mobility shift assay
EPS	Extracellular polymeric substance
Erm	Erythromycin
EtOH	Ethanol

g	Gram(s)
gDNA	Genomic DNA
GFP	Green fluorescent protein
GlcNAc	*N*-acetyl-D-glucosamine
GlcNAc-6-P	*N*-acetyl-D-glucosamine-6-phosphate
GMO	Genetically modified organism
Gm	Gentamicin
GOI	Gene of interest
hms	Hemin storage locus
IPTG	Isopropyl β-D-1-thiogalactopyranoside
Kan	Kanamycin
kb	Kilobase
kDa	Kilodalton
KIM	Kurdistan Iranian Man *Y. pestis* strain
Km	Kanamycin
kV	Kilovolt
L	Litre
LB	Luria Bertani media
M	Molar concentration
min	Minute
ml	Millilitre
mM	Millimolar concentration
mm	Millimetres
MSC	Microbiological safety cabinet
Nal	Nalidixic acid
ng	Nanograms
NGM	Nematode Growth Media
NPNT	No promotor, no terminator
OD	Optical density
ORF	Open reading frame
PBS	Phosphate buffered saline
pCD1	*Yersinia pestis* virulence plasmid
PCR	Polymerase chain reaction

PEG	Polyethene glycol
PFA	Paraformaldehyde
pFra (pMT1)	CO92 Murine toxin plasmid (KIM strain name)
pH	Potenz (power) of hydrogen
pPst (pPCP)	CO92 Pesticin, coagulase and plasminogen activator plasmid (KIM strain name)
QS	Quorum sensing
^{R}	Resistance
rpm	Revolutions per minute
SCS	Sucrose counter selection
SDS	Sodium dodecyl sulphate
SDS-PAGE	Sodium dodecyl sulphate polyacrylamide gel electrophoresis
Sm	Streptomycin
T3S(S)	Type III secretion (system)
TAE	Tris-acetate-EDTA buffer
TB	Terrific broth
Tc	Tetracycline
Tcs	Toxin complexes
TCA	Trichloroacetic acid
TF	Transcription factor
TFBS	Transcription factor binding site
Tris	Tris hydroxymethyl aminomethane
V	Volts
v/v	Volume to volume ratio
w/v	Weight to volume ratio
WGA	Wheat germ agglutinin
x *g*	Times gravitational force
X-gal	5-bromo-4-chloro-3-indolyl-β-D-galactopyranoside
YDMM	*Yersinia* defined minimal media
YOP	*Yersinia* outer protein
YpIII	*Yersinia pseudotuberculosis III* strain
YSA	*Yersinia* selective agar

Ysc	*Yersinia* secretion complex
Δ	Deletion mutant
Ω	Ohm
MOPS	3-(*N*-morpholino)propanesulfonic acid
n/a	Not applicable

Table of Contents

List of Figures

List of Tables

1 Introduction

1.1 History

Throughout history, there has never been a more devastating bacterium than *Yersinia pestis*, the causative organism of plague. Responsible for an estimated 200 million deaths, it has swept across vast swathes of the globe numerous times (Brubaker, 1991; Perry and Fetherston, 1997; Inglesby *et al.*, 2000).

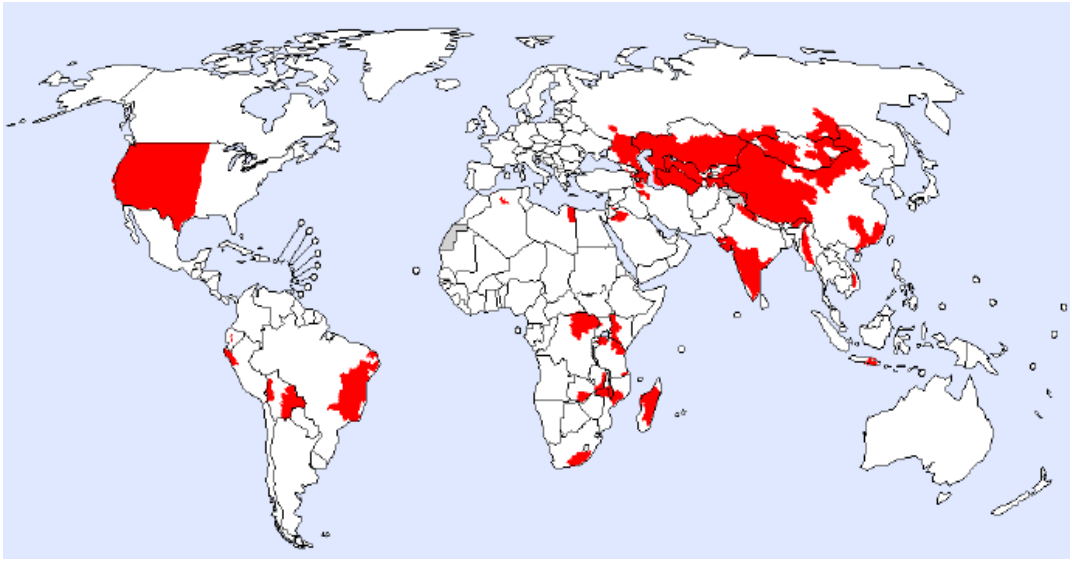

Figure 1.1. Global distribution of natural plague foci as of March 2016. Areas in red show potential plague natural foci based on historical data and current information. Source: WHO/PED, as of 15 March 2016.

There are many countries where natural plague foci still exist, as shown in Figure 1.1. Many of these still regularly have human cases of plague, including Brazil, the DRC, Madagascar, Myanmar, Peru, USA and Vietnam (Zietz and Dunkelberg, 2004). This worldwide distribution that continues to kill hundreds of people every year would suggest that plague still warrants much scientific attention. Indeed, the World Health Organisation (WHO) has recently

reclassified *Y. pestis* as a '(re)emerging dangerous pathogen', warranting its inclusion in the organisation's Emerging and Dangerous Pathogens Laboratory Network (WHO, 2015). Insecticides are currently used successfully to curb outbreaks by killing the flea vector (Zietz and Dunkelberg, 2004) but multidrug resistance is a growing concern for all types of pathogenic bacteria, and could be especially serious in a highly virulent disease such as plague (Galimand *et al.*, 1997).

1.2 The Human Pathogenic *Yersiniae*

Y. pestis is a Gram negative coccobacillus and part of the genus *Yersinia*, which belongs to the family *Enterobacteriaceae* (Gage and Kosoy, 2005). Of the eleven species in the genus, three are medically important, including *Y. pestis.* The other two, *Yersinia pseudotuberculosis* and *Yersinia enterocolitica,* both cause gastroenteritis and are transmitted faecal-orally (Neyt *et al.*, 1997). All three exhibit a biphasic lifestyle and grow in environmental conditions as well as within a mammalian host. *Y. pestis* is transmitted by insect vectors such as fleas, or *via* infected water droplets, causing plague. For the other two, human infection occurs when contaminated food, such as vegetables, is not washed properly (*Y. enterocolitica*) or from undercooked meats in the case of *Y. pseudotuberculosis* [reviewed in (Bearden *et al.*, 2009; Heroven and Dersch, 2014)]. A fourth, *Yersinia ruckeri*, causes redmouth disease in rainbow trout (*Oncorhynchus mykiss*) and other salmonids (Ewing *et al.*, 1978).

Y. pestis evolved from *Y. pseudotuberculosis* around 1,500–20,000 years ago, suggesting a potentially rapid adaptation from a gastrointestinal pathogen to a

mammalian blood-borne disease as these changes are thought to have occurred shortly before the first human pandemic, the plague of Justinian in AD 532 (Achtman *et al.*, 1999; Parkhill *et al.*, 2001; Bobrov *et al.*, 2014). This divergence occurred as a result of the acquisition of both chromosomal and extrachromosomal DNA by *Y. pestis*, as well as inactivation or loss of others, allowing for insect transmission and subcutaneous host entry (Skurnik, Peippo and Ervelä, 2000; Derbise *et al.*, 2010).

The most widely studied modern strains of *Y. pestis* are KIM and CO92. The virulent KIM (Kurdistan Iran man) 10+ strain was originally isolated from a clinical case in 1968 (Deng *et al.*, 2002; Losada *et al.*, 2011). The CO92 (Colorado (1992)) strain was isolated from a case of pneumonic plague, fatally contracted from a domestic cat in the USA (Doll *et al.*, 1994). Despite extensive rearrangement, KIM and CO92 share more than 95% of their chromosomal DNA, although CO92 has roughly 50 kb more (Deng *et al.*, 2002; Morelli *et al.*, 2010). Much research conducted on *Y. pestis* uses non-virulent strains modified from KIM, such as KIM6+, which lacks the virulence plasmid pCD1 (Sun *et al.*, 2014).

1.3 Disease Manifestations

Y. pseudotuberculosis and *Y. enterocolitica* cause the relatively mild gastrointestinal disease, Yersiniosis, in humans which in most cases is not fatal. The disease begins within the digestive system where the bacteria colonise, causing mucosal ulcerations and necrotic sites within the Peyer's patches and spreading to the mesenteric lymph nodes (Butler, 1994).

Symptoms usually include abdominal pain, diarrhoea and fever which last around 1-3 weeks (Leino and Kalliomaki, 1974; Fahlgren *et al.*, 2014). Rare cases can result in complications, including adenitis, arthritis and sepsis (Butler, 1994; Koornhof, Smego and Nicol, 1999).

Y. pestis is responsible for bubonic plague, which occurs following the bite of an infected flea (Hinnebusch, 2005). Thousands of *Y. pestis* cells may be released from the bite and spread though the lymphatic system into nearby lymph nodes where, despite being phagocytosed, they multiply quickly, causing the death of lymphatic tissues (as reviewed by Perry & Fetherston 1997). Symptoms occur around 2-8 days after infection, with fever, chills and headaches occurring, followed by the characteristic swollen lymph nodes, or 'bubos', and occasionally vomiting and nausea and without treatment, has a 40-60% mortality rate (Inglesby *et al.*, 2000; Butler, 2013).

A small percentage of people develop primary septicaemic plague, or go on to develop secondary septicaemic infection from the bubonic form. This presents similarly to bubonic plague with additional sepsis-like symptoms, including necrosis of blood vessels due to intravascular coagulation, leading to gangrene in the extremities such as fingers, toes and nose. This particular symptom is the reasoning behind the name for the second pandemic, the Black Death (Inglesby *et al.*, 2000). Even in the 21st century the death rate for untreated septicaemic plague is extremely high, up to 100%, due to the speed of disease manifestations and delays in diagnosis (Perry and Fetherston, 1997; Butler, 2013).

In around 5% of cases, secondary pneumonic plague can occur from bubonic or septicaemic disease (Sebbane *et al.*, 2006). It is more often contracted

directly *via* infected water droplets from another infected individual (Brubaker, 1991). Pneumonic plague starts with flu-like symptoms and progresses to serious pneumonia, while patients may also present with shortness of breath, haemoptysis and chest pain (Inglesby *et al.*, 2000; Gage and Kosoy, 2005). The untreated death rate for pneumonic plague is estimated to be 80-100% (Zimbler *et al.*, 2015).

1.4 Pathology of *Yersinia* Infections

Most of the *Yersinia* virulence factors responsible for human infections are encoded on a highly conserved virulence plasmid, known as pYV (*Yersinia* virulence) in *Y. pseudotuberculosis,* pYVe in *Y. enterocolitica* and pCD1 (calcium dependence) in *Y. pestis* (Straley and Bowmer, 1986; Bhaduri and Smith, 2011). This 96.2 kb plasmid encodes a number of effector proteins, required by the bacteria to infiltrate host cells, called *Yersinia* outer proteins (YOPs), and the type III secretion system (T3SS), responsible for transporting YOPs into the host (Parkhill *et al.*, 2001; Bhaduri and Smith, 2011; Fahlgren *et al.*, 2014).

One function of secretion systems is to allow bacteria to transport effector proteins directly into the cytosol of host cells. Secretion systems have evolved into seven families across both animal and plant pathogens. The main body of the T3SS export apparatus has a similar structural organisation to flagella and consists of a needle-like structure that is anchored to the bacterial outer membrane (Cornelis, 2006). The *Yersinia* secretion complex (Ysc) 'injectosome' has been well studied and is similar to that of other human

pathogens, such as *Pseudomonas aeruginosa* (Roy-Burman *et al.*, 2001). There are thought to be over twenty types of T3SS, including that found in *Yersiniae* (Cornelis, 2006). It is made up of different Ysc proteins that form a membrane-spanning basal structure and an extracellular needle, as shown in Figure 1.2, taken from (Cornelis, 2002).

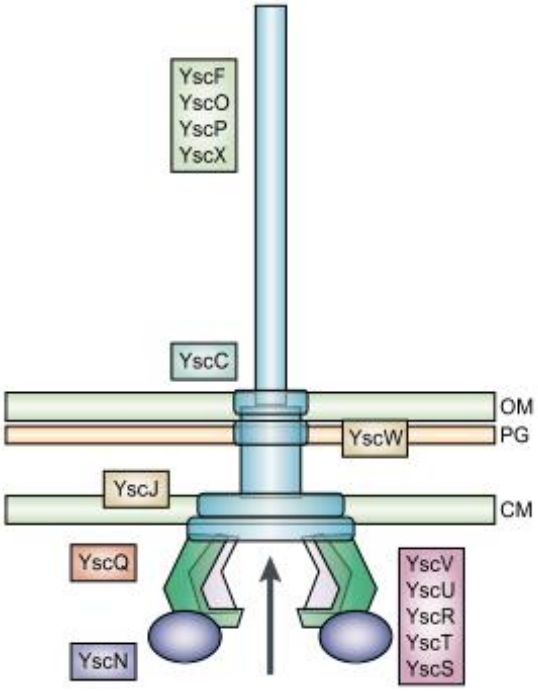

Figure 1.2. Schematic of the Ysc injectosome, taken from Cornelis, 2002. The outer membrane (OM), peptidoglycan (PG) layer and cytoplasmic membrane (CM) of the bacterium harbour a ring of secretin (YscC), supported by YscW, which is a lipoprotein (as is YscJ). YscF, O, P and X form the external part of the needle. The basal body consists of YscV, U, R, T and S. YscN forms the ATPase of the pump and YscQ may localise to the inner cylinder.

In the mammalian host, YOPs interfere with cell signalling responses, enabling the bacteria to create a favourable environment for themselves. YopE, YopH, YpkA/YopO, as well as YopT (found only in *Y. enterocolitica*) disrupt the cytoskeleton and weaken the phagocytic actions of host cells, whilst YopK/YopJ block MAPK and nuclear factor-κB pathways which downregulate

inflammatory responses of cells such as macrophages. The functions of YopM are not clear, although it may affect host gene transcription (Trosky, Liverman and Orth, 2008; Fahlgren *et al.*, 2014). Once *Y. pestis* has invaded and multiplied within the macrophages, there is massive extracellular proliferation, causing severe bacteraemia and the characteristic inflammation and necrosis of lymph and periglandular tissues (Sebbane *et al.*, 2005).

Alongside pCD1, *Y. pestis* has acquired two other unique plasmids which contain additional virulence factors. These are both likely to have facilitated the evolution of *Y. pestis* infection from a gastrointestinal disease to an insect-borne one, enabling invasion of new mammalian hosts and insect vectors (Perry and Fetherston, 1997; Parkhill *et al.*, 2001; Zimbler *et al.*, 2015). The first, a 100-110 kb plasmid known as pFra (or pMT1, standing for murine toxin, in KIM strains) contains the *Yersinia* murine toxin gene (*ymt*), a phospholipase, which allows for survival in the insect gut by protecting the bacteria from cytotoxic digestion products within the blood plasma (Hinnebusch, 2002) and Fraction 1 capsular antigen, encoded by the *caf1* gene, which inhibits phagocytosis by mammalian host cells (Du, Rosqvist and Forsberg, 2002). The other, pPst (or pPCP1, standing for pesticin, coagulase and plasminogen activator in KIM strains) is a 9.5 kb plasmid housing the outer membrane serine protease Pla, which protects the bacteria from the proteolytic action of plasmin in the host's blood and is thought to be essential for the *Y. pestis* subcutaneous infection route (Sodeinde and Goguen, 1989; Cowan *et al.*, 2000; Parkhill *et al.*, 2001). It also contains the bacteriocin pesticin, which prevents the growth (and thus competition) of other *Y. pestis* strains which lack a third gene on the plasmid that codes for pesticin immunity (Brubaker, Beesley and Surgalla,

1965; Sikkema and Brubaker, 1987). These two extra plasmids plus the *hms* genes, a hemin storage locus responsible for a pigmented *Y. pestis* phenotype due to storage of exogenous hemin or Congo Red dye, appear to be vital for the rapid transition from enteropathogenic to flea-borne transmission, as *Y. pestis* strains lacking these factors are incapable of colonising fleas (Pendrak and Perry, 1993; Hinnebusch, Perry and Schwan, 1996; Hinnebusch, Fischer and Schwan, 1998; Wren, 2003).

1.5 Quorum Sensing

The *Yersiniae* are able to control these virulence factors, using a regulatory system known as Quorum sensing (QS). QS is utilised by many bacteria, fungi and other organisms in which individual cells communicate with each other by releasing diffusible signal molecules, allowing them to co-ordinately regulate gene expression in a given environmental situation (as reviewed by Williams 2007). This is a population density dependent system and is important in a number of behaviours in the *Yersiniae*, including controlling pathogenicity, maintaining virulence plasmids, motility and biofilm formation (Atkinson *et al.*, 2006, 2008, 2011; Ng *et al.*, 2018). QS allows for an efficient bi-phasic lifestyle, enabling a temperature-dependent switch between the soil/insect vector and the mammalian host, ensuring energy conservation in the former and effective virulence in the latter (as reviewed by Atkinson & Williams 2009). Those genes switched on at body temperature are termed virulence genes, whilst those switched on in *Y. pestis* at flea temperature (around 22ºC) are termed transmission genes (Hinnebusch, Perry and Schwan, 1996).

QS in Gram negative bacteria depends on the production of diffusible signal molecules such as *N*-acylhomoserine lactones (AHLs). These extensively studied molecules have differing side chain lengths, 3 position substituent and degree of acyl chain saturation (Bobrov *et al.*, 2007; Ortori *et al.*, 2007; Zhang *et al.*, 2011).

Bacteria use the synthase protein family LuxI to produce AHLs which are then released into the environment (Engebrecht and Silverman, 1984). When there is a high enough density of bacteria and an AHL concentration threshold is reached, the signal molecules can then diffuse back into bacterial cells, where they are sensed by LuxR type receptors/transcriptional regulators. The LuxR-AHL complex is able to activate genes in response to environmental stimuli (Fuqua and Winans, 1996; Bobrov *et al.*, 2007). The *Yersiniae* utilise homologues of the LuxI/R system. Although *Y. enterocolitica* only has one QS system (YenI and YenR) (Throup *et al.*, 1995), both *Y. pestis* and *Y. pseudotuberculosis* have two, YspI/R and YpeI/R in *Y. pestis* and YtbI/R and YpsI/R in *Y. pseudotuberculosis* (Atkinson *et al.*, 1999, 2006; Kirwan *et al.*, 2006).

1.5.1 Biofilms

One of the principal QS-regulated phenotypes in *Y. pestis* is the formation of biofilms (as reviewed by Parsek & Greenberg 2005). Physically, biofilms are an aggregation of bacteria embedded in an extracellular polymeric substance (EPS) matrix, either attached to a surface or as a liquid culture biofilm (Bryers 2008). The polysaccharides within the extracellular matrix (ECM), including

poly-*N*-acetyl-D-glucosamine (poly-GlcNAc), are integral to maintaining the structure of the biofilm (Bryers, 2008; Atkinson *et al.*, 2011).

Biofilms typically begin with the attachment of bacterial cells at a solid-liquid interface. The bacteria produce signalling molecules *via* the QS system and when they reach the required threshold, begin producing the exopolymers required for the three-dimensional EPS-bacterial matrix as shown in Figure 1.3 (Donlan, 2002; Sadovskaya *et al.*, 2005; Bryers, 2008). Biofilms can form on many different surfaces, such as medical devices, natural aquatic systems, living tissues and industrial systems to provide protection to the bacteria from a number of environmental stressors such as washing, antibiotics, predators and host immune defences (as reviewed by Donlan 2002). Cells within the biofilms can disperse and form new colonies elsewhere (Bryers, 2008).

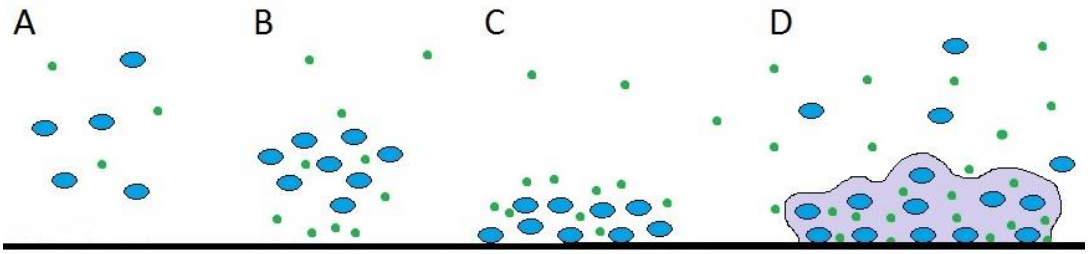

Figure 1.3. Schematic of biofilm development. (A) Indicates contamination with bacteria (blue). (B) Signalling molecules (green) are released. (C) QS of signalling molecules gathers bacteria and bacteria settle on the surface. (D) Bacteria produce EPS, protecting cells from environmental factors.

Aside from its vital role in *Yersinia* poly-GlcNAc EPS formation, GlcNAc plays many other functional roles across a varied range of organisms, such as in bacterial cell walls (e.g. peptidoglycan) and the chitin in fungal cell walls (Konopka, 2012). In the *Yersinia*, poly-GlcNAc is produced *via* the *hmsHFRS* operon, but it is as yet unclear how this system is regulated (Lillard *et al.*,

1997). In *E. coli*, GlcNAc metabolism is regulated by NagC, but there is no evidence that NagC regulates poly-GlcNAc production in any bacterium that makes this polysaccharide (Plumbridge, 1990).

Biofilms are essential for *Y. pestis* to facilitate transmissible infection within its flea vector. The bacteria enter the flea within a blood meal taken from an infected host and begin to aggregate in the midgut in susceptible flea species (Hinnebusch, 2005; Erickson *et al.*, 2006). They then attach to and form biofilms on the proventriculus, a chitinous, barbed valve located between the oesophagus and gut (see Figure 1.4). This allows the flea to absorb the nutrients within the ingested bloodmeal (Service, 2008a).

A

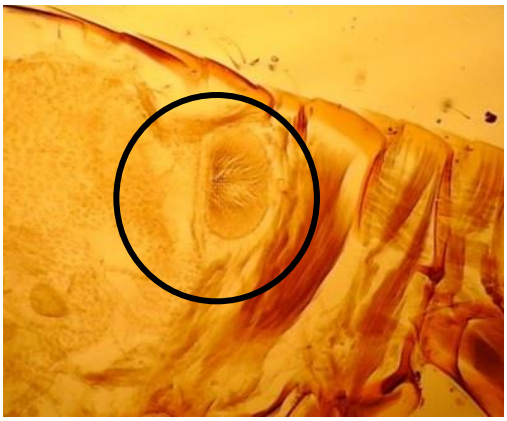

B

Figure 1.4. Images of the *Xenopsylla cheopis* proventriculus. (A) shows a 10x bright field image of the proventriculus (circled) with the midgut to the left and oesophagus to the right. (B) shows a scanning electron microscope image of the spines *of X. cheopis* proventriculus (purple) covered with *Y. pestis* biofilm (green) (Source: National Institute of Allergies and Infectious Diseases).

The *Y. pestis* biofilm spreads to partially or fully block the proventriculus of infected fleas, making it difficult for the insect to take another meal and as a result begins to starve. In the flea's desperate attempts to feed, bacteria (and viruses) are passed to a new host, regurgitated alongside the saliva, which is

used to soften the tissue around the bite site and prevent the blood from coagulating (Service, 2008a; Chouikha and Hinnebusch, 2012). The bacteria are also passed out in the fleas' faeces and can be transmitted when a host rubs it into a bite wound (Service, 2008a). Although *Y. pestis* biofilm formation in fleas has been studied extensively, attenuated, pCD1 negative strains such as KIM6+ are often used, due to health and safety regulations (Kolodziejek *et al.*, 2007; Yoong, Cywes-Bentley and Pier, 2012; Fukuto *et al.*, 2018). Recently, Atkinson *et al.* (2011) described a direct link between biofilms, the TT3S and QS for *Y. pseudotuberculosis* using *Caenorhabditis elegans* models. Biofilm formation was shown to be controlled by AHL-mediated QS, as AHLs were found within the biofilm and strains with mutations in AHL synthase or response regulator genes showed biofilm attenuation. Given these links in *Y. pseudotuberculosis*, it would be useful to determine whether they exist in the fully virulent *Y. pestis.*

1.5.2 The Genetics of Colonisation and Transmission of *Y. pestis* in Insect Vectors – Biofilm formation and GlcNAc

So far, only two loci have been found to be essential for *Y. pestis'* survival in the flea; *ymt*, required for flea colonisation and found on the pFra plasmid, and the *hms* locus, located on the chromosome (Parkhill *et al.*, 2001). The *hms* genes, also present in *Y. pseudotuberculosis*, are essential for *Y. pestis* to form biofilms in the flea midgut and proventriculus, and are responsible for synthesising and transporting biofilm matrix exopolysaccharides (Hinnebusch, Perry and Schwan, 1996). The *hms* genes are separated into a number of

different loci on the chromosome; *hmsB, hmsCDE, hmsT, hmsHFRS* and *hmsP* (Lillard *et al.*, 1997). The *hmsHFRS* operon is vital for *Y. pestis* colonisation and blockage of the proventriculus, but is not thought to be vital for the survival of *Y. pestis* in the midgut (Perry, 2003; Hinnebusch and Erickson, 2008).

Although research on the genetics of biofilm formation and poly-GlcNAc production in *Y. pestis* has focused on the *hmsHFRS* operon, it is also important to consider GlcNAc metabolism and regulation since this sugar monomer is the substrate for poly-GlcNAc production *via* the *hms* gene products (Bobrov *et al.*, 2008). In most Gram negative bacteria the *nagE-nagBACD* regulon is required for the transport and catabolism of extracellular GlcNAc (Plumbridge 1990; Atkinson *et al.* 2011; Wiechmann, Ph.D. Thesis, 2015). The transcriptional regulator NagC acts as a repressor of the *nagE-nagBACD* regulon in the absence of GlcNAc-6-phosphate (GlcNAc-6-P) and is de-repressed by its presence (Konopka, 2012). Despite the role of NagC in GlcNAc metabolism being studied in other organisms, its contribution to poly-GlcNAc biosynthesis in *Y. pestis* is not known.

1.5.3 The GlcNAc Pathway and *nagE-nagBACD* Regulon

Much of what is known about the *nagE-nagBACD* regulon comes from research conducted in *E. coli.* It is known to be responsible for the uptake and metabolism of extracellular GlcNAc and glucosamine (GlcN) and is present in many biofilm-forming species, including *E. coli*, *P. aeruginosa, Y. pseudotuberculosis* and *Y. pestis* (Plumbridge, 1990, 1992; Torruellas *et al.*,

2005; Korgaonkar and Whiteley, 2011). Alongside its role in GlcNAc metabolism, the *nag* regulon is known to have other functions, including chitobiose degradation (Plumbridge and Pellegrini, 2004) and the negative regulation of *galP,* which encodes a galactose transporter (El Gaidi *et al.* 2009).

The two operons, *nagE* and *nagBACD* are on opposing strands of the chromosome, as shown in Figure 4.1. The *nagB* gene codes for GLcN-6-phosphate deaminase, *nagA* codes GlcNAc-6-phosphate deacetylase, *nagC* represses the *nag* regulon and *nagD* codes for a uridine-5'-monophosphatase (UMPase) of the haloacid dehydrogenase (HAD) superfamily, although its function within the GlcNAc metabolism is unclear (Plumbridge, 1990). The *nagE* gene codes for EII^{nag}, a GlcNAc-specific transporter that is part of the phosphotransferase system (Plumbridge, 1990; Hill *et al.*, 2007). A schematic diagram of the NAG pathway is shown in Figure 1.5. Exogenous GlcNAc enters the bacterium and is catabolised by genes within the *nagE-nagBACD* operon, which is likely to be repressed by NagC in the *Yersiniae*, as it is in *E. coli* and *V. fischeri* (Plumbridge, 1991; Miyashiro *et al.*, 2012).

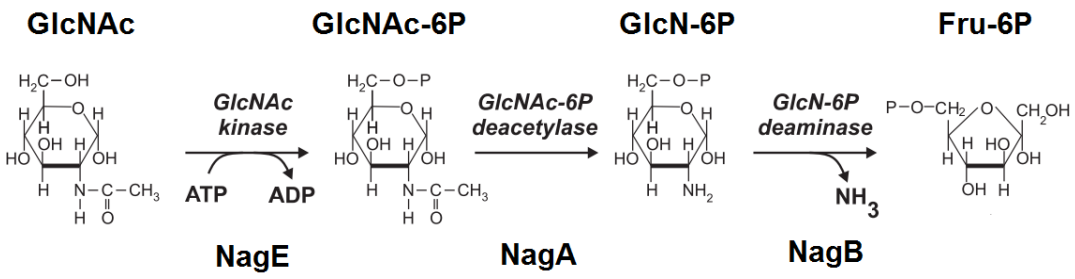

Figure 1.5. The GlcNAc pathway in *E. coli*. Exogenous GlcNAc enters the cell and is catabolised by genes in the *nagE-nagBACD* operon, which is likely to be regulated by NagC.

In the absence of external GlcNAc, NagC represses the *nagE-nagBACD* operon, which degrades GlcNAc, and switches on the *glmUS* operon, which syntheses GlcNAc. When extracellular levels of GlcNAc are high, NagC binds GlcNAc-6-P so relieving the repression of the *nagE-nagBACD* operon, thus switching on GlcNAc degradation, and repressing the *glmUS* operon, so turning off GlcNAc production. These operons are represented schematically in Figure 1.6.

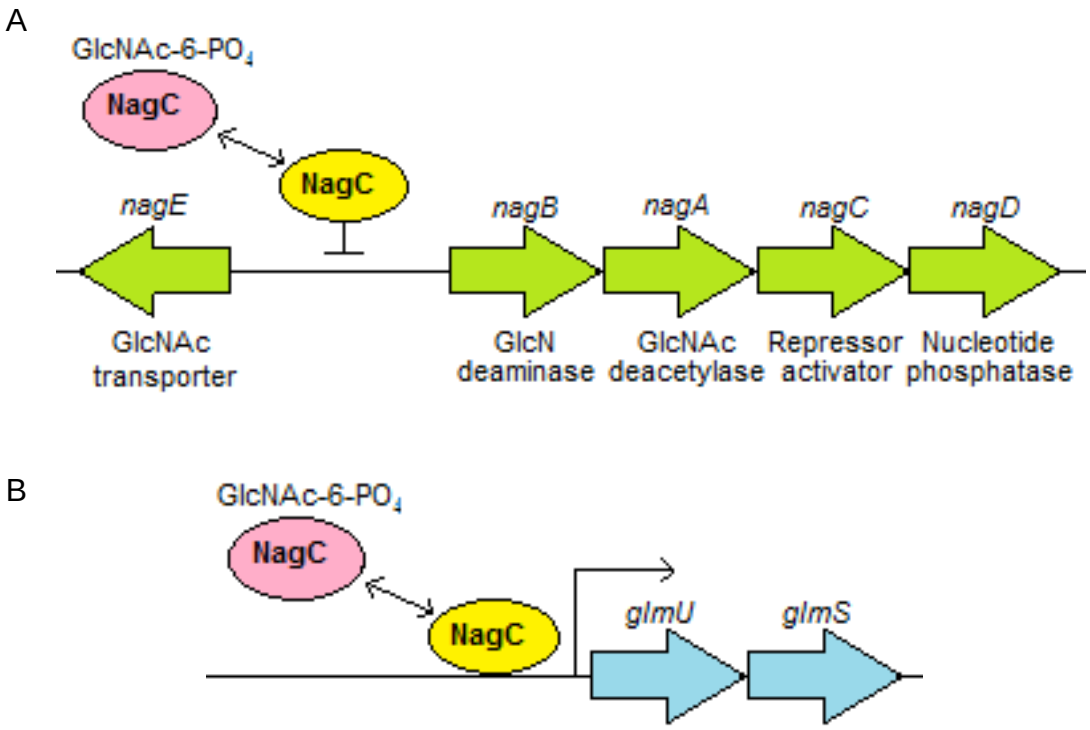

Figure 1.6. Schematic of the *nagE-nagBACD* and *glmUS* operons and their regulation by NagC in *E. coli*. In the absence of GlcNAc-6-P, NagC binds to the *nagE-nagBACD* operon, repressing it and stopping GlcNAc degradation. In the presence of GlcNAc-6-phosphate, NagC does not bind, de-repressing the *nagE-nagBACD* operon, allowing degradation of GlcNAc. In contrast, when GlcNAc-6-P is absent, NagC binds to the *glmUS* operon switching on GlcNAc production. When GlcNAc-6-P is present, NagC does not bind to the *glmUS* operon and GlcNAc is not produced.

The inducer of NagC binding in *E. coli* is GlcNAc-6-P. Figure 1.7 shows the structure of NagC and the docking site of GlcNAc-6-P (Plumbridge, 1991; Pennetier, Domínguez-Ramírez and Plumbridge, 2008).

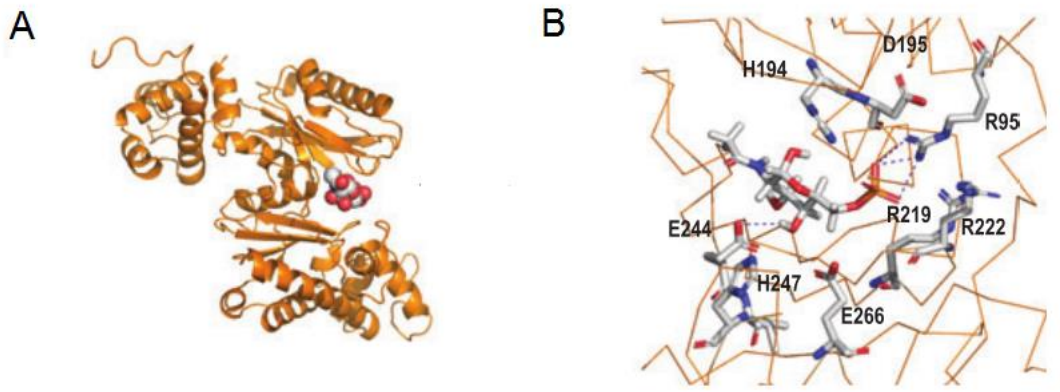

Figure 1.7. Models of the structure of NagC and the binding of GlcNAc-6-P in *E. coli*, taken from Pennetier *et al.* 2008. (A) model of the tertiary structure of NagC (three-subunit model). GlcNAc-6-P is shown as red and grey spheres in the same docking result (B), which has been rotated 90°.

GlcNAc is thought to play a role in the virulence of pathogenic yeast and bacteria and has been shown to be important for host colonisation by *E. coli* and *V. fischeri*, as well as biofilm formation and release of virulence factors by *Streptococcus mutans* (Chang *et al.*, 2004; Ghosh *et al.*, 2011; Kawada-matsuo *et al.*, 2012; Naseem and Konopka, 2015). In *Y. pseudotuberculosis*, NagC and GlcNAc have both been shown to play roles in QS, which regulates virulence and biofilm formation (Wiechmann, Ph.D. Thesis, 2015). A QS gene promoter pulldown study initially suggested that NagC may bind to the QS regulator *ypsR* in *Y. pseudotuberculosis* (Robert Goldstone, unpublished data). However although the regulation of *ypsR* by QS could not be confirmed using reporter gene fusions, NagC was shown to regulate both *Y.*

pseudotuberculosis AHL synthases (*ytbI* and *ypsI*) (Wiechmann, Ph.D. Thesis, 2015). GlcNAc has also been shown to influence QS by inhibiting AHL-dependent gene transcription in *P. aeruginosa* (O. Kimyon *et al.*, 2016). Despite the role of NagC in the metabolism of GlcNAc in other bacterial species and the role of the *hmsHFRS* operon in poly-GlcNAc production in *Y. pestis*, the contribution of NagC as a transcriptional regulator of the GlcNAc metabolic genes *nagE-nagBACD*, *glmUS* or to the *hmsHFRS*-dependent production of poly-GlcNAc has yet to be reported (Plumbridge, 1991; Bobrov *et al.*, 2008).

1.5.4 The *hms* Operons

The *hms* operons play major roles in biofilm blockage of the flea foregut and proventriculus during transmission of plague. The operons are spread across the chromosome and encode genes which synthesise and transport biofilm matrix exopolysaccharides as well as those that synthesise and degrade the second messenger, c-di-GMP (Figure 1.8) (Hinnebusch, Perry and Schwan, 1996), such as *hmsB*, a small RNA that upregulates c-di-GMP production (Fang *et al.*, 2014). In the *hmsCDE* operon, *hmsC* represses *hmsD*, *hmsD* is a diguanylate cyclase producing c-di-GMP and *hmsE* is a peptidoglycan associated lipoprotein (Guo *et al.*, 2015). *hmsT* is also a diguanylate cyclase responsible for c-di-GMP synthesis and *hmsP* is a phosphodiesterase responsible for c-di-GMP degradation (Bobrov *et al.*, 2014; Fang *et al.*, 2014; Guo *et al.*, 2015). The *hmsHFRS* operon is responsible for the synthesis of poly-GlcNAc and contains the genes *hmsH*, encoding an outer membrane

transporter protein, *hmsF*, encoding an outer membrane hydrolase protein and *hmsR* and *hmsS* encoding GlcNAc synthases (Perry, Pendrak and Schuetze, 1990; Pendrak and Perry, 1993).

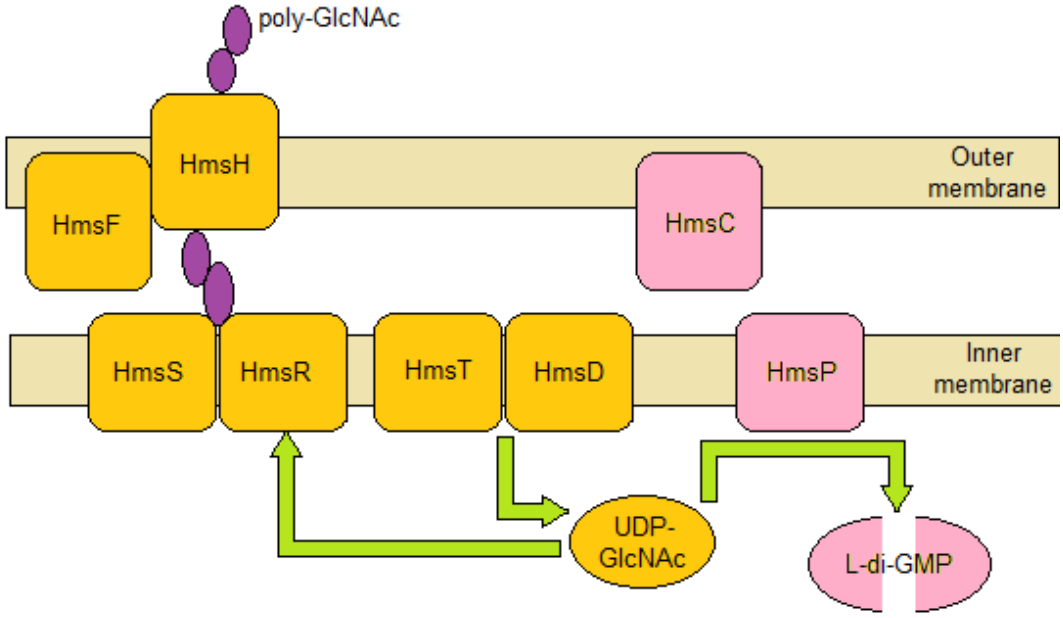

Figure 1.8. Schematic of the roles played by *hms* genes in GlcNAc metabolism for *Y. pestis*. Genes coloured orange are responsible for synthesis of poly-GlcNAc from UDP-GlcNAc and thus biofilm formation, whereas those coloured pink are responsible for the catabolism of UDP-GlcNAc, and thus repression of biofilm formation.

The regulation of the *hms* operons is complex, involving a number of proteins and effectors. RovM increases biofilm formation, by activating transcription of *hmsCDE* and *hmsT*, but indirectly represses *hmsHFRS* and *hmsP* (Liu *et al.*, 2016). CsrA, although a biofilm inhibitor in *E. coli*, enhances biofilm formation in *Y. pestis* and although it does not affect *hmsH*, *hmsP* or *hmsT* transcription, in a Δ*csrA* mutant, deletion of *hmsP*, a phosphodiesterase, showed excessive biofilm production, suggesting an indirect activation of *hmsP* by CsrA (Willias *et al.*, 2015). The cationic polyamines putrescine and spermidine are also vital

for maintaining the levels of HmsR, HmsS and HmsT and therefore biofilm formation (Patel *et al.*, 2006; Wortham *et al.*, 2010). RcsAB supresses biofilm production by repressing the *hmsT*, *hmsCDE* and *hmsHFRS* operons and indirectly activating *hmsP*, the only biofilm inhibiting operon (Fang *et al.*, 2015) (Figure 1.9).

hmsHFRS, found in the *pgm* locus, is responsible for a red pigmented phenotype seen in *Y. pestis* due to the uptake of external hemin or Congo red dye into the bacteria's outer membrane. This occurs at temperatures of 26°C or lower, and corresponds to the environment found in the flea gut, which is hemin-rich (Hinnebusch, Perry and Schwan, 1996). Mutations of this locus results in non-pigmented forms which cannot survive in fleas.

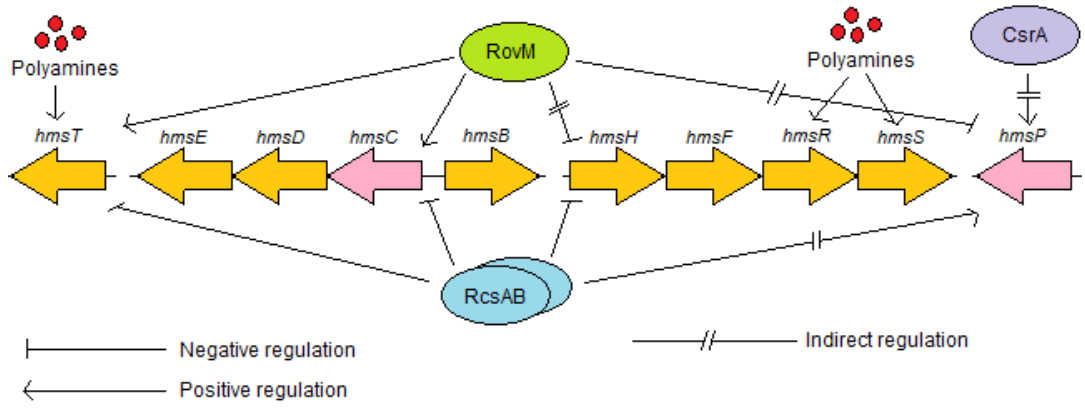

Figure 1.9. Configuration of the *hms* operons on the *Y. pestis* chromosome and the factors that regulate them. Genes coloured orange are involved in poly-GlcNAc synthesis and those in pink are suppressors of poly-GlcNAc synthesis. RovM, CsrA and polyamines positively regulate biofilm formation, whereas RcsAB represses biofilm formation.

1.6 *Y. pestis* Life History

Despite its reputation as one of the deadliest human diseases, plague is a zoonosis, which does not require humans to maintain its populations (Prentice and Rahalison, 2007). Whilst *Y. pseudotuberculosis* and *Y. enterocolitica* are spread through contaminated food and water, *Y. pestis* is transmitted *via* a bite from an infected flea, as well as *via* inhalation of infected water droplets (Perry and Fetherston, 1997). Its natural hosts are mainly rodents, including rats, marmots and ground squirrels (Koornhof, Smego and Nicol, 1999) and it remains within its sylvatic cycles unless close human contact occurs (Gage and Kosoy, 2005). Some of its animal hosts, including rodents, monkeys and pigs are susceptible and may die from the disease whilst others, such as domestic dogs, ferrets and badgers seem to remain highly resistant, experiencing mild or no symptoms (Perry and Fetherston, 1997; Nichols *et al.*, 2014). Plague as a zoonosis can be found in animals on every continent except Australia (Inglesby *et al.*, 2000).

Historically, humans were exposed to the plague because of unsanitary living conditions and close proximity to large, overlapping populations of wild and urban rats. As the plague spread through wild rodent populations, decimating their numbers, fleas needed to find new hosts; first urban rats and then humans (Perry and Fetherston, 1997). In modern times, isolated cases are more likely to occur when people come into contact with infected wild rodents, or if unsanitary conditions and overcrowding occur, such as in refugee camps and prisons (Inglesby *et al.*, 2000).

The most well-known and efficient plague flea vector is *Xenopsylla cheopis* (the Oriental Rat flea), which can be found across sub-tropical Asia (Suyemoto *et al.*, 1956). It favours the black rat (*Rattus rattus*) as its host, although it will take blood meals from a wide range of mammals, including the brown or Norwegian rat (*Rattus norvegicus*) and, if lacking in rodent options, humans (Bacot, 1914a; Dennis *et al.*, 1999; Whitehorn, 2010). It has occasionally been found in temperate areas, however, it is rarely found in cold zones, as it requires warm temperatures to pupate (Roberts and Janovy, 2009). Despite this, the plague travelled as far north as Scandinavia and Greenland, casting doubt as to whether *X. cheopis* is the only vector for plague. Only around 80 flea species have been shown to be susceptible to *Y. pestis* across the world, alongside the 200 species of mammal on which they feed (Pollitzer, 1954; Lorange *et al.*, 2005).

Several studies have tried to identify whether other insect vectors, such as lice, ticks or bed bugs might be involved in transmission (Pollitzer, 1954; Thomas, Karstens and Schwan, 1990; Houhamdi *et al.*, 2006). There is an especially strong case for human lice as potential plague vectors, due to their constantly close proximity to their host. This would have been particularly important in medieval times, due to poor hygiene and the tendency to wear the same clothes for long periods without washing them, making it difficult to reduce infections (Dean *et al.*, 2018).

1.7 Insect Vectors of Plague

1.7.1 Fleas

1.7.1.1 Phylogeny

Fleas, belonging to the order Siphonaptera, are multi-host, haematophagous insects that can be found all over the world including on seabirds in Antarctica (Bacot, 1914a; Krasnov, 2008; Whitehorn, 2010). There are over 2,500 species but relatively few are medically important and whilst the majority feed on mammals, around 5% feed on birds (Russell, 1868; Service, 2008a).

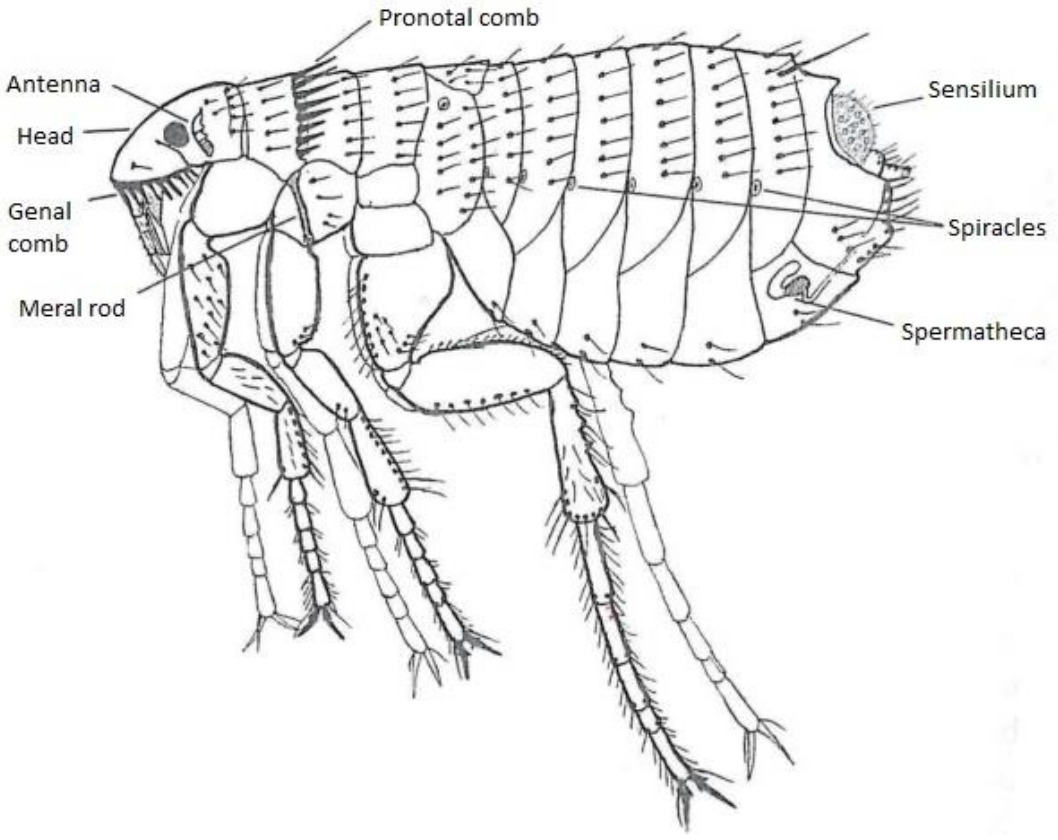

Figure 1.10. Diagram of general flea morphology. Taken from Service 2008a.

They are approximately 1–6 mm in size and have a hair covered, laterally flattened body, as seen in Figure 1.10, which enables them to pass easily though the coat or feathers of the host. They do not have wings, but instead move using their extremely powerful hind legs which are adapted for jumping (Russell, 1868). The female is slightly larger, with a rounded abdomen and a visible spermathecae, the organ used for storing received sperm, as shown in Figure 1.11. The males are smaller, with upturned abdomens and a visible aedeagus, the organ through which they secrete sperm and both sexes take blood meals (Service, 2008a).

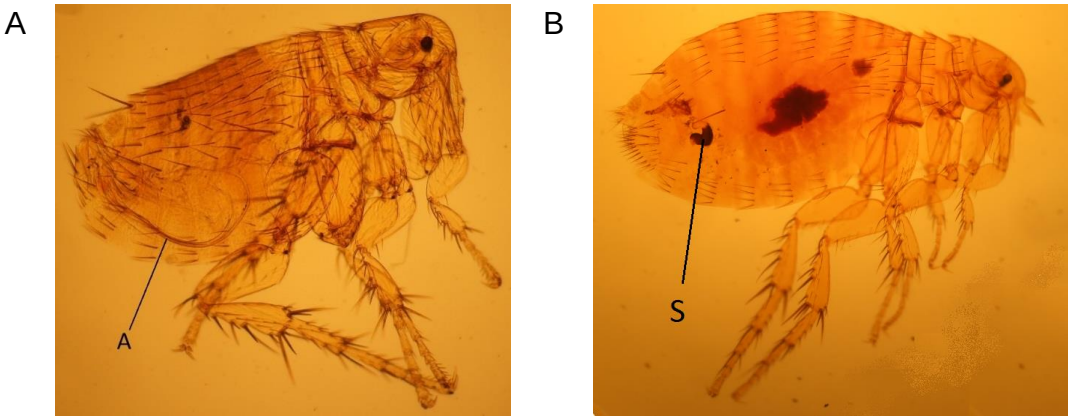

Figure 1.11. Morphology of *X. cheopis*. (A) Male *X. cheopis*, 10x magnification. Note the upturned abdomen and reproductive organ known as the aedeagus (labelled A). (B) Female *X. cheopis*. 10x magnification. Note the rounded abdomen and reproductive organ known as the spermatheca (labelled S).

Different species can be distinguished by the presence or absence of tooth-like combs, found above the mouthparts (genal combs) or at the edge of the first thoracic segment (pronotal combs) (Russell, 1868; Service, 2008a) and also by the shape of the female genitalia (Baker, 2008). Other diagnostic features include the absence of eyes, the mesoplural rod (a thickened structure located above the middle pair of legs), or the sclerotized fossae, a

thickening of the suture joining the antennae, which lie in depressions behind the eyes (Whitehorn, 2010).

1.7.1.2 Morphology and Lifecycle

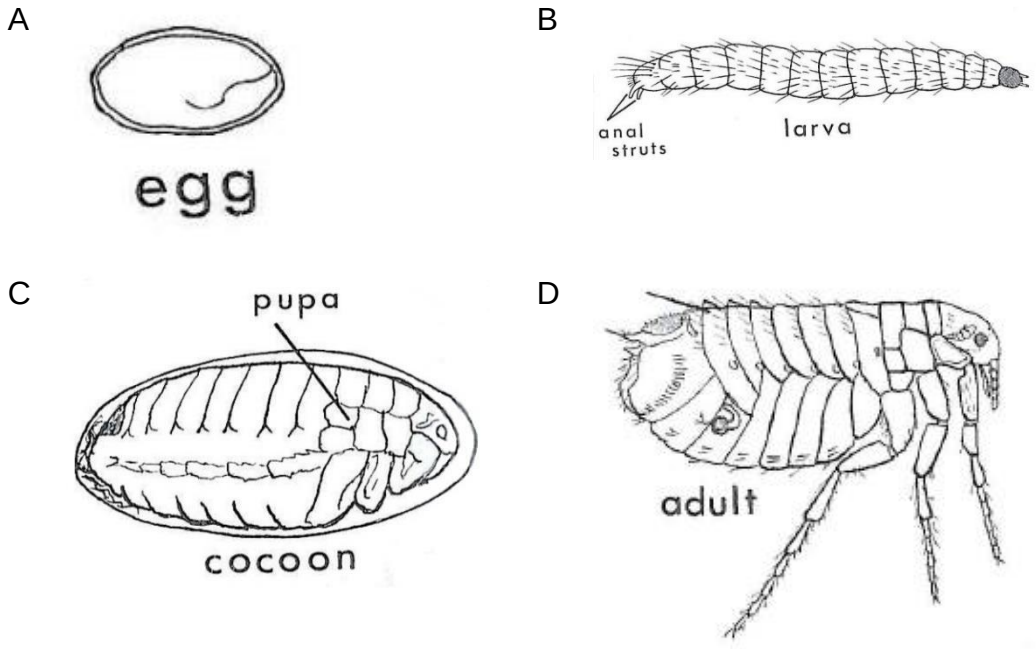

Figure 1.12. Schematic diagrams of the life stages of fleas, taken from Service, 2006. (A) shows the egg stage, (B) the larval stage, (C) the cocoon stage and (D) the final, adult form.

The mouthparts are a complex collection of piercing and sucking tubes along with sensory palps. Needle-like stylets enter the skin of the host and saliva, containing anticoagulants, is injected. The sucking mouthparts then siphon the blood through the pharynx and oesophagus before entering the proventriculus, a cuticle-covered valve between the mouth and midgut with many chitinous, backwards facing spines (Service, 2008a; Whitehorn, 2010). The proventriculus prevents the backflow of blood, whilst the 250–450 spines

pierce the blood cells, aiding digestion and allowing for absorption of nutrients (Lorange *et al.*, 2005; Service, 2008a).

Table 1.1. Flea lifecycle stages explaining the size of the insect and length of time it remains within this stage.

Life stage	Description	Size	Length of time
Eggs	Tiny ovals, yellow or white in colour. Around 300/day are laid per female	0.1–0.5 mm	Once laid, 2-5 days until hatching
Larvae	Segmented 'worms' with anal struts, pale bodies and dark heads. Very sensitive to humidity	40–1000 mm	Larvae live for 2-13 weeks, depending on conditions, then pupate
Pupae	Larvae spin silk cocoons, which are sticky and thus get coated in bedding particles.	Varying, up to 1 cm	Will be in the cocoon for 5-14 days
Adults	Emerge from cocoons as fully formed adults	1–6 mm	Depending on species, live around 10 days, but up to 6-12 weeks

Fleas are only attached to the host when feeding, they are usually found in and around the hosts' nest or den where they also lay their eggs (see Figure 1.12) (Service, 2008a). Females lay 300-1000 eggs in a lifetime, from which a legless larva will emerge. There are 2-3 larval instars, followed by pupation within a cocoon spun from silk found in their salivary glands (Russell, 1868). The length of time for these stages depends on environmental factors such as temperature, but adults tend to live between 10 days to 6 weeks, although

greater than 12 months has been recorded (Service, 2008a). An overview of flea life stages is summarised in Table 1.1.

1.7.1.3 Transmission of *Y. pestis* by the Flea Vector

Fleas have long been known to transmit a number of human diseases such as murine typhus (*Rickettsia typhi*) and certain parasitic cestodes but are perhaps best known as the primary vectors of plague (Service, 2008a). They take a relatively small bloodmeal of around 0.1–0.4 µl, which, although itchy, is not detrimental to the host by itself (Hinnebusch, Jarrett and Bland, 2017). If a bloodmeal is taken from an infected host, the flea is likely to ingest between 2-8 x 10^4 *Y. pestis*, as a natural mammalian infection has been shown to be around 2 x 10^8 CFU/ml and *Y. pestis* requires this high blood titre, with accompanying overwhelming virulence and death rates, in order to establish a successful population within the flea (Jarrett, Deak, *et al.*, 2004; Bland and Hinnebusch, 2016).

The first *Y. pestis*-flea studies were undertaken by the Indian plague commission in the early 1900s where they described early-phase transmission. Prior to the classical biofilm-mediated transmission, which usually requires a 7 day incubation period, fleas are still capable of causing *Y. pestis* infection in naïve hosts, although it usually requires more than one infected insect and results in a transmission rate of 20–70% (as reviewed by B. Joseph Hinnebusch *et al.* 2017). It is thought that this predominantly mechanical transmission may be important in fast-spreading epizootic outbreaks, with infectivity peaking at around 3 days after an infectious blood

meal (Bacot and Martin, 1915; LaRock *et al.*, 2013; Eisen, Dennis and Gage, 2015).

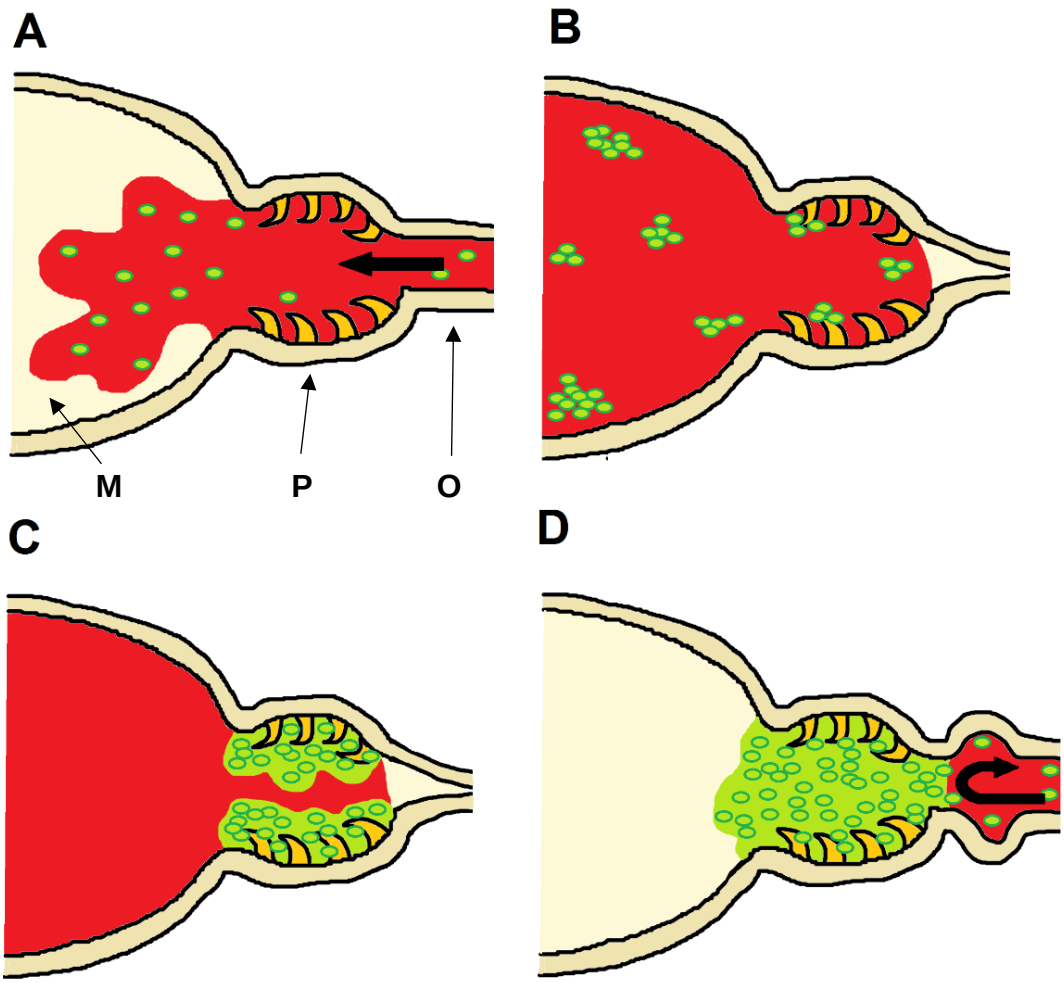

Figure 1.13. Stages of flea blockage by *Y. pestis* (labelled as green ovals). (A) shows an infectious bloodmeal moving from the oesophagus (labelled O) into the midgut (labelled M) through the proventriculus (labelled P). (B) shows *Y. pestis* aggregating together within the midgut, which occurs hours to days after the infected meal. (C) shows *Y. pestis* biofilms, including the exopolysaccharide matrix, beginning to form and cover the spikes of the proventriculus and (D) shows the complete blockage of the proventriculus and a new bloodmeal being infected with regurgitated *Y. pestis* bacteria. Subsequent bloodmeals ingested at stages B, C and D can all transmit *Y. pestis* to the new host with varying levels of efficiency.

The more comprehensively studied, biofilm-mediated method of transmission occurs after early-phase transmission, when bacteria have established

themselves within the flea gut. Bacteria ingested with an infected blood meal begin to replicate within the gut and form aggregates within a few hours to days although these aggregates do not appear to be able to adhere to flea gut epithelial cells or interact with them. They do, however, adhere to the proventriculus, the spines of which are covered by a chitinous cuticle (Figure 1.4). These aggregates eventually form such large clumps that they prevent the flea from excreting the bacteria (Hinnebusch, Jarrett and Bland, 2017).

Due to the speed at which fleas digest their bloodmeals, bacterial aggregations are thought to protect *Y. pestis* from being excreted, as around half of fleas can clear a *Y. pestis* infection during the early stages of infection (Cavanaugh *et al.*, 1956; Lorange *et al.*, 2005). A flea infected with *Y. pestis* can have more than 10^6 bacteria in its gut around for two weeks post an infected bloodmeal (Hinnebusch, Perry and Schwan, 1996). The proventriculus does not have to be fully blocked for plague transmission to occur and the stages of biofilm-mediated transmission are shown in Figure 1.13. Although most fleas die from *Y. pestis* infections relatively quickly, some fleas have been shown to be infective for up to a year post infection and flea faeces in the environment have been shown to remain infective up to three years later (Gage and Kosoy, 2005).

It is unclear whether *Y. pestis* binds directly or uses chitinases to break down the surface of the hydrophobic, acellular, cuticle-covered proventriculus to adhere to it. Chitinases and chitin-binding proteins are found in many marine and soil-dwelling bacteria and are vital for extracting nutrients from chitin, although research has recently identified chitinases as important for mammalian host infection (Frederiksen *et al.*, 2013).

Y. pestis, along with other *Yersiniae* and soil-based species of bacteria produce insecticidal toxin complexes (Tcs) which encode chitinases that break down chitin and provide protection for the bacteria from insect ingestion in the environment (Parkhill *et al.*, 2001; Hurst *et al.*, 2011; Busby *et al.*, 2012). Whilst *Y. pestis* KIM and 91001 strains contain functional copies of these genes, *Y. pestis* CO92 has a frameshift mutation in *tcaB*, and an internal deletion in *tcaC*, suggesting a loss of function and that the Tcs do not play a role in the attachment of *Y. pestis* to the proventriculus, as CO92 is also capable of attachment (Parkhill *et al.*, 2001). *Y. pseudotuberculosis* has been shown to have functional toxin complexes, although no upregulation of these genes occurred when fed to *X. cheopis* as part of a bloodmeal (Erickson *et al.*, 2007). The *hmsHFRS* operon has been shown to be vital for production of the ECM which allows *Y. pestis* to form aggregates and adhere to the proventriculus, but it is unclear exactly how it attaches (Darby *et al.*, 2002).

1.7.2 Lice

1.7.2.1 Phylogeny

Lice can be distinguished into different suborders, the sucking Anoplura and chewing Amblycera, Ischnocera and Rhynchoptirina (Service, 2008b). The chewing lice are mainly parasites of birds and occasionally other mammals. Three sucking varieties affect humans, *Pediculus humanus corporis*, the body louse, *Pediculus humanus capitis*, the head louse, and *Pthirus pubis*, the pubic or ‘crab’ louse.

There appears to be some debate over whether head lice, *P. h. capitis*, and body lice, *P. h. corporis* are different species (Service, 2008b). Their morphology overlaps significantly and cannot be used as a definitive identification tool, however, generally, body lice tend to be darker and larger than head lice (Service, 2008b; Veracx and Raoult, 2012). Current opinion based on genomics appears to suggest that head and body lice have identical genomes bar one gene present in body but not head lice, although there are differences in gene expression levels (Veracx and Raoult, 2012). For simplification, head lice are referred to as *P. capitis* and body lice as *P. corporis* in this text.

1.7.2.2 Morphology and Lifecycle

Lice are small, wingless insects, which vary in colour from pale beige to dark brown. They are flattened dorsoventrally and are softer than fleas, with a leathery tegument (Service, 2008b). General morphology can be seen in Figure 1.14. The mouthparts, unlike most hematophagous insects, are stored within the head. When feeding, the haustellum, armed with barbed teeth, is everted and anchors into the host's skin. Once in place, piercing stylets enter the skin and saliva, containing anticoagulants, is injected to maintain blood flow (Jones, 1998). Blood is then sucked up through the oesophagus and into the midgut for digestion. This system is similar to that of the tsetse fly *Glossina* (Waniek, 2009). Unlike fleas, lice do not have a proventriculus (Service, 2008b; Whitehorn, 2010).

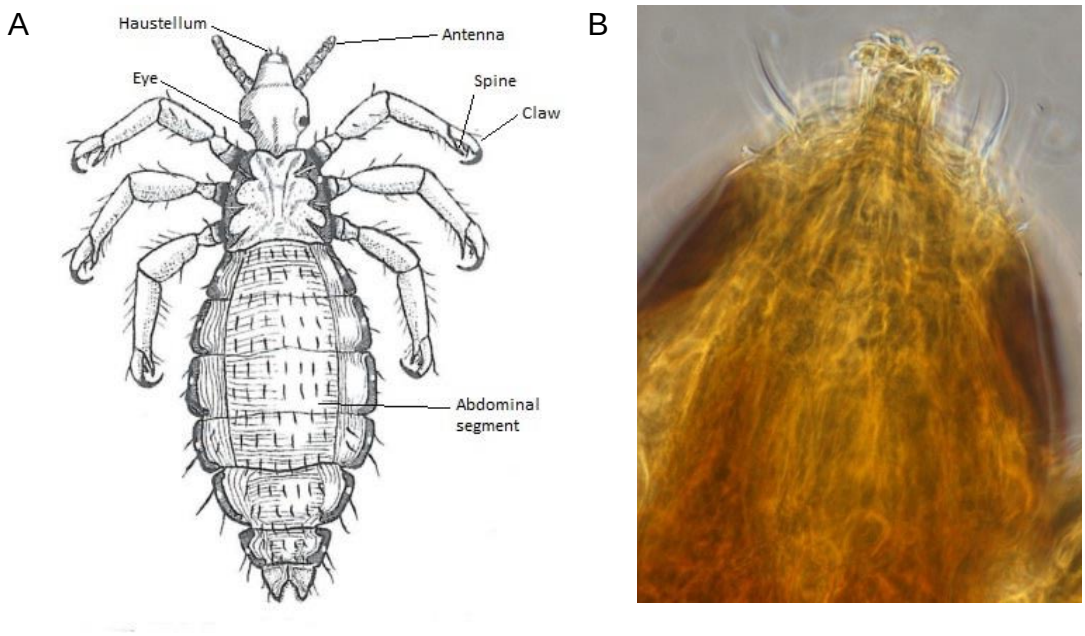

Figure 1.14. Morphology of the human body louse. (A) Diagram of general human louse biology. Taken from Service 2008b. (B) Female *P. capitis* in Euparal. 40x magnification. Note the spiked, everted haustellum.

Like fleas, both sexes take blood meals, although females typically ingest more blood (0.16 µl) compared to males (0.07 µl). Human lice display sexual dimorphism; males are smaller at 2–3 mm, and have a rounded abdomen tip as shown in Figure 1.15. They also have larger front claws compared to the second and third pairs, which enable them to grip the female during mating. Females are larger, 3–4 mm, and have a bifurcated abdomen tip. Their claws are all the same size (Service, 2008b).

A  B 

Figure 1.15 Images showing sexual dimorphism in *P. corporis*. (A) Male *P. corporis*. 10x magnification. Note the rounded terminal abdominal segment and enlarged front claws. (B) Female *P. corporis*. 10x magnification. Note the bifurcated terminal abdominal segment.

All stages of human lice live permanently on the host, head lice in the hair very close to the scalp and body lice within the inner seams of clothes next to the skin. Adults feed between one and five times per day, with head lice feeding more often than body lice (Takano-Lee, Yoon, *et al.*, 2003). Females lay around 6-10 eggs per day onto hairs or in seams, using a strong cement to anchor them in place. The eggs, also known as nits, are oval and white, with an operculum at one end through which the developing embryo receives air (Service, 2008b). The lice are hatched fully developed and live for roughly 2-4 weeks (Whitehorn, 2010). Body lice are capable of withstanding separation from the host for longer than head lice, as the clothes they inhabit are often taken off at night. They can live for up to a week in abandoned clothes before

dying, whereas a head louse separated from its host is likely to die within 24 hours (Service, 2008b).

1.7.2.3 Transmission of *Y. pestis* by the Louse Vector

Large numbers of lice on a host can induce what is known as pediculosis. The skin of such hosts can become tough and scaly and the toxic effects of the louse's saliva can cause fatigue, itchiness and irritability; the person feels 'lousy' (Service, 2008b). Lice are known to transmit louse-borne epidemic typhus (*Rickettsia prowazekii*), epidemic relapsing fever (*Borrelia recurrentis*) and trench fever (*Bartonella quintana*) (Drali *et al.*, 2015). None of these diseases appear to be transmitted in the saliva of the louse, rather the infected faeces is rubbed into the wound or inhaled, or in the case of relapsing fever, by crushing the insects and releasing the spirochetes (Service, 2008b).

Case studies have shown *Y. pestis* concomitant infections with *B. quintana* in Democratic Republic of the Congo (Piarroux *et al.*, 2013; Drali *et al.*, 2015) and experimental rabbit infection studies have shown that *P. corporis* are capable of transmitting *Y. pestis* to a naïve host and that as few as ten lice are needed to transmit an infection (Houhamdi *et al.*, 2006). Little seems to be known about the biology of transmission, or whether, like fleas, biofilm formation is involved with the colonisation of the louse gut.

1.7.3 Colony Husbandry

Different research groups around the world have maintained colonies of both fleas and lice on various feeding systems, but predominantly on live animals, such as rabbits and guinea pigs (Hinnebusch, 2007; Mumcuoglu *et al.*, 2011). Fleas can be kept in glass or plastic jars, at the bottom of which bedding is applied, which allows the fleas to create nests and for the larvae to feed. Hinnebusch (2007) suggests a combination of dry milk, powdered blood, mouse food and sawdust, which can be autoclaved and stored in the freezer. Colonies require a temperature of between 20°C-25°C and a humidity of 75%. It is also suggested that keeping the jars in trays of water stop any mites entering the colony.

As lice spend their entire life cycle close to the host, setting up an artificial system may be more difficult than for fleas and only one strain of *P. corporis* has been adapted for feeding on rabbit blood so far, although a number of groups use this method (Culpepper, 1946; Waniek, 2009). Artificial feeding systems involving reservoirs and processed blood have been successfully implemented at least for experimental purposes if not colony maintenance (Georgi, 1996; Takano-Lee, Yoon, *et al.*, 2003).

1.8 Previous Work and Aims of This Study

The transmission of *Y. pestis via* its insect vectors has been studied for many years and fleas, specifically *X. cheopis*, have long been established as the main culprit, although there are some case studies and experimental papers

(Houhamdi *et al.*, 2006; Bonilla *et al.*, 2009; Drali *et al.*, 2015) that point towards other insects, mainly the human body louse *P. corporis*, due to its very close relationship with the human host.

The scarcity of information regarding the artificial rearing of these insect vectors would suggest that it is not something that has been attempted frequently, although groups have had some successes with artificially-fed infection experiments (Takano-Lee, Velten, *et al.*, 2003; Mumcuoglu *et al.*, 2011; Kernif *et al.*, 2015; Bland and Hinnebusch, 2016). The need to reduce experimental animal usage and the prohibitive ethical framework makes setting up an artificially fed colony of *X. cheopis* and *P. corporis* a more attractive proposition than using animal hosts. Insect work with a CL3 level pathogen such as *Y. pestis* naturally provides extra challenges, yet an artificial, 'fake flea' chitin-based model does not appear to exist, although chitin attachment experiments have been conducted notably with *Vibrio cholerae* (Kirn, Jude and Taylor, 2005).

Due to the highly contagious nature of *Y. pestis*, research has inevitably been difficult. The genetically similar but non-lethal *Y. pseudotuberculosis* has been used as a model organism, as well as attenuated strains of *Y. pestis*, which have had the virulence plasmid pCD1 removed, therefore allowing work to be undertaken at a CL2 level. This study set out to understand the relationships outlined above using the fully virulent CO92 strain at CL3 level.

Although the function of NagC has been extensively studied in other organisms, it has yet to be investigated in *Y. pestis*. Alongside GlcNAc catabolism and biosynthesis, NagC has been shown to influence QS regulation and AHL production in *Y. pseudotuberculosis* (Wiechmann, Ph.D.

Thesis, 2015), so there is a strong possibility that it may have an effect on QS phenotypes, such as virulence factor production (Robert Goldstone, Ph.D. Thesis, 2011, O. Kimyon *et al.* 2016). As it has been shown to play a role in the formation of biofilms in other species, including *Y. pseudotuberculosis*, it is likely that NagC influences the production of biofilms in *Y. pestis* (Sicard et al. 2018; Wiechmann, Ph.D. Thesis, 2015). Given that biofilms are so vital to the transmission of plague within its flea vector, the ability to knock out biofilm production could help to unravel the complex biological mechanisms surrounding flea blockage and plague transmission.

This study set out to understand the relationship between NagC, poly-GlcNAc and biofilm formation, in relation to QS and insect transmission for *Y. pestis*, using *Y. pseudotuberculosis* as a reference, and to build on artificial flea-plague models for use within CL3 conditions.

To elucidate the most suitable conditions for artificially rearing *X. cheopis* and *P. corporis* colonies the following aims were explored to determine:

- The optimal physical conditions in which to maintain insects without an animal host
- The most effective membrane through which insects can feed
- The blood type most suited for artificially rearing insect colonies

To investigate the role of NagC and GlcNAc in QS phenotypes, the following aims were pursued by constructing a *Y. pestis nagC* deletion mutant to compare to a *Y. pseudotuberculosis* Δ*nagC* mutant and examining the consequences for:

- AHL biosynthesis
- YOP production
- Auto-aggregation

To investigate the regulatory role of NagC in poly-GlcNAc biosynthesis, the Δ*nagC* mutant and recombinant NagC protein were utilised to establish:

- The role of NagC in poly-GlcNAc production in *Y. pseudotuberculosis*
- The role of NagC as a DNA binding protein in *Y. pestis*

To develop *in vitro* transmission models to understand the role of NagC in relation to establishment and biofilm formation *in vitro* and within insect hosts, the following aims were established:

- To investigate the impact of *nagC* in *Y. pestis* using the *C. elegans* biofilm model
- To develop a chitin based *in vitro* assay to study *Yersiniae* attachment and biofilm formation
- To determine the impact of *nagC* in *Y. pseudotuberculosis* biofilm production and blockage in relation to *P. corporis*

2 Materials and Methods

2.1 Insect Rearing and Feeding

X. cheopis were obtained from Dr Florent Sebbane at the Institut Pasteur in Lille, France. *P. corporis* colonies were obtained from Carola Kuhn from the Umweltbundesamt in Berlin, Germany.

2.1.1 Colony Maintenance Conditions

Genlab Limited incubators (model INC/50/DIG) were used to maintain colonies. Temperature was controlled *via* the incubator settings and humidity was maintained using different sized plastic trays filled with water. Humidity and temperature were monitored using Bohlender GmbH electronic hygrometers.

Figure 2.1. Image of a flea aspirator. This allowed for the secure transportation of *X. cheopis*.

To move fleas for visualisation *etc*. chilling for five min on a tray of ice was required to immobilise them. A flea aspirator (Figure 2.1) (B100 SEC, Charles Austin Pumps Ltd.) was also constructed, which enabled the insects to be sucked into a large test tube and transported securely. Lice were moved by carefully picking them up with forceps.

2.1.2 Insect Housing

Fleas were maintained in a glass vase (Ikea Ltd.) with a one-inch layer of autoclaved sawdust and larvae food in a ratio of 3:1 for bedding (Figure 2.2(A)). The food portion was taken from Hinnebusch (2007) and contained one-part dried erythrocytes from bovine blood (Sigma-Aldrich Co.), one-part dried skimmed milk (Tesco PLC) and one-part mouse chow (Purina®).

Lice were maintained in modified 60 ml Sterilin™ polystyrene containers (Figure 2.2(B)). A square of voile mesh was placed over the top, secured with an elastic band. The centres of the lids were removed and then screwed over the voile, to ensure insects could not escape, but could breathe and feed through the mesh. A piece of corduroy (500 mm x 200 mm) was placed into the containers. Fluon®, (BioQuip Products Inc.) was used on the edges of the flea vase and insect trays to prevent insects from escaping, as they are unable to grip Fluon with their feet.

A 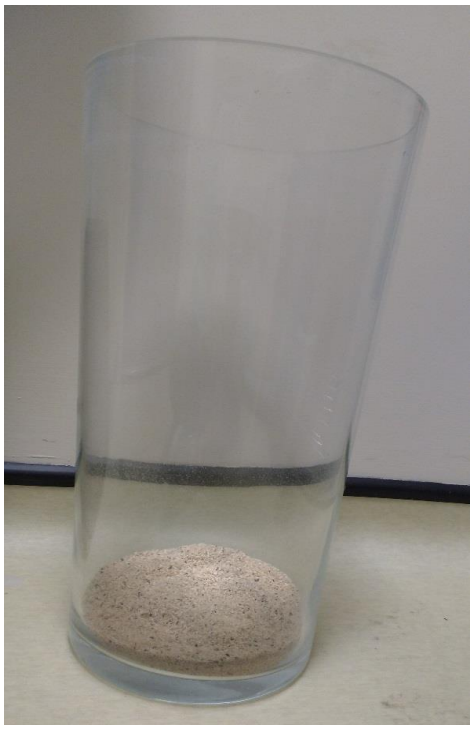 B 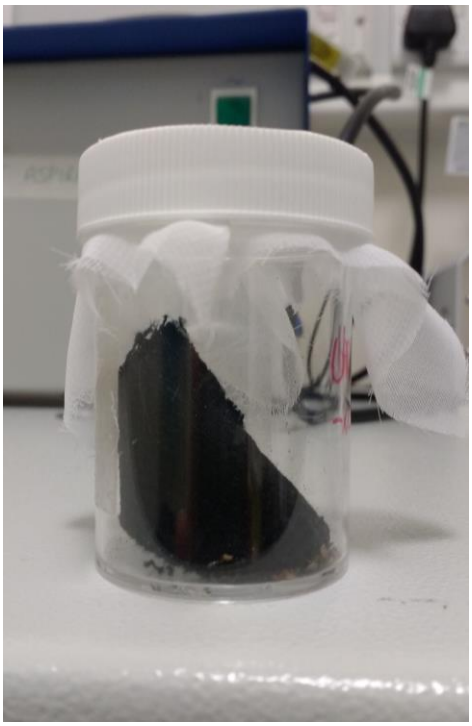

Figure 2.2. Images of insect housing. (A) shows the glass vase in which the *X. cheopis* colony was kept, with a layer of sawdust bedding at the bottom. (B) shows a modified plastic pot with a mesh lid, containing a square of corduroy in which *P. corporis* were kept.

2.1.3 Feeding System

The Hemotek® 5W1 (Hemotek Ltd.) system was used to artificially feed both the lice and fleas, (the setup is shown in Figure 2.3). This enabled the blood to be maintained at a temperature of 37ºC. FU1 feeding arms were connected to the power pack and meal reservoirs screwed into them. Either standard 3 ml (385 mm^2) or micro 1 ml (195 mm^2) were used to contain the blood. Squares of each type of membrane were cut to size and placed over the meal reservoir, secured with an O ring or rubber band and then gently stretched so that there were no creases and the membrane was taut. Under a flame, blood was pipetted into the posterior hole until filled. Plastic plugs provided with the Hemotek system were pressed into place to ensure no spillages. Once used,

the meal reservoirs were cleaned with 2% Distel HLD4L (MediMark Scientific Ltd.) then rinsed thoroughly with sterile water.

A  B 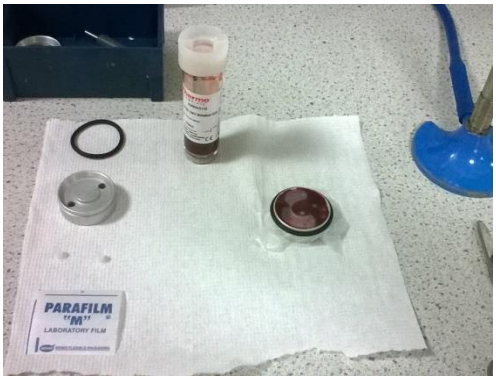

Figure 2.3. Photos showing Hemotek setup. (A) shows the Hemotek artificial feeding system set up in the insect laboratory. (B) shows the preparation of a meal reservoir.

2.1.4 Feeding Materials

Defibrinated sheep blood (SLS Ltd.) and defibrinated rabbit blood (TCS Biosciences Ltd.) were both purchased in vials of 25 ml. Human blood was collected from volunteers and defibrinated.

2.1.4.1 Human Blood

An ethical licence (Number: A051016SA–Steve Atkinson) to collect blood from human volunteer donors was obtained from the School of Life Sciences Ethical Committee. Volunteers were required to pass a health screening and, allowed to donate up to every 8 weeks. 10 ml of blood was taken from the antecubital vein using a syringe and deposited into a Sterilin tube. This was defibrinated using the method modified from (Rodda, 1996). In an microbiological safety cabinet (MSC), 5 glass beads (5 mm) were added to the blood. This was gently

swirled for approximately 5-10 min until the ‘ringing’ of the beads had ceased and a blood clot had formed around them. The liquid blood was then pipetted into a fresh 20 ml Sterilin tube and stored for up to a week, before it was disposed of in accordance with the ethical guidelines stated in the licence.

2.1.5 Membranes

Membranes were tested with the artificial feeding system, including Hemotek’s collagen feeding membrane, Parafilm® M (Bemis Company Inc.) and prepared cadaver mouse skins.

2.1.5.1 Mouse Skin Preparation

Mouse skins were provided by Jeni Luckett (as a by-product from the medical school animal laboratory) in phosphate buffered saline (PBS) (plus penicillin G and streptomycin, both 100 µg/µl). The skins were pinned inner side upwards on a wax dissection tray and, using forceps and a scalpel, the subcutaneous fat layer was removed. The skins were returned to PBS where they could be stored for 2-3 weeks at 4ºC. Tests comparing 1 M NaCl and PBS as a storage medium indicated that NaCl caused the outer layer of the dermis to slough off, making it unsuitable.

2.2 Microbiological Methods

2.2.1 Bacterial Growth Media and Growth Conditions

E. coli was grown at 37ºC, whilst shaking with aeration at 250 rpm in liquid Luria Bertani broth (LB) (Luria and Delbrück, 1943) unless otherwise stated. LB was composed of 10 g/l tryptone (Oxoid™), 10 g/l NaCl, 5 g/l yeast extract (Oxoid™). When grown on plates, 15 g/l agar was added to the medium. *Y. pseudotuberculosis* was also grown on LB modified by reducing NaCl to 5 g/l NaCl, at 22º, 30ºC or 37ºC depending on the growth conditions required. *Y. pestis* requires a richer media and was grown in brain-heart-infusion broth (BHI), using 37 g/L BHI powder (Oxoid™) at 22ºC, 30ºC or 37ºC depending on the growth conditions required. When required, antibiotics were added to cultures as follows; ampicillin (Amp) 100 µg/ml, gentamicin (Gm) 10 µg/ml, erythromycin (Erm) 25 µg/ml, chloramphenicol (Cm) 10 µg/ml, tetracycline (Tc) 10 µg/ml, kanamycin (Kan) 50 µg/ml, nalidixic acid (Nal) 15 µg/ml.

C. elegans were maintained on a lawn of *E. coli* OP50, at 22ºC using nematode growth medium (NGM), containing 2.5 g/l peptone (Difco-Bacto™), 3 g/l NaCl and 17 g/l agar, made up with distilled H_2O. This was autoclaved, then 1 ml/l cholesterol (5 mg/ml in EtOH), 1 ml/l $CaCl_2$ (1 M), 1 ml MgS (1 M) and 25 ml/l KH_2PO_4 (1 M, pH6) was added (Epstein and Shakes, 1995).

Congo red magnesium oxalate (CR-MOX) plates, were used for testing for the presence of the pCD1/pYV virulence plasmid, as described by Surgalla & Beesley (1969) and Riley & Toma (1989). 40 g of tryptic soy agar (Sigma-Aldrich) was mixed with 825 ml distilled water and autoclaved. The following

were added; 80 ml of 0.25 M sodium oxalate (Sigma-Aldrich), 80 ml of 0.25 M magnesium chloride (Sigma-Aldrich), 10 ml of 20% D-galactose (Sigma-Aldrich) and 5 ml of 1% Congo red (Sigma-Aldrich).

2.2.2 Bacterial Strains

Bacterial strains used in this study are listed in Table 2.1.

Table 2.1. Bacterial strains used in this study.

Strain	Description	Reference
	Escherichia coli	
One Shot™ Top10	F- *mcrA* Δ(*mrr-hsd*RMS-*mcr*BC) Φ80*lac*ZΔM15 Δ *lac*X74 *rec*A1 *ara*D139 Δ(*araleu*)7697 *gal*U *gal*K *rps*L (StrR) *end*A1 *nup*G (Amp^R)	Thermo Fisher Scientific
DH5α	K-12 cloning strain [Fφ80*lacZ*ΔM15Δ (*lacZYA-argF*) U169 *recAI endAI hsdR17* (r_K-m_K^+) *supE44 thiI gyri relAI*] (Amp^R)	Hanahan, 1983
S17.1 pDM4	S17.1 containing the suicide vector pDM4 (Cm^R)	Milton *et al.*, 1996
OP50	Uracil auxotroph. A nutrient source for *C. elegans* and control for uninfected worms (Tc^R)	Epstein, 1995
BL21	T7 protein over-expression strain	New England Biolabs®
	Yersinia pestis	
CO92 parent	Parent strain, isolated from a patient who died Colorado, pCD1, pFra, pPst (Erm^R)	Doll *et al.* 1994

Strain	Description	Reference
CO92 *ΔnagC*	CO92 lacking the GlcNAc-operon repressor NagC, ($Erm^{R,}$ Gm^{R})	This study
CO92 *ΔnagC* complemented	pHG327::*nagC* (Erm^{R}, Gm^{R}, Amp^{R})	This study
CO92 pHG327	Control for plasmid (Erm^{R}, Gm^{R}, Amp^{R})	This study
Y. pseudotuberculosis		
YPIII parent pLB1	Parent strain of YpIII harbouring the virulence plasmid pYV. Serotype O:3 (Nal^{R})	Rosqvist *et al.* 1988
YPIII Δ*nagC*	YpIII lacking the GlcNAc-operon repressor NagC (Km^{R})	Wiechmann, Ph.D. Thesis, 2015
YPIII *ΔnagC* complemented	Complementation of YpIII lacking NagC with a functional copy of *nagC* in the *glmS* region of Δ*nagC* (Tc^{R})	Wiechmann, Ph.D. Thesis, 2015
YPIII parent GFP	YpIII harbouring the GFP plasmid p*xylA*p (Amp^{R})	Wiechmann, Ph.D. Thesis, 2015
YPIII Δ*nagC* GFP	YpIII *ΔnagC* harbouring the GFP plasmid p*xylA*p (Amp^{R})	Wiechmann, Ph.D. Thesis, 2015
YPIII *ΔnagC* complemented GFP	YpIII *ΔnagC* complement harbouring the GFP plasmid p*xylA*p (Amp^{R})	Wiechmann, Ph.D. Thesis, 2015
Chromobacterium violaceum		
CV026	Mini-Tn5 mutant of ATCC 31532, does not produce violacein (Km^{R})	McClean *et al.* 1997
CV 12472	Parental strain that produces the pigment violacein	Streichsbier 1983

2.2.3 Molecular Biology Methods

2.2.3.1 Molecular Cloning

2.2.3.1.1 Plasmid Extraction and Restriction Digests

A plasmid extraction kit (Sigma-Aldrich GenElute™ Plasmid Miniprep kit) was used to isolate plasmids following the supplier's instructions but eluted in 50 - 100 µl H_2O and stored at -20ºC. Restriction enzymes (FastDigest, Thermo Fisher Scientific) for digestion of plasmids were used as per the manufacturer's instructions.

2.2.3.1.2 DNA Purification and Gel Electrophoresis

The Monarch® DNA Gel Extraction Kit (New England BioLabs Inc.) was used to purify and clean DNA products, either excised from agarose or from PCR products, following the manufacturer's guidelines. Agarose gel electrophoresis was used to separate DNA products according to mass using (1% (w/v) agarose and 1 x Tris-acetate-EDTA (TAE) buffer [50 x stock solution: 2.0 M Tris-acetate pH 8, 0.05 M ethylenediaminetetraacetic acid (EDTA)]). Invitrogen™ Sybr™ Safe (Thermo Fischer Scientific) (10,000 x in DMSO buffer) was added at a final concentration of 0.1 µl/ml, then 5-20 µl DNA/PCR product was run in 1 x TAE buffer at 70 V for 45 min against 5 µl of Promega 1 kb DNA molecular markers.

2.2.3.1.3 Ligation of the DNA Fragment and Vector

Ligation of digested vector and DNA fragment were undertaken using T4 DNA ligase (Promega) at a ratio of 1:3, then incubated on a 30ºC (30 seconds) and 10ºC (30 seconds) cycle on a thermocycler for 16 h.

2.2.3.1.4 Transformation of Plasmids into Competent Cells

2.2.3.1.5 Electro-Competent Cells

Overnight cultures of *E. coli* Top10 or *Y. pseudotuberculosis* YPIII were diluted to OD_{600} 0.1 in a 250 ml flask containing 100 ml LB. Cultures were grown until early exponential phase (OD_{600} 0.6-0.9), then harvested by centrifugation at 4ºC at 4000 x *g* for 8 min in 50 ml falcon tubes. The cells were washed in 40 ml 10% (v/v) chilled glycerol, then repeated with 20 ml and 5 ml 10% (v/v) glycerol. Cells were then pelleted and resuspended in 500 µl 10% (v/v) glycerol and stored in 50 µl aliquots at -80ºC.

DNA was dialysed against H_2O using Millipore® Membrane filters (Fisher Scientific) for 30 mins then added to thawed competent cells transferred to a 2 mm electroporation cuvette. A BioRad MicroPulser set to 200 Ω, 2.5 V, 25 µF was used to electroporate the cells, which were then recovered in 500 µl of LB and left shaking at 250 rpm for 1–3 h at the appropriate temperature before plating onto LB agar containing the required antibiotics.

2.2.3.1.6 Chemical-Competent Cells

Y. pestis overnight cultures grown in medium A (YLB broth supplemented with 10 mM $MgSO_4.7H_20$ and 0.2% glucose) (Nishimura *et al.*, 1990) were diluted to 1/10 and further incubated in medium A until they reached OD_{600} 0.5-0.9. Cells were collected by centrifuging at 13,000 x *g* for 1 min and washed in medium A. Cells were pelleted at 13,000 x *g* for 1 min and resuspended in 50 µl media A and 250 µl medium B (36% (v/v) glycerol, 12% polyethene glycol (PEG) (MW7500), 12 mM $MgSO_4.7H_20$ added to YLB-broth (pH 7.0), sterilized by filtration) (Nishimura *et al.*, 1990) and stored in 50 µl aliquots at -80ºC. 1 ng DNA was added to thawed chemical-competent cells and kept on ice for 20 min before heat shocking at 37ºC for 1 min. Cells were returned to ice for a further 5 min before being plated on BHI agar with the appropriate antibiotics.

2.2.3.2 Plasmids Used in This Study

All plasmids used in this study are listed in Table 2.2.

Table 2.2. Plasmids used in this study.

Plasmid	Description	Source
pGEM®T Easy	High copy number cloning vector (Amp^R)	Promega
pDM4	Suicide vector: *mob*RK2, *ori*R6K (*pir* requiring). *sacBR* of *Bacillus subtilis* (Cm^R)	Milton *et al.* 1996
pHG327	Complementation vector low copy number (Amp^R)	Stewart *et al.* 1986
pEX18Gm	Gm^R, oriT+, sacB+, gene replacement vector, MSC from pUC18 (Gm^R)	Hoang *et al.* 1998
pCOLD1	Cold shock expression system vector	Qing *et al.* 2004
p*xyl*Ap	Vector harbouring GFP (Amp^R)	Stephan Heeb

2.2.3.3 Genomic DNA Extraction

Genomic DNA (gDNA) was extracted using the GenElute™ Bacterial Genomic DNA Kit (Sigma Aldrich) according to manufacturer's instructions, then eluted into H_2O and stored at 4ºC.

2.2.3.4 Polymerase Chain Reaction

Polymerase chain reactions (PCRs) were used with either Go Taq® DNA polymerase (Promega) or Q5® High-Fidelity DNA polymerase (NEB). A 50 µl PCR reaction typically consisted of 0.2 µl DNA polymerase, 5 µl reaction buffer

(Promega or NEB), 1 µl of 10 µM forward and reverse primer, 1 µl of 20 mM nucleotides (dNTPs) and approximately 1 ng DNA. This was made up to 50 µl using H_2O. PCR conditions depended on the length of the final DNA product length and the melting temperature of the primers and were performed according to the supplier's instructions. Primers used in this study are listed in Table 2.3.

Table 2.3. Primers used in this study. Underlined sections of the primer sequences are restriction enzyme recognition sites.

Primer name	Sequence (5' – 3')	Restriction Enzyme	Source
GmR_F	CGTCTAGAGTCGATGTTTGATGTTATG	*XbaI*	This study
GmR_R	ACGGTACCTTAGGTGGCGGTACTTG	*KpnI*	This study
*nagC*_UP_F	GCCTCGAGGTGTCGAACATGTCGGTATC	*XhoI*	This study
*nagC*_UP_R	TCGGTACCGCGTCTAGACAATTGCCGGGTGATTTTG	*KpnI, XbaI*	This study
*nagC*_DW_F	CTCTCGAGACTGGTACCGCTCAATGGTGTCTTGCTG	*XhoI, KpnI*	This study
*nagC*_DW_R	ATACTAGTGCGTCTCACCGACAATAAC	*SpeI*	This study
M13_F	GTAAAACGACGGCCAGT	-	Joanne Purves (unpublished)
M13_R	CAGGAAACAGCTATGAC	-	Joanne Purves (unpublished)

Primer name	Sequence (5’ – 3’)	Restriction Enzyme	Source
Gm_out_F	CACTTTGATATCGACCCA	-	Natalie Barratt, Ph.D. Thesis, 2018)
Gm_out_R	CTGCTGCGTAACATCGT	-	Natalie Barratt, Ph.D. Thesis, 2018
Gm_NoPro_*XbaI*	CGTCTAGAGTCGATGTTTGATGTTATG	*XbaI*	This study
Gm_NoTerm_*KpnI*	ACGGTACCTTAGGTGGCGGTACTTG	*KpnI*	This study
YPCO92_*nagC*_F	GGTTTATGCGTAGACGAAAA	-	This study
YPCO92_*nagC*_R	GGCAATAAAACGTGCACC	-	This study
*nagC*_F_*XbaI*	TATCTAGAGCGAGTAACTTTATTGATGA	*XbaI*	This study
*nagC*_R_*HindIII*	ATAAGCTTTGTTTATATTACTCATTTAGCG	*HindIII*	This study
Gm_F_*EcoRI*	AGCGAATTCGGCGATATCGGATCATTC	*EcoRI*	This study
Gm_R_*XbaI*	TACCTCTAGAGTCCGAGGAGCTTTATG	*XbaI*	This study
NagC_F_*NdeI*	ACTTTACATATGAGCACCGGCGGACAAGCA	*NdeI*	This study
NagC_R_*XhoI*	CTTTCACTCGAGCGGGTGAGTTTCTAGCAAACGT	*XhoI*	This study
*nagBACD*_F1	ATCACTCATCTTGGAGTG	-	This study

Primer name	Sequence (5’ – 3’)	Restriction Enzyme	Source
*nagBACD*_R (Cy5)	CATCGTGCACCTCTTTGA	-	This study
*glmUS*_F1	TAACTTGGGTATATATGATGTG	-	This study
*glmUS*_R (Cy5)	CATAAGCAACCTGATAACT	-	This study
*hmsHFRS*_F1	GTCATTGATAATCTACTTTGC	-	This study
*hmsHFRS*_R (Cy5)	CATTATATAACCCTTAAGCC	-	This study

2.2.3.5 DNA Sequencing

The purity and quantity of the DNA was checked using a Nano Drop® 1000 spectrophotometer (Fisher Scientific). Sanger sequencing (Sanger and Coulson, 1975) was conducted at Source Bioscience, Science Park, Nottingham, UK.

The results were analysed in SnapGene® Viewer 3.0.3 (GSL Biotech LLC) and Artemis Release 16.0.0 (Wellcome Trust, Sanger Institute, Pathogen Genomics Group).

2.3 Genetic Modifications

2.3.1 Genetic Mutations

2.3.1.1 Gene Modifications using the Suicide Plasmids pDM4

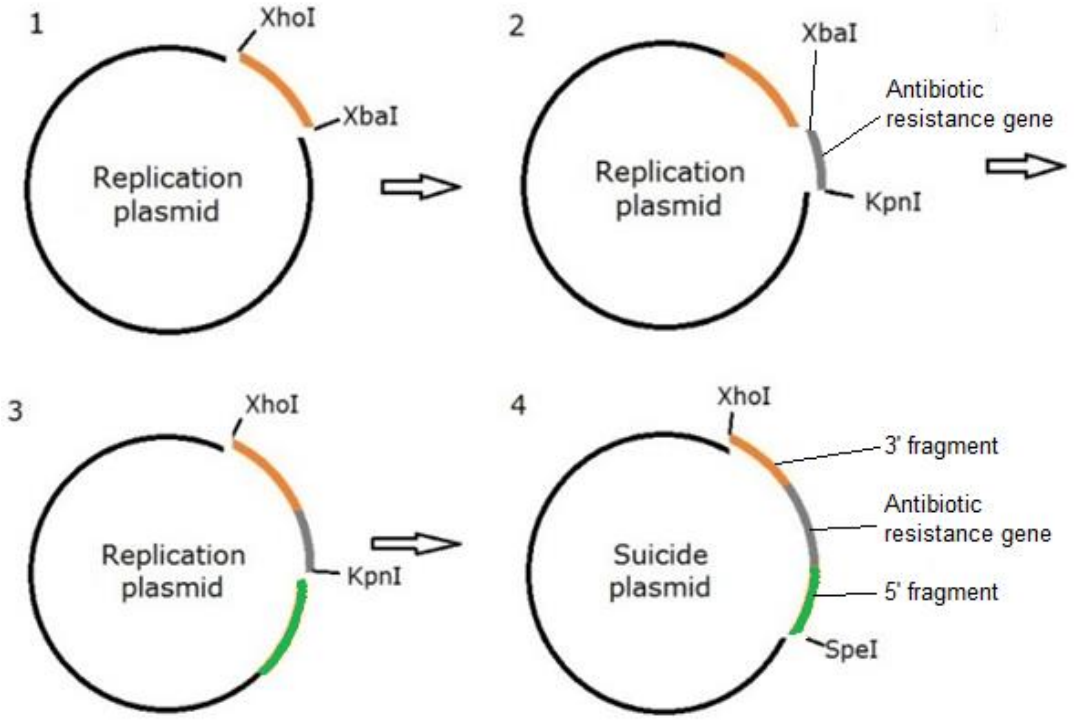

Figure 2.4. Schematic of the deletion-insertion cloning strategy. 1. The 3' fragment (orange), flanked by *XhoI* and *XbaI* restriction sites is cloned into a replication plasmid (pGEM-T easy) (black). 2. The antibiotic resistance cassette (grey), flanked by the restriction sites *XbaI* and *KpnI* is ligated into the replication plasmid containing the 3' fragment. 3. The 3' fragment and antibiotic resistance cassette is cut out using the restriction sites *XhoI* and *KpnI* and ligated into the replication plasmid containing the 5' fragment (green), flanked by *KpnI* and *SpeI* restriction sites. 4. The disrupted gene, including the 3', 5' fragment and antibiotic resistance cassette is ligated into a suicide vector (pDM4).

Mutations were made utilising the sucrose sensitive suicide plasmid pDM4 (Table 2.2). Most of the target gene was deleted and replaced by a gentamicin

cassette, as described in Atkinson *et al.* 2008. Primers were used to amplify the upstream (*nagC*_UP_F and *nagC*_UP_R) and downstream (*nagC*_DW_F and *nagC*_DW_R) gene fragments and antibiotic cassette. Each was then cloned into pGEM®T Easy (Table 2.2) and transformed into the Top10 strain of *E. coli* (Table 2.1). The gentamicin cassette was excised from pGEM-T Easy and cloned into vector containing the upstream fragment. This construct was then again excised from pGEM-T Easy and cloned into pGEM-T Easy containing the downstream fragment, creating an upstream-antibiotic-downstream insert. The whole construct was excised from pGEM-T Easy and sub-cloned into the suicide plasmid pDM4 (Table 2.2) and transformed into S17-1 *E. coli* (Table 2.1), as shown in Figure 2.4.

After incubation at 30ºC for 24 h, the bacteria were scraped off the plate using a culture loop, resuspended in 200 µl BHI and plated onto *Yersinia* selective agar (YSA) agar (58 g/L YSA (Oxoid™) autoclaved, then 4 ml YSA supplement (Oxoid™) (suspended in 1 ml EtOH and 1 ml distilled H_2O per vial)) to inhibit *E. coli* and promote *Y. pestis* growth. Plates were incubated at 30ºC until single colonies appeared. These colonies were then serially patched onto BHI plates containing gentamicin, gentamicin and 12% (w/v) sucrose, chloramphenicol and a non-selective plate. Those colonies able to grow on sucrose and gentamicin, but not chloramphenicol (the antibiotic resistance cassette encoded on pDM4) were screened for the mutation by PCR. If only single crosses occurred (those colonies growing on gentamicin and chloramphenicol, but not sucrose), it was possible to counter-select for the *sacBR* system on pDM4 by incubating these colonies for 24 h at 30ºC shaking at 250 rpm with aeration in BHI with 12% (w/v) sucrose and gentamicin, then plated onto BHI

agar containing gentamicin to improve the chances of double crosses occurring.

2.3.1.2 Genetic Complementation

To ascertain whether the effects observed were caused by mutation, a plasmid containing a functional copy of the mutated gene was introduced into the mutant strain, which should revert the phenotype back to the wild type. A copy of the intact gene was amplified with the primers *nagC*_UP_*XbaI* and *nagC*_DW_*HindIII*, using PCR and ligated into pGEM-T Easy, before being excised and sub-cloned into pHG327 (Obrist and Miller, 2012) (Table 2.2). The pHG327 vector containing the gene was then transformed into *Y. pestis* CO92 (see Appendix **Error! Reference source not found.** for confirmation gel).

2.4 Phenotypic Assays

2.4.1 Analysis of AHL Production

To analyse the production of AHLs by *Y. pestis* and *Y. pseudotuberculosis*, the extraction method described by Ortori was followed (Ortori *et al.*, 2007). 10 ml of culture was grown in BHI MOPS (pH 6.8) (3-(*N*-morpholino)propanesulfonic acid) at 22ºC or 37ºC until they reached mid log phase, which was identified using OD_{600} readings. The cultures were centrifuged and filter sterilised using a 0.2 µm filter.

For analysis by mass spectrometry, undertaken by Nigel Halliday, (Bruker HCT Plus), 3 ml of supernatant containing AHLs was mixed with an internal standard (d9-C5-AHL, final concentration 10 µM) and 1.5 ml 100% acidified ethyl acetate. The deuterium component of the internal standard enables identification of and differentiation from C5-AHL by mass spec and the resulting concentration was used as a control marker. The samples were vortexed for 30 s and centrifuged at 3000 rpm for 10 min. The organic layer containing the soluble AHLs was removed to a fresh tube. The addition of acidified ethyl acetate was repeated twice more, resulting in 4.5 ml of pooled sample. This was dried using a centrifugal evaporator, resuspended in 10 µl acetonitrile and the AHLs were analysed using liquid chromatography-mass spectrometry (LC-MS/MS), as developed by Ortori *et al.*, 2007.

2.4.2 Analysis of Proteins

2.4.2.1 Extraction of *Yersinia* Outer Proteins

YOPs from *Y. pestis* and *Y. pseudotuberculosis* were extracted using the method described by Trülzsch, 2004, with modification for CL3 conditions. CFU counts were undertaken to ensure that the OD_{600} were equivalent for each strain of *Y. pseudotuberculosis* and *Y. pestis* (data not shown). Cultures at OD_{600} 0.1-1.0 were diluted and plated onto BHI plates, then colonies counted after a 24 h incubation. Cells were grown overnight in 10 ml BHI at 22ºC and then diluted to an OD_{600} of 0.1 in BHI containing 0.2% (w/v) glucose, 20 mM sodium oxalate (NaOx) and 20 mM magnesium chloride ($MgCl_2$).

Cultures were incubated at 22ºC for 2 h then, to induce YOP expression and release into the growth medium, shifted to 37ºC for 3 h. The culture was centrifuged to remove bacterial cells and the subsequent supernatant removed and filter sterilised with a 0.2 µm filter. The YOPs were extracted from the supernatant by incubating with 1 ml 100% (w/v) trichloroacetic acid (TCA) for 30 min, before centrifugation at 10,000 x *g* at 4ºC for 10 min. The proteins were then resuspended in 500 µl of 10% (w/v) sodium dodecyl sulphate (SDS) and re-precipitated with 1 ml ice cold acetone for 30 min on ice. Proteins were pelleted at 16,000 x *g* for 30 min at 4ºC then washed in 300 µl ice cold acetone and centrifuged at 16,000 x *g* for 10 min at 4ºC. The final pellet was air dried and resuspended in 30 µl phosphate buffered saline (PBS).

2.4.2.2 Sodium Dodecyl Sulphate Polyacrylamide Gel Electrophoresis (SDS-PAGE)

YOP samples for SDS-PAGE were boiled in 2 x SDS loading buffer (1 ml Tris pH 6.8, 4 ml 10% (w/v) SDS, 1 ml 1% (w/v) bromophenol blue, 2 ml glycerol, 560 µl 2-mercaptoethanol) before loading on an SDS-PAGE gel (12% (w/v) acrylamide) in 1 x SDS running buffer (3.0 g Tris, 14.4 g glycine and 1 g SDS in 1000 ml H_2O. An NEB Prestained Broad Range Protein Ladder (11-245 kDa) was used as a molecular marker, which was run at 150 V for 80 min. Gels were stained with Coomassie Blue to visualise proteins.

To quantitively analyse YOP bands, gel images were processed using the imaging software ImageJ (NIH). Each lane was highlighted and the density peaks (bands within the lane) were analysed to provide a percentage of the

total size of all the highlighted peaks (bands). The numbers provided were arbitrary, so each was calculated as a percentage difference compared with the parental peak for each YOP.

2.4.3 Aggregation Assay

Bacteria were grown for 17 h in YLB (*Y. pseudotuberculosis*) or BHI (*Y. pestis*) at 22ºC, 30ºC and 37°C, then cultures were diluted to OD_{600} 2.0-3.0 in fresh medium and left statically in a 1.0 mm cuvette for up to 2 h at 22°C, as described by Atkinson (1999) and observed visually for sedimentation of cells. The presence of small, red colonies on CR-MOX plates indicated the presence of pCD1/pYV; larger, pinkish white colonies indicated the absence of the plasmid. To identify the aggregation rate, the optical densities of the cultures were read at 10 min (*Y. pseudotuberculosis*) or 15 min (*Y. pestis*) intervals over 2 h. When cultures aggregate, the aggregations settle at the bottom of the cuvette, causing the optical density in the remaining media to decrease. All cultures were diluted to an OD_{600} of 1.5 to start. The rate of aggregation was derived from the sedimentation data and expressed as the change in turbidity (the optical density at OD_{600} nm) per minute.

2.4.4 GlcNAc Production Assay

To analyse the amount of GlcNAc a bacterial strain produced, cultures were grown for 24 h in YLB at 22ºC and 37ºC and 40 µl was spotted onto a microscope slide and allowed to dry. 20 µl 1/1000 WGA was added to the spot

and incubated at room temperature in the dark for 45 min. These were examined using confocal microscopy and the fluorescence analysed using the Volocity 2.0 (Perkin Elmer) software package. The fluorescence channel required for each image was measured and then analysed using the mean of the sum fluorescence. The GFP-labelled *Y. pseudotuberculosis* complemented Δ*nagC* strain cloned by Wiechmann (Ph.D. Thesis, 2015) (Table 2.1) continually lost fluorescence despite repeated attempts to transform it with different plasmids containing GFP (p*xylA*p, pME6032, pBluescript) so for subsequent experiments, the complemented Δ*nagC* strain was stained using 10 µM SYTO®9 (ThermoFisher Scientific).

2.4.5 Protein Purification and Binding Site Identification

2.4.5.1 *In Silico* Identification of Transcription Factor Binding Sites

To identify potential DNA binding targets for NagC both *in silico* and experimental approaches were adopted. Putative NagC binding domains were identified using the RegPrecise database and Softberry BPROM websites. The RegPrecise website enables transcriptional regulons to be searched and reconstructed by comparative genomics using a selection of reference genomes, including *Y. pestis* KIM. The database was used to identify NagC transcription factor binding sites (http://regprecise.lbl.gov/RegPrecise/regulon.jsp?regulon_id=11428).

Information such as position upstream from the gene, score (the probability of

this being a binding site rather than a background motif) and binding site sequence was displayed, as shown in Table 4.1.

As the *hmsHFRS* operon was not identified using the RegPrecise database, the SoftBerry BPROM website (http://www.softberry.com/berry.phtml?topic=bprom&group=programs&subgroup=gfindb) was used to identify whether NagC had a potential binding site upstream of the operon. The SoftBerry website uses an annotator pipeline to enable identification and automatic annotation of genes, operons and potential promoters and terminators from sequence data. A ~500 bp upstream section of sequence was pasted into the search engine which then identified the binding domain, as well as the -35 and -10 regions. This *in silico* analysis enabled appropriate primer sites to be identified to ensure the binding sites were included in the probes.

2.4.5.2 Protein Cloning and Expression

To identify potential DNA binding targets for NagC both *in silico* and experimental approaches were adopted. Putative NagC binding domains were identified using the Softberry BPROM and RegPrecise database websites. The *nagC* gene was amplified using the primers NagC_F_*NdeI* and NagC_R_*XhoI* (Table 2.3). The PCR product (see Appendix **Error! Reference source not found.**) was cut with restriction enzymes then ligated into the cold shock expression vector pCOLD1 (Table 2.2). This construct was transformed into *E. coli* BL21, as described by Takara Bio Inc. and cold-shock induction of gene expression was carried out by simultaneous addition of 1 mM isopropyl- β-

thiogalactopyranoside (IPTG) upon temperature downshift to 4ºC. (Qing *et al.*, 2004) and grown on an LB plate containing 10 µg/ml ampicillin. A colony was picked to make an overnight culture, before 4 ml was inoculated into 600 ml terrific broth (TB) (Sigma Aldrich) with 10 µg/ml ampicillin. This was grown at 37ºC until it reached an OD_{600} of 0.6-0.9 and then pelleted at 4000 x *g* for 15 min at 10ºC. The pellets were resuspended in 2 x 30 ml cell suspension buffer (10 mM Tris pH 7.5, 10% glycerol, 5 mM $MgCl_2$) modified from (Miyashiro *et al.*, 2012) and stored at -80ºC.

NagC was purified with the help of Dr Philip Barderlang, using methods modified from (Bornhorst & Falke 2000). The pellet was sonicated (amplitude 8, 10 second pulse, 1 min off, 10 min process time) using the Sonic Dismembrator (Fisher ScientificTM) to break open the cells. This was then centrifuged at 4000 x g for 30 min and the clear supernatant filtered through a nickel column and washed with a low imidazole (10 mM) buffer (50 mM NaP (pH 7.5), 10% glycerol, 500 mM NaCl, 1 mM EDTA, 2 mM DTT). This was followed by approximately 20 ml high salt wash (50 mM NaP (pH 7.5), 2.5 M NaCl) before washing with a further 15 ml of the low imidazole buffer and 60 µl samples were taken to run on an SDS-PAGE gel to ensure protein quality. The proteins were run on the ÄKTAprime plus (GE Healthcare Life Sciences) and eluted with a gradient introducing a high imidazole (0.5 M) buffer (50 mM NaP (pH 7.5), 10% glycerol, 500 mM NaCl, 1 mM EDTA, 2 mM DTT). This eluted NagC (~46 kDa) in an increasing imidazole gradient into 2 ml fractions (fractions 14 (328 mM imidazole), 15 (343 mM), 16 (357.7 mM), 17 (367.5 mM), 18 (377.3 mM), 19 (396.9 mM), 20 (411.6 mM) and 21 (416.5 mM). 1 ml of low imidazole buffer and 30 mM DTT was added to each fraction and 60 µl

samples of each fraction were run on an SDS-PAGE gel to ascertain protein quantity, which was shown to be very pure (see Appendix 8.3).

The fractions with protein (numbers 14 to 21) were pooled and dialysed overnight (50 mM NaP (pH 7.5), 10% glycerol, 500 mM NaCl, 1mM EDTA, 2 mM DTT) to remove impurities. The dialysis buffer was UV transparent, allowing the quantification of NagC using UV absorbable spectroscopy on a Nanospec®II (Nanometrics Incorporated) and its molar extinction coefficient, calculated from its amino acid sequence using the ExPASy ProtParam tool (https://web.expasy.org/protparam/). The concentration was calculated to be 14.35 µM. This was run through a VivaSpin®6 column (Sartorius AG) to concentrate as per the manufacturer's instructions (8,000 xg 3x30 minutes) and re-dialised overnight as before. The concentration was then re-measured on a Nanospec®II. The final concentration was 28.7 µM (1,35 mg/ml-1) and this was aliquoted and stored at -80°C until further use.

2.4.5.3 Electrophoretic Mobility Shift Assay

To ascertain whether there were DNA-protein interactions, an electrophoretic mobility shift assay (EMSA) was undertaken, as modified from (Hellman and Fried, 2007). The putative NagC DNA binding domains were identified in the promotor regions of *nagE-nagBACD*, *glmUS* and *hmsHFRS* which were amplified using *nagBACD*_F1, *nagBACD*_R, *glmUS*_F1, *glmUS*_R, *hmsHFRS*_F1 and *hmsHFRS*_R primers, as described in Table 2.3. The reverse primer for each of these was labelled with the Cyano dye Cy5, allowing fluorescence to be quantified using the Odyssey® CLx Infrared Imaging

System (Li-Cor Biosciences). For the binding reaction, 10 nM of DNA probe was incubated with 100 nM protein in the presence of 0.9 µl of 1 µg/µl poly-dIdC in TE buffer, 1.8 µl 5 x binding buffer (50 mM Tris HCL (pH 7.5), 750 mM KCl, 2.5 mM EDTA (pH 8.0), 0.5% Triton-X 100 and 62.5% glycerol), 1.8 µl 10 mM DL-Dithiothreitol (DTT), 0.1 µl 100 x bovine serum albumin (BSA), made up to 9 µl with dH_2O. To dilute protein samples, protein dilution buffer (10 mM Tris-HCl (pH 7.5), 2 mM DTT and 10% glycerol made up to 1 ml with dH_2O) was added.

This was incubated at room temperature for 30 min, then 1 µl loading dye (Promega) added and run for 60 min at 110 volts on a 0.7% agarose gel, using 0.5 x TBE buffer (45 mM Tris-borate and 1 mM EDTA). All DNA-protein binding experiments were also run in the presence of 10 mM GlcNAc-6-P and 10 mM GlcNAc (Sigma-Aldrich) to identify whether it had an effect and 500 nM cold DNA competitor and non-specific DNA probe to rule out non-specific binding.

2.4.5.4 'Fake flea' *In vitro* Chitin Substrate Aggregation Assays

A 'fake flea' model was developed, testing chitin from shrimp shells (Sigma-Aldrich), chitin resin beads (New England BioLabs Inc.) and dissolved chitin attached to glass coverslips as a substrate for bacterial attachment and biofilm formation. Substrates was prepared as follows; 200 µl chitin beads were washed twice in 200 µl PBS and added to a 5 ml YLB culture of GFP-tagged *Y. pseudotuberculosis* with the appropriate antibiotics. 0.5 g of sterile chitin flakes were added to a 5 ml YLB overnight culture. Other media were also tested, including 50% YLB and *Yersinia* defined minimal media (YDMM) (1×

M9 minimal salts (Gibco), 4 g.l^{-1} glucose, 4 g.l^{-1} casamino acids, 10 mM $MgCl_2$, 5 mM K_2SO_4, 10 g.l^{-1} thiamine) as defined by Lavander *et al.* (2006).

For the chitin-coated coverslips, chitin from shrimp shells was dissolved as described by Moustafa *et al.* (2007). Briefly, 5 g of chitin powder (Sigma-Aldrich) was slowly added to 60 ml 37 % HCl, and gently shaken at 200 rpm at room temperature overnight. This mixture was added to 200 ml ice cold 95% ethanol and again stirred overnight at room temperature. It was then centrifuged at 5000 x *g* for 20 minutes at 4ºC and the precipitate transferred to a glass funnel with filter paper (Whatman™). It was washed with sterile distilled water until the colloidal chitin became neutral (pH 7.0) and then stored at 4ºC. 100 µl of 1:10 poly-L-lysine (Sigma-Aldrich) was added to positively charge the coverslips, incubated at room temperature for 5 min, washed off and allowed to dry at room temperature for 24 h. 200 µl 1:2 dissolved chitin (approximately 12.5 mg) was applied to each coverslip and allowed to dry overnight, then sterilised using UV. To test the effect of blood products on bacterial adhesion to a chitin surface, 10% of either bovine serum or heat inactivated bovine serum was added to PBS containing 1 mM $MgCl_2$ and $CaCl_2$. 100 µl was placed onto a chitin covered coverslip and incubated at 37ºC for 30 min to allow for adherence. The excess serum was then blotted off and the coverslip placed into the culture tube.

The ‘fake flea’ model optimal conditions are defined as follows:

- Dissolved chitin (as described by (Moustafa *et al.*, 2007)) attached to a glass coverslip pre-treated with poly-L-lysine (100 µl 1:10) for 5 min at room temperature

- A 48 h incubation period at either 22ºC or 37ºC
- 5 ml YDMM as an incubation media within a 50 ml Sterilin tube
- The addition of 100 µl 10% heat inactivated bovine serum, incubated on the coverslip for 30 min at 37ºC
- The use of 4% PFA as a fixative (24 h incubation at room temperature)

2.4.6 *Y. pestis* Biofilm Formation on *C. elegans*

2.4.6.1 *C. elegans* Maintenance

C. elegans (wild-type N2 Bristol), were obtained from the *Caenorhabditis* Genetics Centre, University of Minnesota, USA) and sub-cultured every 2-3 days for maintenance. 400 µl OP50 *E. coli* (Table 2.1) was spread onto NGM plates and allowed to dry. A 1 cm x 1 cm piece of agar from an existing worm plate was then transferred onto the fresh plate and incubated at 22°C until required.

2.4.6.2 *Y. pestis* Biofilm on *C. elegans* Assays

C. elegans biofilm infection assays were conducted as described by Joshua *et al.* 2003 and Atkinson *et al.* 2011, although required modification for CL3 conditions. 5 ml overnight cultures were grown at 30ºC. Cultures were diluted to OD_{600} 1.0 for *Y. pseudotuberculosis* and 0.4 for *Y. pestis*. 400 µl was applied to an NGM plate. 30 worms were either directly picked onto the plates using a micro-lance (CL2) or transferred to an Eppendorf, then pipetted onto an NGM

plate (CL3). The plates were sealed using Parafilm M and incubated at 22ºC for 24 h. To score biofilms on the worms, each plate was disinfected and placed into a ziplock bag and transferred to a microscope. Each worm was given a biofilm severity index (BSI) score, determined by rating the size of the biofilm from 0-3 and calculated as follows:

$$Biofilm\ severity\ index\ (\%) = \left\{\left[\sum\left(\frac{severity\ \times number\ of\ worms\ in\ this\ level}{(highest\ severity\ \times total\ number\ of\ worms)}\right)\right]\right\} \times 100$$

0 = no biofilm, 1 = small biofilm (often) around the buccal cavity, 2 = large, mono-focal biofilm, 3 = very large, multi-focal biofilm (Atkinson *et al.*, 2011)**.**

2.4.7 *Y. pseudotuberculosis* Colonisation of *P. corporis* Assay

Twenty *P. corporis* were placed into a feeding house, consisting of a 3 x 3 cm cardboard tube (Crayford Tubes Ltd.), with mesh glued across each end (see Figure 3.9). This diameter enabled the feeding houses to fit snugly to the meal reservoirs, allowing contact between the membrane and mesh. All insects remained within these houses for the duration of the experiment.

For each bacterial strain to be tested, 200 µl OD_{600} 1.0 (approximately 2 x 10^8 bacteria) *Y. pseudotuberculosis* was added to the blood, alongside 2 µl rhodamine labelled wheat-germ agglutinin (WGA) to stain poly-GlcNAc. The sealed meal reservoir was then placed onto the Hemotek feeding arm and the feeding houses containing insects placed on top. Insects fed for approximately 1 h before being placed into an incubator at 30ºC and 75% relative humidity.

To kill insects and bacteria for imaging, lice were submerged in 500 µl 4% paraformaldehyde (PFA) for 24 h. To ensure bacteria were killed, sample

insects were crushed and plated out onto an LB plate for 24 h to check for growth. Insects were washed twice in distilled H_2O and placed in 30 µl of FluoroGel mounting medium (GeneTex Inc.) on a 1 mm Academy cavity slide (Smith Scientific Ltd.). A coverslip was placed over the top before being allowed to harden for 24 h.

2.4.8 Microscopy

2.4.8.1 Dissection Microscope

A dissecting microscope (Nikon SMZ1000, Nikon) was used for examining bacterial colonies, transferring *C. elegans* between NGM plates and examining *Y. pseudotuberculosis* biofilm formation on *C. elegans* under CL2 conditions. Under CL3 conditions, the AMG Evos® xl core digital microscope was used for examining *Y. pestis* biofilms on *C. elegans*. For detection of the bacteria within the biofilm, *Y. pseudotuberculosis* YPIII strains were transformed with p*xyl*Ap, a plasmid containing the gene encoding green fluorescent protein (GFP) (see Table 2.2).

2.4.8.2 Confocal Microscopy

Confocal microscopy was undertaken using both a Zeiss LSM700 confocal microscope (for chitin assays) and a Zeiss Elyra PS.1 super resolution microscope (louse assays). Images were analysed using Zen software (Karl Zeiss AG). Insects were fed GFP labelled *Y. pseudotuberculosis*, with the

addition of 1 µl rhodamine-labelled wheat germ agglutinin (WGA) (Vector Laboratories) per 1 ml of blood. Insects were imaged using 100-fold magnification. To quantify the fluorescence emitted by *Y. pseudotuberculosis* in *P. corporis*, louse images were processed using the software Volocity 6.3 (PerkinElmer Inc.).

2.4.8.3 Scanning Electron Microscopy

All scanning electron microscopy (SEM) work was done with the help of Kathryn Thomas, from the Department of Engineering, University of Nottingham. Samples were prepared using methodology adapted from Horisberger & Rosset (1977). Chitin coverslips were washed with 100 µl PBS before being fixed with 3% glutaraldehyde for 30 min, washed three times with 1 ml 0.1 M cacodylate buffer and stored in 1 ml cacodylate buffer. The samples were then post-fixed with 1 ml of 10 g.l-1 osmium tetroxide in 0.1 M cacodylate buffer for 30 min, then dehydrated in ethanol in ascending concentrations (50%, 70%, 90% then 100% ethanol). Each concentration was used twice successively for 10 min before moving on to the next concentration, in 1 ml volumes. A final wash of 1 ml of 100% ethanol was left on for 10 min before the samples were treated twice with 1 ml hexamethyldisilazine for 5 min. The samples were mounted on aluminium stubs and coated with gold-palladium in a sputter coater (K550; Emitech, East Grinsted, UK). The samples were viewed at 30 kV accelerating voltage in a JEOL JSM-6060LV scanning electron microscope (JEOL, Tokyo, Japan) at several magnifications.

2.5 Containment Level 3 Methods

2.5.1 General Safety Principles

Special measures and protocols were adopted for Containment Level 3 (CL3) work, due to the high risk of infection with *Y. pestis*. Comprehensive training, was necessary before being signed off as competent to work in the CL3 laboratory. All work at CL3 level was undertaken in a Class I MSC. All *Y. pestis* cultures were always double contained when outside of the MSC (e.g. on a taped petri dish within a modified carry case). Protocols from the CL2 were adapted for the CL3, which included different disposal methods and mandatory cleaning steps with 2% Distel (Star Lab Group) of equipment, plates, tubes and gloves. All items and the MSC itself were cleaned with liberal amounts of 2% Distel and left for 3 min before being removed.

A gown style lab coat was worn, then a pair of CL3 standard gloves, then oversleeves and then a second pair of gloves when in the MSC. To minimise the risk of spills and exposure a maximum volume of 20 ml liquid culture was used. To minimise aerosol formation, before putting cultures in the centrifuge or heat block, all tubes and pipettes were wiped down with 2% Distel and left for 3 min. All waste from the MSC was disposed of in sweetie jars (Sigma Aldrich). All waste-filled sweetie jars, lab and lobby waste went through the autoclave in the CL3 suite before being removed and autoclaved again *via* the general waste route.

3 The Use of Artificial Feeding Systems for the Maintenance of the Oriental Rat Flea *Xenopsylla cheopis* and the Human Body Louse *Pediculus (humanus) corporis*

3.1 Introduction

The breeding of haematophagous insects has provided an extra challenge over insects that do not feed on blood. Finding a suitable captive animal host can prove difficult, especially when the insect is host specific. Most historical colonies were set up using mammals such as mice or rabbits as blood sources and many research groups still use these systems. Animal welfare issues, rearing and maintenance costs make establishing new colonies using an artificial method of feeding insects an attractive prospect.

Many groups have utilised various artificial systems to carry out insect infection experiments and most of these rely on equipment that heats blood to 'body' temperature (Georgi and Wade, 1989; Takano-Lee, Velten, *et al.*, 2003; Mumcuoglu *et al.*, 2011; Bland and Hinnebusch, 2016). The blood must be either pumped through the system or prevented from clotting *via* defibrination or the addition of anticoagulants. Commercial systems such as Hemotek® are available which consist of a power unit with 'feeding arms', into which can be screwed temperature-adjustable meal reservoirs. Blood is placed in a reservoir, covered with a membrane and placed into the insect enclosure. This has proved extremely successful for the maintenance of certain insects, such as mosquitoes and bed bugs for some groups, including the London School of Hygiene and Tropical Medicine and the Pirbright Institute (Cheryl Whitehorn and Adrian Zagrajek, personal communications), as well as experimentally for insects including lice, fleas and mosquitoes (Luo, 2014; Bland and Hinnebusch, 2016; Sangaré *et al.*, 2016).

Problems can arise when weaning insects off laboratory hosts and on to artificial systems as ideally this should be introduced over time to minimise shock to the insects but requires the two systems to be run concurrently for long periods (Florent Sebbane, Institut Pasteur, Lille, France and Cheryl Whitehorn, LSHTM, London, UK, personal communications).

Further complications arise when experiments involve CL3 organisms such as *Y. pestis* as working with large mammals in such high containment laboratories presents a major challenge. Transmission and pathology studies have used rabbits, guinea pigs and mice as models, although some groups circumnavigate the CL3 requirement by using attenuated *Y. pestis* strains that can be employed under CL2 conditions (Qi *et al.*, 2010).

3.1.1 Current Colonies of *X. cheopis*

Flea colonies are used for research on the transmission of flea-borne diseases such as plague, murine typhus and tapeworms, as well as for testing pesticides. Colonies of *X. cheopis* are currently maintained in the USA and also the Institut Pasteur in Lille, France. Although both groups have attempted artificial feeding systems for experimental purposes, they maintain their colonies using blood obtained *via* the exsanguination of neonatal mice (Florent Sebbane, Institut Pasteur, Lille, France, personal communication).

Since flea colonies are being maintained on animals, there is little literature regarding artificially administered blood types (Kernif *et al.*, 2015; Bland and Hinnebusch, 2016). Although fleas have an indirect lifecycle, feeding on a number of mammalian hosts, *X. cheopis* are primarily rat parasites and

therefore rat blood is likely to be the preferred option. Despite the commercial availability of animal-reared fleas, artificial systems appear to be more difficult to maintain and no published evidence was found of any groups attempting to artificially maintain colonies of *X. cheopis* or other flea species (Kernif *et al.* 2015, Florent Sebbane, Institut Pasteur, Lille, France, personal communicaton).

3.1.2 Current Colonies of *P. corporis*

Both body and head lice have been extensively investigated for their roles in disease transmission and for insecticide susceptibility studies. Animal-fed *Pediculus* spp. colonies, including Mumcuoglu's laboratory in Israel (which no longer maintains this colony) (Mumcuoglu *et al.*, 2011) and the current colony at the Umweltbundesamt (Federal Environment Agency) in Berlin, Germany, have fed or currently feed their lice on live rabbits. Artificial feeding systems involving reservoirs and processed blood have been successfully used (Georgi, 1996; Takano-Lee, Yoon, *et al.*, 2003), however, these systems appear to have been used for experimental feeding, rather than colony maintenance.

As lice naturally feed up to five times a day (Bonilla *et al.*, 2009), modifications to their lifecycle are likely to be necessary when feeding in a laboratory setting. Human lice are extremely susceptible to starvation compared to other haematophagous insects (Waniek, 2009) and Takano-Lee (2003) suggested that when reared *in vitro*, approximately 50% of the population dies within 20–35 h of feeding. As lice spend their entire life cycles close to or on their natural

hosts, mimicking their living conditions artificially is also likely to be more difficult than for fleas, especially for eggs and newly hatched insects.

Like fleas, louse colonies have traditionally been maintained on live animals, such that much of the information available on blood types for use in artificial feeding systems is experimental. Due to the direct lifecycle of *Pediculus* spp., living only on their natural human host, human blood is by far the most commonly used. There is a debate as to whether antibiotics should be added, with some groups suggesting that they stop blood degrading and have no adverse effects on the lice (Takano-Lee, Velten, *et al.*, 2003), whereas others suggest that certain antibiotics (as well as certain anticoagulants) can be fatal (Kosta Mumcuoglu, Hebrew University of Jerusalem, Israel, personal communication). It appears to be difficult to maintain *P. corporis* long term (as reviewed by Cole 1966) and it appears that globally there are no artificially reared colonies.

3.2 Specific Research Aims

Although artificial feeding systems have been used for experimental purposes, the lack of colonies sustainably maintained using such systems for both *X. cheopis* and *P. corporis* suggest that this is not a simple task, but the need to reduce the use of experimental animals, plus the impracticality and health and safety requirements of taking mammals into a CL3 lab for experimental *Y. pestis* research make the development of an artificially fed colony maintenance system highly desirable.

There are multiple possibilities for blood types, including commercially available sheep and rabbit defibrinated blood, as well as human ex-blood bank stocks. Utilising fresh blood from human donors is also an option, especially for *P. corporis*. Equally, there are many feeding membrane options available, including a mouse skin method for *X. cheopis* research group in Lille (Florent Sebbane, Institut Pasteur, Lille, France, personal communication), Parafilm M used by the LSHTM (Cheryl Whitehorn, LSHTM, UK, personal communication) and Pirbright Institute (Adrian Zagrajek, Pirbright Institute, UK, personal communication) and a collagen membrane produced by Hemotek.

This chapter aims to ascertain for artificially maintained colonies of *X. cheopis* and *P. corporis* the most appropriate:

- Housing conditions, including optimum humidity and temperature
- Equipment for establishing an artificial feeding system
- Blood type and processing method for optimal insect survival and fecundity
- Membrane through which insects can feed successfully

3.3 Results

3.3.1 Artificially Fed *X. cheopis* Colonies

A thorough literature review of flea maintenance was conducted and a survey of groups who currently or in the past had maintained colonies of *X. cheopis* or other flea species. The results of this survey are outlined in Table 3.1.

Table 3.1. Literature review of *X. cheopis* colony conditions. The majority of research using artificial membrane feeding systems is short term for experimental purposes, rather than for long term colony maintenance.

Reference	Florent Sebbane	Hinnebusch (2002)	Hudson (1958)	Krishnamurthy (1966)	Kernif (2015)	Bland (2016)
Flea pre-study conditions	Neonatal mice fed	Neonatal mouse fed	Kept in large cages with cats and dogs and allowed to feed	From an established colony or a trapped rat	Artificially fed *Ctenocephalides felis felis*	*C. felis felis* (feeds more often than *X. cheopis*)
Temperature	22ºC	20-25°C	26.6ºC	24-28ºC	No information	25ºC
Humidity	75%	75%	80%	65–75%	No information	75%
Light/dark cycle	Photophobic	No information	No information	Eggs kept in the dark	No information	No information
Storage	Glass gallon jars	Glass gallon jars	No information	Breeding cages 45 cm x 30 cm x 40 cm deep	No information	High walled container

Reference	Florent Sebbane	Hinnebusch (2002)	Hudson (1958)	Krishnamurthy (1966)	Kernif (2015)	Bland (2016)
Bedding	See Hinnebusch (2002)	3:1 autoclaved sawdust to larvae food	100 parts sawdust, 2-5 parts larval food	Sterile sand and wood shavings; depth of 1.5 cm	No information	No information
Egg culturing	No information	No information	No information	Hatched in test tubes and pupae sieved	28°C and 70% humidity. Kept in plastic beakers with mesh	No information
Feeding system	Neonatal mice	Neonatal mice	Cat or dog in a cage	Albino rats	‘Artificial dog machine' (Wade and Georgi 1988)	Hemotek
Feeding frequency	Tuesdays and Thursdays. Starve fleas for 5 days, for a 95% feed rate	Twice a week (Monday and Thursday)	Possibly every day	No information	Inconclusive	Monday-Friday for 8 h

Reference	Florent Sebbane	Hinnebusch (2002)	Hudson (1958)	Krishnamurthy (1966)	Kernif (2015)	Bland (2016)
Feeding length	Takes about 20-30 min	1 h	No information	No information	No information	8 h per day
Feeding incentives	n/a	n/a	n/a	n/a	No information	Sterile gauze fitted over to aid attachment and feeding
Membrane	n/a	n/a	n/a	n/a	Parafilm M	Parafilm M
Blood amount	n/a	n/a	n/a	n/a	No information	Sterile gauze fitted over the membrane to aid attachment
Blood type	Neonatal mouse	Neonatal mouse	Canine/feline	Rat	Citrated porcine blood	Sterile defibrinated sheep blood

Reference	Florent Sebbane	Hinnebusch (2002)	Hudson (1958)	Krishnamurthy (1966)	Kernif (2015)	Bland (2016)
Blood feeding temperature	36.9ºC (animal body temperature)	Animal body temperature	Animal body temperature	Animal body temperature	A temperature differential of 10ºC between fleas and blood	37ºC
Blood storage temperature	n/a	n/a	n/a	n/a	4°C	No information
Blood storage length	n/a	n/a	n/a	n/a	Up to 3 weeks	No information

From this information, and taking into account the equipment available, the most appropriate conditions are outlined in Table 3.2. An *X. cheopis* colony was obtained from Dr Florent Sebbane (Institut Pasteur, Lille, France). Briefly, fleas were kept in a glass jar with a layer of bedding. The temperature in the incubator was maintained at 24ºC, humidity at 75%. To feed, the Hemotek arm was either placed into the main colony jar or a number of fleas were fed within a large glass test tube.

Table 3.2. Proposed optimal conditions for maintaining an artificially fed *X. cheopis* colony.

Condition	Best option(s)	Reasoning
Temperature	24ºC	Approximately the median temperature used by those consulted
Humidity	75%	Most common humidity described in the literature
Light/dark cycle	Dark (low light required)	Fleas are photophobic
Storage	Glass vases, 40 cm tall	*X. cheopis* jump to an average height of 7 cm. Maximum recorded 9 cm (Rothschild *et al.* 1973)
Bedding	3 parts autoclaved sawdust to 1 part larvae food (equal parts dried blood, mouse chow and dried skimmed milk)	As for original colony
Egg culturing	Within the colony	As for original colony

Condition	Best option(s)	Reasoning
Feeding system	Hemotek, start with mouse skins and human defibrinated blood	Simpler than the ‘thistle’ does not require assembling
Feeding frequency	Every day initially	More feeding attempts should increase success
Feeding length	A few hours	Long enough to feed, membrane will dry out over time
Membrane	Mouse skin, Parafilm M and collagen membranes to be tested	Original colony successful with mouse skins, collagen easier to maintain, Parafilm M is an alternative
Blood amount	1 ml in meal reservoir	3 ml reservoir wastes blood
Blood type	Defibrinated human, rabbit or sheep	Rabbit and sheep blood are commercially available, humans are also natural hosts of *X. cheopis*
Blood feeding temperature	37ºC (host body temperature)	Attempt to make situation as realistic as possible
Blood storage temperature	4ºC	Freeze-thawing degrades blood, room temperature may allow bacterial/fungal growth
Blood storage length	One week	Ethical stipulation

3.3.1.1 Condensation Influences Meal Reservoir and Insect Housing Orientation

As fleas are naturally opaquer than lice, this made it harder to differentiate between fed and non-fed individuals, as shown in Figure 3.1, However, peristaltic movement of the digestive system of recently fed fleas could be observed, which helped fed individuals.

A  B 

Figure 3.1. Comparison of a non-fed and fed *X. cheopis*. (A) a non-fed male *X. cheopis* with a small, dark gut containing blood from an older blood meal. (B) a recently fed female *X. cheopis*, with a full abdomen and bright red liquid blood meal.

The length of feeding depends on the membrane used, if less than 20 min the fleas will not have enough time to feed effectively. More than 1 h and the membrane (especially the collagen membrane) dehydrated and a gap between the membrane and mesh resulted such that the insects could not access the blood.

Feeding was attempted both by placing the feeding arm and meal reservoir into the flea colony vase and also by placing a number of individuals into a large glass test tube and placing the meal reservoir at one end, with feeding permitted through a mesh. When fed within the flea vase, it was impossible to

count positive feeders, which made it difficult to assess success rates. Feeding individuals were countable with the test tube method, but condensation was an issue. When the entire colony was fed using the Hemotek, they preferred the collagen membrane to the mouse skin or Parafilm M.

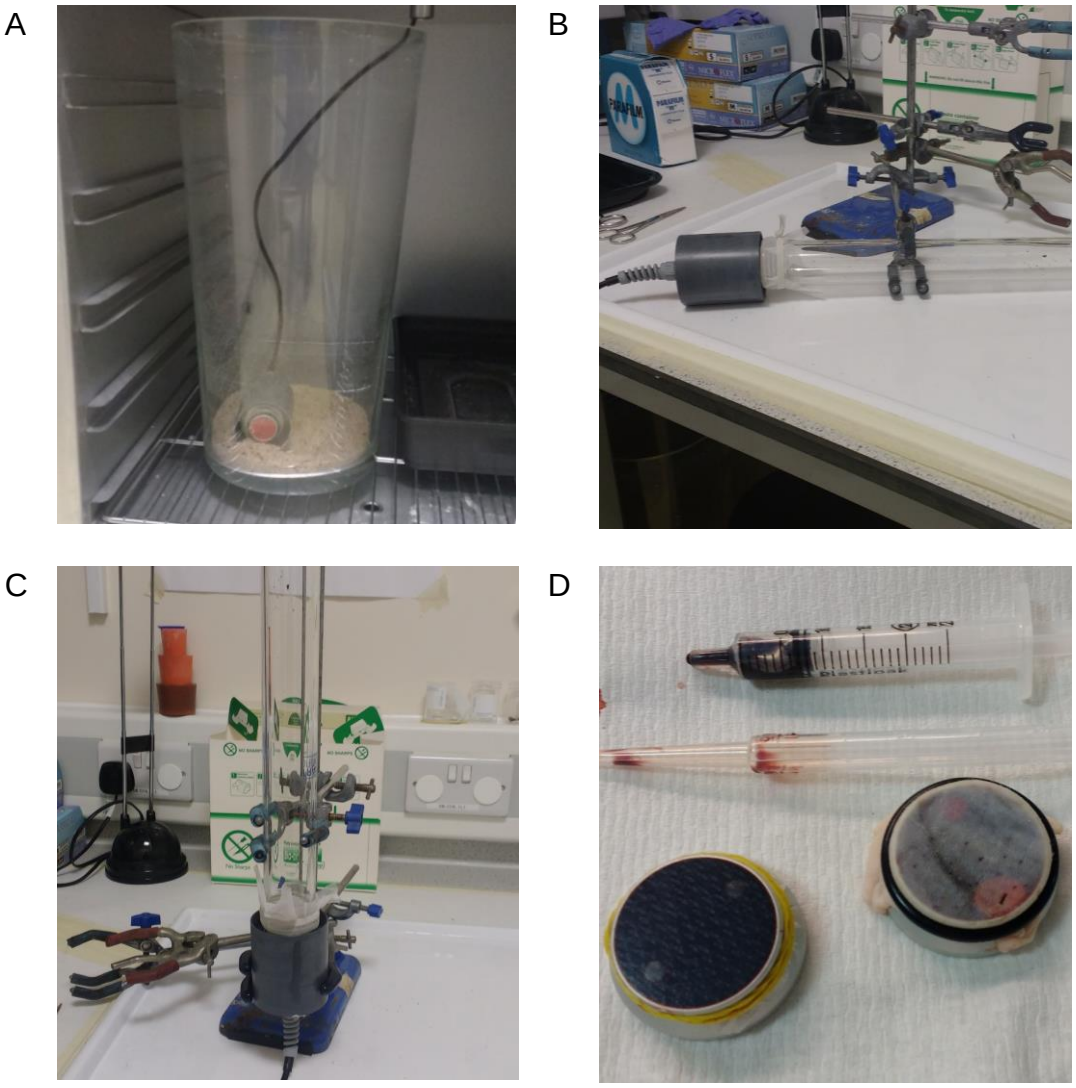

Figure 3.2. A-D illustrate the different feeding configurations for *X. cheopis*. (A) meal reservoir placed into the colony vase. (B) feeding test tube placed side-on to the meal reservoir. (C) feeding test tube placed above the meal reservoir. (D) collagen (left) and a mouse skin (right) membrane fitted over a meal reservoir.

When fed within the main colony vase, the position of the meal reservoir could not easily be changed, however, it was possible to try different orientations in

the test tube, using a clamp stand, as shown in Figure 3.2. When the test tube was placed on top of the meal reservoir, it allowed better access, but condensation was a problem. If the tube was placed sideways, next to the meal reservoir, there was less condensation, but the fleas did not move towards the membrane. When the meal reservoir was placed on top of the test tube, fleas could not reach it, thus this set-up was not tested.

3.3.1.1.1 Human Blood Provided the Greatest Feeding Success Rate for *X. cheopis*

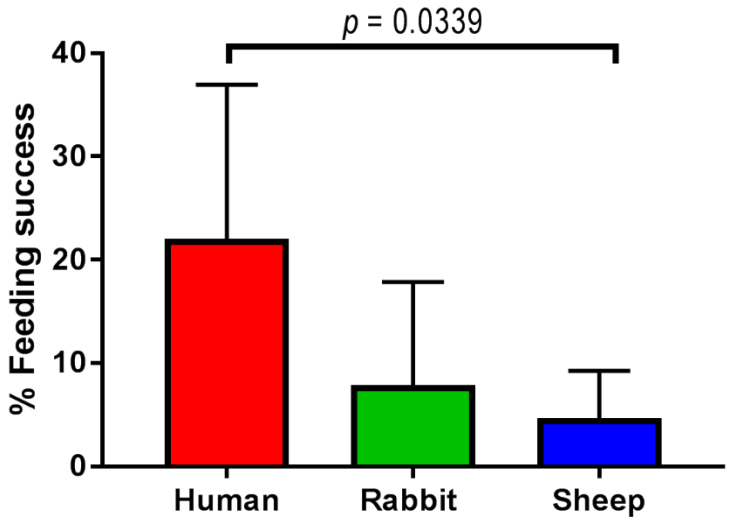

Figure 3.3. Impact of blood types on *X. cheopis* feeding success rates. The sample size for each was n=20, *P*-values were calculated using one-way ANOVA and Tukey's multiple comparison test.

Three different types of defibrinated blood were tested; human, rabbit and sheep. Although rats are the main host of *X. cheopis*, rat blood was prohibitively expensive for long term colony maintenance, so was not tested. None of the blood types tested produced particularly good feeding success

rates, although human blood generated a twofold increase in feeding rate compared with rabbit and sheep blood, as shown in Figure 3.3. All blood types tested had a variable feeding success rate, as often no fleas would feed at all. It was therefore difficult to determine reproducibly the impact of blood type on flea survival.

3.3.1.1.2 Feeding Membrane Type Did Not Influence *X. cheopis* Feeding Success Rates

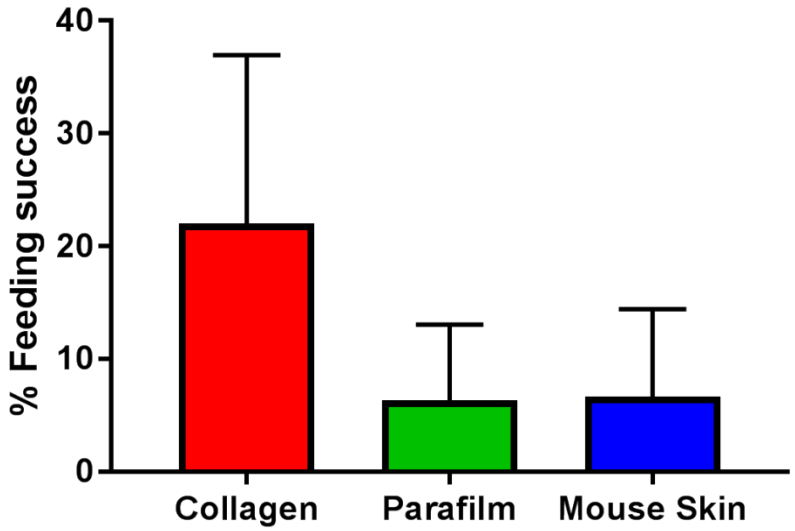

Figure 3.4. The effect of membrane types on *X. cheopis* feeding success rates. The sample size for each was n=20, *P*-values were calculated using one-way ANOVA and Tukey's multiple comparison test, no significant differences were found.

Each of the membranes tested had benefits and limitations. Despite contrary reports from Dr Sebbane (Institut Pasteur, Lille, France), the fleas preferred the collagen membrane, as shown in Figure 3.4. It was difficult to get the fleas to feed consistently, consequently many feeding attempts scored zero. The collagen membrane did not yield significantly higher feeding success rates

compared with the mouse skin or Parafilm M, most likely due to the unreliable feeding behaviour of the fleas. However, fleas appeared to prefer it, as they spent less time probing it before commencing feeding, compared with Parafilm M or mouse skin membranes (Figure 3.5).

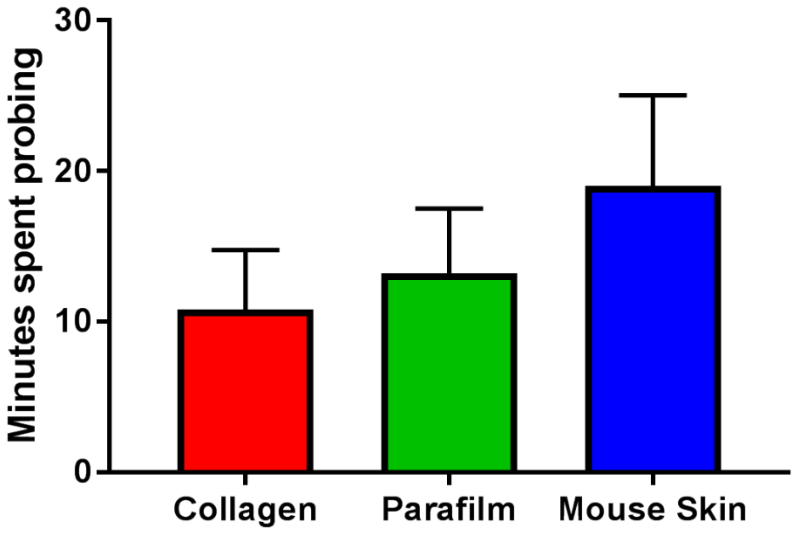

Figure 3.5 Minutes *X. cheopis* spent probing each membrane before feeding. Despite being the most 'natural' the mouse skin required the most probing. The sample size for each was n=5, *P*-values were calculated using one-way ANOVA and Tukey's multiple comparison test, no significant differences were found.

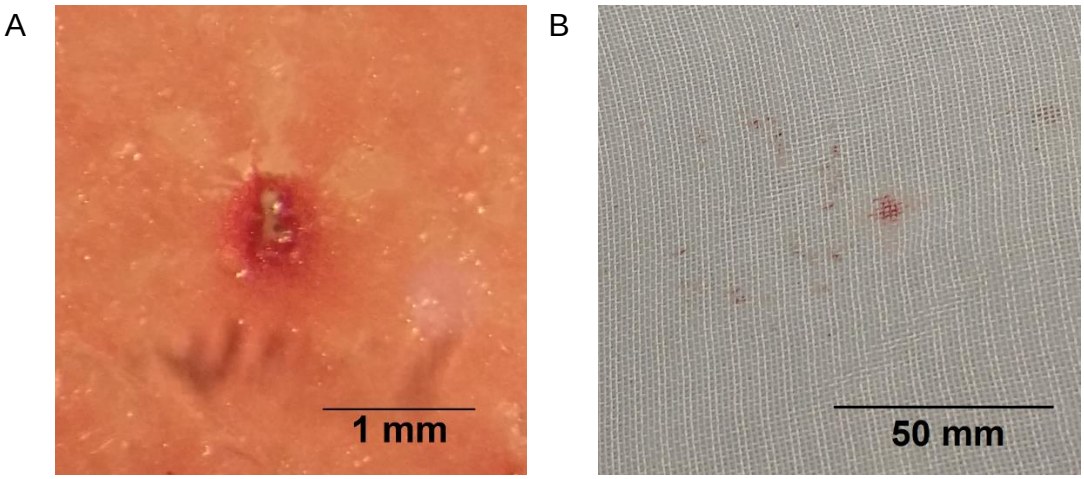

Figure 3.6. Evidence of flea feeding. (A) Flea stylet piercing holes on a collagen membrane, 10x Nikon dissecting microscope (B) blood spots on a mesh sheet that covered a feeding membrane, indicating insect feeding.

Feeding through the collagen membrane did not appear to be a mechanical issue; when the membrane was examined under the Nikon dissecting microscope, small probing holes could be seen pierced through it. The mesh that covered it also had small blood spots, indicating that the membrane had been pierced (Figure 3.6).

3.3.2 Artificially Fed *P. corporis* Colonies

An extensive literature review was conducted, as well as personal communications with groups who currently held, or who had previously held colonies in the past. This information was compiled as Table 3.3.

Table 3.3. Literature review of colony maintenance conditions for *P. corporis*. The majority of research using artificial membrane feeding systems are experimental, rather than for long term colony maintenance.

Conditions	Carola Kuhn	Habedank (1999)	Takano-Lee (2003)	Takano-Lee (2003)	Yoon (2006)	Schrader (2008)	Mumcuoglu (2011)
Louse pre-study conditions	Rabbit-adapted *P. humanus*	Rabbit-adapted *P. humanus*	Rabbit-adapted *P. humanus*	Human-fed strains of *P. capitis*	Human-fed strains of *P. capitis*	Rabbit-adapted *P. humanus*	Rabbit-adapted *P. humanus*
Temperature (feed day)	32°C	31°C	30-31°C	No information	No information	32°C	30±1°C
Temperature (non-feed day)	25°C	19-22ºC	No information	No information	No information	25°C	30±1°C
Humidity (feed day)	70%	70%	60–75%	No information	No information	45–55%	60–70% (Cole 1966)
Humidity (non-feed day)	70%	70–80%	No information	No information	No information	45–55%	60–70%
Light/dark cycle	No information	Darkness	No information	No information	No information	No information	No information

Conditions	Carola Kuhn	Habedank (1999)	Takano-Lee (2003)	Takano-Lee (2003)	Yoon (2006)	Schrader (2008)	Mumcuoglu (2011)
Storage	Petri dishes within an incubator	No information	No information	No information	No information	Glass petri dishes (closed but not sealed)	No information
Bedding	5 x 5 cm cotton corduroy cloth	No information	Folded piece of black felt	No information	No information	5 x 5 cm cotton corduroy cloth	No information
Egg culturing	No information	No information	60–70% relative humidity	No information	31±1°C, 70–80%	Eggs incubated at 32°C until hatched	No information
Feeding system	Rabbit fed	Glass dish/ membrane/ glass ring on a hot plate	Automatic feeding system	Magnetic stirred vessel system	Magnetic stirred vessel system	Rabbit fed	Glass feeding 'thistle', maintained on rabbits

Conditions	Carola Kuhn	Habedank (1999)	Takano-Lee (2003)	Takano-Lee (2003)	Yoon (2006)	Schrader (2008)	Mumcuoglu (2011)
Feeding frequency	Fed Monday, Tuesday, Wednesday and Friday	Fed each weekday	Continuous for 7 days and then cleaned	No information	No information provided	4-5 times per week	4 times a week
Feeding length	Removed after 30 min	60-90 min. Seen to finish feeding after 15-30 mins	Continuous	No information	No information	15 min	30 min
Feeding incentives	n/a	Thermotaxis was enough to induce feeding	Hair tufts	Hair tufts	200-300 hair strands, 23 mm in length	No information	Bundle of hairs to
Membrane	n/a	Parafilm M	Nescofilm-silicone sandwich	Silicone-reinforced Parafilm M layer (around 13 µm thick)	Silicone-reinforced Parafilm M membrane	No information	5 x 5 cm Parafilm M membrane

Conditions	Carola Kuhn	Habedank (1999)	Takano-Lee (2003)	Takano-Lee (2003)	Yoon (2006)	Schrader (2008)	Mumcuoglu (2011)
Blood amount	n/a	2-3 ml	Continuous	1 ml	No information	No information	2 ml
Blood type	Rabbit	Preserved human blood - expired blood donations	A+ Plasma and RBCs (treated with penicillin and streptomycin)	Human ex-blood bank. Treated with antibiotics	A+ Plasma and RBCs (treated with penicillin and streptomycin)	No information	Different human blood types
Blood feeding temperature	Mammalian body temperature	38°C	No information	30°C	No information	No information	37±1°C
Blood storage temperature	n/a	4°C or 27°C	Blood 2 - 4°C, plasma -20°C	Blood 2-4°C, plasma -20°C	No information	No information	4-5°C

Conditions	Carola Kuhn	Habedank (1999)	Takano-Lee (2003)	Takano-Lee (2003)	Yoon (2006)	Schrader (2008)	Mumcuoglu (2011)
Blood storage	n/a	As fresh as possible. After 14 days larvae fed as well, but not adults	No information	Up to 8 weeks	No information	No information	Diminished over 26 weeks. Would not feed at 26 weeks

Based on this information, the best conditions for our colony and thus the first attempted conditions were as follows in Table 3.4. Three *P. corporis* colonies were obtained from Dr Carola Kuhn (Umweltbundesamt, Federal Environment Agency, Berlin, Germany). Briefly, lice were kept in modified Sterilin pots within an incubator at 32ºC and 70% humidity. To feed, the Hemotek was either placed on top of the louse housing pots, or individual lice were picked onto a meal reservoir surrounded by a cardboard collar.

Table 3.4. Proposed optimum conditions for artificially reared *P. corporis* colony maintenance.

Conditions	Best conditions	Reasoning
Temperature (feed day)	32°C	Most common temperature cited in the literature, same as original colony conditions
Temperature (non-feed day)	25°C	Don't want to slow them too much, but need to stop metabolising their meals too quickly, same as original colony conditions
Humidity (feed day)	70%	Most common humidity used in the literature, original colony conditions
Humidity (non-feed day)	70%	Most common humidity used in the literature, original colony conditions
Light/dark cycle	Darkness (dim light when feeding)	Lice are photophobic
Storage	Modified Sterilin sample pots	Visible colony, good ventilation
Bedding	Cloth	Original colony conditions

Conditions	Best conditions	Reasoning
Egg culturing	Remaining at feeding temperature/ humidity	Original colony conditions
Feeding system	Hemotek meal reservoirs	Easier than the ‘thistle’, does not require assembling
Feeding frequency	Daily to begin with. Up to 5/week	Need to optimise feeding, but then reduce as very labour/resource intensive
Feeding length	An hour	Require potentially up to 30 min to feed, don’t want the membrane to dry out
Feeding incentives	Hair tufts	Attempt to make situation as realistic as possible
Membrane	Test collagen, Parafilm M and mouse skin membranes	Collagen membranes are easier to maintain, mouse skins and Parafilm M have been used successfully in other groups
Blood amount	1 ml	3 ml meal reservoirs waste blood
Blood type	Defibrinated human and rabbit blood	Lice are human parasites, but the original colony was fed on rabbits. Sheep blood is also commercially available
Blood feeding temperature	37°C (host body temperature)	The same temperature as host
Blood storage temperature	4°C	Freeze-thawing degrades blood, room temperature may allow bacterial/fungal growth
Blood storage length	Short as possible, no more than one week	Ethical approval

3.3.2.1 A High Humidity is Vital to Maintain Artificially Reared *P. corporis*

Lice were kept at 32ºC on days when they were to be fed or otherwise at 25ºC (*e.g*. over weekends) with a minimum humidity of 75%. Keeping lice at 32ºC without feeding caused dehydration and death. However, constant maintenance at 25ºC meant that they didn't feed as well, as at this temperature they go into hibernation mode.

3.3.2.2 *P. corporis* Feeding Success is Affected by Multiple Feeding Conditions

Figure 3.7. Image of *P. corporis* successfully feeding on the Hemotek collagen membrane. Note the swollen, red abdomen containing the new blood meal.

Figure 3.7 shows a louse successfully feeding on the Hemotek collagen membrane. Figure 3.8 shows the difference between a louse that has not recently fed and one that has. The large, red, swollen gut as seen in Figure 3.8(B) is characteristic of a recently fed louse with a fresh blood meal, compared to the gut of a louse that has not fed within 24 hours (Figure 3.8(A)), which is much smaller in comparison with the overall abdomen size, and much darker, due to the old, digested blood. Peristaltic movement of the digestive systems of lice during and directly after feeding could be observed. Identifying fed lice was much easier than for fleas, as they could be observed under a microscope without chilling to immobilise and they are less opaque, allowing the blood meal and peristalsis to be observed, even without the use of a microscope.

A

B

Figure 3.8. Comparison of a non-fed and fed *P. corporis*. (A) a non-fed *P. corporis* with a small, dark gut containing blood from a previous blood meal. (B) a recently fed *P. corporis*, with a full, red blood meal.

The optimal feeding time was approximately 1 h; less than 20 min, and the lice were unable to probe and feed in time. If they were left for more than 1 h the membrane dehydrated and the insects could not feed through it. This was most pronounced with the collagen membrane. It was easier to feed the lice within a cardboard tube rather than a plastic pot, as there was much less condensation.

The position of the meal reservoir in relation to the feeding house was also investigated, as shown in Figure 3.9. Placing the feeding house on top of the meal reservoir allowed better access, although condensation was an issue with the plastic pots, but not the cardboard tubes.

Placing the feeding house underneath or alongside the meal reservoir required a bridge for the lice to climb. Corduroy squares and human hair bundles were evaluated but neither was as effective as locating the feeding house on top of the meal reservoir. The feeding success rate also appeared to be higher for adult and 3rd instar lice; this may have been purely mechanical, as younger insects have smaller mouthparts and may have been unable to pierce the membrane. 1st instar lice were too difficult to track when not contained but did not appear to feed through any of the membranes.

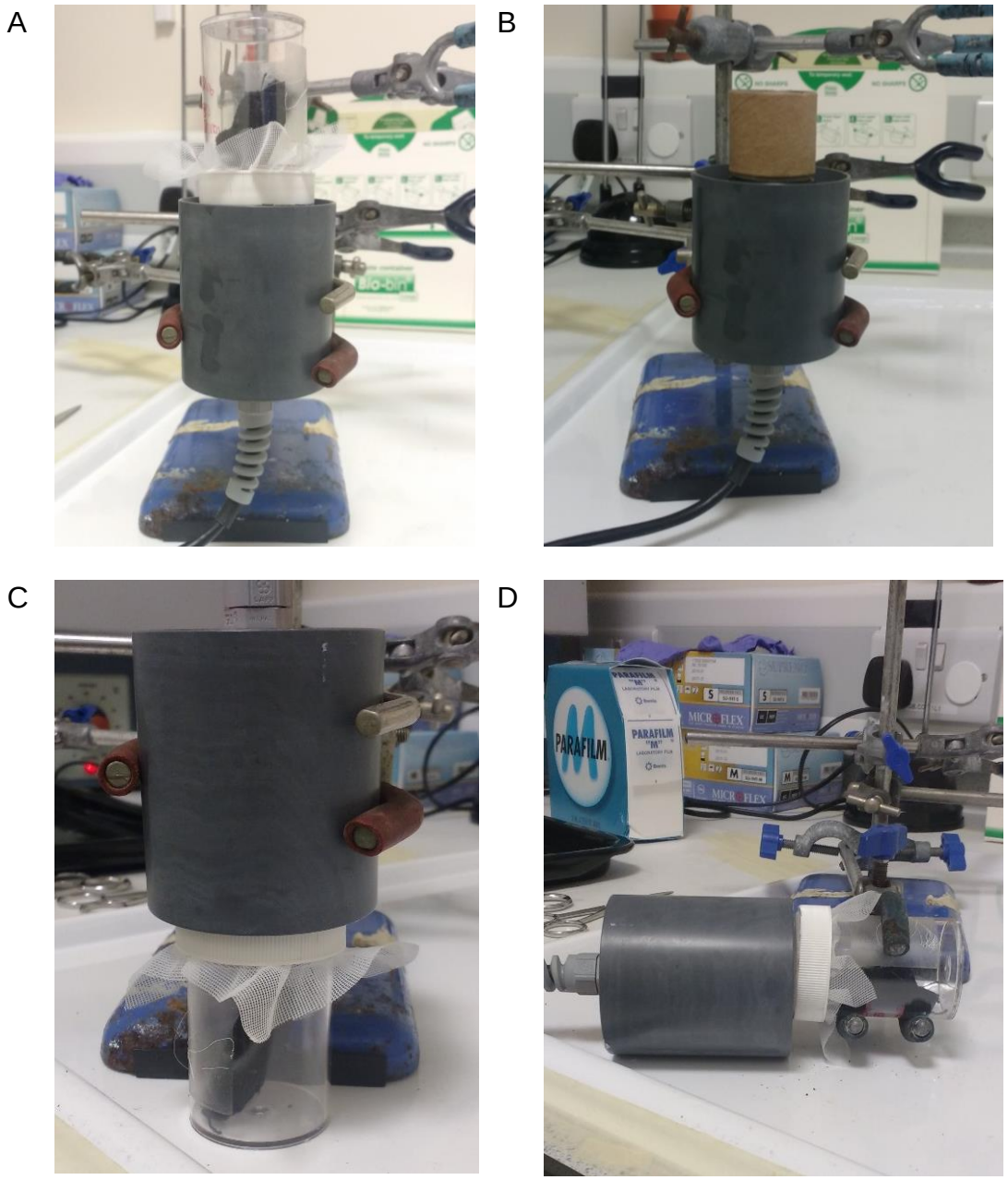

Figure 3.9. (A-D) Lice feeding positions and incentives. (A) Plastic feeding house placed above the meal reservoir. (B) Cardboard feeding house placed above the meal reservoir. This orientation was the most effective way of feeding *P. corporis*. (C) Feeding house placed below the meal reservoir and (D) Feeding house alongside the meal reservoir.

3.3.2.2.1 Human Blood is Preferred when Maintaining *P. corporis* Colonies Artificially

Three different defibrinated blood types were tested for *P. corporis*; sheep, rabbit and human. All were tested using the collagen membrane. Although there were no significant differences in feeding success rates when analysed using one-way ANOVA and Tukey's multiple comparison test, the lice feeding success rate was highest when fed on human blood, (Figure 3.10), despite the original colony being fed on live rabbits. Rabbit blood was expensive and was subsequently found to contain streptomycin sulphate (0.09%), penicillin G (0.04%) and neomycin trisulphate (0.10%), which may affect the lifespan of the lice fed on it. Sheep blood (SLS), contained no antibiotics and was considerably more cost effective, but did not provide a comparable feeding rate to human blood, as sheep are not a natural host for *P. corporis*.

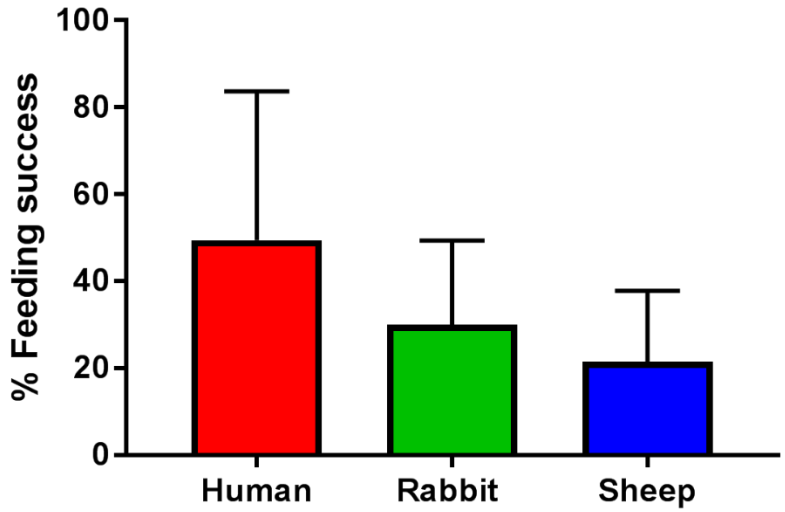

Figure 3.10. Effect of different blood types on *P. corporis* feeding success rates. The sample size for each was n=20, *P*-values were calculated using one-way ANOVA and Tukey's multiple comparison test. No significant differences were found.

Although feeding success rates showed no significant differences between blood types, the survival rate of *P. corporis* was affected by blood type. Rabbit blood negatively affected the survival rate of the lice, whilst sheep and human were comparable with each other. Only around 20% of lice fed rabbit blood were still alive 2 days post-feeding, compared with human and sheep blood, which were both around 75% survival by day 2. All lice fed rabbit blood died by 3 days post-feeding, compared with 6 days post-feeding for those fed sheep blood and 7 days post feed for those fed human blood (Figure 3.11).

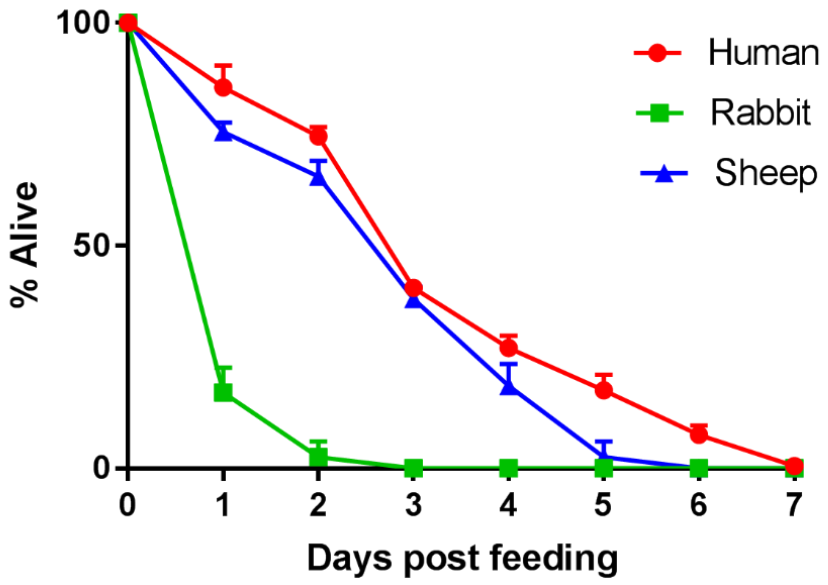

Figure 3.11. *P. corporis* survival rates with different blood types. n=20.

With all three blood types, a small percentage of the fed lice turned bright red and died very quickly, which Houhamdi (2002) suggests is a result of louse gut epithelial cell rupture and blood meal erythrocytes spreading into the haemolymph (Figure 3.12).

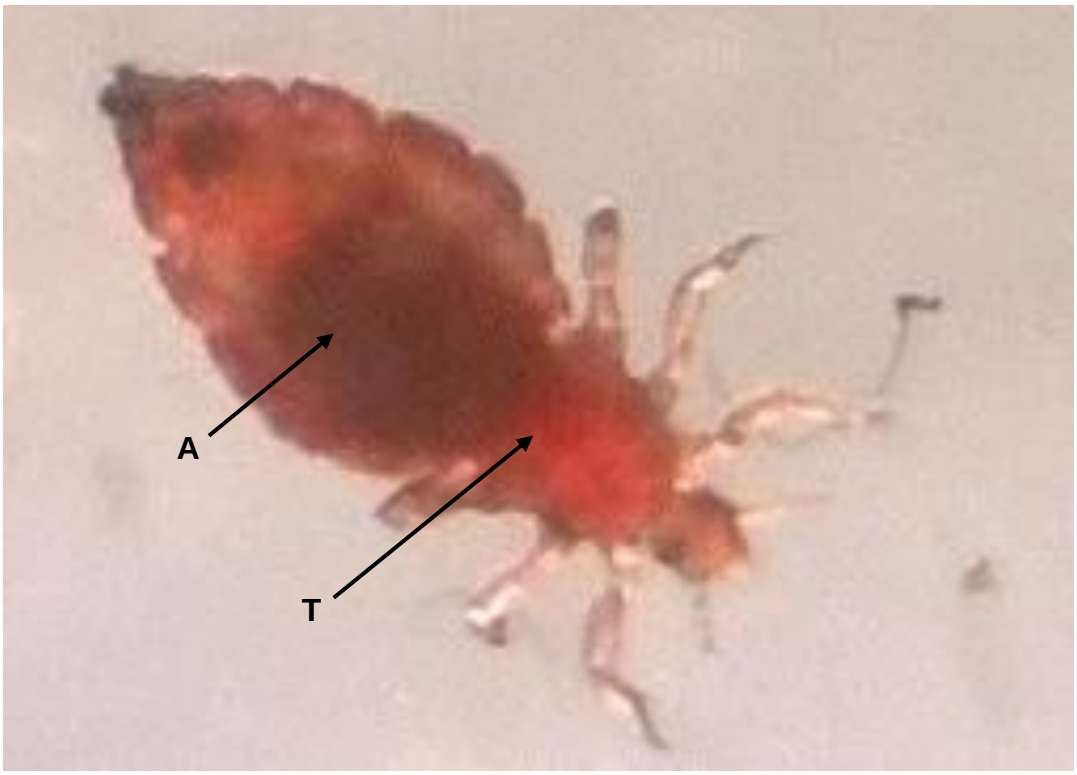

Figure 3.12. An example of *P. corporis* haemolytic epithelial cell rupture. Note the red colouration across the entire abdomen (A) and thorax (T), as well as in the legs.

3.3.2.2.2 Collagen Membranes Produce the Highest Feeding Rates when Artificially Feeding *P. corporis*

Parafilm M, collagen and mouse skin membranes were all tested using human defibrinated blood. Again, highly variable feeding rates were observed for all three, however the collagen membrane was preferred by the lice (Figure 3.13). On the collagen membrane, *P. corporis* settled more readily and spent less time probing, whereas insects on the Parafilm M and mouse skin membranes spent much longer walking around, sometimes not settling at all (Figure 3.14). Feeding on the Parafilm M membrane was negligible, and no louse was observed to feed through the mouse skin membrane.

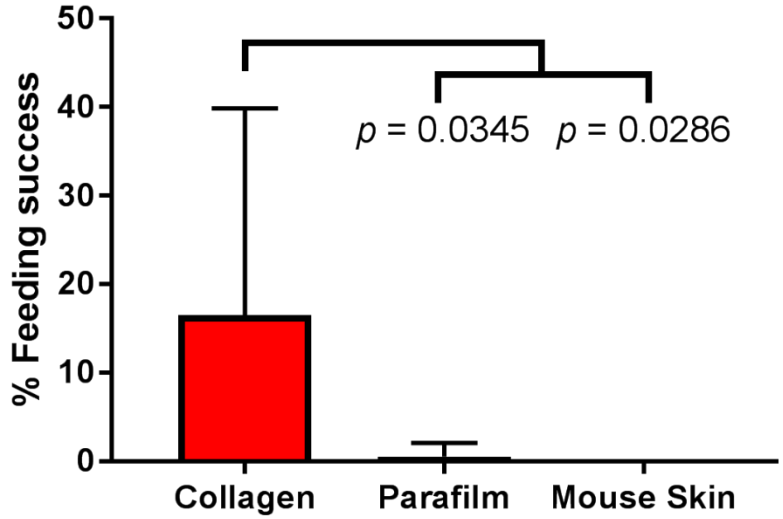

Figure 3.13. Effect of different membranes on *P. corporis* feeding success rates. The sample size for each was n=20, *P*-values were calculated using one-way ANOVA and Tukey's multiple comparison test.

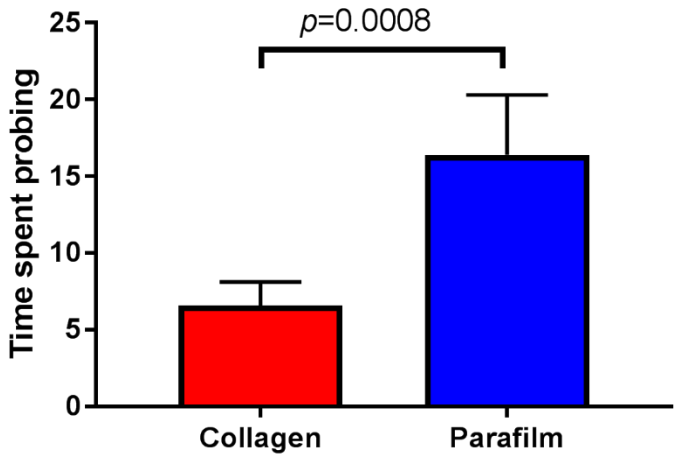

Figure 3.14. Minutes spent probing by *P. corporis* on different membranes. Lice spent longer probing on the parafilm membrane before feeding than on the collagen membrane. The mouse skin membrane was not included, as none of the lice fed on it. The sample size for each was n=5, *P*-values were calculated using an unpaired T test.

Parafilm M had less condensation issues, though was more prone to splitting and therefore spillage. It was also more difficult to stretch over the meal reservoir. When mouse skins were used as membranes, the lice did not feed

at all, which may be due to the thickness of the skin in comparison to the lice's relatively short mouthparts.

3.4 Discussion

The results presented in this chapter show that environmental conditions are important for the survival of colonies, most notably for *P. corporis*, which rapidly die if humidity is not controlled within its preferred range of 70-80%. Both fleas and lice feed best when fed through collagen membranes and they both prefer human blood over rabbit or sheep, although for the rabbit blood, this is likely to be a consequence of antibiotics present.

3.4.1 *X. cheopis* Colonies

Although the *X. cheopis* colony survived for approximately 3 months, noticeable hatching of new insects did not occur. The fleas were maintained in a large glass jar on bedding used by other groups (Hinnebusch 2007) and were both maintained and fed at 22ºC, with humidity maintained at 70%. Fleas spend much of their indirect lifecycles in the nests of hosts and should be capable of withstanding temperature and humidity fluctuations much better than the lice. Neither temperature nor humidity influence flea longevity (Krishnamurthy, 1966).

Fleas are naturally photophobic, often living in darkness in the host's den or climbing to sheltered places on the host to feed, such as thick fur or armpits (Service, 2008a) and this was generally found to be the case with the flea

colony, with insects naturally gravitating away from strong lights and preferring to feed in dim light. To assess flea feeding success rates, they needed to be anaesthetised by chilling, which may have adversely affected their lifespan.

The type of blood did not seem to affect *X. cheopis* feeding success rates although they were observed to prefer human defibrinated blood. This may be because it was the freshest of the bloods tested, having been collected on the day or day before insect feeding. Both the rabbit and sheep blood had to be shipped and was potentially a week old or more by the time feeding occurred. The discovery that the rabbit blood contained antibiotics (streptomycin sulphate (0.09%), penicillin G (0.04%) and neomycin trisulphate (0.10%)) may have also detrimentally affected the flea's desire to feed (Kernif *et al.*, 2015), although the feeding success rates for all three blood types was so low it was impossible to determine whether antibiotics influenced flea longevity. As fleas naturally feed on multiple hosts, unlike lice, which live their entire lives on single hosts (Service, 2008a), the feeding success rates between blood types would not be expected to be particularly different.

X. cheopis seemed to prefer the Hemotek collagen membrane over the mouse skin or Parafilm M, despite Florent Sebbane (Institut Pasteur, Lille, France) suggesting they had less fleas feeding on the collagen membranes compared to mouse skins. In this study, the collagen membrane had a slightly higher feeding success rate than mouse skin or Parafilm M, as well as a shorter probing time, suggesting that the insects felt this to be the most natural. Despite the mouse skin being physically closest to what the fleas had been previously fed on, in this study, the fleas did not appear to feed that successfully. This is possibly due to the preparation procedure or antibiotics

required to keep it sterile, or the thickness of the skin, which is difficult to process evenly, making some areas too thick for the fleas to reach the blood through. Due to processing, the mouse skins did not maintain sterility and had to be disposed of after a couple of weeks, thus could not be prepared in batches, making them a time-consuming option.

The fleas thrived best in the glass vase, where they had bedding, plus other fleas, mimicking natural colony conditions. However, it was very difficult to count the number of insect feeders within the colony. Condensation was not an issue when feeding within the main colony vase, as there was plenty of space for evaporation compared with when feeding within a glass tube. The fleas did not survive as long when maintained in the glass tubes, due to smaller amounts of bedding and protection, however, it was easier to manipulate them and count the number that had fed. The fact that they were easier to manipulate (*i.e.* chilling to observe them) may also have negatively impacted on their lifespan. Condensation on the sides of the tube was also a real issue as the fleas tended to get stuck and drown in it, or, if a filter paper ring was placed inside to soak up moisture, the fleas would become wedged and were not able to feed. When feeding was in progress, the Hemotek meal reservoir needed to be periodically detached from the feeding tube to allow the condensation to evaporate for about ten min.

There was no real option to change the position of the meal reservoir within the main colony, although the fleas had no problem reaching and staying on the membrane and within a few min of it being placed in the vase, insects were observed to be probing across the whole surface of the membrane and Hemotek heating arm. When feeding within the tube, clamping the tube on top

of the meal reservoir allowed better access to the membrane, but greatly increased the condensation and therefore the chance of insects drowning. Having the meal reservoir clamped at the top of the tube meant that the fleas could not access the membrane. Laying the feeding tube and meal reservoir side by side (ensuring a tight seal between the two) proved to be a good middle ground; the fleas were able to jump or crawl onto the membrane, but the condensation build up appeared to be slightly less.

3.4.2 *P. corporis* Colonies

The physical conditions in which the lice were kept had a much more noticeable effect on their longevity compared to the fleas, most obviously temperature and humidity. Colonies did not survive for longer than three weeks, a much shorter time than the fleas. Lice kept constantly at 32ºC dehydrated and died as, although feeding was attempted every day, they would not always feed to maintain their liquid intake. Lice kept at lower temperatures and then brought up to feeding temperature were better feeders. The increase in temperature needed to be approximately 12 h before feeding took place, otherwise the lice were sluggish and did not feed well. It is difficult to replicate *P. corporis*' natural feeding habits within the laboratory, as in their natural environment, body lice are known to take more than five small bloodmeals a day (Waniek, 2009). With the equipment and time available in this study, it was impossible to mimic this, as even feeding once a day was extremely time consuming.

The correct humidity was vital to stop the lice from dehydrating in the incubator, and a relative humidity of at least 70% was required. This was true even at the lower, 'hibernation' temperature, as *P. corporis* are extremely susceptible to desiccation (Waniek, 2009).

Although other groups have suggested that haematophagous insects are sensitive to light-dark cycles (Cheryl Whitehorn, LSHTM, London), it did not seem to have much of an effect on the colonies in this study. However, the majority of the experiments were conducted in as low light as possible. The lice were capable of feeding with the lights on and off, but preferred not to be in bright, direct light. When given the choice, they would attempt to squeeze into enclosed areas, such as the gap between the membrane and the mesh or cardboard sleeve. When there was no protection (*i.e.* when lice were placed on an 'open' meal reservoir membrane without a cardboard sleeve) they would not settle or feed and instead continued to walk off the membrane (usually in the opposite direction to the light source) and hide under the meal reservoir. When the cardboard sleeve was added, they fed much more readily.

All three blood types tested had relatively large variation in feeding rates, as sometimes none of the lice would feed at all, which was similar to the fleas. *P. corporis'* feeding rate was much greater when fed on human blood compared to rabbit or sheep blood, although this is to be expected, as naturally *P. corporis* are obligate human parasites (Service, 2008b). The decision to use fresh, defibrinated human donor blood rather than blood bank stocks which contain anticoagulants may have contributed to the feeding success rate, as anticoagulants are known to decrease fecundity in body lice (Mumcuoglu *et al.* 2011) as well as cat fleas as previously noted (Kernif *et al.* 2015) and the age

of the blood is likely to have had an effect on feeding success rates and louse survival, as both Habedank (1999) and Mumcuoglu (2011) have suggested that feeding rates decrease with time, due to blood chemistry deterioration.

Although the rabbit blood produced a relatively high feeding rate, the lice that ingested it were observed to die more quickly than those that were fed on human blood and the discovery that the rabbit blood contained antibiotics may have been a factor in this, as the addition of antibiotics (in this case streptomycin sulphate (0.09%), penicillin G (0.04%) and neomycin trisulphate (0.10%)) is thought by some groups to lower louse fecundity and life expectancy (Takano-Lee, Velten, *et al.* 2003).

Sheep blood (SLS), contained no antibiotics and was considerably more cost effective, but did not confer a very successful feeding rate. The fact that this colony has never fed on sheep blood before and weaning from one blood type to another is difficult, would suggest that sheep blood would not be a suitable food source for this colony, unless it were possible to wean the lice slowly onto it from their original blood supply (in this case, live rabbit blood) (Carola Kuhn, Umweltbundesamt, Berlin, Germany).

Human blood is the natural food source of *P. corporis* and results from this study concur with this, as it had the highest feeding success rate and a similarly high survival rate. This would suggest that it is the most appropriate blood source when rearing *P. corporis* artificially.

The type of membrane used also had a large effect on feeding success rate. *P. corporis* preferred the collagen membrane which was thin enough for them to feed through, but sturdy and flexible enough to not break when the lice pierced it with their mouthparts, which sometimes occurred with the Parafilm

M. A complication with the collagen membrane was that a lot of moisture evaporated though it, meaning that the blood dried out quicker than the other membranes and condensation caused some insects to drown in the feeding house.

An attempt to soak the collagen membranes overnight in sterile water did not make a difference to the evaporation rate, however, usually 1 h was long enough for the insects to probe and feed before the blood dried too much for them to access it. The collagen membrane also had a smooth and rough side, the latter of which a Hemotek representative suggested would be most effective. However, when this was tested, the side of the membrane facing the lice seemed to make no difference. The Parafilm M membrane was also successful and is used by many other groups to feed haematophagous insects artificially. It was also more prone to splitting, making it less of a prospect for experimental CL3 work. The mouse skin membrane was not successful, as the lice did not seem to be able to penetrate it at all as, unlike fleas which feed with a long stylus, lice feed using the shorter haustellum (Russell, 1868; Buxton, 1940). They did not settle, indicating they did not want to feed on the mouse skin, despite it being a natural substance, which may be due to the skin's processing.

The length of time that the insects were left on the membrane to feed depended on the membrane, although less than 20 min on any membrane tested was not enough time for the lice to probe and find a suitable spot to pierce. More than 1 h and the collagen membrane became too dehydrated, although this was less of an issue with the Parafilm M or mouse skin membrane, which lost less water to evaporation. The collagen membrane

could be rehydrated by dabbing with damp tissue, but lice got stuck in any standing water and did not feed as readily compared to a fresh membrane.

The lice could not feed when a mesh was placed over the membrane, as their mouthparts are likely too short to reach the membrane. Feeding lice by individually placing them onto the membrane is not an acceptable long-term solution as large scale colony maintenance would be extremely time consuming. Hand picking onto the membrane was also not a practical method for feeding juvenile lice as they were impossible to track. Given that *P. corporis* showed very poor feeding rates when required to pierce though mesh to reach the membrane, it provides a real colony maintenance issue, as well as a containment level 3 laboratory issue, as insects must be doubly contained at all times in the presence of *Y. pestis*, which would significantly reduce experimental feeding success rates.

The position of the feeding house relative to the meal reservoir made a large difference to the feeding success rates. Placing the feeding house on top of the meal reservoir allowed better access to the membrane but increased condensation, whereas placing the house underneath the meal reservoir required a bridge to allow to the lice to reach the membrane. Placing each side by side allowed lice to access membrane, as there was observed chemotaxis towards it, although condensation was still a problem, although less than placing the feeding house on top (Buxton, 1940). The position of the louse housing and meal reservoir could be altered with the use of clamp stand.

Placing the lice on top of the membrane allowed sustained insect contact with the membrane. Overall this was far more effective than any other orientation

and far outweighed the condensation problems, which were largely eliminated when the cardboard collar was used in place of the plastic Sterilin pots.

In an effort to make conditions as realistic as possible, different items were used to mimic hair strands between the cloth patch on which the lice were maintained and the membrane of the meal reservoir. Pullen & Meola (1995) used dog hair as a 'bridge' for their feeding system, and this technique was replicated using a small tuft of human hair, tied with a rubber band and used as a bridge. Cloth and filter paper was also tried, but it did not alter feeding behaviour. Adults probed the most, along with 3rd instar lice, but the smaller ones seemed incapable of feeding through the mesh. Feeding by transferring on to the membrane of the younger instars was not attempted, as they were difficult to keep track of (even with the cardboard collar) and therefore were likely to get lost.

Despite the colonies not surviving using artificial feeding methodology, it was still possible to undertake insect infection experiments using *Y. pseudotuberculosis* due to feeding success, by importing batches as and when needed for experiments.

3.4.3 Summary

Both *X. cheopis* and *P. corporis* proved difficult and time consuming to maintain artificially and consequentially, the colonies could not be propagated, despite some success with *P. corporis* egg hatching.

The results of this chapter show that:

- Blood type does not affect *X. cheopis* feeding rates, although defibrinated human blood was preferred
- *X. cheopis* prefer feeding through collagen membranes compared to Parafilm M and mouse skin membranes
- Blood type does not affect *P. corporis* feeding success rates, although human blood was preferred
- Rabbit blood containing antibiotics negatively affected *P. corporis* longevity compared with human and sheep blood
- *P. corporis* prefer feeding through collagen membranes compared to Parafilm M and mouse skin membranes
- *P. corporis* are very susceptible to fluctuations in temperature and humidity but *X. cheopis* can withstand greater ranges

Despite this new knowledge regarding *X. cheopis* and *P. corporis'* preferences regarding blood types and feeding membranes, we were unable to maintain either colony. Artificially maintaining haematophagous insects is time consuming and more work needs to go into establishing the most favourable environmental conditions that mimic the natural host.

4 The Role of NagC in the Expression of *Y. pseudotuberculosis* and *Y. pestis* Quorum Sensing Phenotypes and the Regulation of Poly-GlcNAc

4.1 Introduction

Despite the difficulties involved in insect colony maintenance described in the previous chapter, it was still important to ascertain the role of NagC in relation to biofilm formation in an insect vector, as well as its potential contribution to other phenotypes including QS in *Y. pestis,* as GlcNAc has been shown to inhibit Lux-R-dependent QS in other organisms including *Chromobacterium violaceum* and *Pseudomonas aeruginosa* (Ö. Kimyon *et al.*, 2016).

Table 4.1. Predicted transcription factor binding sites for *Y. pestis* KIM genes based on RegPrecise 4.0 database (**Novichkov** *et al.*, 2013)**. This suggests that NagC is predicted to regulate both the *nagE-nagBACD and glmUS* operons. Conserved TT and AA pairs crucial for NagC binding are underlined.**

Locus	Name	Position	Score	Sequence
Y1203	*nagE*	-176	6	TTTAATTTGCGTTACGAAATAAT
Y1203	*nagE*	-270	5.2	ATTTTTTCGGATGATAAAATAAG
Y2551	*manX*	-206	5.1	ATTTTTTCACTGACTAAAATAAA
Y1251	*chbB*	-242	5	CTTATTTCGTCAAGAAAAAAATT
Y1202	*nagB*	-245	6	ATTATTTCGTAACGCAAATTAAA
Y1202	*nagB*	-151	5.2	CTTATTTTATCATCCGAAAAAAT
Y4133	*glmU*	-235	4.8	CTTGTTTTCTGTCGTAAAATAAG

The function of NagC has yet to be studied in *Y. pestis* but poly-GlcNAc has been shown to form a vital part of the biofilm ECM in the *Yersiniae* and the deletion of *nagC* would suggest the constitutive degradation, due to de-repression of the *nagE-nagBACD* operon and inhibition of synthesis due to the lack of *glmUS* transcription, of poly-GlcNAc and thus diminished production of

biofilm in *Y. pseudotuberculosis* (see Figure 1.6 in Section 1.5.3) (Wiechmann, Ph.D. Thesis, 2015). The repressor/activator roles of NagC for the *Yersiniae* can be predicted by using its DNA-binding transcription factor site (TF) to search for transcription factor binding sites (TFBS) in the upstream regions of target genes. The helix turn helix domain of NagC was identified at amino acid position 34-55, (ISRIQIADLSQLAPASVTKITR) using www.uniprot.org. Using the online RegPrecise database, TBFS were identified for the *Y. pestis* KIM strain, as shown in Table 4.1 (Novichkov *et al.*, 2013). As the *hmsHFRS* operon was not identified as interacting with NagC by the RegPrecise database, the online SoftBerry BPROM tool, which uses a gene prediction algorithm, based on Markov chain models of coding regions, was used to identify a putative NagC binding region upstream of the *hmsHFRS* operon in *Y. pseudotuberculosis* and *Y. pestis*.

As well as its role as a DNA binding protein, NagC was suggested to influence QS alongside poly-GlcNAc (Wiechmann, Ph.D. Thesis, 2015). Promoter pull-down experiments suggested that NagC binds to the promotor of the LuxR homologue *ypsR* in *Y. pseudotuberculosis* (Goldstone, unpublished data). In addition, GlcNAc has been reported to inhibit QS through competitive inhibition of AHL-binding to LuxR proteins and hence AHL-dependent gene transcription in both *C. violaceum* and *P. aeruginosa* (Ö. Kimyon *et al.*, 2016). In *C. violaceum*, production of the purple pigment violacein was downregulated by low millimolar concentrations of GlcNAc (Ö. Kimyon *et al.*, 2016). Given that GlcNAc affects AHL signalling, it is possible that it may also affect the QS phenotypes that are regulated by AHLs and YpsR in *Yersinia*.

In the *Yersiniae*, there are two signalling pathways. The first employs LuxI/R homologue pathways and the second utilises autoinducer 2 (AI-2), a furanone derived from the LuxS pathway (Bobrov *et al.*, 2007; Yu *et al.*, 2013). *Y. pseudotuberculosis* produces over 20 different AHLs *via* YpsI and YtbI, with the most abundant and most biologically relevant being the 3-oxo- substituted C6, C7 and C8 AHLs and the unsubstituted C6 and C8 compounds (Ortori *et al.*, 2007). *Y. pestis* produces *N*-hexanoyl-homoserine lactone (C6), *N*-(3-oxohexanoyl)homoserine lactone (3-oxo-C6) and *N*-octanoyl-homoserine lactone (C8), alongside *N*-(3-oxooctanoyl)-homoserine lactone (3-oxo-C8) (Gelhaus *et al.*, 2009). AHL production in *Y. pestis* and *Y. pseudotuberculosis* is affected by both temperature and environmental pH (Yates *et al.*, 2002; Kirwan *et al.*, 2006) although in *Y. pestis*, it has been suggested that AHLs do not affect biofilm formation in fleas (Jarrett, Deak, *et al.*, 2004).

Wiechmann (Ph.D. Thesis, 2015) has shown that GlcNAc increases the expression of *ytbR* and *ytbI* at 22ºC and 37ºC and decreases the expression of *ypsR* at 22ºC, and that GlcNAc influences *nagC* expression. If GlcNAc influences AHL signalling and production by inhibiting LuxR/AHL interactions, there may be a complex interplay between the GlcNAc pathway and QS. It is possible that NagC and GlcNAc may influence the expression of QS phenotypes such as the T3SS, auto-aggregation and biofilm formation, the latter of which will be explored in Chapter 5. Previous research indicated that, for *Y. pestis*, QS was not involved in plague virulence in mice nor in the ability of *Y. pestis* to colonize and block fleas despite biofilms being vital for flea blockage (LaRock *et al.*, 2013).

The *Yersinia* virulence factors known as YOPs are delivered into mammalian host cells by the T3SS, allowing bacteria to infiltrate host cells and cause disease (as reviewed in Cornelis 2002). If GlcNAc, regulated by NagC, affects QS regulation, it is possible that the deletion of *nagC* may disrupt the T3SS and YOP expression in *Y. pestis*. Although Wiechmann (Ph.D. Thesis, 2015) has shown that NagC had no effect on production of YOPs in *Y. pseudotuberculosis*, it would be of interest to see whether this is also the case in *Y. pestis,* as its mammalian host infection route is very different.

Sample and Mehigh (1989) showed that the presence of pPla prevents *Y. pestis* revealing a full YOP profile *in vitro* in culture supernatants, as although they are all produced, YOPs undergo rapid post-translational degradation facilitated by outer membrane plasminogen activator/coagulase activity (PAC). *In vivo*, YOPs are directly injected into host cells, but after 2 h *in vitro*, the YOP profile is likely to be reduced (Sample, Fowler and Brubaker, 1987; Mehigh, Sample and Brubaker, 1989; Sodeinde and Goguen, 1989).

Hinnebusch (2017) has shown that the biofilm which blocks the proventriculus of fleas begins with smaller aggregations of bacteria within the gut, which do not contain poly-GlcNAc, but may include blood meal components. As such, auto-aggregation, a known virulence phenotype expressed at 37ºC in pYV+ *Y. pseudotuberculosis*, could potentially be used by *Y. pestis* as a precursor to biofilm formation at flea body temperature.

It has been suggested that although *Y. pestis* can aggregate after incubation at 28ºC, it is incapable of aggregation at 37ºC, due to its expression of Fraction 1 Capsular protein (Caf1), an adhesin on the pFra plasmid which is absent in *Y. pseudotuberculosis* (S. Felek and E. S. Krukonis, unpublished observations,

as reviewed by Felek *et al.* 2010). Caf1 is thought to facilitate the change in infection route from *Y. pseudotuberculosis* which requires the ability to adhere to gut epithelial cells, to *Y. pestis* which needs to disseminate away from the site of infection, which it can do more effectively as single cells. Whilst Erickson *et al.* (2008) proposed that larger amounts of poly-GlcNAc are produced at flea rather than mammalian temperature in *Y. pestis*, Yoong *et al.* (2012) suggests that *Y. pestis* produces more poly-GlcNAc at 37ºC. *Y. pseudotuberculosis* exhibits maximal auto-aggregation and biofilm formation *via* QS at 37ºC, suggesting that these functions are more important in mammalian gut epithelial cell infections (Atkinson *et al.*, 1999, 2011). There are thought to be two auto-aggregation pathways, one mediated by YadA hydrophobic interactions and the other linked to virulence and antibiotic resistance (Rosqvist, Skurnik and Wolf-Watz, 1988; Paerregaard *et al.*, 1991). Wiechmann (Ph.D. Thesis, 2015), showed that a *Y. pseudotuberculosis* Δ*nagC* mutant enhanced QS-mediated auto-aggregation, so it will be useful to discover whether NagC plays a role in *Y. pestis* auto-aggregation.

4.2 Specific Research Aims

NagC has established roles in *E. coli, V. fischeri* and *Y. pseudotuberculosis* but is yet to be studied in *Y. pestis*. As *nagC* has 99% sequence identity across the whole gene between *Y. pseudotuberculosis* and *Y. pestis*, it would suggest that the gene has the same or a similar function in both. A Δ*nagC* mutant had previously been constructed by Wiechmann (Ph.D. Thesis, 2015) in *Y. pseudotuberculosis*, but needed to be constructed in *Y. pestis*.

The AHL profile has been elucidated in *Y. pestis* at 37ºC but given that NagC has never been studied in *Y. pestis*, the consequences of a *nagC* mutation for AHL production is currently unknown (Kirwan *et al.*, 2006). Similarly, the ability of *Y. pestis* to produce YOPs has also been investigated, but not in the context of the presence or absence of NagC, which is known to regulate GlcNAc, which in turn is known to inhibit the QS system in other bacterial species (Sample, Fowler and Brubaker, 1987; Sodeinde *et al.*, 1988; Mehigh, Sample and Brubaker, 1989; Sodeinde and Goguen, 1989).

Given that bacterial aggregates appear to be the precursor to proventriculus biofilm formation in fleas, it is possible that NagC may also play a role in the auto-aggregation of *Y. pestis* at flea body temperature (Hinnebusch, Jarrett and Bland, 2017). In comparison, *Y. pseudotuberculosis* does not have a flea stage and does not aggregate at 22ºC (Wiechmann, Ph.D. Thesis, 2015).

As NagC is likely to control transcription of the GlcNAc operons *glmUS* and *nagE-nagBACD,* and potentially *hmsHFRS* in *Y. pestis*, it is important to ascertain whether the removal of *nagC* affects the ability of *Yersinia* to produce poly-GlcNAc, as this is likely to influence its ability to produce biofilm.

A *Y. pestis* Δ*nagC* deletion mutant was constructed to ascertain whether NagC affected QS and QS-phenotypes in *Y. pestis* at both flea and mammalian body temperatures. These assays were performed in parallel with the *Y. pseudotuberculosis* Δ*nagC* mutant for comparison*;* some of these assays are repeats of previous work done by Wiechmann (Ph.D. Thesis, 2015), some are entirely novel, as indicated below. Some experiments could only be completed in *Y. pseudotuberculosis* due to licencing constraints. To answer the questions

raised above, the Δ*nagC* mutants were used in phenotypic assays where relevant at flea/soil or mammalian temperatures to ascertain whether:

- NagC affects AHL production by *Y. pestis* and *Y. pseudotuberculosis*
- NagC regulates YOP secretion of *Y. pestis*
- NagC affects auto-aggregation of *Y. pestis*
- NagC affects the ability of *Y. pseudotuberculosis* to produce poly-GlcNAc
- NagC in *Y. pestis* binds to the promotor regions of the GlcNAc synthesis operon *glmUS,* the poly-GlcNAc synthesis operon *hmsHFRS* and the external GlcNAc transport/catabolic operon *nagE-nagBACD* in the presence or absence of GlcNAc-1-P or GlcNAc-6-P

4.3 Results

4.3.1 Construction of a *Y. pestis ΔnagC* Mutant

To investigate the effect of NagC on QS phenotypes and biofilm formation in *Y. pestis*, an in-frame insertion-deletion of *nagC* was constructed by replacing part of the gene with a gentamicin resistance cassette between bases 171 and 1184 of the *nagC* gene using a suicide plasmid conjugation system as described in Milton *et al.* 1996.

Figure 4.1 shows the gentamicin insertion in *nagC* within the *nagE-nagBACD* operon being exchanged for the gentamicin cassette. The primers *nagC*_UP_F, *nagC*_UP_R, *nagC*_DW_F and *nagC*_DW_R (Table 2.3) were used to amplify in-frame upstream (UP) and downstream (DW) fragments (384

bp and 305 bp respectively) from *Y. pestis* CO92 wild-type genomic DNA which were then T-cloned into the amplification vector pGEMT-easy (Table 2.2).

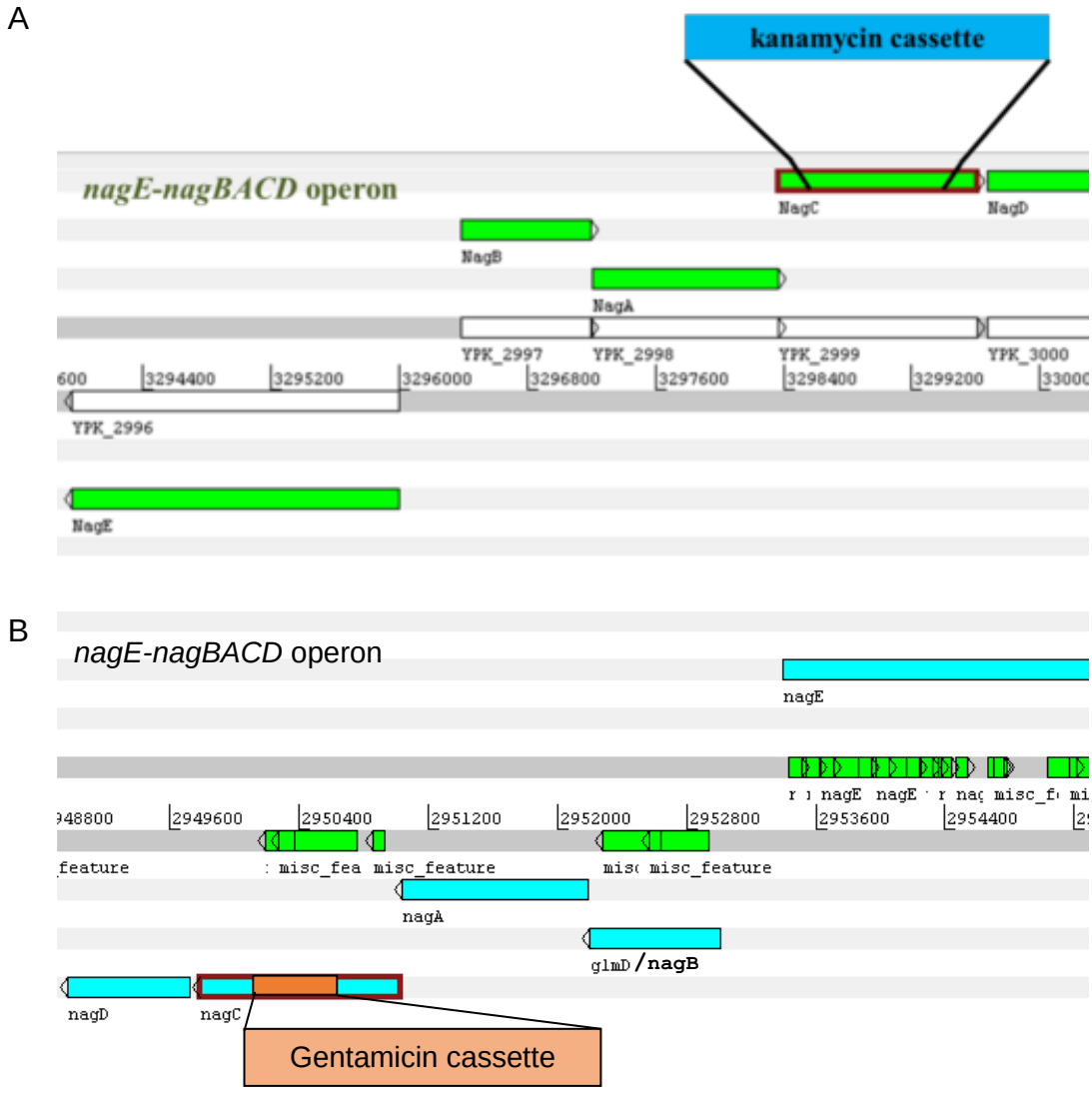

Figure 4.1. Schematic description of the mutation of *nagC*. (A) *Y. pseudotuberculosis nagE-nagBACD* arrangement showing substitution of part of *nagC*, taken by Wiechmann (2015). (B) *Y. pestis nagC* mutation in this study by substituting 1013 bp of *nagC* with a gentamicin cassette.

The gentamicin resistance cassette was amplified from the pEX18 plasmid (Hoang *et al.*, 1998) using the primers Gm_NoPro_*XbaI* and Gm_NoTerm_*KpnI* (Table 2.3). The gentamicin cassette was then ligated into

pGEMT-Easy::UP, which contained a section of *nagC,* using the *XbaI* and *KpnI* restriction sites before UP:GmR was excised and ligated into the pGEMT-Easy::DW plasmid using the *XbaI* and *SpeI* restriction sites. This completed *ΔnagC* cassette was ligated into the suicide vector pDM4 (see Appendix **Error! Reference source not found.** for confirmation gel), before being mated with wild-type CO92 *Y. pestis*. This created a disrupted gene, in which the gentamicin resistance cassette replaced part of the gene. The parent gene was 1230 bp compared to the *ΔnagC* mutant, which was 790 bp, including the gentamicin cassette.

Conjugation generally results in a single crossover, which can be forced *via* sucrose counter-selection into a double crossover. Mutants were screened by PCR using YPCO92_*nagC*_F and YPCO92_*nagC*_R primers (Table 2.3) (see Appendix image 8.2) based approximately 50 bp outside of the mutant, resulting in a 1391 bp fragment (see Appendix **Error! Reference source not found.** for agarose gel confirmation images). Once the mutation of *nagC* was confirmed by sequencing, a functional copy of *nagC* was inserted into the plasmid pHG327 (Stewart *et al.*, 1986) using the primers *nagC*_F_*XbaI* and *nagC*_R_*HindIII* (Table 2.3) (see Appendix image 8.3 and 8.4). pHG327::*nagC* was transformed into the CO92 *ΔnagC Y. pestis* strain and the empty pHG327 vector transformed into wild-type CO92 *Y. pestis* to serve as a control for any effects of the plasmid vector (see Appendix **Error! Reference source not found.** for agarose gel confirmation images). PCR was used to screen for successful transformants using combinations of the primers M13_F, M13_R and *nagC*_UP_F (Table 2.3) and sent for sequencing at Source Bioscience (see Section 2.2.3.5). When the sequence of *nagC* for *Y. pestis* and *Y.*

pseudotuberculosis was compared *in silico*, the sequences were 99% homologous and results obtained for one species are therefore likely to be the same for the other. The promoter regions for *nagE-nagBACD*, *glmUS* and *hmsHFRS* were 99%, 100% and 99% homologous respectively. Sequence data is shown in Appendix 8.38.3. This strong homology is useful, as parts of this study could only be conducted on *Y. pseudotuberculosis* for health and safety reasons, but results are likely transferrable to *Y. pestis*.

4.3.2 The Influence of NagC on QS

4.3.2.1 NagC Influences AHL Production in *Y. pseudotuberculosis* or *Y. pestis*

AHLs are produced by many Gram negative bacteria, allowing them to regulate gene expression in a cell density-dependent manner. As NagC regulates the production, uptake and catabolism of GlcNAc, it is possible that Δ*nagC* mutants may produce different AHL profiles in *Y. pseudotuberculosis* and *Y. pestis,* compared to the parent strains (Miyashiro *et al.*, 2012).

To ascertain whether NagC influenced the production of AHLs and therefore QS, AHLs were extracted as described in section 2.4.1. Growth curve data for *Y. pseudotuberculosis* were obtained from Slater (Ph.D. Thesis, 2017) and Wiechmann (Ph.D. Thesis, 2015) at both 22ºC and 37ºC. The concentration of deuterated *N*-pentylhomoserine lactone (d9-C5-AHL) (used as an internal standard) was within 2 standard deviations of the mean in 99% of *Y. pseudotuberculosis* and 100% of *Y. pestis* samples (Figure 4.2). Given the co-

extraction of the internal standard alongside the AHLs, this high level of reproducibility suggests the extraction of AHLs was successful and that subsequent AHL analysis data is reliable.

Results obtained in this study were from bacteria harvested at mid-log phase. AHL production patterns may have been different if harvested at stationary phase, as QS is reliant on bacterial cell density.

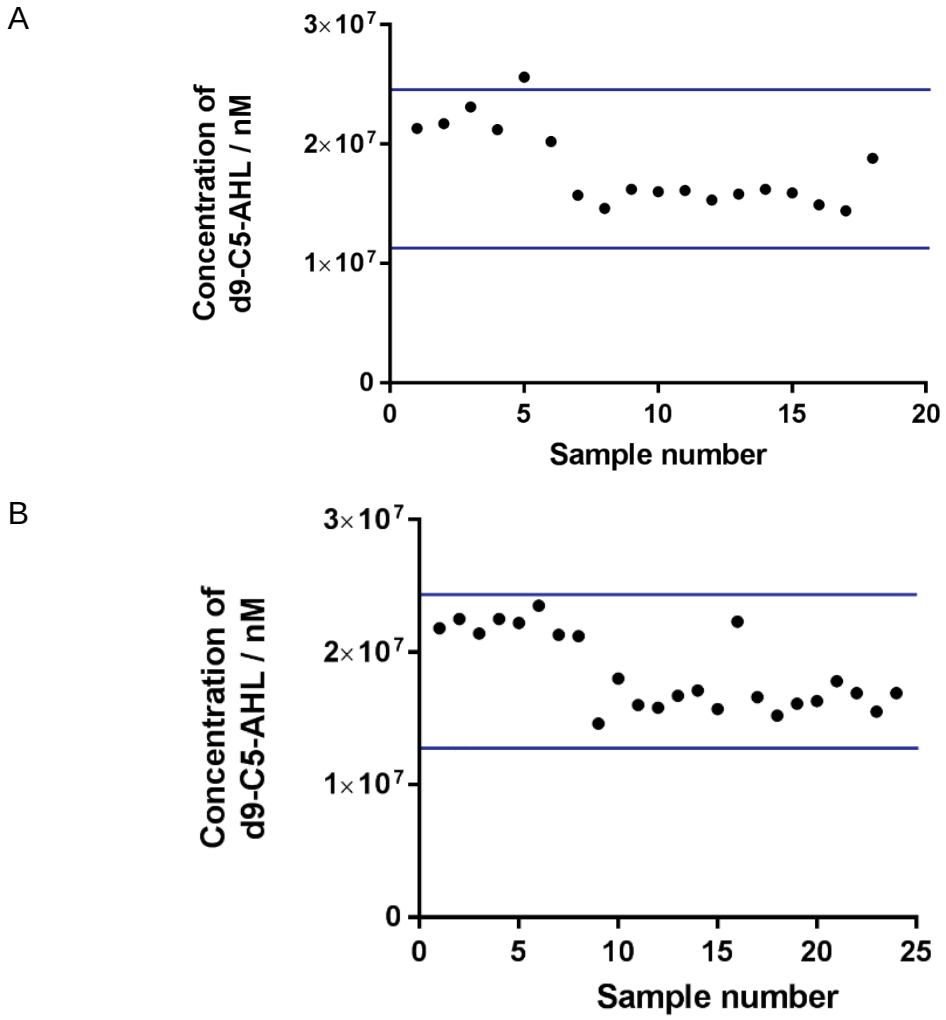

Figure 4.2. The concentration of d9-C5-AHL extraction from each sample as an indicator of AHL extraction efficiency. +/- 2 standard deviations are marked with a blue line, within which 99% of *Y. pseudotuberculosis* (A) and 100% of *Y. pestis* data falls.

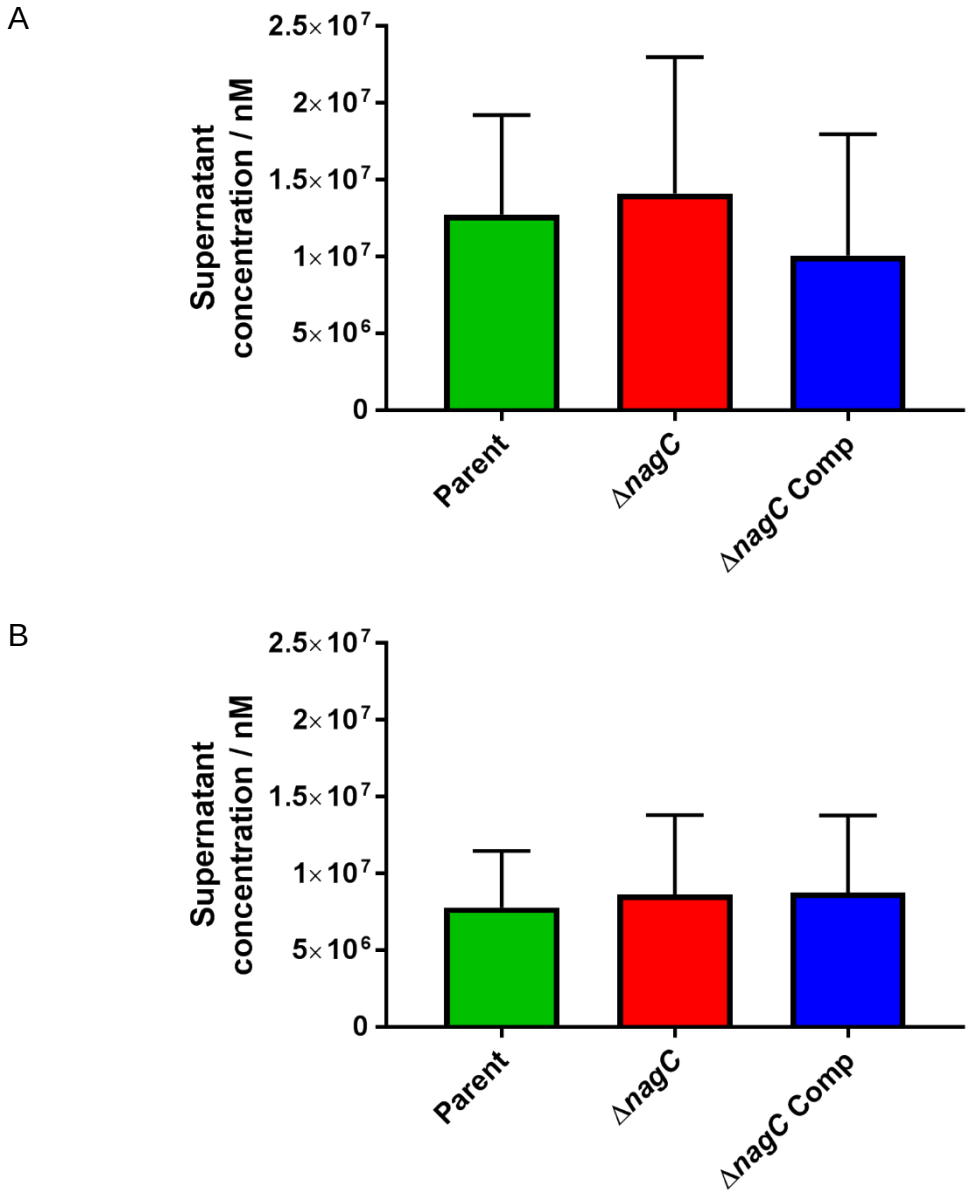

Figure 4.3. Total AHL production for *Y. pseudotuberculosis*, shown for (A) 22ºC and (B) 37ºC. There are no significant differences in total AHL production between the parent, Δ*nagC* or complemented Δ*nagC* strains. The data represent the average ± SD of three different experiments.

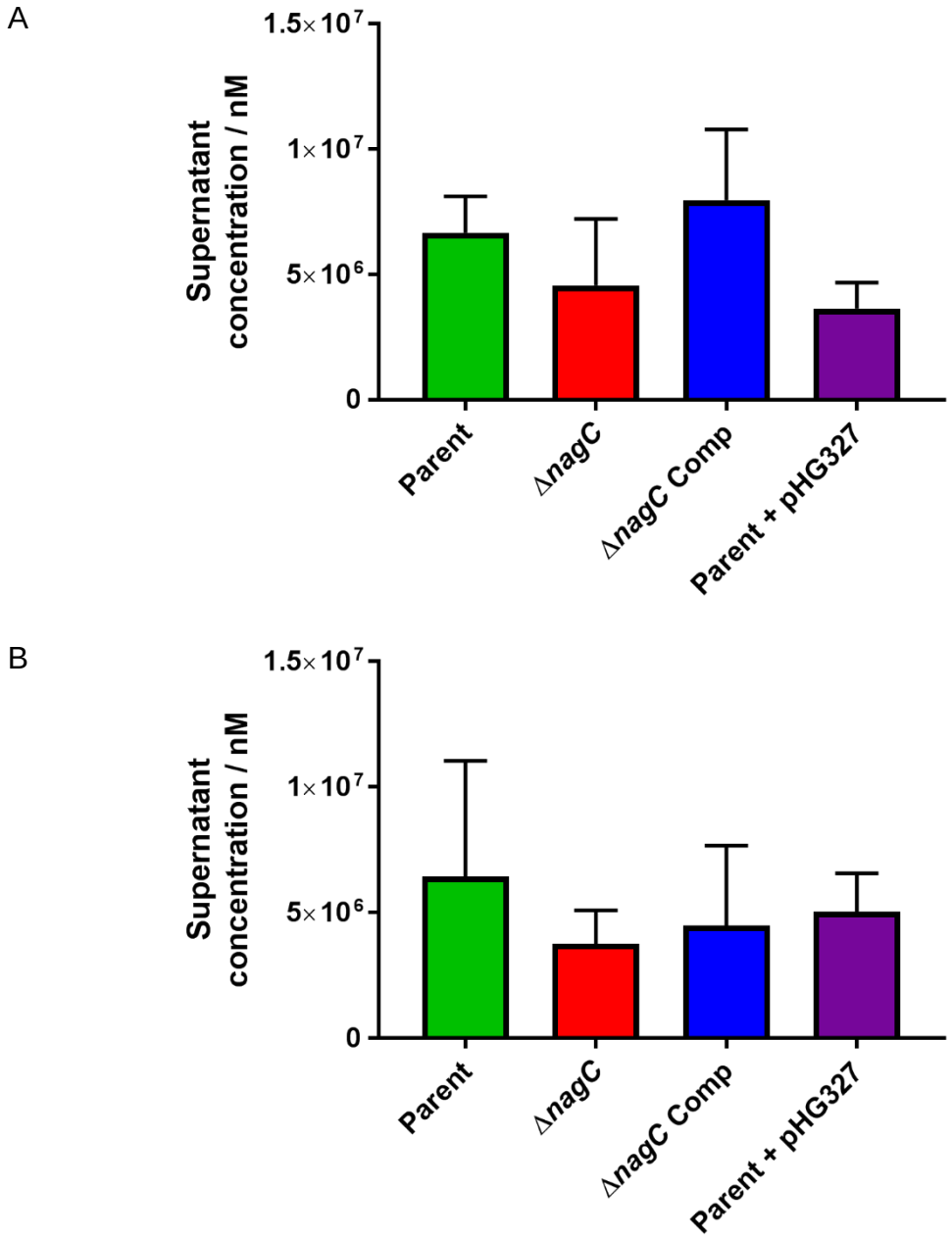

Figure 4.4. Total AHL production for *Y. pestis* is shown for (A) 22ºC and (B) 37ºC. There are no significant differences in total AHL production between the parent, Δ*nagC* mutant, complemented Δ*nagC* or parent + pHG327 strains. The data represent the average ± SD of three different experiments.

Despite the regulation of GlcNAc by NagC, which itself has been shown to inhibit AHL production in *Y. pseudotuberculosis* (Wiechmann, Ph.D. Thesis, 2015), the deletion of *nagC* does not appear to affect the total AHL production for either *Y. pseudotuberculosis* or *Y. pestis*, as there were no significant

differences in the concentrations of AHLs produced by the Δ*nagC* mutant compared to parent, as shown in Figure 4.3 for *Y. pseudotuberculosis* and Figure 4.4 for *Y. pestis*. This was shown to be the case at both 22ºC and 37ºC.

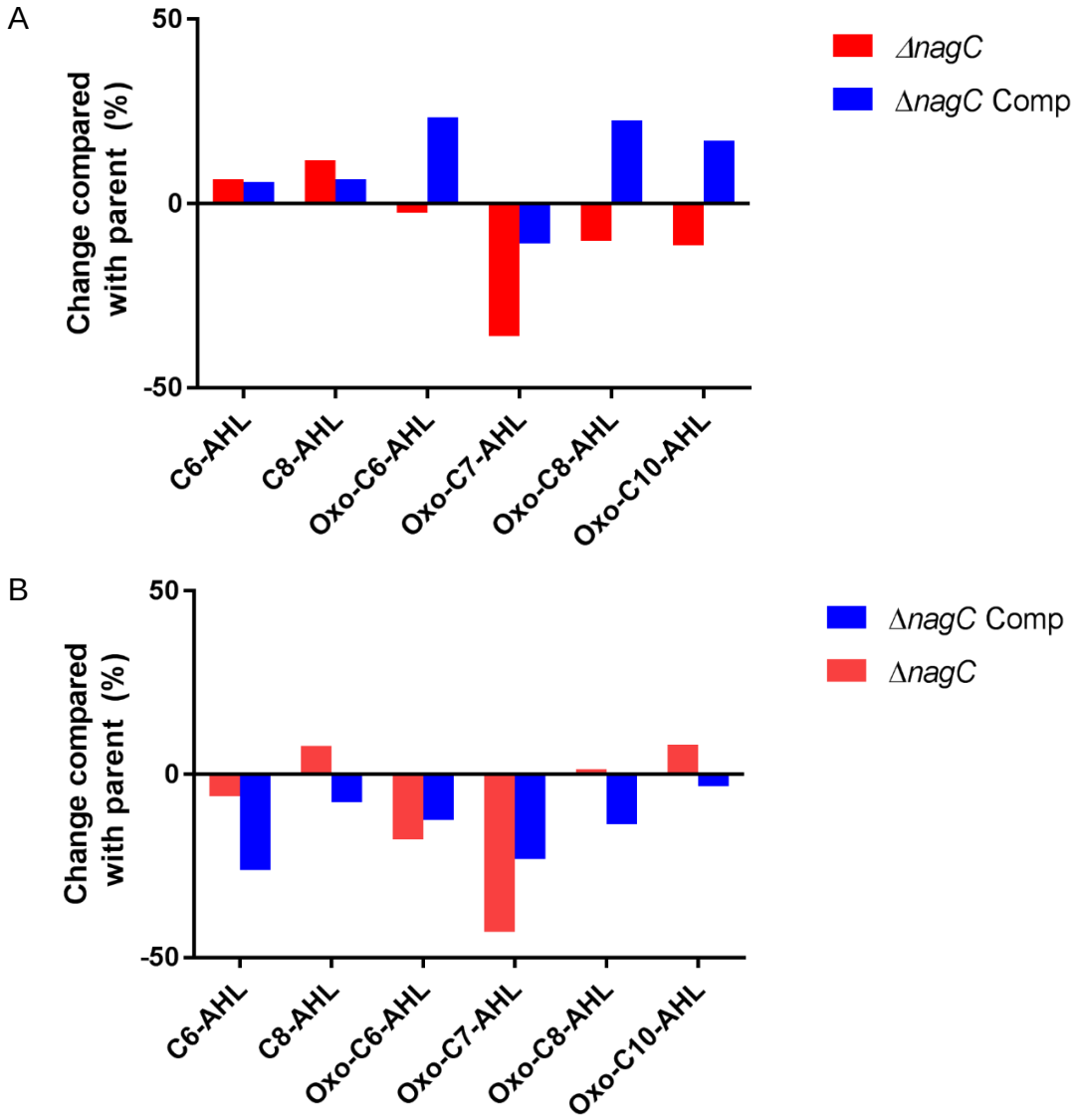

Figure 4.5. Percentage change in *Y. pseudotuberculosis* AHL production in the Δ*nagC* mutant and complemented Δ*nagC* mutant, compared to the parent strain. At 22ºC (A) the Δ*nagC* mutant showed a slight reduction in Oxo-C6, Oxo-C8 and Oxo-C10. At 37ºC (B) the Δ*nagC* mutant exhibited slight increases in C8, Oxo-C8 and Oxo-C10.

Although NagC did not appear to affect the overall AHL levels, its effect on the AHL profile was investigated for more subtle changes. Changes in the production of the six most prevalent AHLs produced by the *Yersiniae* were

measured at 22ºC and 37ºC for both *Y. pseudotuberculosis* and *Y. pestis*, as shown in Figure 4.5 (*Y. pseudotuberculosis*) and Figure 4.6 (*Y. pestis*).

When each individual AHL was measured for both *Y. pseudotuberculosis* and *Y. pestis* some minor differences were seen. The amounts of C6, C8, Oxo-C6, Oxo-C7, Oxo-C8 and Oxo-C10 were all identified using mass spectrometry and the expression for the Δ*nagC* mutant and complemented Δ*nagC* strain were plotted as a percentage of the parental strain.

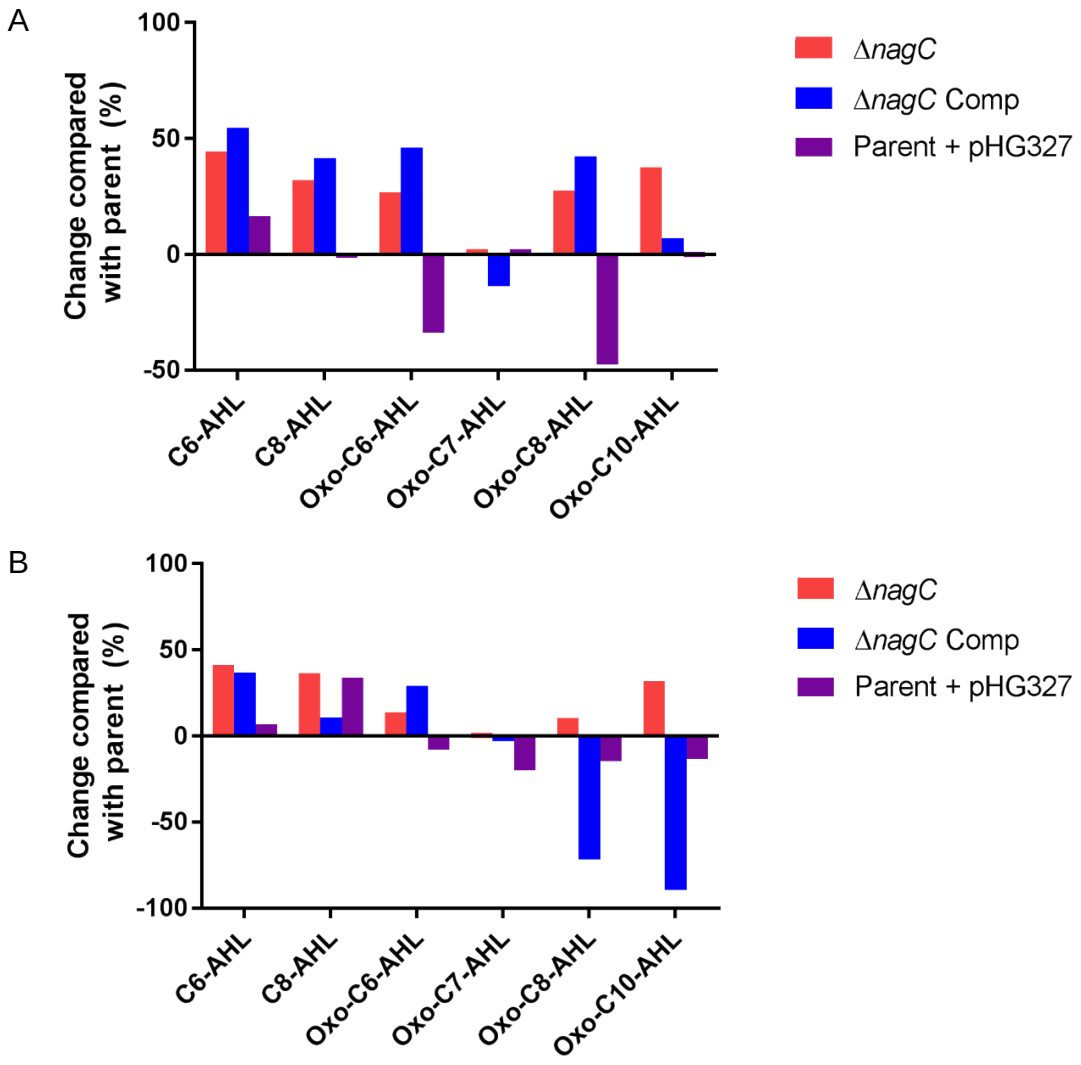

Figure 4.6. Percentage change in *Y. pestis* AHL production in the Δ*nagC* mutant, complemented Δ*nagC* mutant and parent + pHG327, compared to the parent strain. At 22ºC (A) the Δ*nagC* mutant showed a slight increase in Oxo-C10. At 37ºC (B) the Δ*nagC* mutant showed slight increases in Oxo-C8 and Oxo-C10.

The *Y. pseudotuberculosis* Δ*nagC* mutation resulted in a slight reduction of about 20% of Oxo-C8 and Oxo-C10 at 22ºC, whilst the complemented Δ*nagC* strain showed an increase compared to the parent strain. The Δ*nagC* mutant showed increased levels of less than 10% of C8, Oxo-C8 and Oxo-C10 at 37ºC. For *Y. pestis,* the Δ*nagC* mutant showed increased Oxo-C10 at both 22ºC (+40%) and 37ºC (+30%).

4.3.2.2 NagC Influences YOP Secretion in *Y. pseudotuberculosis* and *Y. pestis*

Secretion of the T3SS effector proteins occurs at the mammalian body temperature of 37ºC, with YOPs being secreted *in vitro* only in the absence of Ca^{2+} (Perry and Brubaker, 1987), although some *Yersinia* QS mutants have lost this regulation, secreting YOPs at 30ºC in the presence of Ca^{2+}, showing that loss of QS results in the dysregulation of T3S (Atkinson *et al.*, 2011). Although Wiechmann (Ph.D. Thesis, 2015) showed that the *Y. pseudotuberculosis ΔnagC* mutant did not show altered YOP secretion, it was important to determine whether NagC had the same effect in *Y. pestis*.

Figure 4.7 and Figure 4.8 show that, under YOP inducing conditions, the *ΔnagC* mutant shows a similar YOP profile as the parent and complemented strain in *Y. pseudotuberculosis* and *Y. pestis* respectively, although the *Y. pseudotuberculosis* Δ*nagC* complemented mutant over-expressed YOPs and the *Y. pestis* Δ*nagC* complemented mutant produced fewer. The Δ*nagC Y. pestis* and *Y. pseudotuberculosis* complemented mutants were cloned in different ways. For *Y. pestis in vitro*, the plasminogen activator protease on the

pPst plasmid breaks down YOPs secreted into culture supernatants, which accounts for the fact that SDS-PAGE gel bands produced in this study were not as strong as those produced in *Y. pseudotuberculosis*, despite being processed in the same manner (Sample *et al.* 1987).

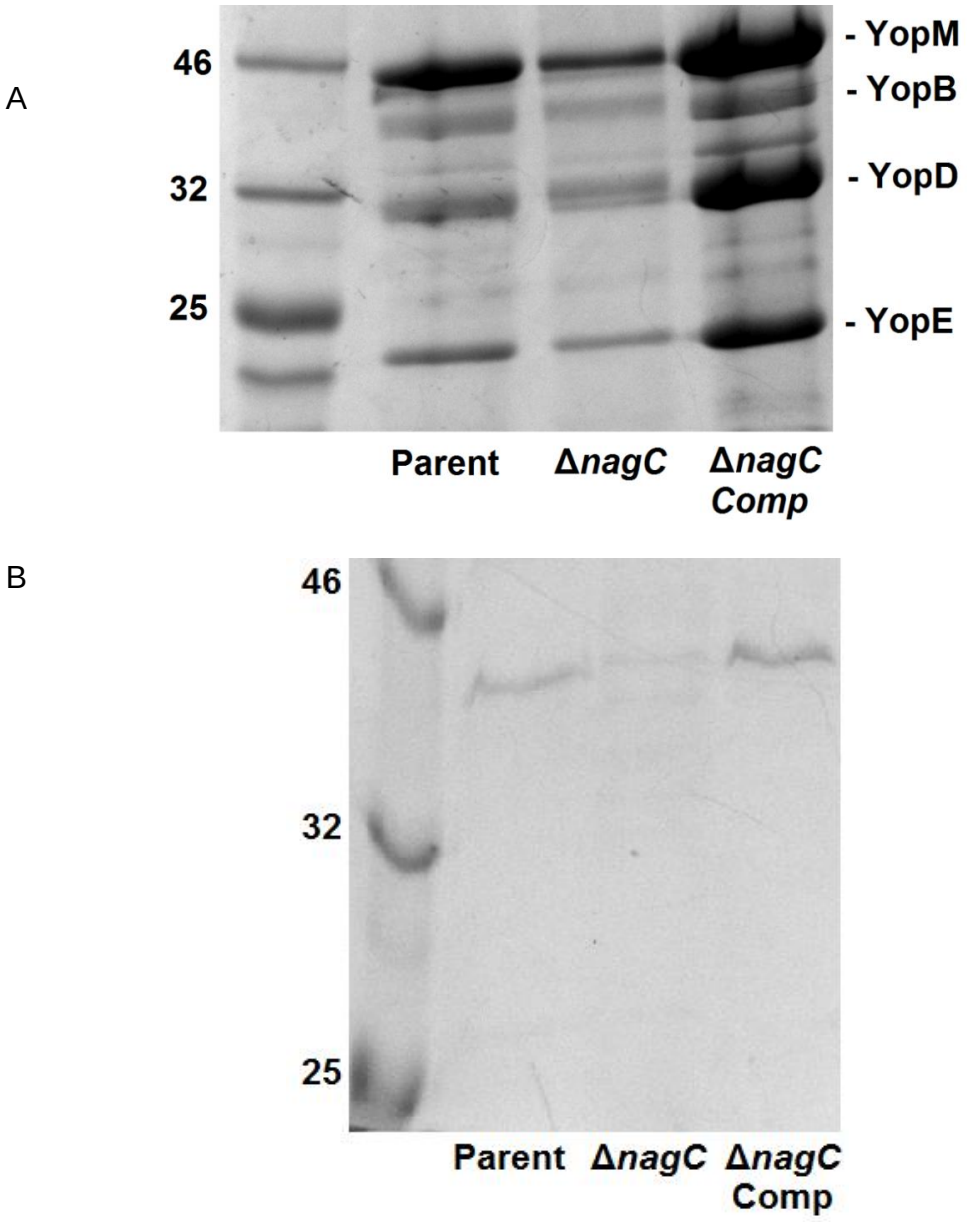

Figure 4.7. *Y. pseudotuberculosis* YOP secretion assay. (A) parent, Δ*nagC* mutant and the Δ*nagC* complemented mutant grown in the absence of Ca^{2+} at 37ºC show the same YOP profile as the parent and complemented strain. The Δ*nagC* complemented mutant appears to overexpress YOPs. (B) shows an uninduced control. The NEB Prestained Broad Range Protein Ladder (11 - 245 kDa) was used as a molecular mass marker.

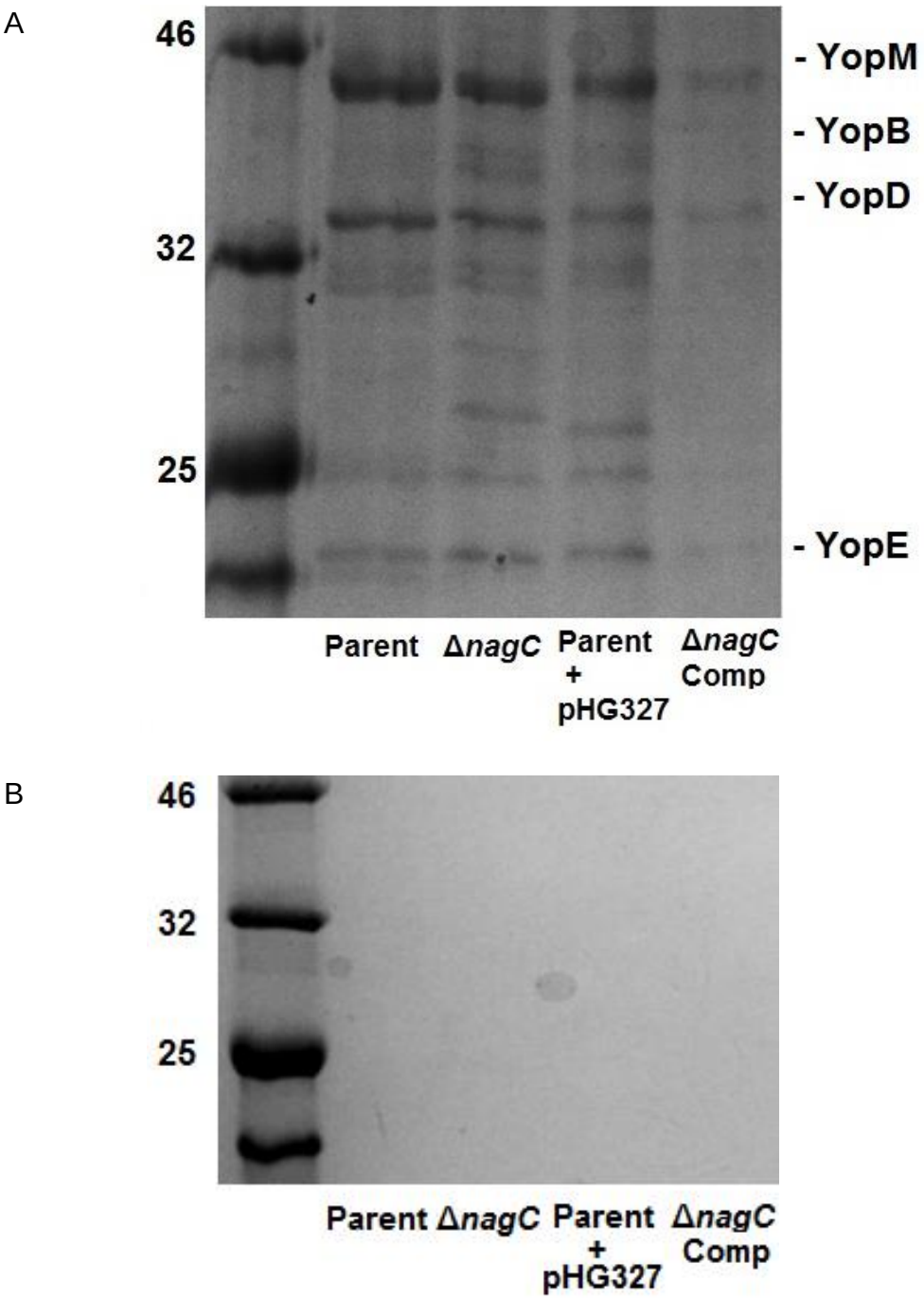

Figure 4.8. *Y. pestis* YOP secretion assay. (A) parent, Δ*nagC* mutant and the Δ*nagC* complemented mutant grown in the absence of Ca^{2+} at 37ºC shows the same YOP profile as the parent and complemented strain. In comparison to the *Y. pseudotuberculosis* Δ*nagC* complemented mutant, the *Y. pestis* Δ*nagC* complemented mutant shows fewer YOPs. (B) uninduced control. The NEB Prestained Broad Range Protein Ladder (11 - 245 kDa) was used as a molecular mass marker.

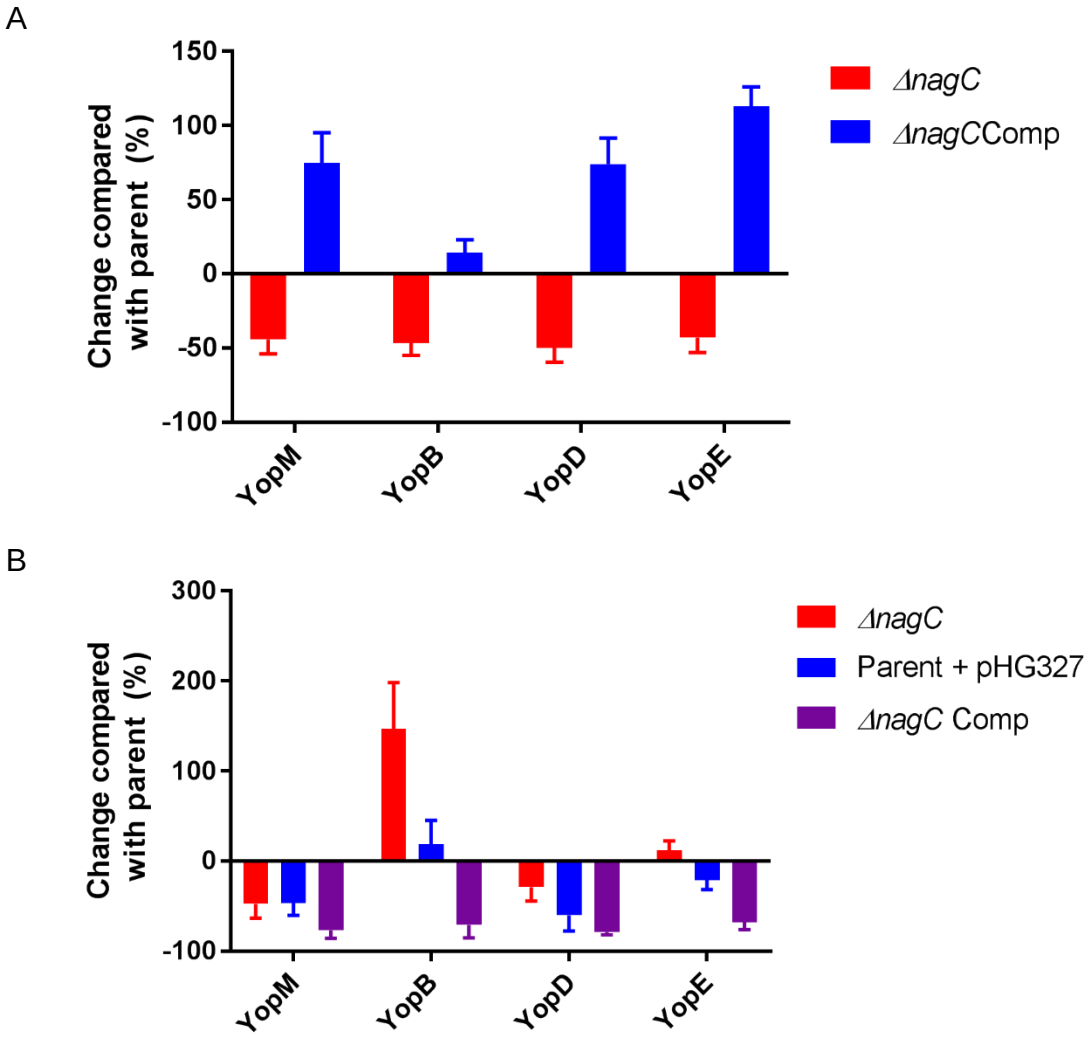

Figure 4.9 Percentage change in (A) *Y. pseudotuberculosis* and (B) *Y. pestis* YOP expression in the Δ*nagC* mutant and complemented Δ*nagC* mutant, compared to the parent strain. The sample size for each was n=3.

Further information was revealed when YOP band densities for *Y. pseudotuberculosis* and *Y. pestis* were analysed using ImageJ (NIH), as described in section 2.4.2.2, as a percentage of the parental band as shown in Figure 4.9. All YOPs identified in *Y. pseudotuberculosis* were under-expressed by around 45% in the Δ*nagC* mutant, whereas all YOPs were upregulated in the complemented Δ*nagC* mutant by 75-100% apart from YopB, which was upregulated by approximately 10%. The picture in *Y. pestis* was less clear-cut, but YopM and YopD production was reduced in the Δ*nagC*

mutant, the complemented Δ*nagC* mutant and the parent + pHG327. In contrast, YopB was upregulated in the Δ*nagC* mutant by approximately 100% and YopD upregulated by 20%.

4.3.2.3 NagC Influences the Rate of Auto-Aggregation in *Y. pseudotuberculosis*, but not in *Y. pestis*

Y. pseudotuberculosis auto-aggregation is promoted at 37ºC by YadA on the pYV plasmid (El Tahir and Skurnik, 2001). In addition, YadA-independent but T3SS-dependent auto-aggregation has been reported by Wiechmann (Ph.D. Thesis, 2015) and Barrett (Ph.D. Thesis, 2018), who have shown that mutants that reduce auto-aggregation also lack YOP secretion. In *Y. pestis, yadA* has naturally been disrupted by a frameshift mutation and is non-functional, although *Y. pestis* does auto-aggregate at 28ºC under certain conditions (Rosqvist, Bolin and Wolf-Watz, 1988). Restoring a functional YadA for *Y. pestis* results in attachment of bacteria to the flea bite site in mammalian hosts and the inability to disseminate into the host (Eitel *et al.*, 2002). The inability of *Y. pestis* to aggregate at 37ºC may also be due to its expression of Fraction 1 Capsular protein (Caf1), an adhesin on the pFra plasmid which is absent from *Y. pseudotuberculosis* (S. Felek and E. S. Krukonis, unpublished observations, as reviewed by Felek *et al.* 2010). As auto-aggregation is important for *Y. pseudotuberculosis* at mammalian temperatures, allowing the bacteria to attach to mammalian epithelial gut cells (Heise and Dersch, 2006), and aggregation for *Y. pestis* appears to be more important at flea body

temperature (Hinnebusch and Erickson, 2008), it is possible that there are different mechanisms for each species.

Firstly, to ascertain whether the *Y. pseudotuberculosis* and *Y. pestis* strains contained the pYV/pCD1 plasmid, which is vital for auto-aggregation in *Y. pseudotuberculosis* (Wiechmann, Ph.D. Thesis, 2015) colonies were plated onto CR-MOX plates as described by Surgalla & Beesley (1969). All colonies were small and red in colour, indicating that the virulence plasmids were present (as shown in Figure 4.10).

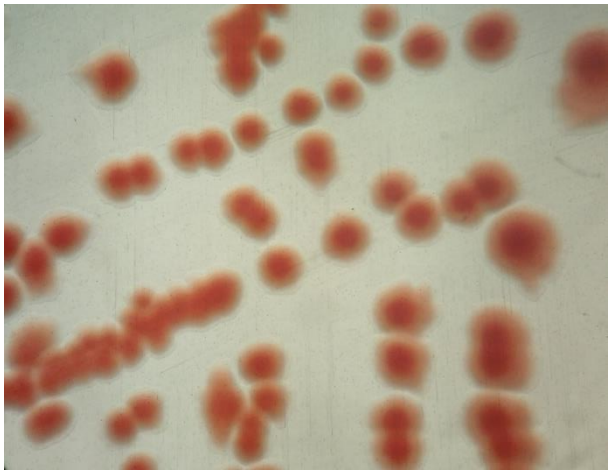

Figure 4.10. Congo red plates showing small, red colonies of *Y. pseudotuberculosis* that express the pYV virulence plasmid (with the same morphology as *Y. pestis* pCD1 positive colonies). Image taken on the Nikon dissecting microscope (4x).

After incubation at 22ºC and then allowed to aggregate statically at 22ºC, neither *Y. pseudotuberculosis* nor *Y. pestis* auto-aggregated after 2 h, as shown in Figure 4.11.

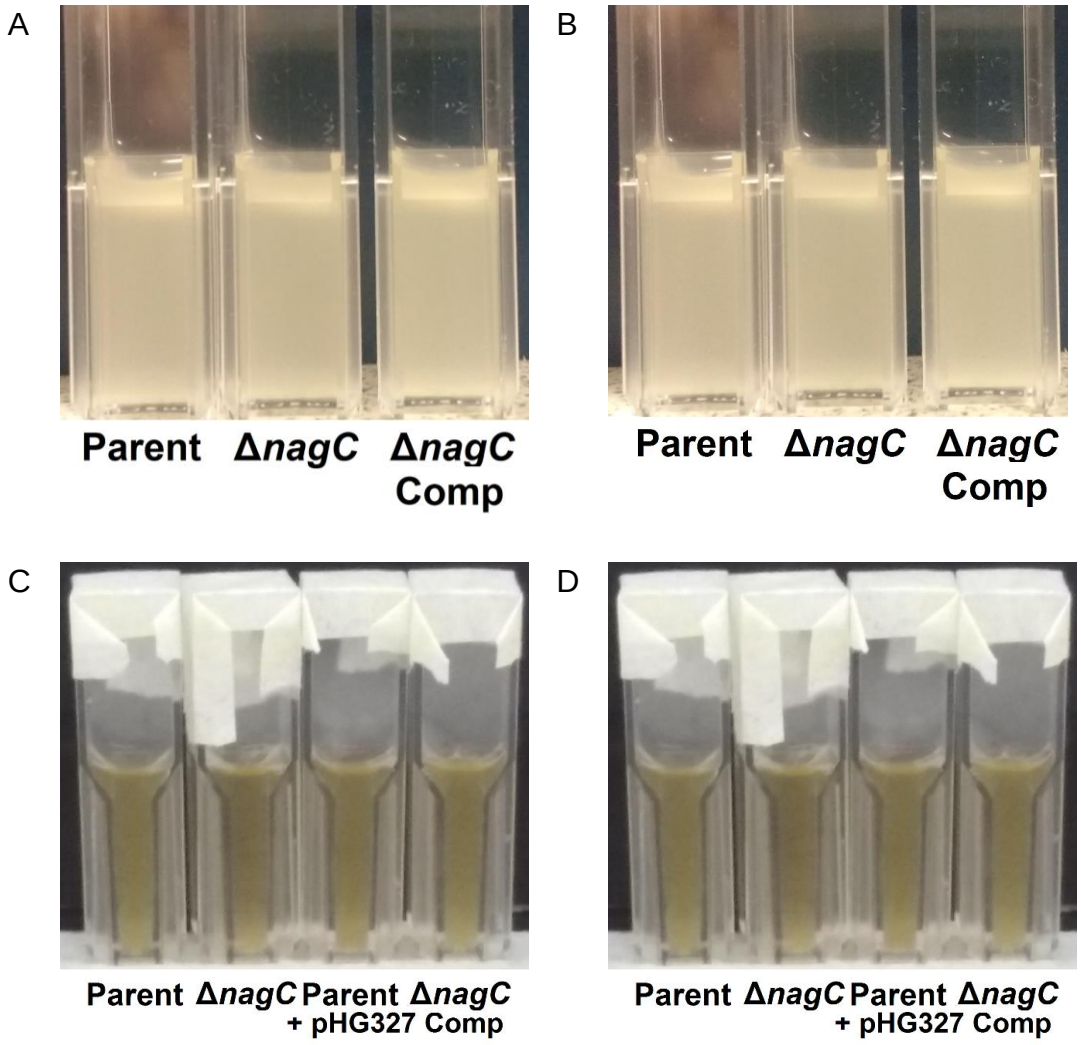

Figure 4.11. Cell aggregation assays of *Y. pseudotuberculosis* and *Y. pestis* Δ*nagC* and Δ*nagC* complement compared with the respective parent strain when grown at 22ºC. (A) *Y. pseudotuberculosis* after 1 h at 22ºC and (B) after 2 h, showing that it does not aggregate under these conditions. (C) and (D) *Y. pestis* after 1 and 2 h respectively at 22ºC. *Y. pestis* also does not aggregate under these conditions.

After incubation at 37ºC, then left to aggregate statically at 22ºC, after 1 h the *Y. pseudotuberculosis* parent and complemented Δ*nagC* strains had both aggregated and the Δ*nagC* mutant had begun to aggregate. After a further hour, the Δ*nagC* mutant had further aggregated. By contrast, under the same conditions at 37ºC, none of the *Y. pestis* strains had aggregated after 2 h.

Figure 4.12 shows *Y. pseudotuberculosis* and *Y. pestis* cultures at 37ºC after 1 h and 2 h.

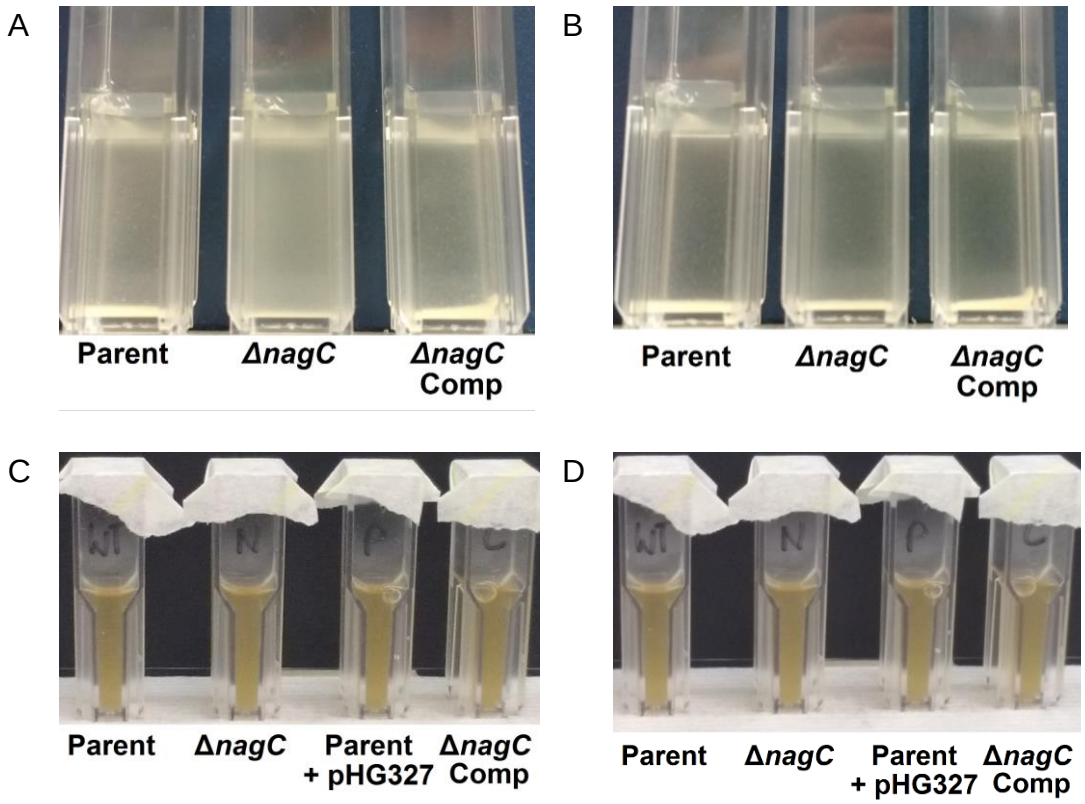

Figure 4.12. Cell aggregation assays of *Y. pseudotuberculosis* and *Y. pestis* Δ*nagC* and Δ*nagC* complement compared to the respective parent strain grown at 37ºC. (A) *Y. pseudotuberculosis* after being left static for 1 h at 22ºC and (B) after 2 h. The Δ*nagC* mutant takes longer to settle but does still aggregate. (C) and (D) *Y. pestis* aggregation after 1 and 2 h respectively left static at 22ºC. *Y. pestis* does not clump at 1 h or 2 h under the same conditions as *Y. pseudotuberculosis*.

As the *Y. pseudotuberculosis* Δ*nagC* mutant appeared to aggregate more slowly, the aggregation rates of each strain were tested. Only *Y. pseudotuberculosis* grown at 37ºC aggregated, but there was a difference in the rate of aggregation between the Δ*nagC* mutant and the parent and complemented Δ*nagC* strain. Whilst the sedimentation rate for the parent was 0.0046 OD_{600} nm U min^{-1} (SD ±0.00004) and the complemented Δ*nagC* mutant

was 0.0043 OD_{600} nm U min^{-1} (SD ±0.00001), the Δ*nagC* mutant was slower, at 0.0025 OD_{600} nm U min^{-1} (the fraction of the turbidity in the supernatant subtracted from unity) (SD ±0.00004) (Figure 4.13).

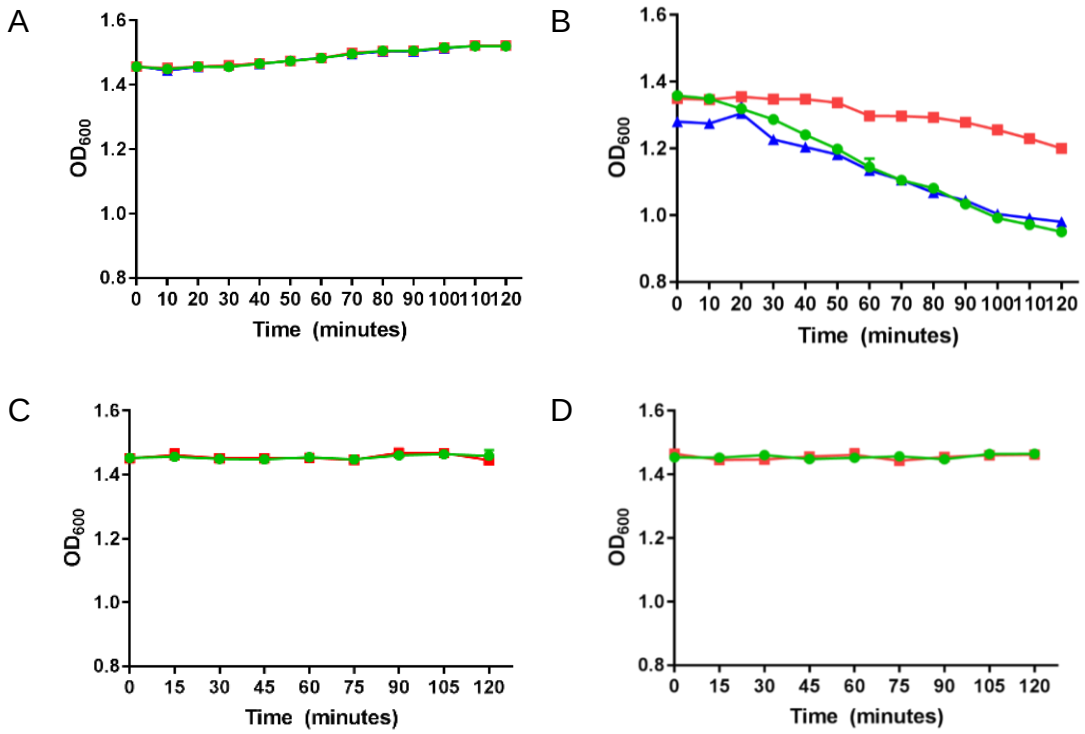

Figure 4.13. Sedimentation assays showing the rates of auto-aggregation for *Y. pseudotuberculosis* (A and B) and *Y. pestis* (C and D); strains are parent (green), Δ*nagC* (red) and complemented Δ*nagC* (blue, *Y. pseudotuberculosis* only) (A) *Y. pseudotuberculosis* at 22ºC, which shows no aggregation for any strains and (B) a decrease in the rate of aggregation of the Δ*nagC* mutant at 37ºC compared to the parent and complemented strain. (C) *Y. pestis* strains at 22ºC and (D) 37ºC. *Y. pestis* does not aggregate. The complemented strain for *Y. pestis* was not tested. The sample size for each was n=3.

4.3.3 NagC Influences the Amount of poly-GlcNAc Produced *by Y. pseudotuberculosis* at 37ºC but not 22ºC

As NagC has been shown to be important for biofilm formation on *C. elegans* (Wiechmann, Ph.D. Thesis, 2015), and slowed the rate of auto-aggregation in *Y. pseudotuberculosis*, it was important to identify the mechanism involved. As NagC regulates GlcNAc biosynthesis and catabolism metabolism in different bacteria, it was logical to ascertain whether the *Y. pseudotuberculosis* Δ*nagC* mutation influenced poly-GlcNAc production. Figure 4.14 shows confocal images of the strains grown at 22ºC, which all showed similar levels of poly-GlcNAc, when stained with a wheat germ agglutinin (WGA)-rhodamine conjugate. Figure 4.15 shows strains grown at 37ºC. Compared to the parent and complemented Δ*nagC* strain, the Δ*nagC* mutant showed a lower level of rhodamine fluorescence and hence reduced poly-GlcNAc production.

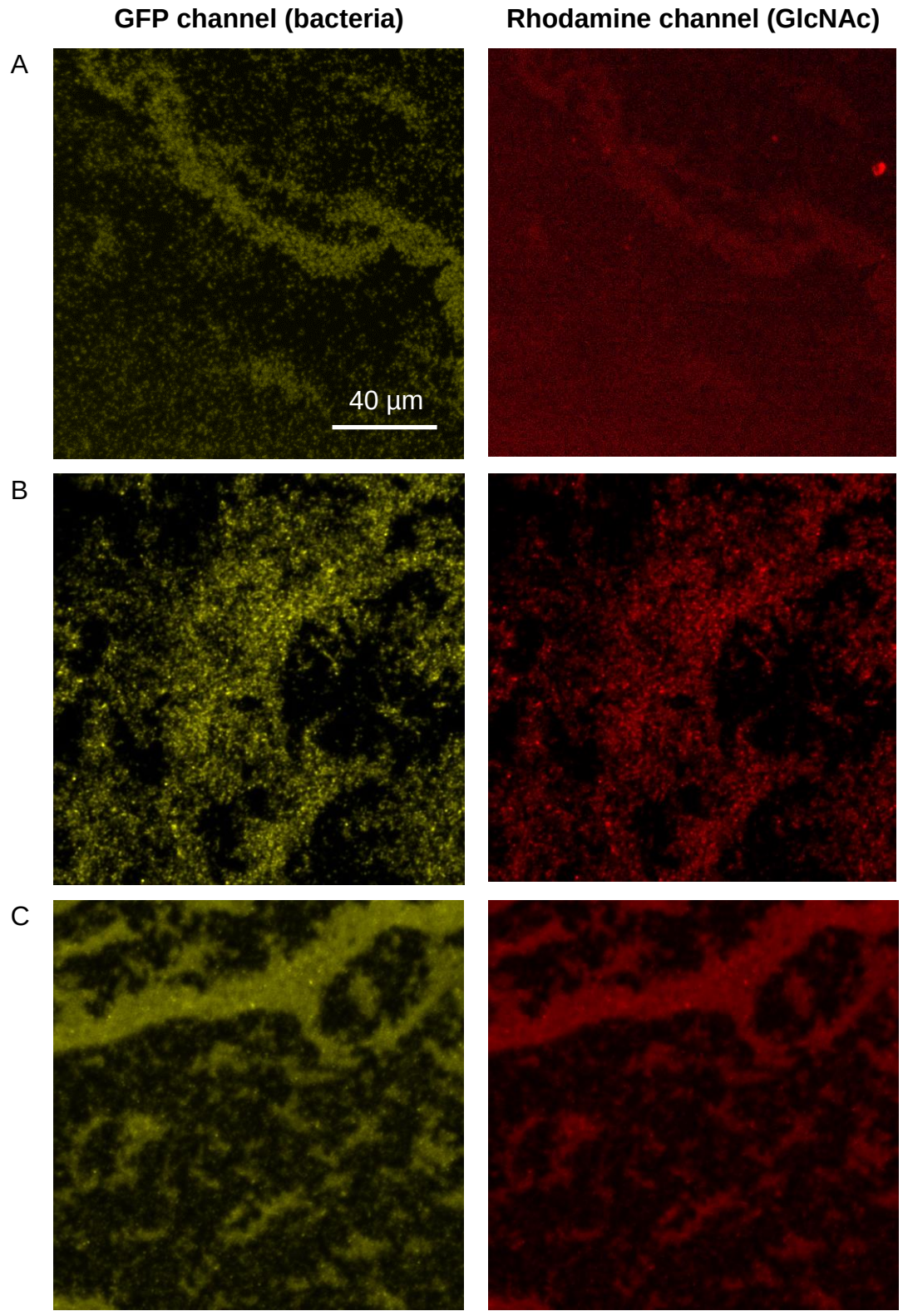

Figure 4.14. Confocal microscopy images showing the production of WGA stained poly-GlcNAc by GFP-labelled *Y. pseudotuberculosis* at 22ºC. A) parent strain, B) Δ*nagC* and C) complemented Δ*nagC* strain. All strains show similar levels of GlcNAc production at 22ºC. Taken at 10x.

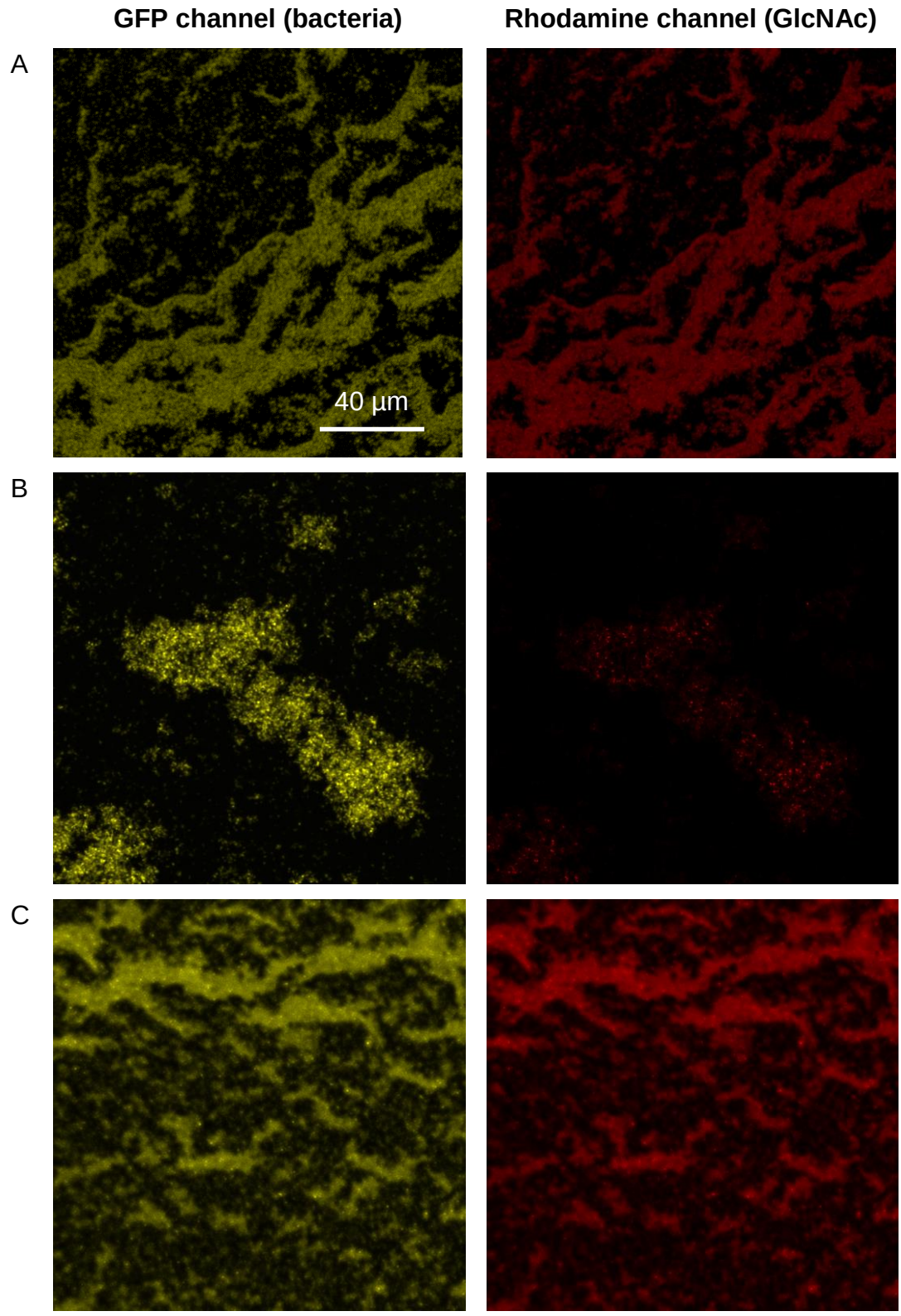

Figure 4.15. Confocal microscopy images showing the production of WGA stained poly-GlcNAc by GFP-labelled *Y. pseudotuberculosis* at 37ºC. A) parent strain, B) Δ*nagC* and C) complemented Δ*nagC* strain. The Δ*nagC* mutant shows approximately two-fold reduction in GlcNAc production at 37ºC. Taken at 10x.

The images obtained from confocal microscopy were processed using Volocity software to find the sum of the mean intensity of rhodamine fluorescence for each strain at both temperatures. Figure 4.16(A) shows no significant differences in rhodamine intensity at 22ºC, suggesting that NagC does not affect GlcNAc production at this temperature. However, at 37ºC, the fluorescence intensity of the Δ*nagC* mutant is 3 times lower than that of the parent strain, and 2.5 times lower than the complemented strain, suggesting that NagC plays a role in poly-GlcNAc regulation in *Y. pseudotuberculosis* at this temperature Figure 4.16(B).

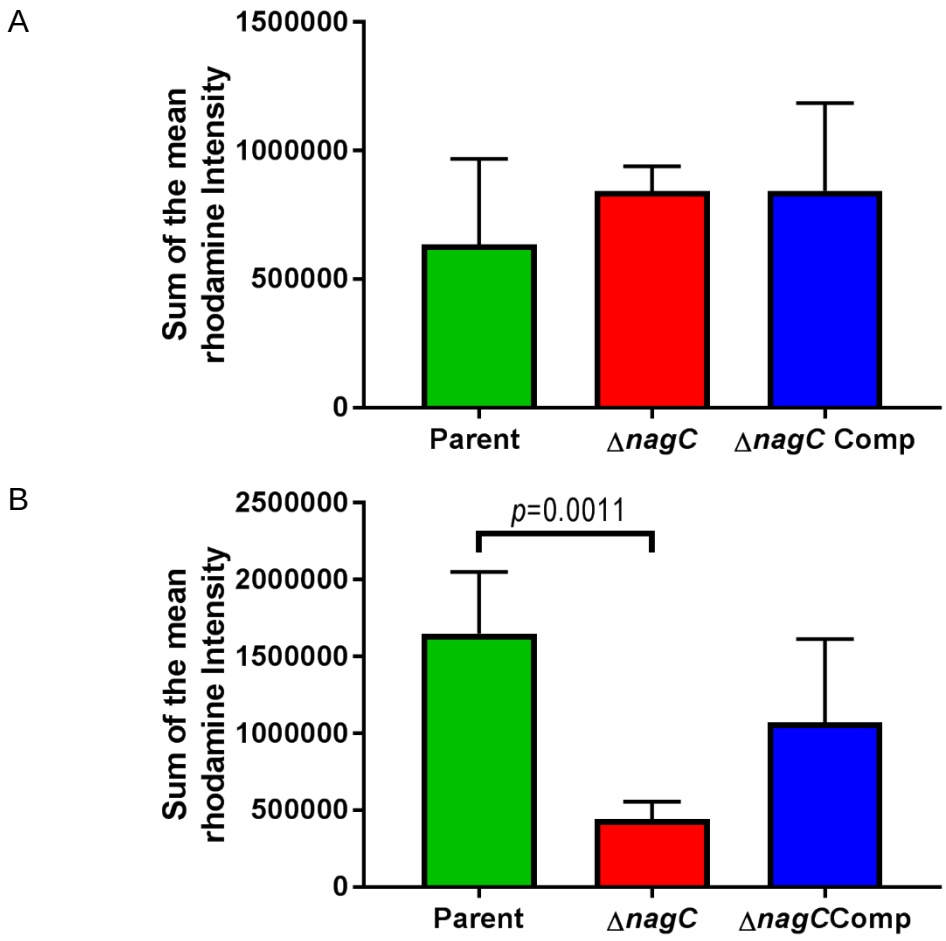

Figure 4.16. Poly-GlcNAc production by *Y. pseudotuberculosis* is affected by NagC at 37ºC, but not 22ºC. The sample size for each was n=3, *P*-values were calculated using one-way ANOVA and Tukey's multiple comparison test. Higher levels of poly-GlcNAc was produced at 37ºC (B) than at 22ºC (A).

Fluorescence intensity was compared for each strain using the same data, as shown in Figure 4.17. The parent strain produced 2.5 times more poly-GlcNAc at 37ºC than it did at 22ºC, whereas production decreased by 2-fold in the Δ*nagC* mutant. The complemented strain increased in line with the parent strain, but not to a significant extent.

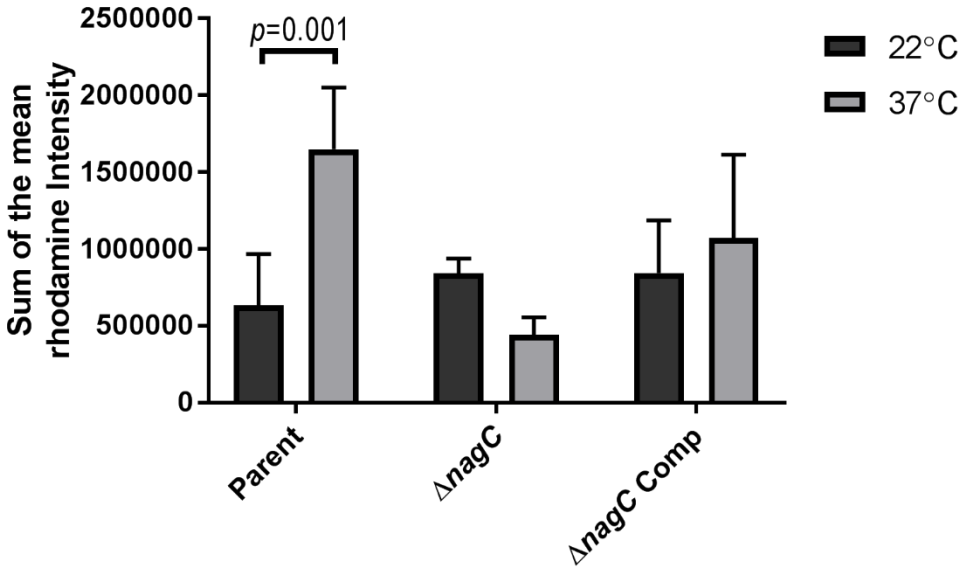

Figure 4.17. Comparison of poly-GlcNAc production by *Y. pseudotuberculosis* parent, Δ*nagC* and complemented Δ*nagC* strains at 22ºC and 37ºC. At 22ºC, all three strains produced similar levels of poly-GlcNAc, whereas at 37ºC, the parent strain produced significantly more and the Δ*nagC* mutant produced less. The sample size for each was n=3, *P*-values were calculated using two-way ANOVA and Sidak's multiple comparison test.

To ensure that the WGA stain was binding specifically to the poly-GlcNAc, 10 mM exogenous GlcNAc was added to the WGA-fluorescent probe and incubated, then processed and imaged as described in section 2.4.4. Figure 4.18 shows that the addition of excess GlcNAc blocks the binding of the fluorescently labelled WGA probe to the poly-GlcNAc produced by *Y. pseudotuberculosis*.

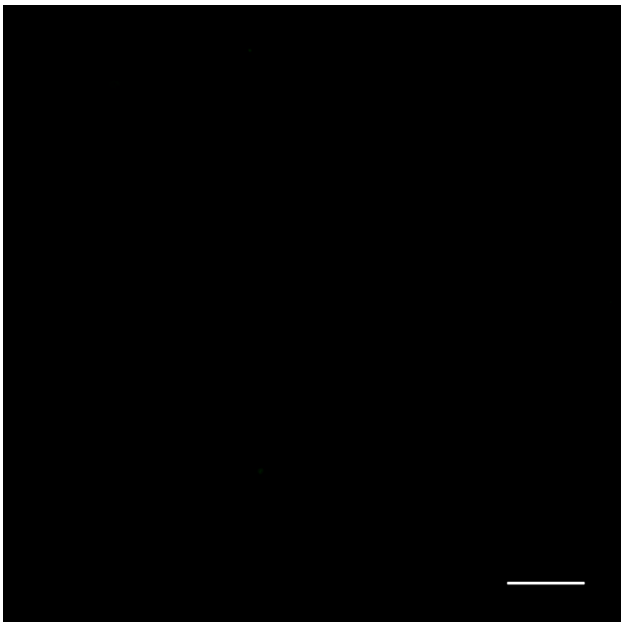

Figure 4.18. GlcNAc control experiment showing that an excess of exogenous GlcNAc blocks the WGA-fluorescent probe from binding to poly-GlcNAc produced by parental *Y. pseudotuberculosis*. Scale bar represents 40 µm.

4.3.3.1 Exogenous GlcNAc Restores the Ability of the *Y. pseudotuberculosis* Δ*nagC* Mutant to Produce Poly-GlcNAc

Exogenous GlcNAc was added to determine whether it restored the ability of the Δ*nagC* mutant to produce poly-GlcNAc. Strains were incubated for 24 h with or without GlcNAc, imaged using confocal microscopy and processed using Volocity as above. Figure 4.19 shows that without additional GlcNAc, the Δ*nagC* mutant produces approximately 3.5 times less poly-GlcNAc, whereas when 1 mM exogenous GlcNAc is added, the ability of the Δ*nagC* mutant to produce poly-GlcNAc is restored back to that of the parent strain.

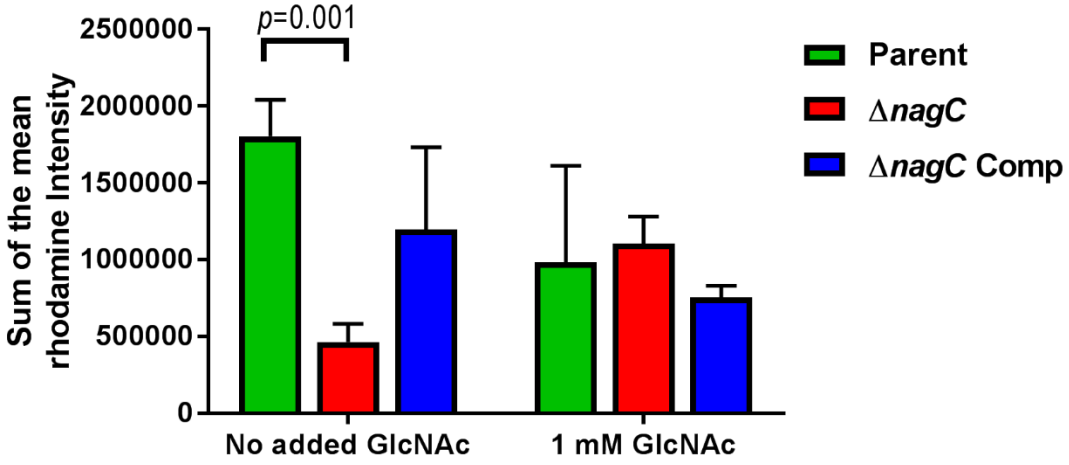

Figure 4.19. Exogenous GlcNAc at 37ºC restores the ability of the Δ*nagC* mutant to produce poly-GlcNAc. The sample size for each was n=3 (biological replicates), *P*-values were calculated using two-way ANOVA and Sidak's multiple comparison test. Attachment was quite variable across the coverslips, which may account for the large error bars.

4.3.4 NagC Binds to the *Y. pestis* Promoters for the GlcNAc Uptake/Catabolism (*nagE-nagBACD),* Biosynthesis *(glmUS)* and poly-GlcNAc Biosynthesis *(hmsHFRS)* Operons

As the Δ*nagC* mutant produces less poly-GlcNAc than the parental strain and NagC is known to act as a transcriptional regulator in *E. coli* and *V. fischeri* (Plumbridge, 1991; Miyashiro *et al.*, 2012), ascertaining the role of NagC in the regulation of GlcNAc metabolism in *Y. pestis* was the next logical step. This required the cloning, expression and purification of a his-tagged *Y. pestis* NagC protein for use in DNA-binding studies (see Appendix images 8.5 and 8.6). Electrophoretic mobility shift assays (EMSA) were undertaken as described in section 2.4.5.3 and by Hellman & Fried (2007). As GlcNAc-6-P is the inducer of NagC binding in *E. coli,* the experiment was repeated with 10 mM GlcNAc-6-P and GlcNAc as a control (Plumbridge, 1991). Since non-denaturing gels are used for EMSAs, a ladder is not used, but sizes of the

probes have been indicated. *Y. pseudotuberculosis* NagC was not tested due to time constraints.

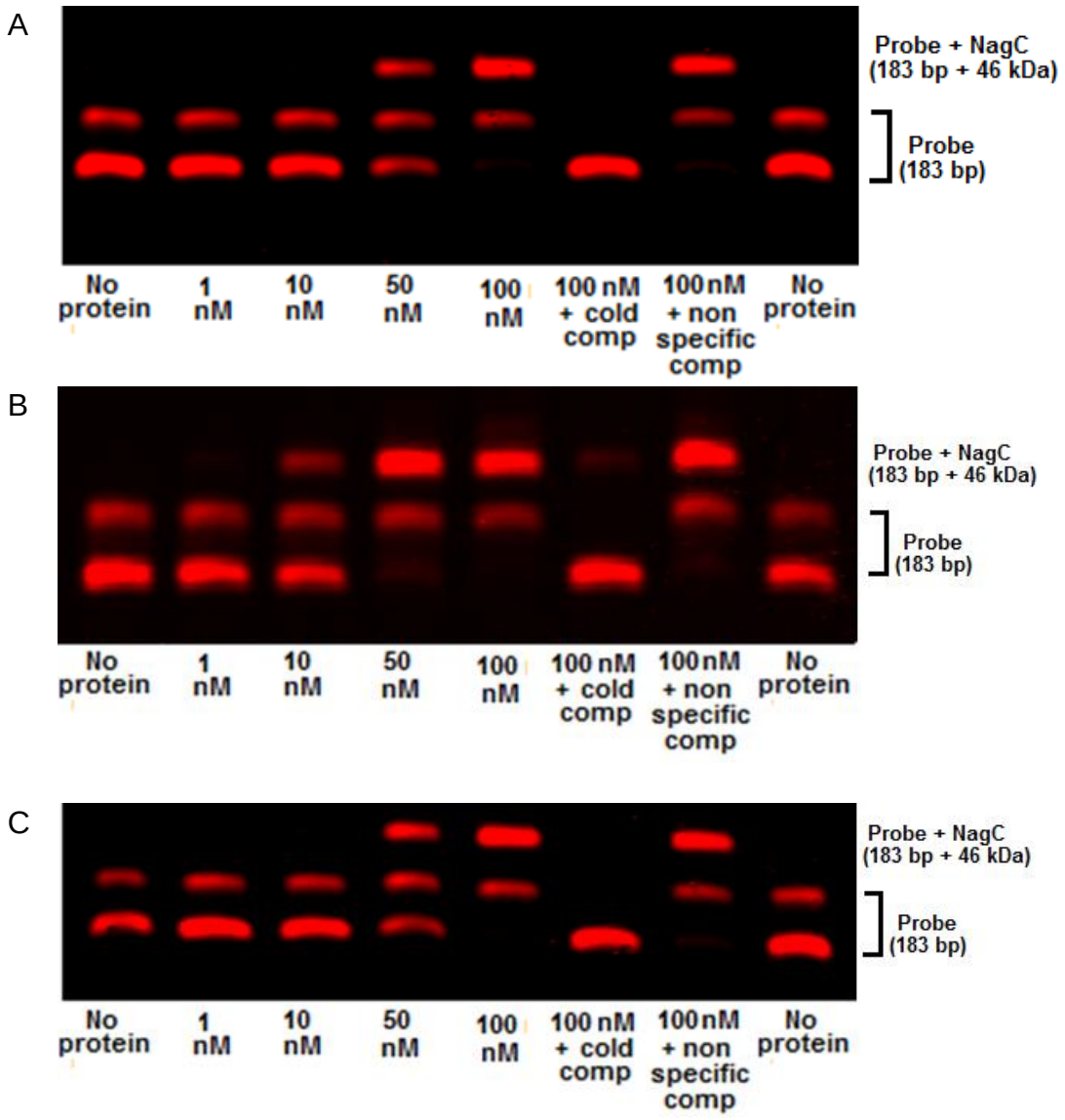

Figure 4.20. Incubation of NagC with a *nagE-nagBACD* promoter probe (183 bp) results in a DNA band shift. At 100 nM of NagC all of the probe had bound to the protein. When incubated in the presence of 500 nM cold DNA competitor, the fluorescent probe was outcompeted and unable to bind to the protein. In the presence of a non-specific DNA competitor, the fluorescent probe was still able to bind, indicating that NagC specifically binds to the *nagE-nagBACD* operon. The presence of 10 mM exogenous GlcNAc-6-P increases binding and enables NagC to bind at lower concentrations. (A) no GlcNAc-6-P, (B) 10 mM GlcNAc-6-P and (C) 10 mM GlcNAc.

Different concentrations between 0.1 and 2000 nM of NagC were incubated with 10 nM *nagE-nagBACD*, *glmUS* and *hmsHFRS* promoter regions to facilitate binding. NagC bound to the *nagE-nagBACD* promoter region in the absence (Figure 4.20(A)) and presence of 10 mM GlcNAc-6-P (Figure 4.20(B)) and 10 mM GlcNAc (Figure 4.20(C)). The addition of GlcNAc-6-P, but not GlcNAc increases affinity and enables NagC to bind at lower concentrations.

100 nM NagC was found to be sufficient for a full band shift and when incubated with 500 nM cold competitor (identical probe without the Cy5, see Table 2.3), the fluorescent probe was outcompeted and remained unbound. When incubated with a non-specific probe (the *nagC* downstream region cloned in section 4.3.1), NagC was still able to bind to the fluorescent *nagE-nagBACD* probe, indicating specific binding. The *nagE-nagBACD* probe ran at two distinct positions on the agarose gel, indicating possible differences in DNA configuration. NagC bound to only one of these bands. This band could not be seen when cold competitor was added, as this fluorescently labelled probe in this configuration represented only a small percentage of the overall DNA concentration (110 nM).

This experiment was repeated with the *glmUS* promoter. Like the *nagE-nagBACD* probe, NagC bound optimally to the *glmUS* probe at 100 nM of protein (Figure 4.21(A)). Two bands were identified when NagC bound to the *glmUS* probe, suggesting that there may multiple binding sites, or that NagC bound as a multimer. The addition of GlcNAc-6-P (Figure 4.21(B)) did not influence the sensitivity, but did increase the intensity of the second band. The addition of GlcNAc (Figure 4.21(C)) did not influence the sensitivity either, but reduced the intensity of the second DNA-protein band.

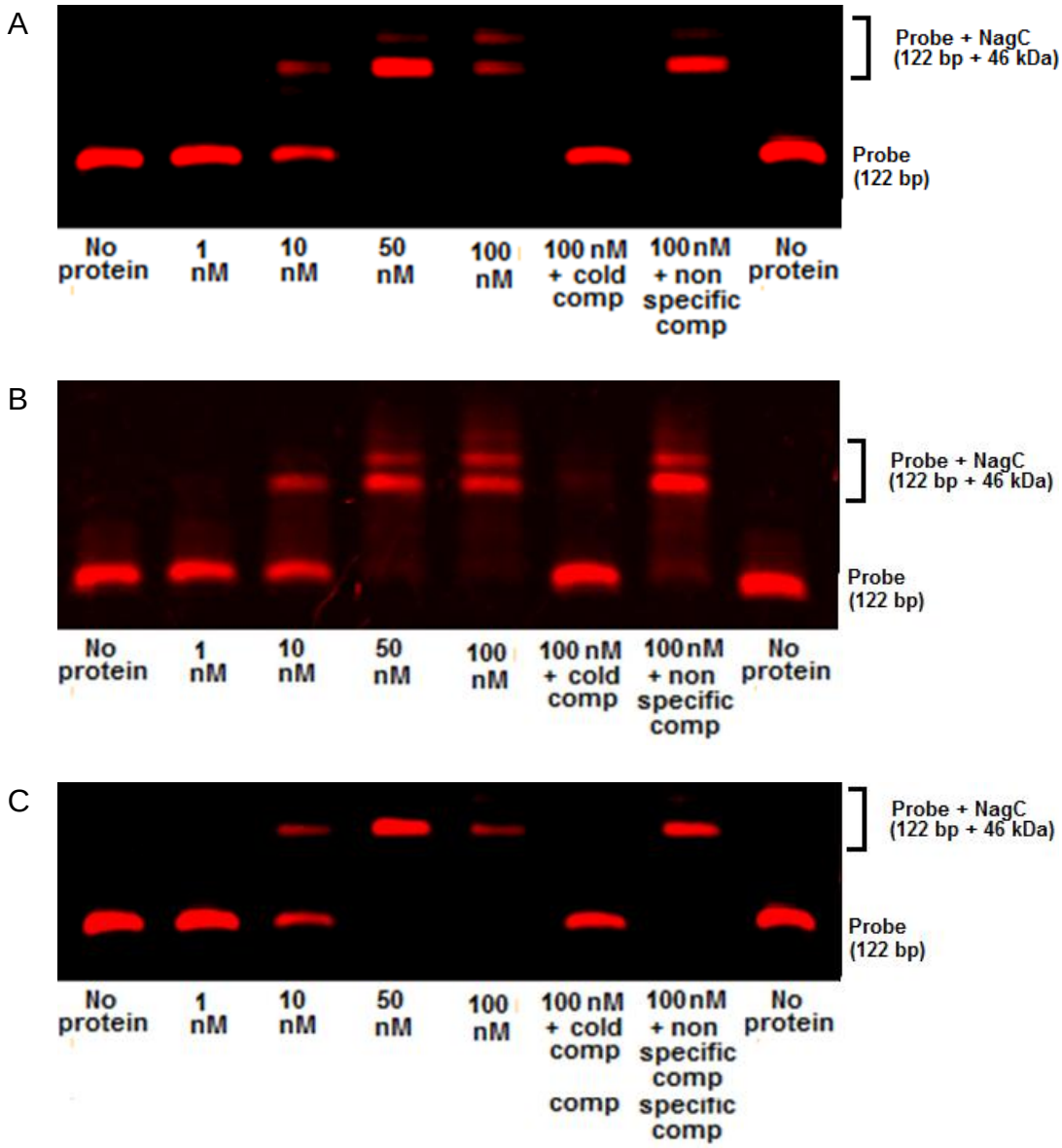

Figure 4.21. Incubation of NagC with a *glmUS* promoter probe (122 bp) results in a DNA band shift. At 100 nM of NagC all of the probe had bound to the protein. When incubated in the presence of 500 nM cold competitor, the fluorescent probe was outcompeted and unable to bind to the protein. In the presence of a non-specific competitor, the fluorescent probe was still able to bind, indicating that NagC specifically binds to the *glmUS* operon. The presence of 10 mM exogenous GlcNAc-6-P does not affect binding but in the presence of GlcNAc the second complex observed in (A) and (B) was less apparent. (A) no GlcNAc-6-P, (B) 10 mM GlcNAc-6-P and (C) 10 mM GlcNAc.

As the RegPrecise database does not provide sequence data, a putative NagC binding site was identified in the upstream region of *hmsHFRS,* a known poly-GlcNAc synthesis operon in *Y. pestis,* using the online SoftBerry BPROM tool

(Figure 4.22) (Darby *et al.*, 2002; Bobrov *et al.*, 2008). The RegPrecise database predicted putative NagC binding sites to be between -151 to -270 bp upstream of the genes. SoftBerry predicted that the putative NagC binding site was -214 bp upstream of *hmsH* in *Y. pseudotuberculosis* and *Y. pestis*.

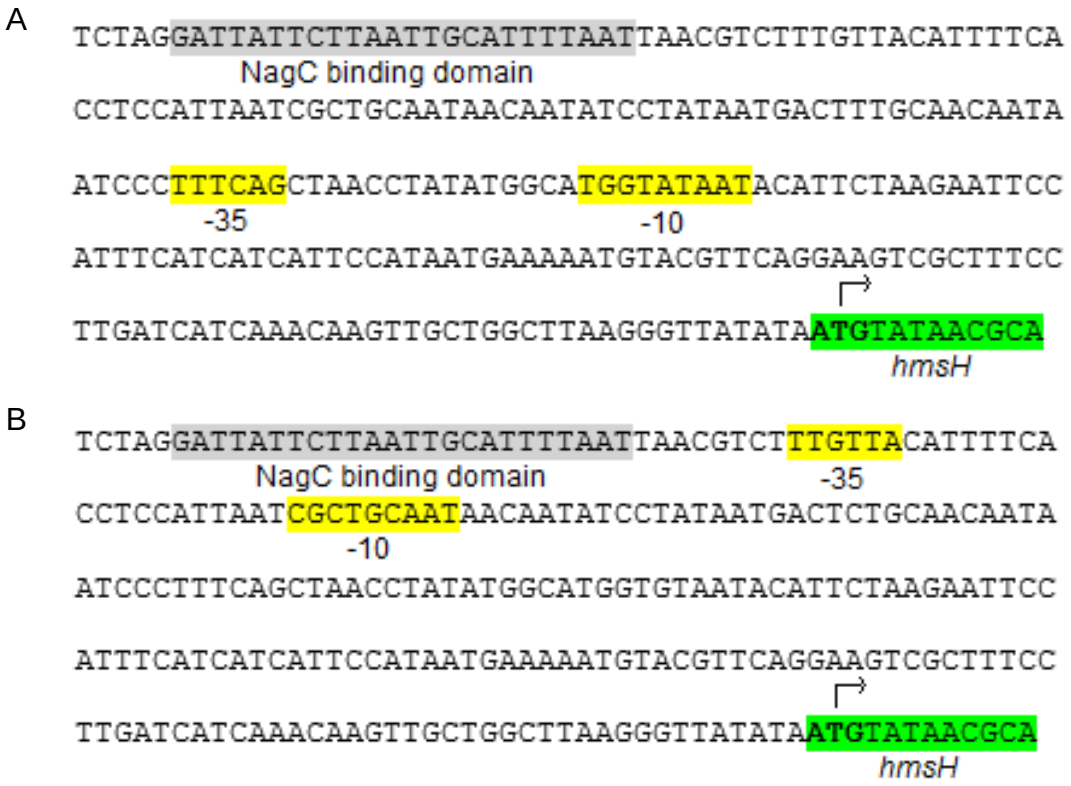

Figure 4.22. Nucleotide sequence for the *hmsHFRS* promoter region in (A) *Y. pestis* and (B) *Y. pseudotuberculosis*. The putative NagC binding site (grey) and -35 and -10 regions (yellow). The translational start codon for the *hmsH* gene (green) is labelled with an arrow.

When this experiment was repeated with *hmsHFRS*, there was no binding of NagC to the probe at 100 nM of protein. Multiple concentrations were tried, from 0.1-2000 nM. The probe band shifted at around 500 nM, indicating a much lower affinity of NagC for the *hmsHFRS* promoter region, but failed to produce a clear band, instead becoming stuck in the well at the top of the gel, potentially forming a large complex and producing a smear.

A

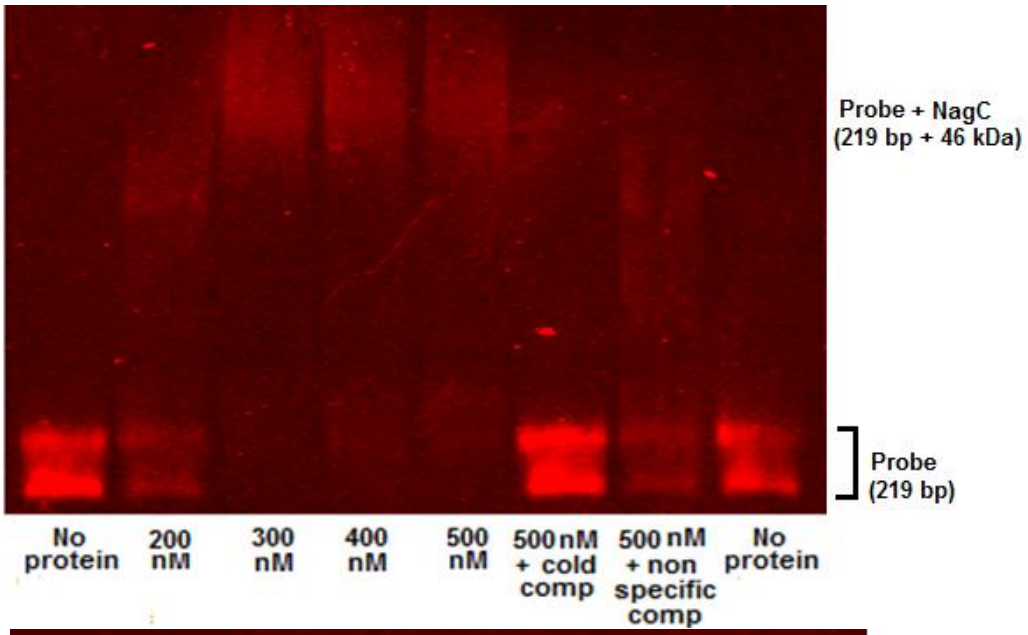
Probe + NagC
(219 bp + 46 kDa)
Probe
(219 bp)
No protein
200 nM
300 nM
400 nM
500 nM
500 nM + cold comp
500 nM + non specific comp
No protein

B

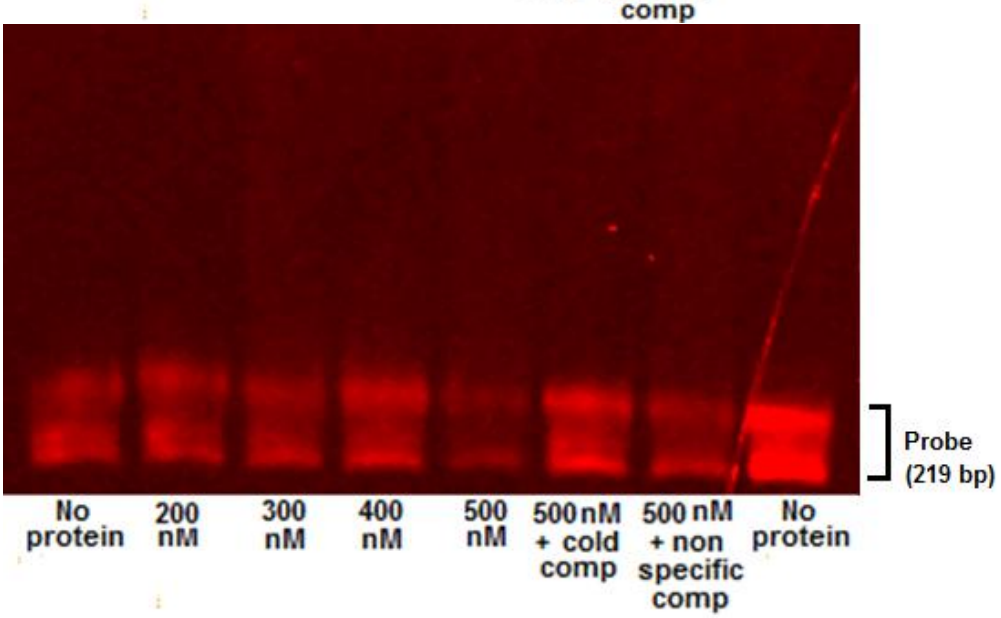
Probe
(219 bp)
No protein
200 nM
300 nM
400 nM
500 nM
500 nM + cold comp
500 nM + non specific comp
No protein

C

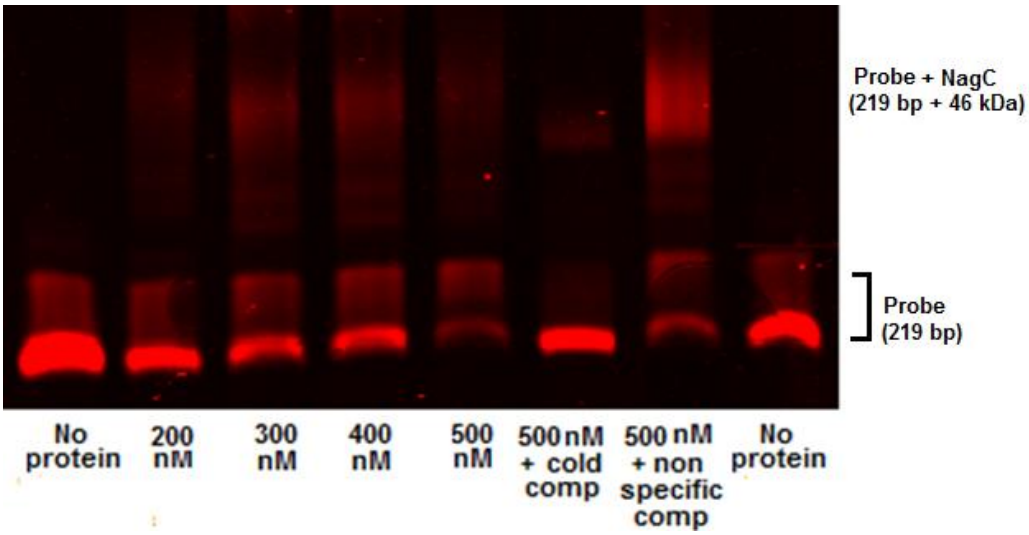

Figure 4.23 Incubation of NagC with the *hmsHFRS* promoter probe (219 bp) results in a DNA band shift. At 500 nM NagC most of the probe bound to the protein. Although band shifts produced a smeared band when incubated in the presence of 500 nM cold competitor, the fluorescent probe was outcompeted and unable to bind to the protein. In the presence of a non-specific competitor, the fluorescent probe was still able to bind, indicating that NagC specifically binds to the *hmsHFRS* operon. The presence of 10 mM exogenous GlcNAc-6-P prevented NagC from binding to the *hmsHFRS* probe. (A) no GlcNAc-6-P (B) 10 mM GlcNAc-6-P (C) 10 mM GlcNAc.

To test whether the band shift was due to NagC binding, 500 nM cold competitor and non-specific competitor was added (Figure 4.23(A)). When an excess of cold competitor was added, the majority of the fluorescent DNA probe remained unbound and when non-specific competitor was added, less fluorescent probe remained unbound, indicating that there was a degree of specific binding of NagC to the *hmsHFRS* probe. When 10 mM GlcNAc6-P (Figure 4.23(B)) but not GlcNAc (Figure 4.23(C)), was added, NagC did not bind to the fluorescent probe, suggesting that, GlcNAc-6-P inhibits the binding of NagC to the *hmsHFRS* operon. The *hmsHFRS* probe also exhibited two DNA configurations like the *nagE-nagBACD* probe, only one of which bound to NagC. The addition of GlcNAc did not influence binding, although did reduce the intensity of the second complex when NagC bound to *glmUS*.

4.4 Discussion

The results of this chapter indicate that NagC has some influence on QS *via* the production of AHLs in *Y. pestis* and *Y. pseudotuberculosis*. NagC appears to have some influence on YOP production in *Y. pseudotuberculosis* and *Y. pestis*, and its loss appears to slow the rate of auto-aggregation in *Y. pseudotuberculosis.* NagC affects the production of poly-GlcNAc in *Y. pseudotuberculosis* at 37ºC but not 22ºC and the addition of exogenous GlcNAc restored the Δ*nagC* mutant to the parental phenotype. For *Y. pestis*, NagC was shown to bind to the promoter regions of the *nagE-nagBACD* and *glmUS* metabolic operons and the *hmsHFRS* poly-GlcNAc biosynthesis operons, indicating that it is a regulator of both GlcNAc metabolism and poly-GlcNAc biosynthesis. The QS system is complex and controlled by many genes, so it is possible that the loss of NagC may be recovered by redundancy *via* other genes and proteins.

There was no difference in the overall production of total AHLs between the parent, Δ*nagC* mutant and complemented Δ*nagC* strains in either *Y. pestis* or *Y. pseudotuberculosis,* however, when individual AHLs were measured, some differences could be seen when C6, C8, Oxo-C6, Oxo-C7, Oxo-C8 and Oxo-C10 were identified using mass spectrometry. The different AHLs each species produces can control different responses, which would suggest that the subtle reductions and increases in AHLs produced by *Y. pestis* and *Y. pseudotuberculosis* in the absence of NagC in this study may have some influence on QS phenotypes, although this appears to be a complex system with many factors involved (Atkinson *et al.*, 1999; Götz-Rösch *et al.*, 2015).

When *Y. pestis* YOPs were extracted, the Δ*nagC* mutant was shown to overexpress YopM, YopB, YopE and YopD in *Y. pseudotuberculosis*, indicating that NagC may play a role in virulence phenotypes. In *Y. pestis*, YopB was highly overexpressed in the Δ*nagC* mutant, although the overall YOP expression picture appears to be more complicated than for *Y. pseudotuberculosis*, which may be explained by the fact that *Y. pestis* YOPs are degraded *in vitro* as described by Mehigh and Sample (1989), but still showed the same profile as *Y. pseudotuberculosis*. As YOPs are not induced at 22ºC, they are unlikely to play a vital role in the survival of *Y. pestis* within the flea host (Perry, 2003). The Δ*nagC* complemented strains overexpressed (*Y. pseudotuberculosis*) and underexpressed (*Y. pestis*) YOPs compared with the parental strain. That they were constructed in differing ways (*Y. pseudotuberculosis* using the Tn7 insertion system and *Y. pestis* using pHG327) may account for the variation in YOP production.

The *Y. pseudotuberculosis* Δ*nagC* mutant auto-aggregated more slowly than the parental strain, which potentially contradicts the results of Wiechmann (Ph.D. Thesis, 2015), who states that the Δ*nagC* mutant enhances auto-aggregation in *Y. pseudotuberculosis*. However, whereas Wiechmann's study used microscopy to identify density of aggregations, it did not look at aggregation rate, so the two studies are not identical. The fact that *Y. pestis* was not shown to form aggregates at 37ºC agrees with Felek (2010) and Rosqvist's (1988) suggestions that Caf1 and a mutation in YadA may inhibit the ability of *Y. pestis* to form aggregations at mammalian body temperature. That it did not aggregate at 22ºC would suggest that either aggregation is not the precursor to biofilm formation or, more likely, there are factors in the flea

gut or blood meal that may mediate aggregation. It has been suggested that although poly-GlcNAc is not initially part of the aggregations found in early infection of flea guts and that bacterial aggregations do not form around a fibrin complex, components from the blood meal are likely to be incorporated into the extracellular matrix as the biofilm matures (Hinnebusch, Fischer and Schwan, 1998; Jarrett, Sebbane, *et al.*, 2004; Chouikha and Hinnebusch, 2012; Hinnebusch, Jarrett and Bland, 2017). It is possible that the degradation of YOPs *in vitro* affects the ability of *Y. pestis* to auto-aggregate, as aggregation has been shown to be a T3SS-mediated phenotype (Anja Wiechmann, Ph.D. Thesis, 2015). Mutations in the T3SS genes *lcrV*, *yscF* and *yscJ* inhibit auto-aggregation and YOP secretion (Barrett, Ph.D. Thesis, 2018). Whilst the results of this study suggest that NagC does not influence *Yersiniae* auto-aggregation under the conditions tested, the Δ*nagC* mutant was shown to slow aggregation in *Y. pseudotuberculosis* in comparison with *Y. pestis* at 37ºC. This furthers research completed by Wiechmann (Ph.D. Thesis, 2015) and indicates that NagC may in fact play a role in the auto-aggregation of *Y. pseudotuberculosis* in the mammalian infection process. The results of this chapter suggest that poly-GlcNAc may assist in the auto-aggregation mechanism of *Y. pseudotuberculosis*, as we have also shown that the Δ*nagC* mutant produces less poly-GlcNAc, although there is not a complete cessation of production. It is therefore possible that this is the reason behind the decrease in the auto-aggregation rate in the *Y. pseudotuberculosis* Δ*nagC* mutant (Petrova and Sauer, 2012).

The results from this chapter show that *Y. pseudotuberculosis* produces more poly-GlcNAc at 37ºC compared to 22ºC. This is likely to be due to *Y.*

pseudotuberculosis requiring biofilm more at mammalian temperatures than in the soil to aid host infection (Atkinson *et al.*, 2008). For *Y. pestis*, it appears to be unclear whether it produces more poly-GlcNAc at 22ºC compared to 37ºC. Erickson *et al.* (2008) suggested that it is likely to be maximal at flea temperatures, as *Y. pestis* requires biofilm to block the insect host and thus be transmitted more effectively. However, another study suggests that *Y. pestis* KIM and CO92 strains produce more at mammalian temperatures and only avirulent strains produce maximal poly-GlcNAc at flea temperature (Yoong, Cywes-Bentley and Pier, 2012). As previously stated, it is likely that, especially during the early phase of mammalian infection, biofilms would be detrimental to the dissemination of bacteria though the lymphatic system, although the production of poly-GlcNAc and therefore biofilm may be important for *Y. pestis* to avoid destruction by the mammalian immune system (Erickson *et al.*, 2008; Felek *et al.*, 2010; Yoong, Cywes-Bentley and Pier, 2012).

In *E. coli*, NagC directly binds to the promoter regions of the *nagE-nagBACD* and *glmUS* operons, responsible for GlcNAc degradation and synthesis respectively (Plumbridge, 1991). This study set out to identify whether this was the case in *Y. pestis*, plus whether it bound to the *hmsHFRS* promoter, responsible for poly-GlcNAc production and biofilm formation (Lillard *et al.*, 1997). This chapter showed that NagC bound to the promoter regions of *nagE-nagBACD*, *glmUS* and *hmsHFRS*, indicating that NagC may play a similar DNA binding role in *Y. pestis* as it does in *E. coli* and other organisms (Plumbridge, 1995; Sun *et al.*, 2015).

The addition of GlcNAc-6-P resulted in an apparent increase in the affinity of the *Yersinia* NagC for the *nagE-nagBACD* promoter region. This is an

unexpected finding given that NagC from *E. coli* acts as a repressor at the *nagE-nagBACD* promoter which is de-repressed by GlcNAc-6-P such that on an EMSA, no band shifts are is observed (Pennetier, Domínguez-Ramírez and Plumbridge, 2008). In contrast to *E. coli* where two protein DNA complexes are observed on EMSAs when NagC binds to the *nagE-nagB* intergenic region (Pennetier, Domínguez-Ramírez and Plumbridge, 2008), only one complex was observed for *Yersinia* (Figure 4.19) Further work will be required using *nag* promoter fusions and DNA footprinting to confirm that the regulation of *nagE* and *nagBACD* by NagC in *Yersinia* is different from that in *E. coli*.

Although the EMSA results were not as definitive for the *hmsHFRS* probe as for the *nagE-nagBACD* and *glmUS* probes, the use of cold and non-specific DNA competitor controls and the identification of the NagC binding domain *in silico* indicate that NagC bound specifically to the promoter region of the *hmsHFRS* operon. This new link between NagC and *hmsHFRS* suggests an important role for NagC in the complex genetic regulation of biofilm formation of *Y. pestis* in the mammalian host and insect vector (Lillard *et al.*, 1997). The addition of GlcNAc-6-P, but not GlcNAc, increased the ability of NagC to bind to the *nagE-nagBACD*, but did not affect binding to *glmUS*. The addition of GlcNAc-6-P prevented NagC from binding to the *hmsHFRS* promoter region.

As this chapter has demonstrated a DNA binding role for NagC in *Y. pestis*, we propose the following actions of NagC on the GlcNAc metabolism. In the absence of GlcNAc-6-P, NagC represses the *nagE-nagBACD* operon, which internalises and degrades extracellular GlcNAc, and switches on the *glmUS* and *hmsHFRS* operons, which produce GlcNAc and poly-GlcNAc respectively. In the presence of GlcNAc-6-P, it is likely that *nagE-nagBACD* is de-repressed

and the *glmUS* and *hmsHFRS* operons inhibited. This is shown schematically in Figure 4.24.

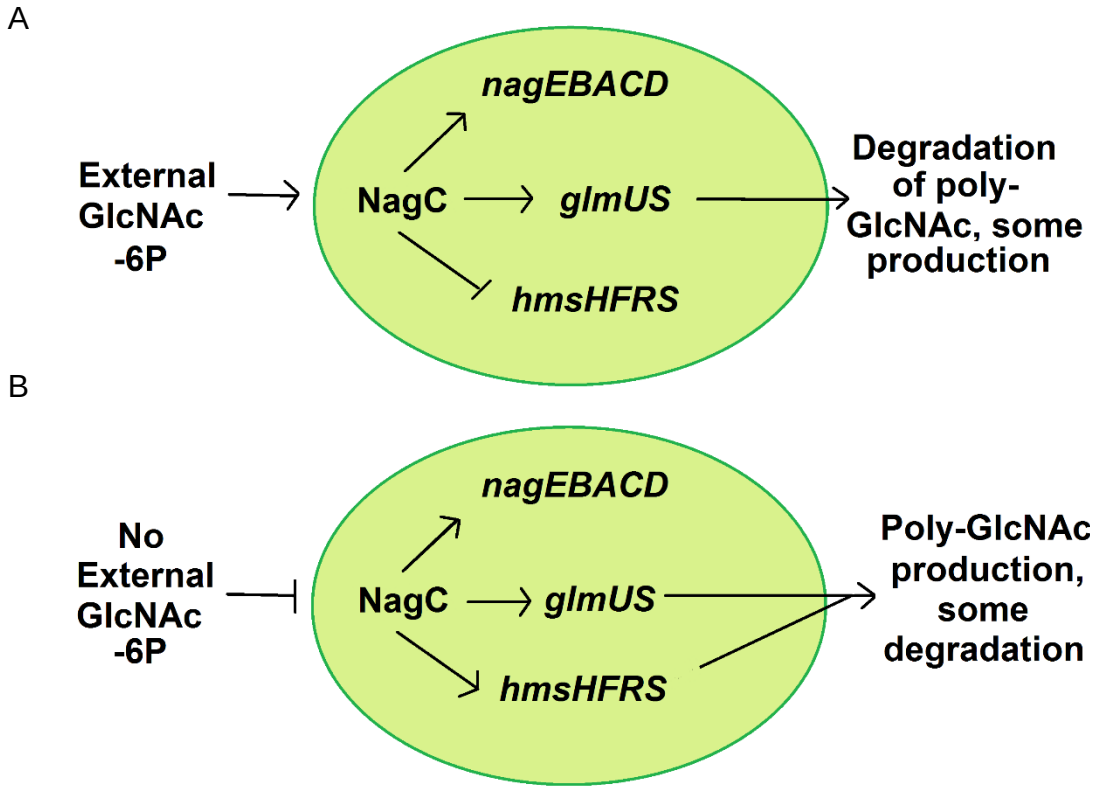

Figure 4.24. Schematic diagram of the NagC regulation of the *nagE-nagBACD*, *glmUS* and *hmsHFRS* operons in the presence and absence of external GlcNAc-6-P in *Y. pestis*. (A) When there is external GlcNAc-6-P present, NagC is likely to de-repress the *nagE-nagBACD* operon which degrades GlcNAc-6-P and repress the *glmUS* and *hmsHFRS* operons. (B) When there is no external GlcNAc-6-P present, *nagC* represses the *nagE-nagBACD* operon, preventing GlcNAc-6-P degradation and switches on the *glmUS* and *hmsHFRS* operons, enabling the production of GlcNAc for cell wall peptidoglycan biosynthesis and poly-GlcNAc.

4.4.1 Summary

After cloning and complementing a Δ*nagC* mutant in *Y. pestis*, it can be concluded that:

- NagC does not affect the overall production of the total *Y. pestis* or *Y. pseudotuberculosis* AHL QS signal molecules although does affect production of specific AHLs, such as Oxo-C10-AHL
- A lack of NagC promotes overexpression of YOPs for *Y. pseudotuberculosis* at 37ºC, as well as influencing YOP expression in *Y. pestis* at 37ºC
- NagC has no effect on the ability of *Y. pestis* to auto-aggregate at either 22ºC or 37ºC
- NagC slows auto-aggregation at 37ºC in *Y. pseudotuberculosis*
- NagC influences the amount of poly-GlcNAc *Y. pseudotuberculosis* produces at 37ºC
- NagC is a DNA binding protein that binds to the *nagE-nagBACD, glmUS* and *hmsHFRS* promoters in *Y. pestis*
- The addition of GlcNAc-6-P increases the binding of NagC to the *nagE-nagBACD* promoter region and blocks binding of NagC to the *hmsHFRS* promoter region. It does not affect the ability of NagC to bind to the *glmUS* promoter region in *Y. pestis*.

5 Development of *In Vivo* and *In Vitro* Insect Models to Study the Role of NagC in Biofilm Formation in the *Yersiniae*

5.1 Introduction

The results presented in Chapter 3 show that developing artificially fed insect colonies is extremely complex and time consuming. In addition to difficulties obtaining GMO licences, the use of established alternative models such as *C. elegans*, alongside insect infection assays using CL2 *Y. pseudotuberculosis* are practical alternatives. *C. elegans* has been a useful model host for studying the virulence of human pathogens (Tan and Darby, 2006; Roberts and Janovy, 2009). In the *Yersiniae*, it has been used to investigate mechanisms of biofilm formation on a living surface (Epstein and Shakes, 1995; Darby *et al.*, 2002; Styer *et al.*, 2005). Biofilms are especially important for *Y. pestis*, as they are required for the blockage of the flea proventriculus, and thus transmission of plague (as reviewed in Zhou & Yang 2011). Studies conducted by Derby *et al.* (2002) have shown that both *Y. pestis* and certain strains of *Y. pseudotuberculosis* can form biofilms on *C. elegans* and that mutations in the *hmsHFRS* operon will render them unable to form a biofilm. Given that Chapter 4 showed that NagC binds to the *hmsHFRS* operon promoter, the deletion of *nagC* is likely to impact on the ability of *Y. pestis* to form biofilm on *C. elegans*. *Y. pseudotuberculosis* strains are not usually capable of forming biofilms on *C. elegans*, although the YPIII strain has a mutation in *phoP*, which enables it to produce biofilm (Pisano *et al.*, 2014). For *Y. pseudotuberculosis* YPIII, QS is required for biofilm formation on *C. elegans,* as double AHL synthase mutants *(ΔypsI/ΔytbI*) and AHL response regulator mutants (*ΔypsR/ΔytbI*) cause severe reduction and delay in biofilm development (Atkinson *et al.*, 2011; Joshua, Atkinson, Robert J. Goldstone, *et al.*, 2015). AHLs were present in the

biofilms on *C. elegans*, which further implicates a role for QS in biofilm formation. The loss of NagC significantly reduces the ability of *Y. pseudotuberculosis* to form biofilms on the surface of *C. elegans* and the addition of exogenous GlcNAc restored biofilm production back to parental levels (Wiechmann, Ph.D. Thesis, 2015). Given these results in *Y. pseudotuberculosis*, it made sense to explore the contribution of NagC to biofilm formation of *Y. pestis* on *C. elegans*.

5.1.1 Fleas and Experimental *Yersinia* Infections

The colonisation of fleas by *Y. pestis* has been studied extensively but the use of fleas in *Y. pestis* transmission experiments is challenging, to the extent that many modern research groups rely on the avirulent pCD1 negative strains such as KIM6+ (Hinnebusch, 2005; Yoong, Cywes-Bentley and Pier, 2012). The role of biofilms in the blockage of fleas has been studied mainly by the manipulation of the poly-GlcNAc synthesising *hmsHFRS* operon (Hinnebusch, Perry and Schwan, 1996) and to date, there is no literature on the role of NagC in *Y. pestis*, or its contribution to biofilm formation/regulation in insect vectors. *Y. pseudotuberculosis*, including YPIII, has not been shown to form biofilms within the flea vector. Rather than colonising the gut of the insect like *Y. pestis*, it is not thought to multiply, instead causing acute diarrhoea, resulting in the expulsion of the bacteria and often causing death of the flea (Erickson *et al.*, 2006, 2007). This appears to involve expression of the poly-GlcNAc hydrolase NghA by *Y. pseudotuberculosis* that is absent from *Y. pestis* and may interfere with biofilm formation and colonisation in insect vectors (Erickson *et al.*, 2008).

Due to complications with GMO licencing, this study was unable to undertake the intended *in vivo Y. pestis* insect infection studies. Instead, an *in vitro* chitin-based attachment model was developed using *Y. pseudotuberculosis* to mimic the flea gut environment, which could then be transferred to a CL3 environment to study *Y. pestis*-chitin interactions in future. The flea proventriculus is made of cuticle, similar to the exoskeleton, which is composed of a network of secreted proteins and chitin (Hinnebusch, 1997). To accurately model the proventriculus, it is important to consider the other substances which may be present. As Hinnebusch (2017) has shown that gut epithelial cells do not appear to be involved in bacterial colonisation, but that blood components are thought to contribute to the aggregation of *Y. pestis* in early stage infections, it was important to ascertain whether blood factors affect the ability of the *Yersiniae* to adhere to and proliferate on a chitinous surface. Blood serum, which is part of the blood meal, is known to increase bacterial attachment and thus may be important in the attachment of *Y. pestis* to the proventriculus (Gallardo-Moreno *et al.*, 2002; Hinnebusch, Jarrett and Bland, 2017).

5.1.2 Lice and Experimental *Yersinia* Infection

Due to the primary focus on fleas as vectors for *Y. pestis* transmission, there have been relatively few studies on other potential insect vectors, such as human lice. There have been several case studies published regarding naturally *Y. pestis*-infected human lice, most of which are reported from Africa, suggesting that lice can transmit or at least contract plague from an infected host. Reports from the Democratic Republic of the Congo have shown human

lice to be vectors of epidemic typhus, trench fever, relapsing fever and, rarely, also *Y. pestis* (Drali *et al.*, 2015)**.** Experimental louse-plague models have also been conducted. Lice were fed on infected rabbits, then allowed to feed on uninfected animals, showing that they were capable of transmitting plague to naïve rabbits, and also of excreting viable *Y. pestis* in their faeces, although there was a high louse mortality rate and they were unable to lay eggs, suggesting that *Y. pestis* infections are highly detrimental to louse survival (Houhamdi *et al.*, 2006).

The infection of *P. corporis* with *Y. pseudotuberculosis* has received very little attention and the role of biofilm in infection remains to be investigated. It is known that infection with *Enterobacteriaceae* mostly causes the death of the lice within 48 h and that *Y. pseudotuberculosis* kills 60 - 70% of *P. corporis* when administered intrarectally, although some individuals were able to clear the infection (Krynski and Becla, 1965). The virulence mechanisms employed by *Y. pseudotuberculosis* during lice infections are not known and the role of poly-GlcNAc or NagC in regulating virulence biofilm formation in the louse is also unknown.

5.2 Specific Research Aims

Much of the known insect vector-*Y. pestis* biofilm research has focused on the *hmsHFRS* operon, and as this study has shown that NagC binds to the promoter of *hmsHFRS*, investigating the impact of NagC on biofilm formation in insect models is an important next step. Given this knowledge, and that previous work by Wiechmann (Ph.D. Thesis, 2015) showed that NagC reduced

the ability of *Y. pseudotuberculosis* to form biofilms on *C. elegans*, it is important to determine whether NagC plays a role in the colonisation of insect vectors and subsequent biofilm formation by the *Yersiniae*.

Testing the Δ*nagC Y. pestis* mutant in the *C. elegans* model and developing an *in vitro* 'fake flea proventriculus' using *Y. pseudotuberculosis* would help to further elucidate the role of NagC in controlling attachment and biofilm formation. The mechanisms through which a human body louse can transmit plague are not well understood, and whether NagC and biofilm formation play a role in its interaction with *Y. pseudotuberculosis* or *Y. pestis* has not yet been investigated. This study aims to infect *P. corporis* with *Y. pseudotuberculosis* in an attempt to understand this relationship.

Although the previous chapter showed that NagC had no effect on QS phenotypes in *Y. pestis*, the corresponding *Y. pseudotuberculosis* Δ*nagC* mutant exhibited a reduction in poly-GlcNAc production. Work by Wiechmann (Ph.D. Thesis, 2015) has previously shown that for *Y. pseudotuberculosis* YPIII, the Δ*nagC* mutant is significantly impaired in biofilm production on *C. elegans*. As *C. elegans* has been used as a biofilm model for *X. cheopis* blockage, it was important to utilise this established model to test the *Y. pestis* Δ*nagC* mutant (Darby *et al.*, 2002; Styer *et al.*, 2005).

Much previous research on *Y. pestis* interactions with insects has been undertaken with attenuated strains, but this study aimed to use the fully virulent CO92 strain. This posed problems, as there is little information in the literature regarding CL3 methodology concerning insect experiments. Due to the constraints of live insect work, a 'fake flea proventriculus' chitin substrate

model was developed using *Y. pseudotuberculosis*, to aid future understanding of the interaction of *Y. pestis* with chitin surfaces.

In this study, a Δ*nagC* deletion mutant was used to ascertain:

- The contribution of NagC to *Y. pestis* biofilm formation and colonisation of *C. elegans*

A ‘fake flea’ chitin model was also developed for *Y. pseudotuberculosis* to provide an *in vitro* version of the flea proventriculus to study the *Y. pestis* - chitin interaction. The following parameters were examined to establish the optimal conditions:

- Type of chitin substrate
- The length of incubation time
- The type of growth medium used to incubate the cultures
- The addition of serum
- The addition of paraformaldehyde as a fixative for CL3 work

Once optimal conditions were ascertained, the ‘fake flea’ model was then used to determine the role of:

- NagC in biofilm formation on a chitin surface

The role of NagC has not been studied in relation to the colonisation of *P. corporis* by the *Yersiniae*. GFP-tagged *Y. pseudotuberculosis* was used to:

- Determine the localisation of *Y. pseudotuberculosis* in infected *P. corporis*

- Investigate the impact of mutating *nagC* on infection of *P. corporis* with *Y. pseudotuberculosis*

5.3 Results

5.3.1 The Impact of Mutating *nagC* on *Y. pestis* Biofilm Formation on *C. elegans*

5.3.1.1 Fewer *Y. pestis* are Required for *C. elegans* Biofilm Assays Compared to *Y. pseudotuberculosis*

As NagC is a regulator of GlcNAc in both *E. coli* and in *Y. pestis* (Chapter 4), and poly-GlcNAc is the chief constituent of the exopolysaccharide component of the ECM of *Yersiniae* biofilms (Titgemeyer *et al.* 1994; Bobrov *et al.* 2008), it was important to establish whether deleting *nagC* would affect the *Y. pestis* biofilm phenotype. It has also been shown that QS expression in *Y. pseudotuberculosis* is influenced by NagC and that the AHL deletion mutant Δ*ypsI*/Δ*ytbI* produces less biofilm on *C. elegans* (Atkinson *et al.*, 2011).

To investigate biofilm formation on *C. elegans*, the *Y. pestis* CO92 parent, Δ*nagC* mutant, parent + pHG327 and genetically complemented Δ*nagC* strains were plated onto NGM media, then *C. elegans* were placed onto the plates. *Y. pseudotuberculosis* YPIII parent, Δ*nagC* and complemented Δ*nagC* experiments were run in parallel as a comparison. *C. elegans* were examined for biofilm formation after 24 h and scored using the biofilm severity index (BSI)

method, as described in Section 2.4.6.2 (Atkinson *et al.* 2011; Wiechmann, Ph.D. Thesis, 2015).

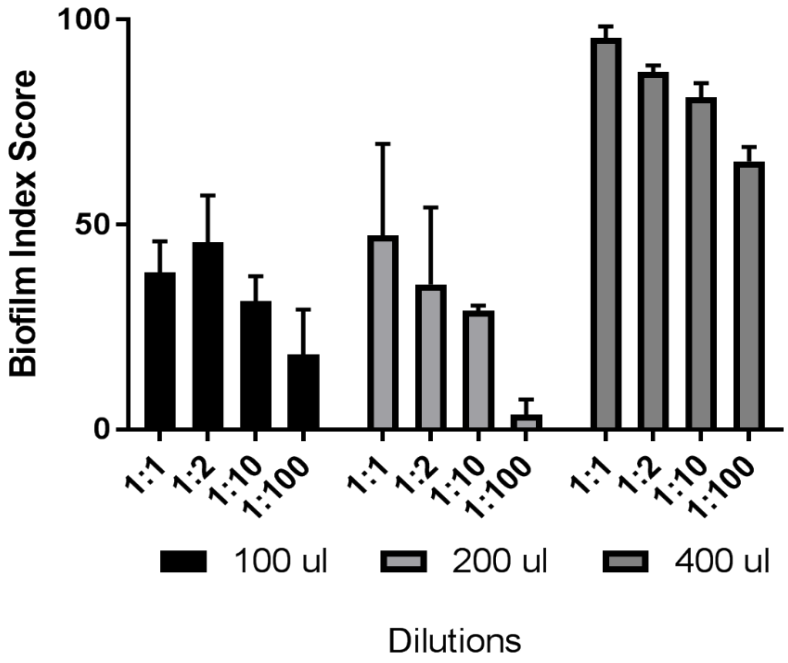

Figure 5.1. Biofilm severity index scores for the calibration assay of *Y. pestis* on *C. elegans*. An OD_{600} of 0.4 was used and dilutions of 1:1, 1:2, 1:10 and 1:100 and volumes of 100, 200 and 400 µl were tested. Undiluted overnight cultures of 400 µl were used for subsequent experiments. The sample size was n=3 (biological replicates).

Calibration of the assay was required for *Y. pestis*, as the OD_{600} needed for *Y. pseudotuberculosis* (OD_{600} 1.0) to form biofilms was too high for *Y. pestis*, which, at that density, overwhelmed and killed most of the worms with biofilm (Atkinson *et al.*, 2011). Various dilutions were tried and 400 µl of undiluted overnight culture at an OD_{600} 0.4 was found to provide the most reproducible results (see section 2.4.6.2) and was used for subsequent *Y. pestis* experiments (see Figure 5.1).

5.3.1.2 NagC is Important for *Y. pestis* Biofilm Formation on *C. elegans*

When repeated in this study, the *Y. pseudotuberculosis* YPIII parent strain did form some biofilm, mainly on the anterior and tail of *C. elegans*, which agrees with the results obtained by Wiechmann (Ph.D. Thesis, 2015) Atkinson *et al.* (2011) and Joshua *et al.* (2015). In comparison, the Δ*nagC* mutant did not appear to produce biofilm on any of the worms and had a biofilm severity index (BSI) score of 0.

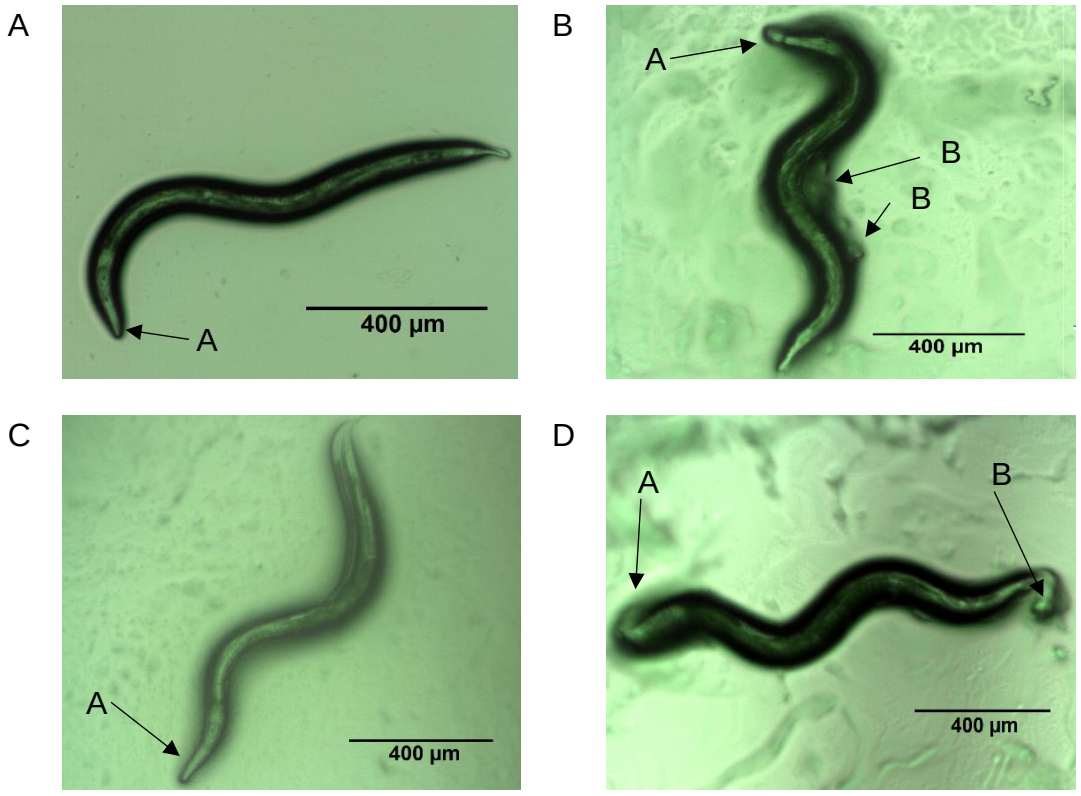

Figure 5.2. Biofilm formation on *C. elegans* by *Y. pseudotuberculosis.* (A) shows a negative control *C. elegans*, fed with *E. coli* OP50, (B) shows *C. elegans* with *Y. pseudotuberculosis* parent strain, (C) shows *C. elegans* with the Δ*nagC* strain and (D) shows a worm with biofilm from the complemented Δ*nagC* strain, all at 10x magnification. Arrows labelled A indicate the anterior of the worm. Arrows labelled B indicate biofilm.

Complementing the Δ*nagC* mutant restored biofilm formation and BSI score to a similar level to the parent strain. Figure 5.2 shows images of *Y. pseudotuberculosis* biofilms on *C. elegans* taken on the AMG Evos® xl core digital microscope using a 10x lens. Figure 5.3 shows the BSI scores for *Y. pseudotuberculosis* which are approximately 20% for the parent and complemented Δ*nagC* strain, but 0% for the Δ*nagC* mutant.

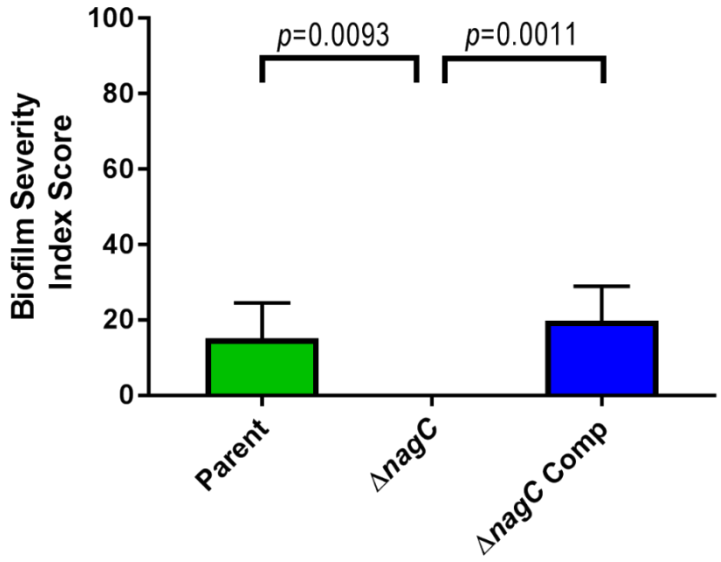

Figure 5.3. *Y. pseudotuberculosis* Δ*nagC* mutant produces less biofilm on *C. elegans* compared to the parent and complemented Δ*nagC* strains. The sample size for each was n=3, *P*-values were calculated using one-way ANOVA and Tukey's multiple comparison test.

In comparison with *Y. pseudotuberculosis*, the *Y. pestis* CO92 parent strain produced high levels of biofilm along the whole body of *C. elegans*, with a mean BSI score for the parental strain of around 80%, 4 times greater than the mean biofilm severity score for the *Y. pseudotuberculosis* YPIII parent strain. As with *Y. pseudotuberculosis*, mutating *nagC* in *Y. pestis* produced a significant reduction in amount of biofilm formed on *C. elegans*. The addition

of pHG327 did not largely affect the ability of *Y. pestis* to form biofilms and the complemented Δ*nagC* strain showed partial restoration of biofilm levels. Figure 5.4 shows images of *Y. pestis* biofilms on *C. elegans* using the AMG Evos® xl core digital microscope imaged with either a 10x or 20x lens. Figure 5.5 shows the BSI scores for *C. elegans* on *Y. pestis* plates, showing a 16-fold decrease in BSI score for the Δ*nagC* mutant compared to the parental strain. Carrying the empty pHG327 vector did not affect the ability of *Y. pestis* to form biofilms on *C. elegans*.

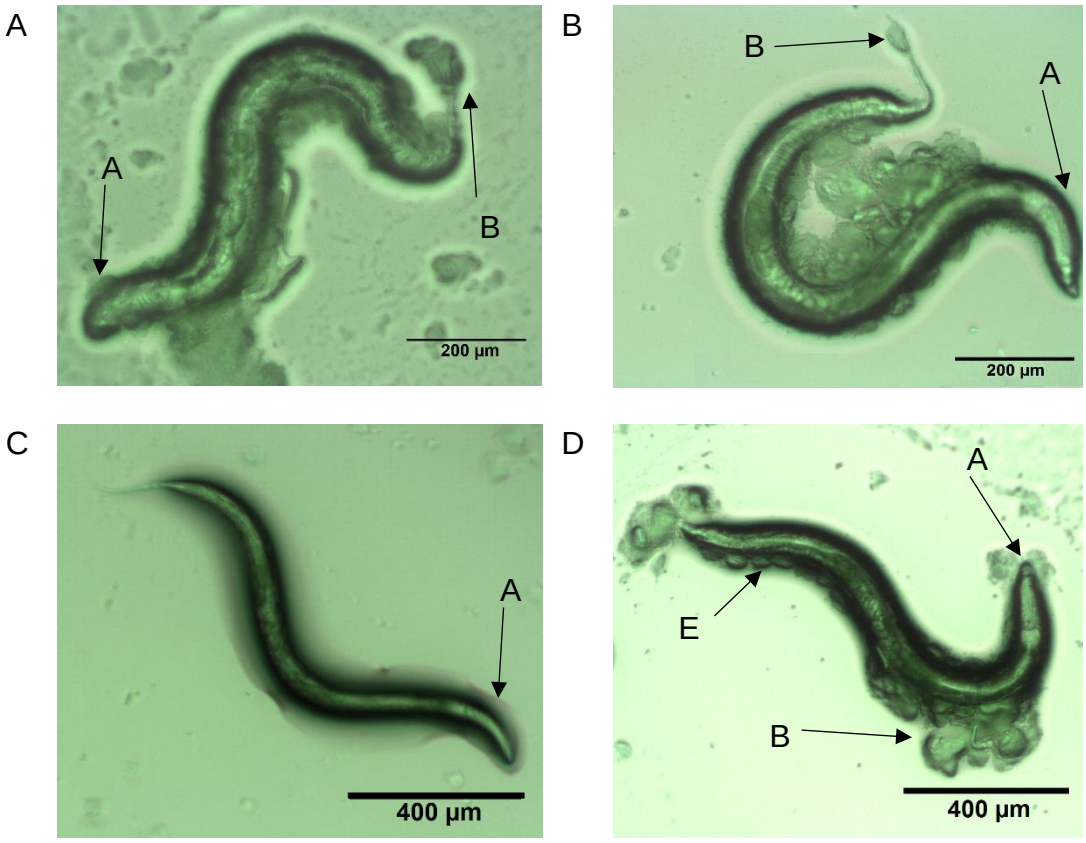

Figure 5.4. Biofilm formation on *C. elegans* by *Y. pestis*. (A) shows *C. elegans* with *Y. pestis* parent strain biofilm (20x magnification), (B) shows a worm with parent + pHG327 (10x magnification) (C) shows a worm with *Y. pestis ΔnagC* (20x magnification), and (D) shows a worm with the complemented Δ*nagC* strain (10x magnification). The parent + pHG327 strain exhibited similar levels of biofilm to the parent. Arrows labelled A indicate the anterior of the worm, arrows labelled B indicate biofilm and arrows labelled E indicate eggs attached to adult worms.

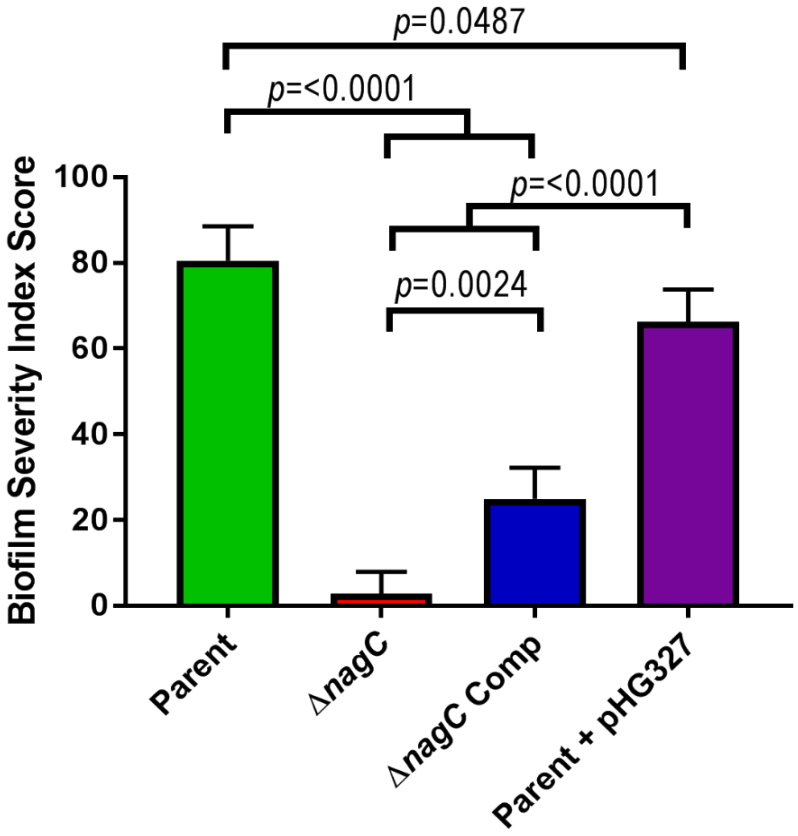

Figure 5.5. The *Y. pestis ΔnagC* mutant produces less biofilm on *C. elegans* than the parent strain. Complementing *ΔnagC* partially restores *Y. pestis*' biofilm formation. The sample size for each was n=3, *P*-values were calculated using one-way ANOVA and Tukey's multiple comparison test.

The parental strain of *Y. pestis* also affected the movement of *C. elegans* on agar plates. Worm trails for worms fed *E. coli* OP50 show symmetrical, 'S' shaped pathways through the bacterial lawn. In comparison, those fed parent strain *Y. pestis* show much tighter 'hairpin' pathways, which are much less regular (Figure 5.6). Worms fed the *ΔnagC* mutant exhibited a smooth path, as when fed *E. coli* OP50.

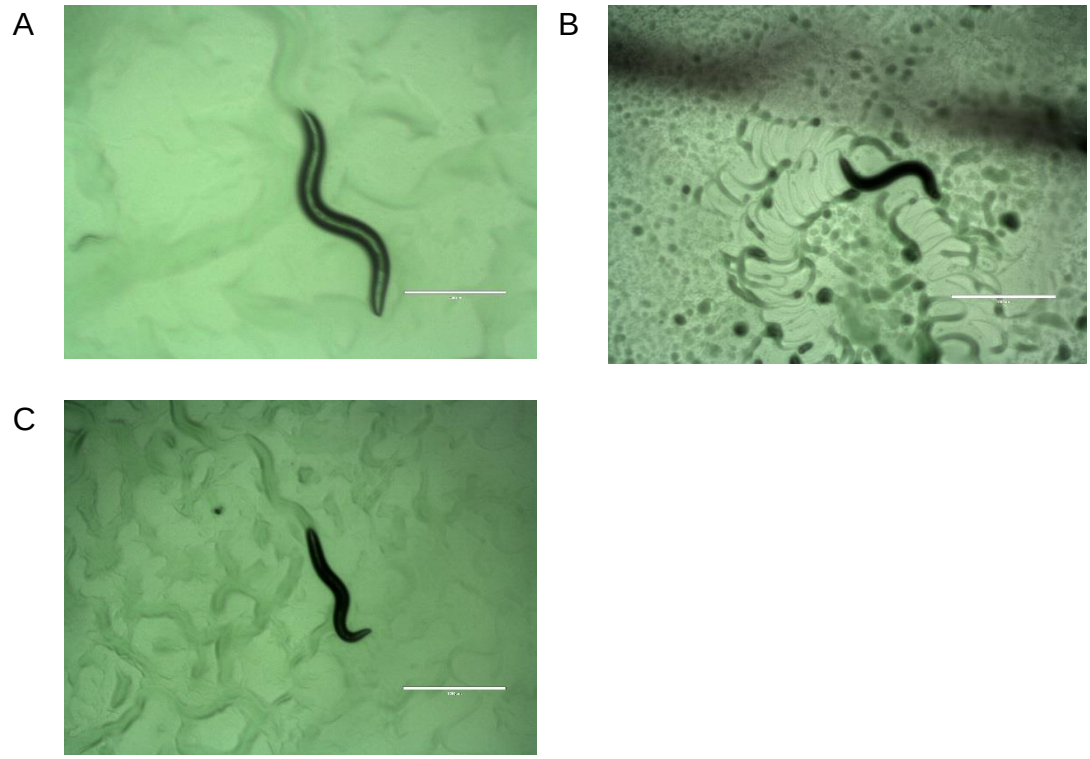

Figure 5.6. *Y. pestis* parent strain causes *C. elegans* migration patterns to change. (A) an uninfected *C. elegans* (fed *E. coli* OP50), which produces a neat, symmetrical 'S' shaped migration path through the bacterial lawn. (B) a worm fed *Y. pestis* parent strain. The movement pattern for these worms becomes disrupted and they form tight hairpin bends in their movement. (C) the mutation of Δ*nagC* restores the worm migration pattern to that of *E. coli* OP50. Worms fed the Δ*nagC* mutant exhibited a smooth, 'S' shaped path, similar to *E. coli* OP50. Scale bars indicate 400 µm.

5.3.2 Development of an *In vitro* 'Fake Flea' Proventriculus Biofilm Model

Y. pestis is known to block fleas by forming large biofilms on the proventriculus, a chitinous, spiky valve linking the oesophagus and gut (Bacot and Martin, 1915). However, the use of live insects in a CL3 laboratory is challenging and a 'fake flea' *in vitro* model was developed to circumnavigate this issue. Preliminary assays were conducted to ascertain whether *Y. pseudotuberculosis* can attach to chitin using chitin resin beads (New England Biolabs) (see section 2.4.5.4 for methodology).

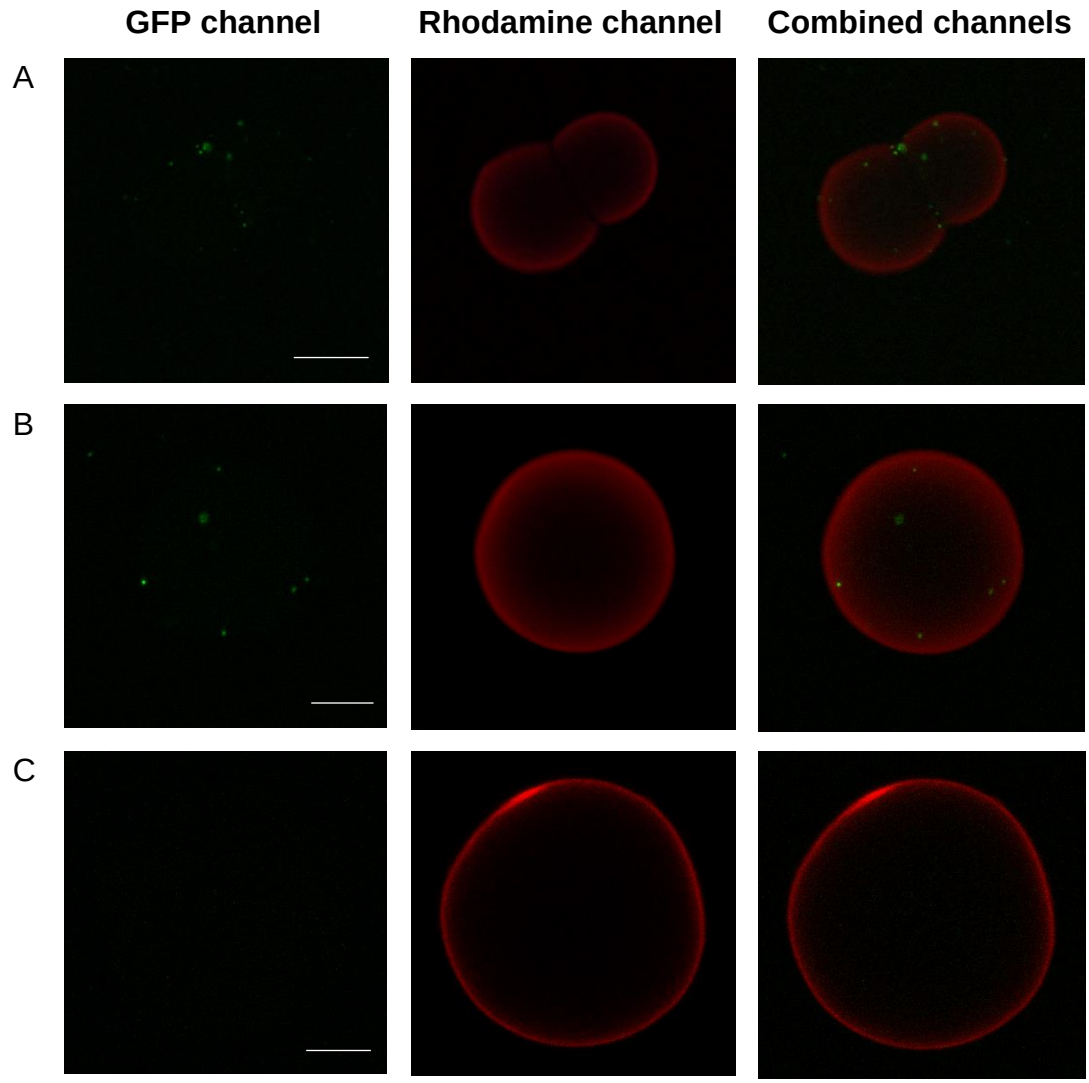

Figure 5.7. Confocal microscopy images showing GFP-labelled *Y. pseudotuberculosis* binding to chitin beads after an incubation of 24 h. Row (A) shows the parent strain at 22ºC, (B) shows the parent strain at 37ºC and (C) shows the negative control, without *Y. pseudotuberculosis*. There was little attachment of bacteria to the chitin beads. The red rhodamine fluorescence is a consequence of the WGA lectin binding directly to the chitin. Scale bars represent 20 µm.

Figure 5.7 shows that there was little attachment of the GFP-labelled parent strain *Y. pseudotuberculosis* to the beads (around 1-5 bacteria were seen to attach per bead), especially at 22ºC, so further chitin substrates were tested for better attachment.

5.3.2.1 Chitin Coated Coverslips as Substrates for the 'Fake Flea' Model

Due to the sparse attachment of *Y. pseudotuberculosis* to the chitin beads, the same assay was undertaken using chitin flakes from shrimp shells (Sigma Aldrich), as well as chitin coated onto glass coverslips. To utilise chitin as a surface substrate, it was dissolved, as described by Moustafa *et al.* (2007) in section 2.4.5.4. Different amounts of chitin were tested on the coverslips (data not shown). Larger volumes tended to crack and fall off, whereas smaller volumes were more easily dislodged when dried.

When imaged using confocal microscopy, the flakes and coverslips showed a much greater level of attachment compared to the beads (Figure 5.8 and Figure 5.9 respectively), which was confirmed when the images were processed using Volocity to ascertain the sum of the mean GFP intensity. There were similar levels of GFP fluorescence intensity when the flakes and the coverslips were compared. All the chitin surfaces showed a lower fluorescence intensity at 22ºC compared to 37ºC, indicating that there is more attachment at mammalian body temperatures.

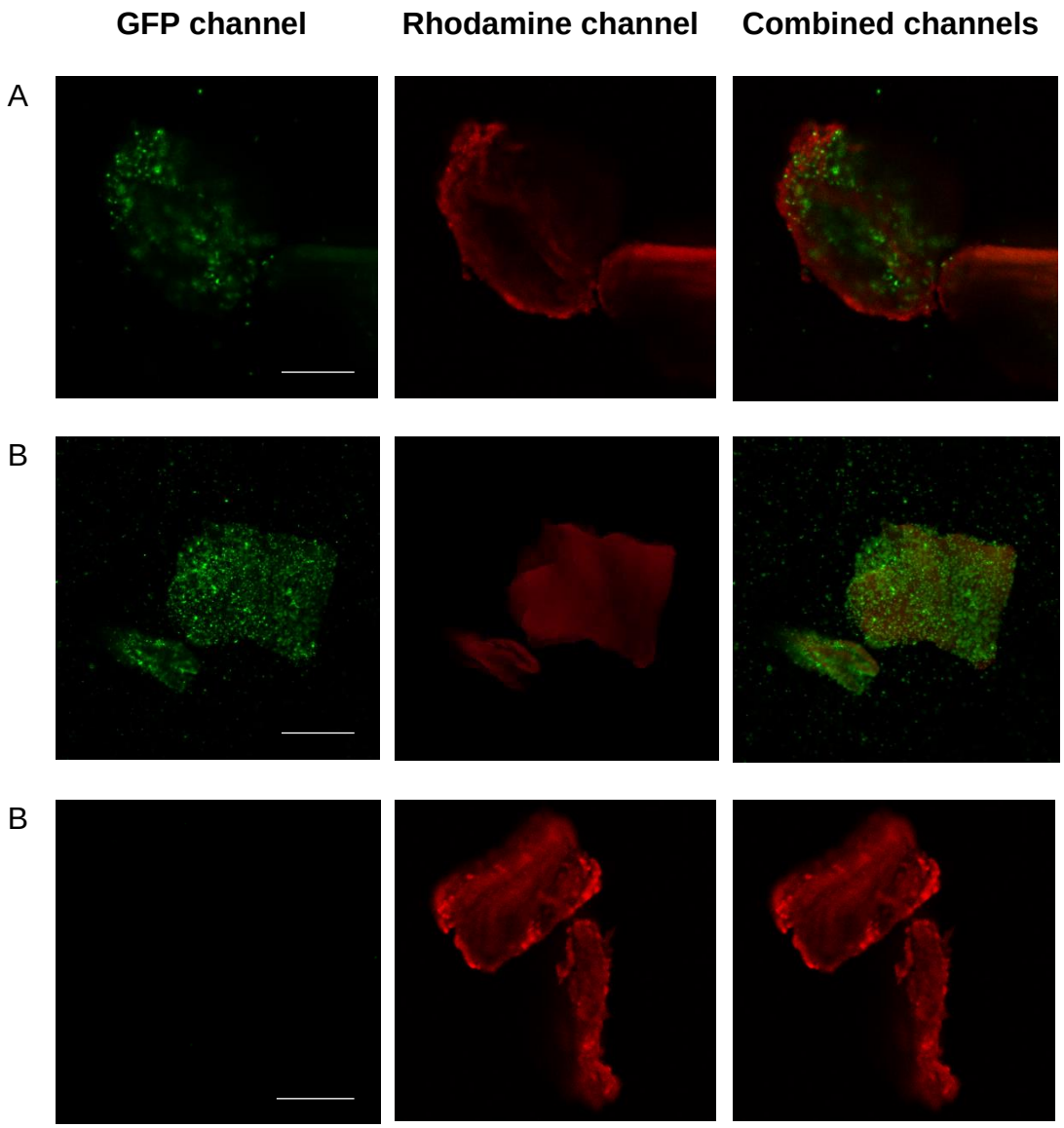

Figure 5.8. Confocal microscopy images showing GFP-labelled *Y. pseudotuberculosis* binding to chitin flakes after 24 h incubation. Row (A) shows the parent strain at 22°C, (B) shows the parent strain at 37°C and (C) shows the negative control, without *Y. pseudotuberculosis*. The red rhodamine fluorescence is a consequence of the WGA lectin binding directly to the chitin. Scale bars represent 50 µm.

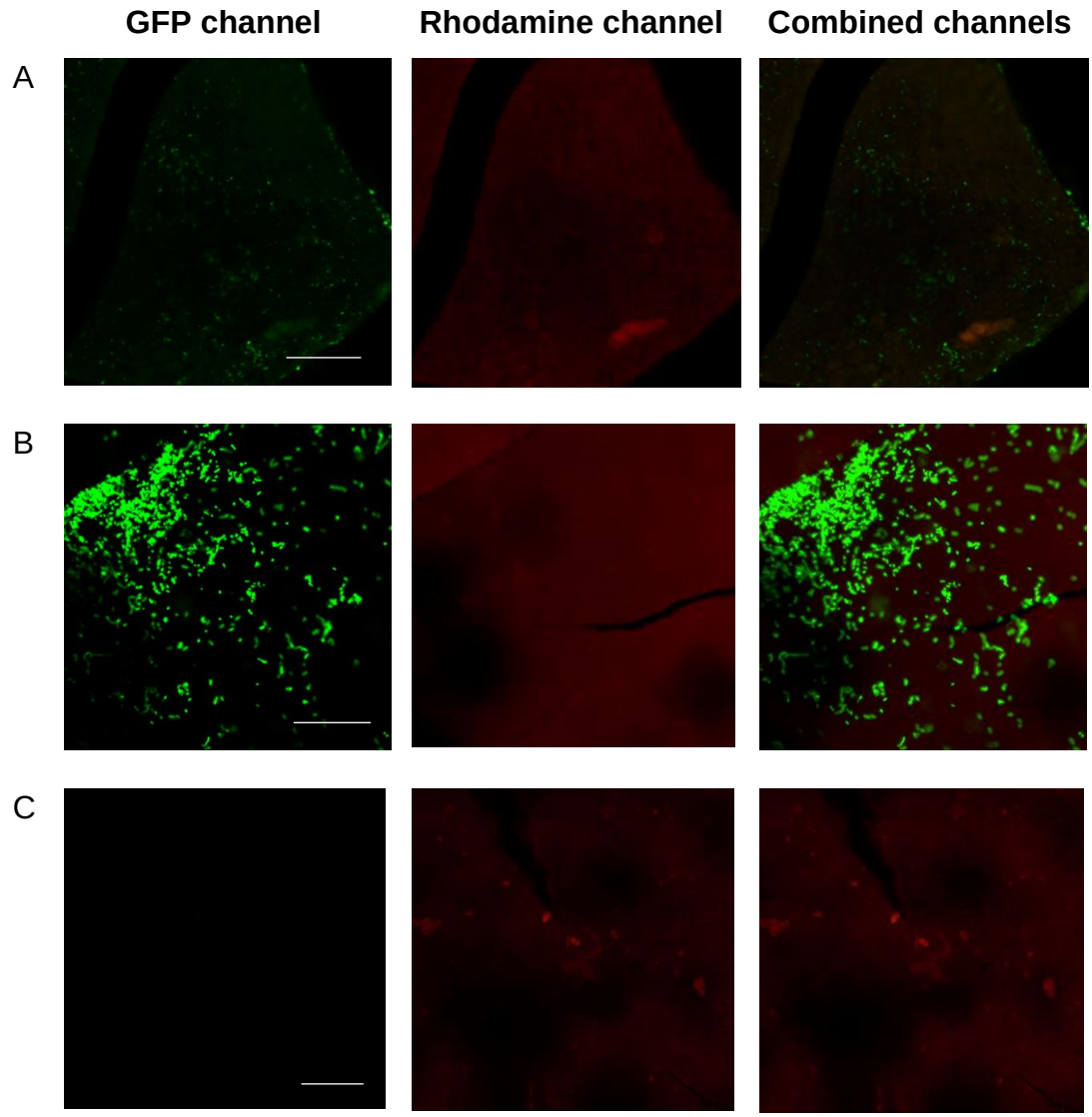

Figure 5.9. Confocal microscopy images showing GFP-labelled *Y. pseudotuberculosis* binding to chitin coverslips after 24 h incubation. Row (A) shows the parent strain grown at 22ºC, (B) shows the parent strain grown at 37ºC and (C) shows the negative control, without *Y. pseudotuberculosis*. The red rhodamine fluorescence is a consequence of the WGA lectin binding directly to the chitin. Scale bars represent 20 µm.

The sum of the mean GFP intensity was then compared between the three chitin surfaces; beads, flakes and coverslips. Figure 5.10 shows that the beads recorded a relatively low level of fluorescence intensity compared to the flakes and coverslips, which were similar at both 22ºC and 37ºC. At 22ºC, the flakes showed a 2-fold increase and coverslips showed a 1.5x increase in

fluorescence intensity compared to the beads, whereas at 37ºC, both the flakes and coverslips showed a tenfold increase in fluorescence intensity compared to the beads, showing that there is a much stronger attachment of *Y. pseudotuberculosis* to the flakes and coverslips.

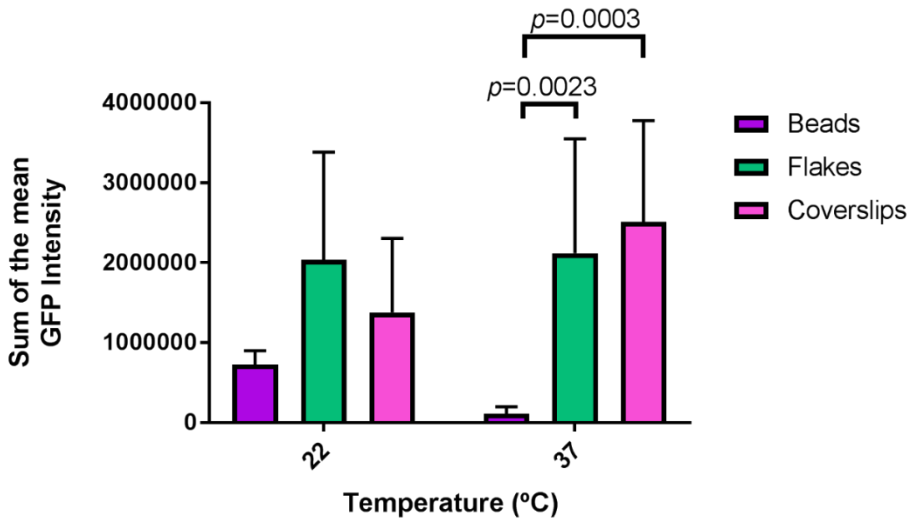

Figure 5.10. Attachment of *Y. pseudotuberculosis* to chitin beads, flakes and coverslips after 24 h incubation. There was significantly more attachment at 37ºC on the flakes and coverslips, compared to the beads. The sample size for each was n=3, *P*-values were calculated using two-way ANOVA and Tukey's multiple comparison test.

To ascertain whether the variation in surface attachment was due to differences in the surface area of the beads and flakes, the surface areas were measured using the Zen Blue software package (Carl Zeiss AG). Figure 5.11 indicates that there was no significant difference between the chitin beads and the flakes, as both had surface areas of between 1000 - 9000 μm^2. As the beads were a more uniform, spherical shape, as shown in Figure 5.12, a rough estimate of an average total surface area was estimated at 31 mm^2. The flakes all varied in their measurements and working out an average total surface area

was not possible. The coverslips, in comparison, had a much smoother and more uniform surface.

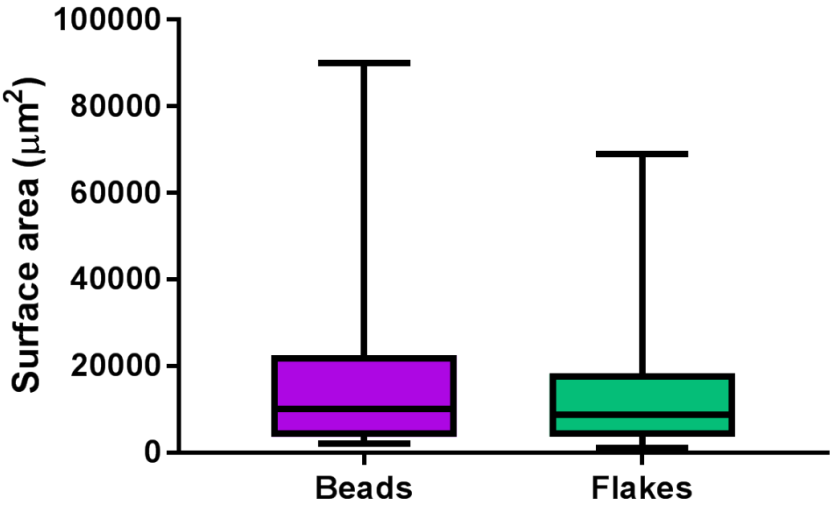

Figure 5.11. Comparison of the surface areas of the chitin beads and flakes. The surface areas are very similar, which suggests that surface area is not the reason for greater attachment of *Y. pseudotuberculosis* to chitin flakes compared with beads. n=20.

As the chitin beads and flakes were of a comparable surface area, but the flakes and coverslips showed comparable attachment, scanning electron microscopy (SEM) was used to investigate whether there were differences in the texture of the surfaces. Samples were processed as adapted from Horisberger & Rosset (1977) (see section 2.4.8.3).

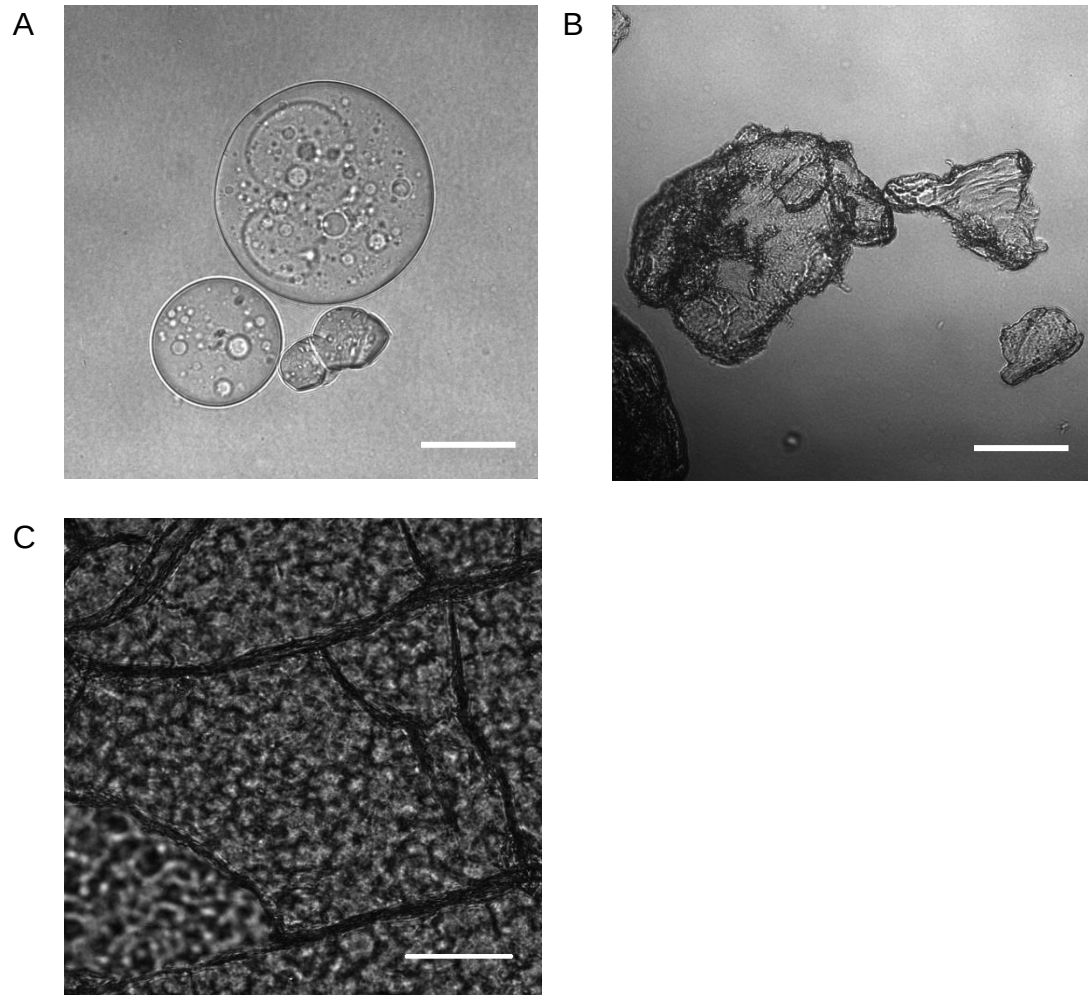

Figure 5.12. Microscope images showing the shapes of (A) chitin beads, (B) chitin flakes and (C) chitin-coated coverslips. The beads show a much more uniform shape, whereas the flakes were more variable. Although the chitin covered coverslips showed cracks from the drying process, the surface was generally much smoother than that of the flakes. Scale bars represent 100 µm.

Figure 5.13 shows that whilst the surface area of the coverslips were relatively smooth, the surface of the flakes was much rougher, with crevices in which bacteria could gather, making it harder to wash off 'unattached' bacteria. Similarly, although *Y. pseudotuberculosis* is capable of attaching to the surface of the chitin coverslips, they can also get caught in chitin surface fractures.

A

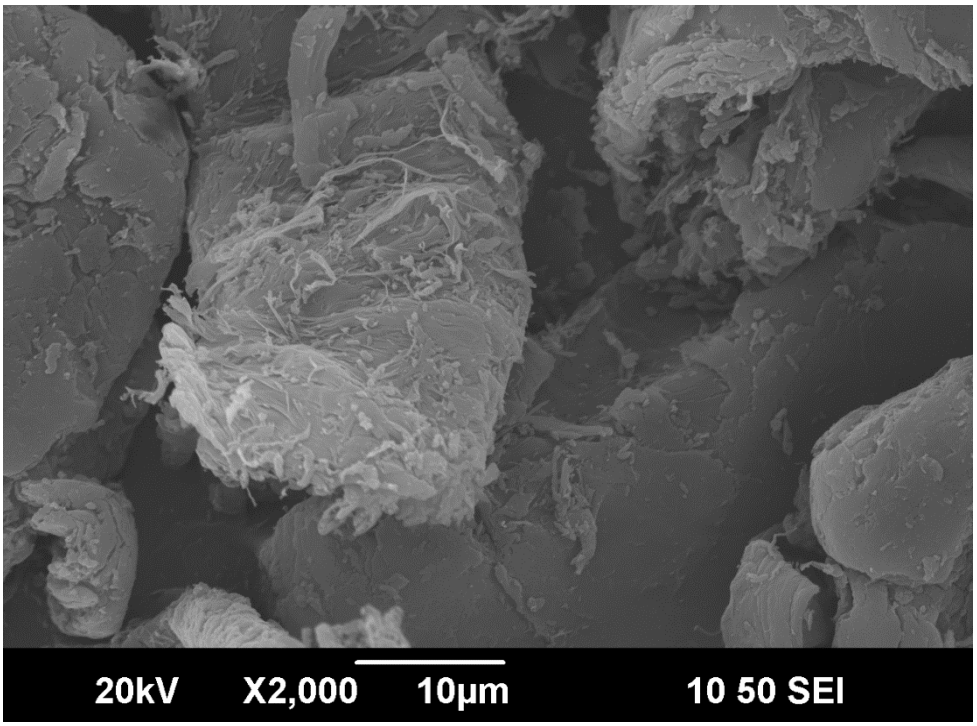

B

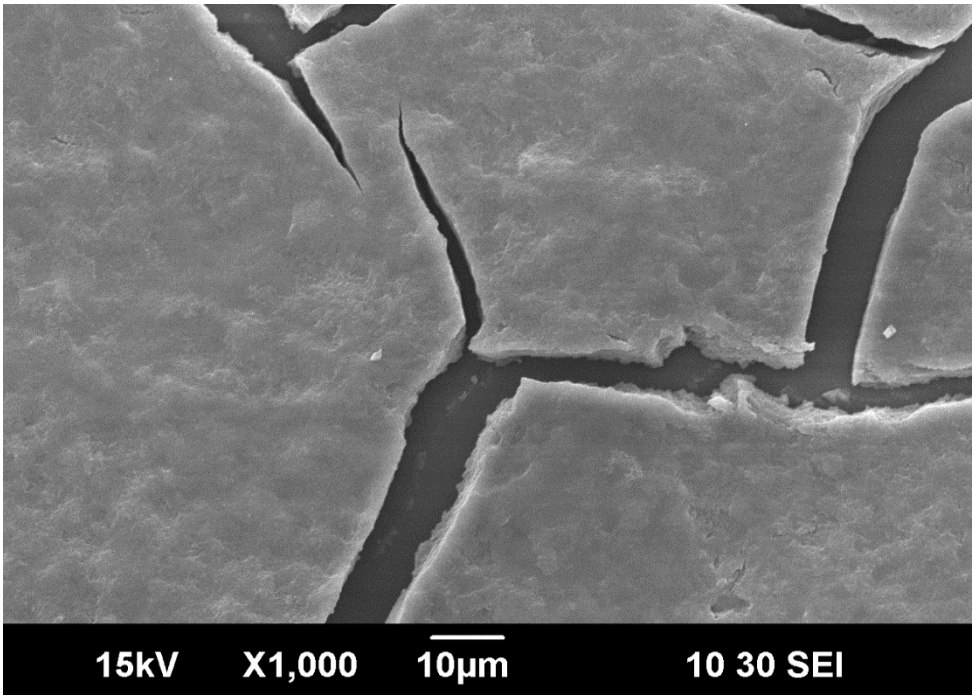

Figure 5.13. Scanning electron microscopy images showing the surface textures of (A) the chitin flakes at 2000x magnification and (B) a chitin coverslip at 1000x magnification. The surface of the chitin coverslips is smoother than that of the flakes, despite the *Y. pseudotuberculosis* attachment being similar for both.

As there was little bacterial attachment to the beads and the flakes had extremely variable surface areas chitin coated coverslips were used for the 'fake flea' experiments.

5.3.2.2 Identifying Optimal Incubation Conditions for the 'Fake Flea' Model

The length of the incubation period was tested to ascertain whether higher bacterial attachment could be achieved. Cultures of GFP-labelled *Y. pseudotuberculosis* were incubated at both 22ºC and 37ºC for 24 h, 48 h and 1 week, stained with rhodamine-labelled WGA and imaged using confocal microscopy. These experiments gave mixed results, as Figure 5.14 shows. At 22ºC, there was no significant difference in the amount of fluorescence intensity recorded for the different incubation periods. However, at 37ºC, a 48 h incubation period showed a significant increase in fluorescence intensity compared to 24 h and 1 week. Very little attachment occurred after 1 week, suggesting that bacterial aggregates may have detached from the coverslip, or possibly lysed.

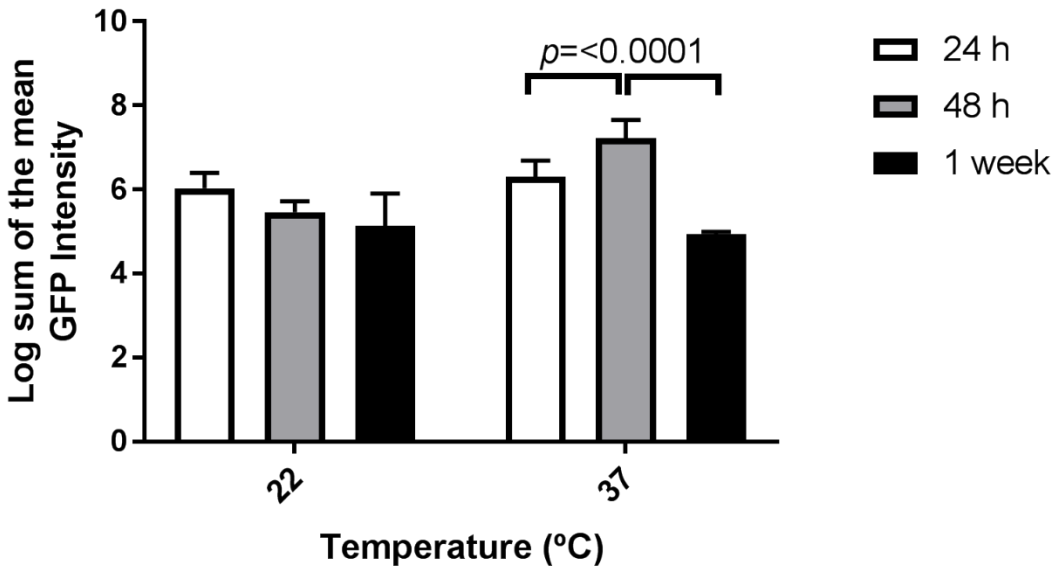

Figure 5.14. Influence of incubation period on the attachment of *Y. pseudotuberculosis* to chitin coverslips at 22ºC and 37ºC. There were no significant differences in attachment at 22ºC, but an incubation of 48 h provided the greatest attachment at 37ºC. The sample size for each was n=3 (biological replicates), P-values were calculated using two-way ANOVA and Tukey's multiple comparison test.

Different media were tested, as *Y. pseudotuberculosis* are most likely to form biofilm in low nutrient conditions. The results of this experiment are shown in Figure 5.15, which shows that although none of the media tested resulted in significantly more attachment than the others, YDMM showed a slight increase over YLB or 50% YLB at both 22ºC and 37ºC. As this was the lowest nutrient medium, this result is in line with previous observations (Barratt, Ph.D. Thesis, 2018).

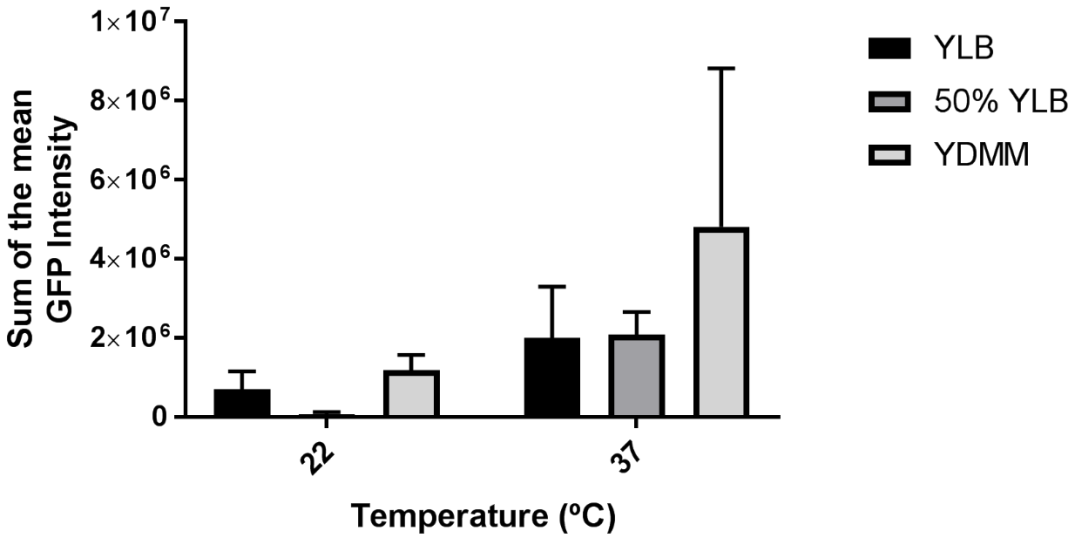

Figure 5.15. Attachment of GFP-labelled *Y. pseudotuberculosis* grown in different media to chitin coverslips. There were no significant differences between the media tested, although YDMM appeared to have a slightly higher mean GFP intensity reading, especially at 37ºC. The sample size for each was n=3 (biological replicates), P-values were calculated using two-way ANOVA and Tukey's multiple comparison test.

Blood components play a role in early phase aggregation of *Y. pestis* in the flea gut (Hinnebusch, Jarrett and Bland, 2017). Figure 5.16 shows that the addition of either bovine serum or heat inactivated bovine serum does not appear to significantly affect the GFP intensity and therefore attachment of GFP-labelled *Y. pseudotuberculosis* to chitin coverslips, although addition of serum, especially when heat inactivated, showed a slight increase in attachment at 37ºC compared to the negative control chitin coverslip. As the heat inactivated serum appeared to slightly increase attachment at both 22ºC and 37ºC, it was utilised in further experiments.

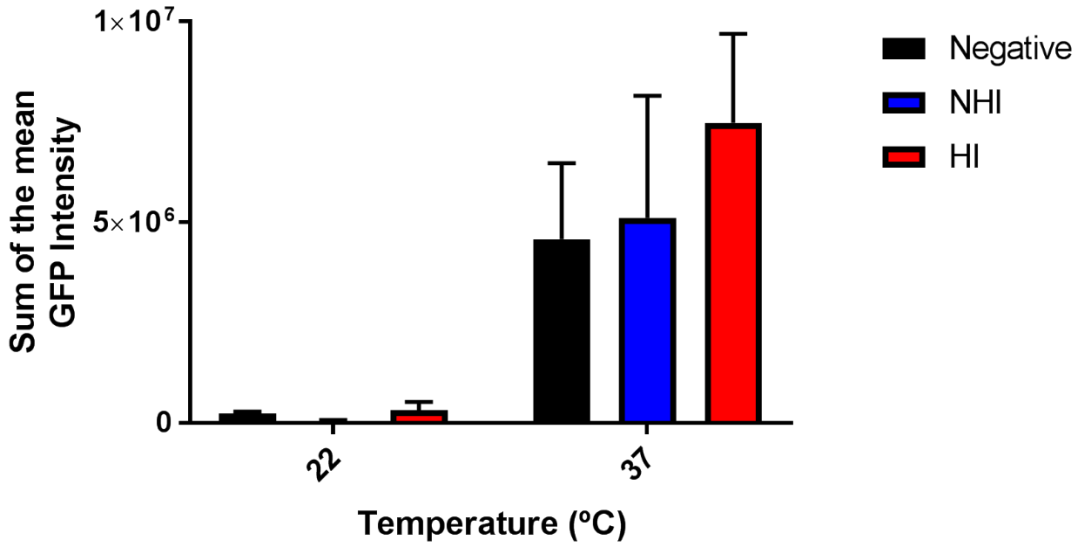

Figure 5.16. Surface conditioning of chitin coverslips with bovine serum or heat inactivated bovine serum had no significant effect on the attachment of GFP-labelled *Y. pseudotuberculosis*. The sample size for each was n=3, P-values were calculated using two-way ANOVA and Tukey's multiple comparison test.

To enable this protocol to be utilised for *Y. pestis* experiments, the bacteria need to be certifiably killed before leaving the CL3 suite. Paraformaldehyde (PFA), which causes covalent crosslinks between proteins and therefore should both kill bacteria and crosslink the cells to the chitin surface, would be used. Consequentially the impact of PFA on GFP intensity was evaluated (Zarda *et al.*, 1997). Figure 5.17 shows that there were no significant differences between the PFA-treated and non-treated coverslips at either 22ºC or 37ºC, suggesting that the addition of PFA to kill *Y. pestis* would not affect the GFP fluorescence.

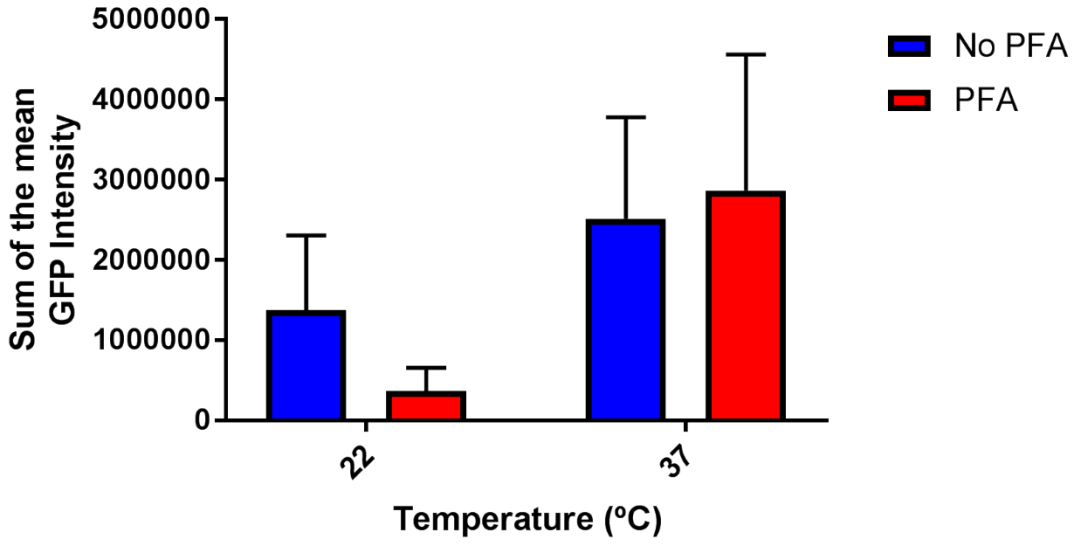

Figure 5.17. Effect of PFA on the attachment of GFP-labelled *Y. pseudotuberculosis* to chitin coverslips. No significant differences between the paraformaldehyde treated and non-treated coverslips at either 22ºC or 37ºC were observed. The sample size for each was n=3, P-values were calculated using two-way ANOVA and Sidak's multiple comparison test.

5.3.2.3 Deletion of *nagC* Reduces Biofilm Formation by *Y. pseudotuberculosis* on a Chitin Surface

Once the optimal conditions for creating a fake flea model were established, the assay was used to identify whether the deletion of *nagC* affected the ability of *Y. pseudotuberculosis* to chitin surfaces. Cultures were grown at 22ºC and 37ºC for 48 h in YDMM with the appropriate antibiotic in the presence of heat inactivated bovine serum and a chitin-coated coverslip. The coverslips were stained as described above (with the addition of SYTO-9 for the complemented Δ*nagC* strain) and imaged using confocal and scanning electron microscopy. At 22ºC, the Δ*nagC* mutant showed no significant reduction in attachment compared to the parental and complemented Δ*nagC* strains (Figure 5.18).

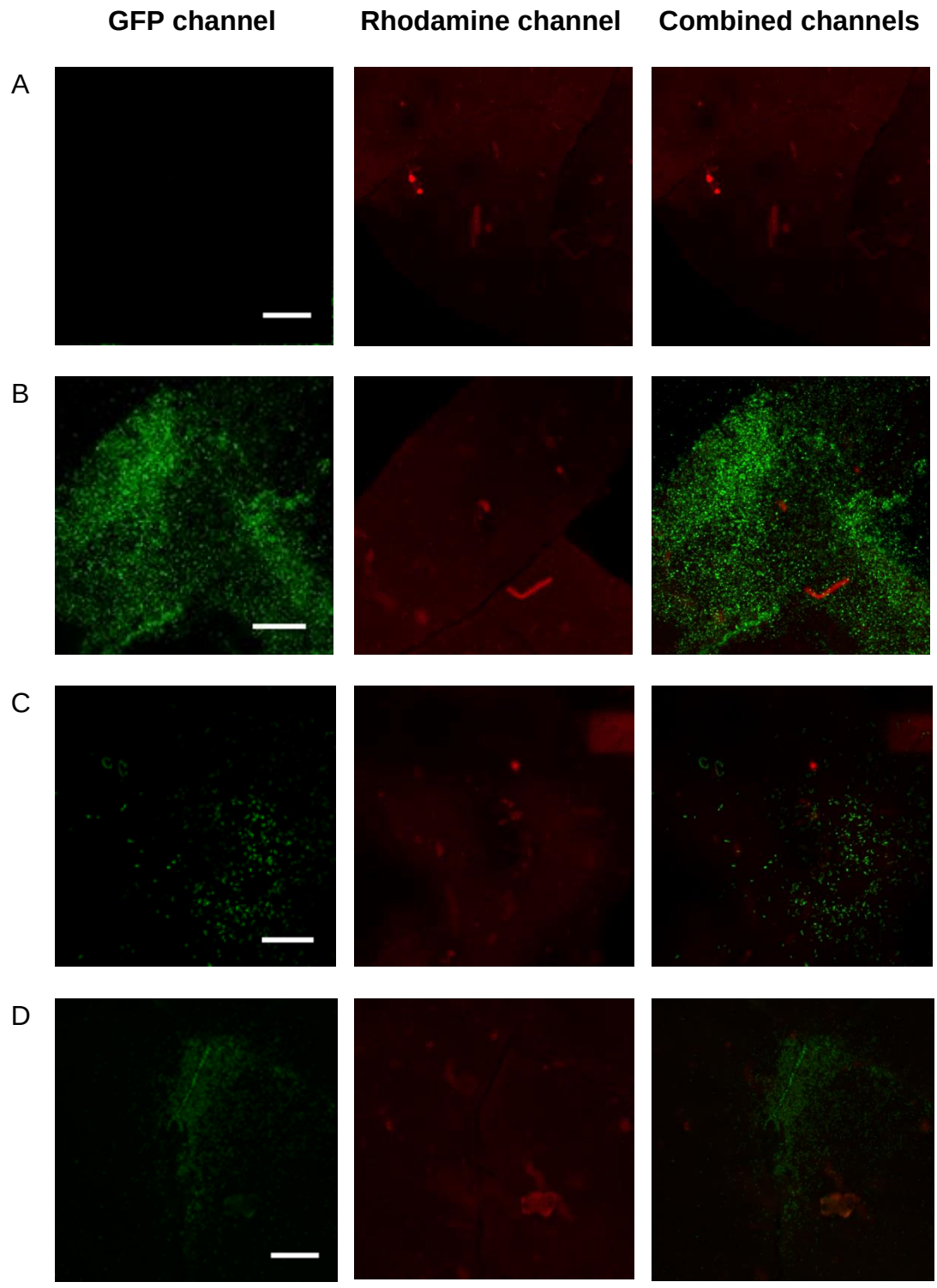

Figure 5.18. Confocal images showing that detection of *Y. pseudotuberculosis* on chitin coated coverslips at 22ºC. (A) shows the negative control with no bacteria, (B) the parental strain, (C) the Δ*nagC* mutant and (D) the complemented Δ*nagC* strain. Scale bars represent 20 µm.

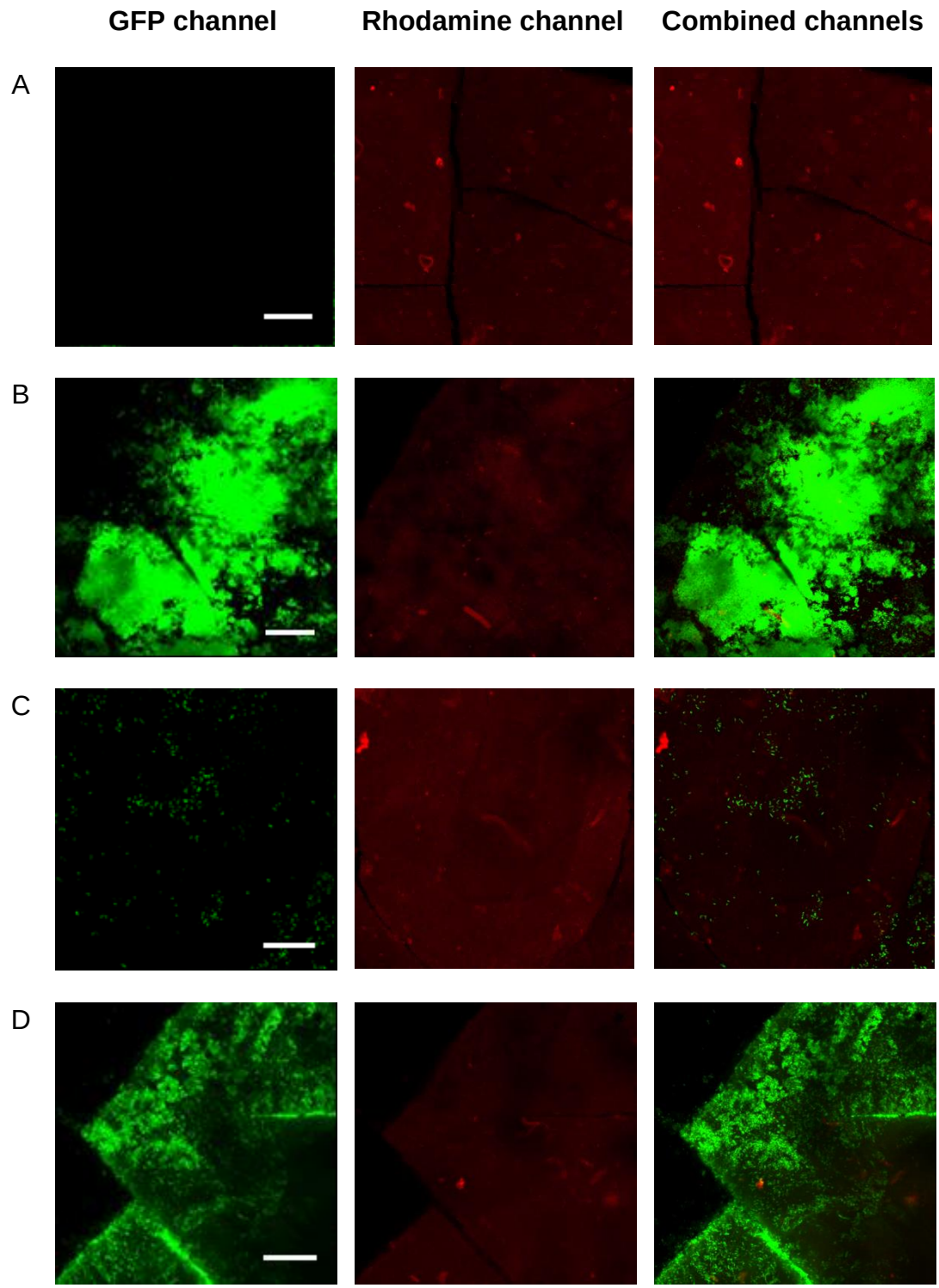

Figure 5.19. Confocal images showing attachment of *Y. pseudotuberculosis* at 37°C to chitin coated coverslips. (A) shows the negative control with no bacteria, (B) the parental strain, (C) the Δ*nagC* mutant and (D) the complemented Δ*nagC* strain. Scale bars represent 20 µm.

At 37ºC however, the Δ*nagC* mutant showed a severe reduction in attachment (Figure 5.19). When the sum of the mean fluorescence intensity was measured, attachment was shown to be almost 30 times greater for the parental strain compared to the Δ*nagC* mutant at 37ºC (Figure 5.20). Attachment was 3.5 times greater at 37ºC than 22ºC for the parental strain indicating larger biofilm formation at virulence temperatures.

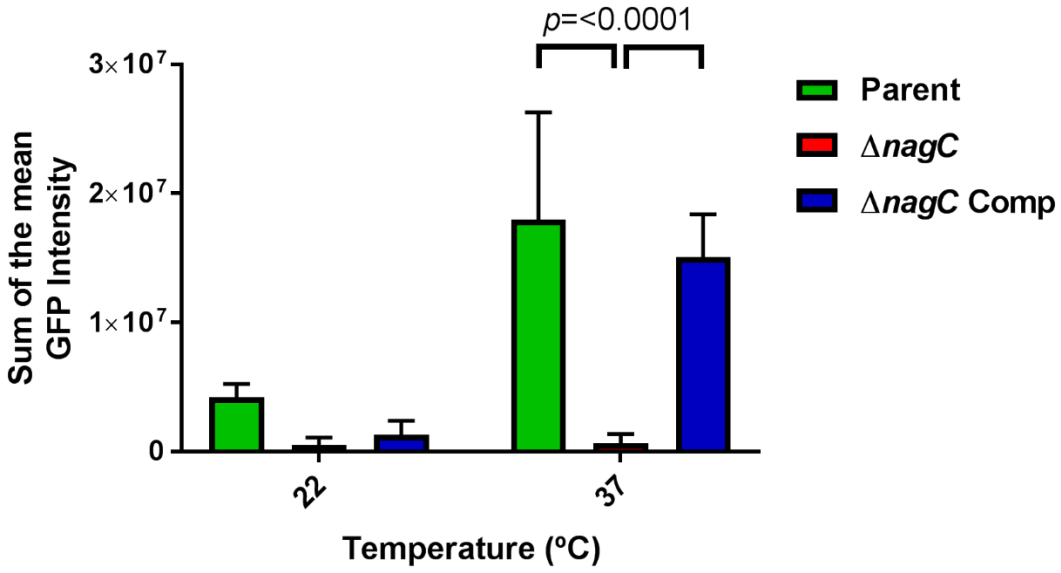

Figure 5.20. Quantification of *Y. pseudotuberculosis* parent, Δ*nagC* and complemented Δ*nagC* strain when grown on chitin covered coverslips in YDMM for 48 h in the presence of heat inactivated bovine serum at 22ºC or 37ºC. At mammalian temperature, the Δ*nagC* mutant shows a significant reduction in the GFP intensity and therefore attachment, whilst the complemented Δ*nagC* strain is restored to the parental phenotype. The sample size for each was n=3 (biological replicates), *P*-values were calculated using two-way ANOVA and Tukey's multiple comparison test.

Confocal Z stack images were taken to further analyse *Y. pseudotuberculosis* attachment and biofilm formation on chitin-coated coverslips. Using the Comstat 2 plugin for ImageJ (National Institute of Health), the biomass and surface coverage of the *Y. pseudotuberculosis* attachment were quantified.

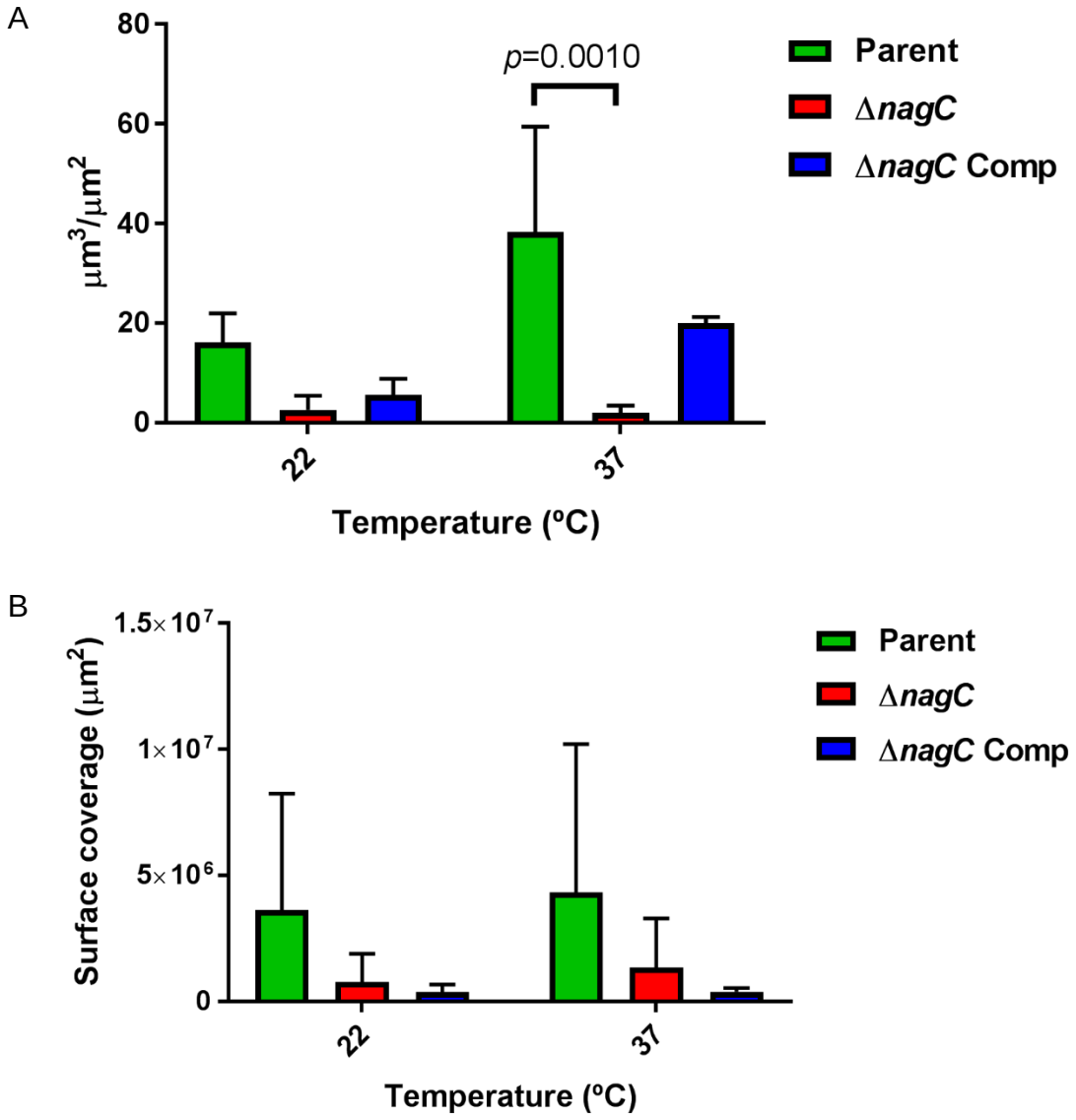

Figure 5.21. *Y. pseudotuberculosis* biofilm development on chitin-coated coverslips quantified as bacterial biomass (A) and surface coverage (B). At 22ºC there are no significant differences in either the biomass or the surface coverage when the Δ*nagC* mutant is compared to the parental and complemented Δ*nagC* strains. At 37ºC, although there was no significant difference in surface coverage, there was around 8 times less Δ*nagC* mutant biomass present compared to the parental strain. The sample size for each was n=3, P-values were calculated using two-way ANOVA and Tukey's multiple comparison test.

Figure 5.21 shows that at 22ºC there were no significant differences in either the biomass or the surface coverage when the Δ*nagC* mutant was compared to the parental and complemented Δ*nagC* strain, which correlates with the confocal results obtained. At 37ºC, although there were no significant

differences in surface coverage, it was reduced for the Δ*nagC* mutant. There was around 8 times less biomass present for the Δ*nagC* mutant compared with the parental strain which suggests that although the bacteria attach, they are unable to proliferate on the surface, develop into microcolonies and subsequently form a mature biofilm.

To further elucidate whether ECM and therefore biofilm was being produced by the bacteria attaching to the chitin surface, samples were imaged using SEM (Figure 5.22). Whilst confocal microscopy and image processing had already shown that the Δ*nagC* mutant showed less attachment and biomass at 37ºC compared to the parental strain, it was difficult to confirm the presence of poly-GlcNAc and therefore biofilm ECM using WGA staining. Figure 5.22 shows the chitin surface after being incubated for 48 h in the presence of (A) the parental strain of *Y. pseudotuberculosis* and (B) the Δ*nagC* mutant. The parental strain showed a thick, multicellular layer of bacteria with accumulations of ECM around the cells which almost completely obscures the chitin. The Δ*nagC* mutant, in contrast, only attached in small numbers and showed no signs of ECM surrounding the bacteria.

A

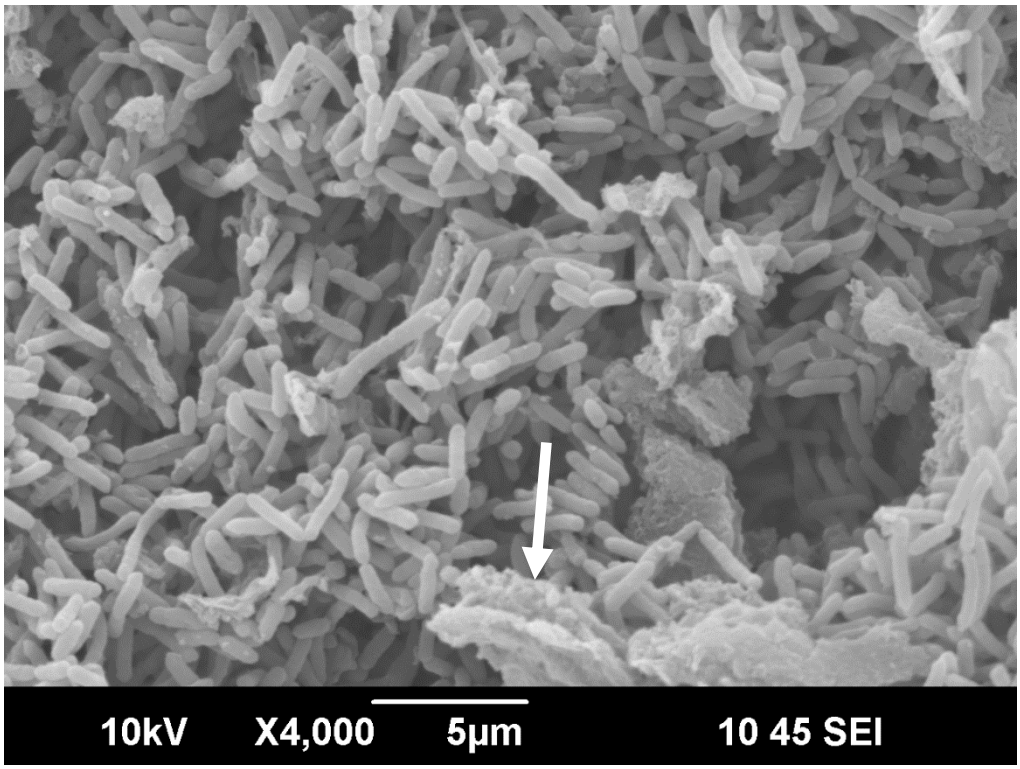

B

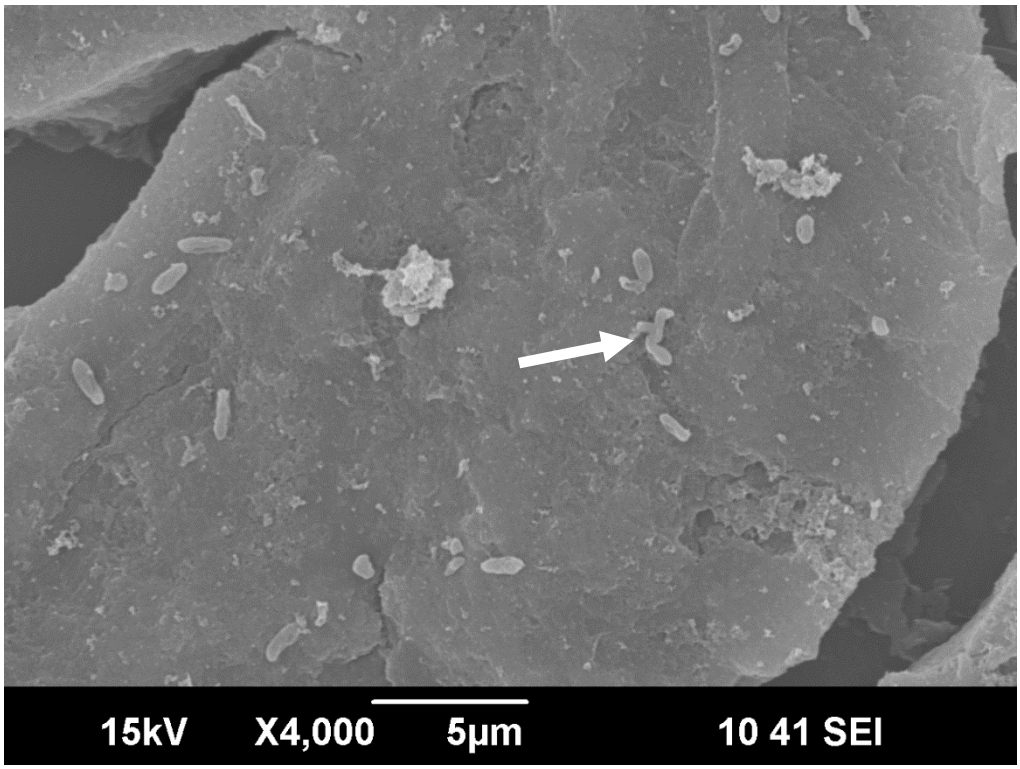

C

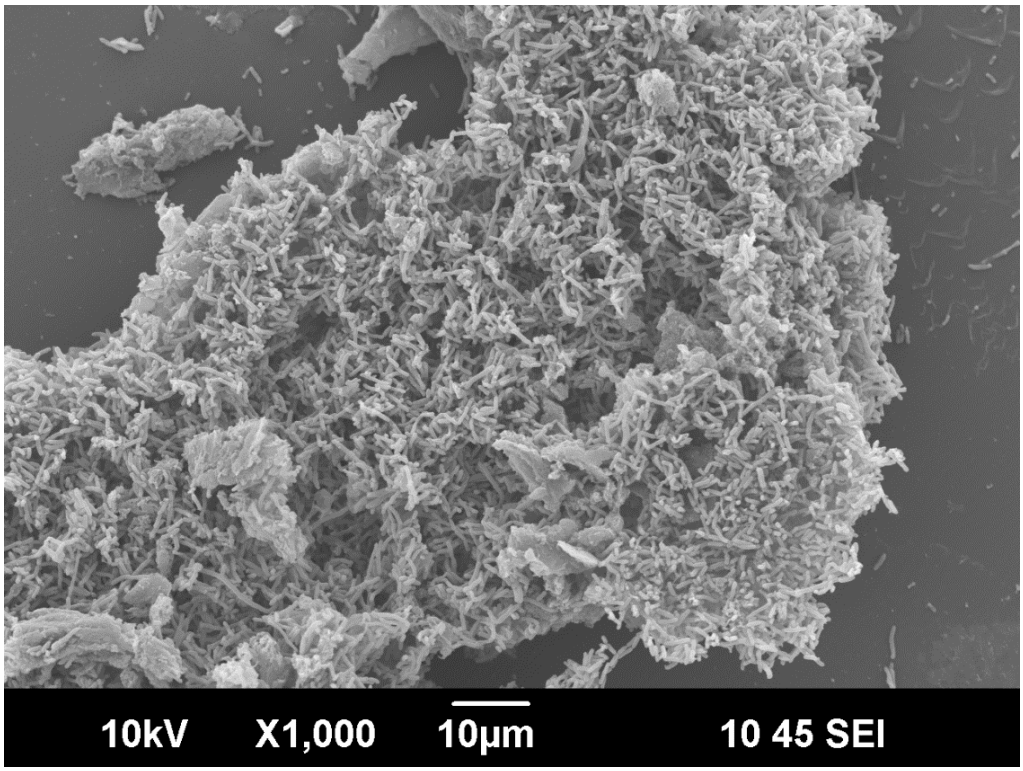

Figure 5.22. SEM images of *Y. pseudotuberculosis* parental strain (A) and the Δ*nagC* mutant (B) on a chitin surface. Each image was taken at 4,000x magnification. Whilst the parental strain created a thick, multicellular aggregation, with evidence of ECM (arrowed), the Δ*nagC* mutant showed only single cellular attachment (arrowed) to the chitin surface, and no evidence of ECM formation. (C) multicellular aggregation was restored when the Δ*nagC* mutant was complemented (image taken at 1,000x magnification, to show the extent of aggregation).

5.3.2.4 Exogenous GlcNAc Restores Attachment of the *Y. pseudotuberculosis* Δ*nagC* Mutant to Chitin

To determine whether the addition of exogenous GlcNAc could restore the chitin attachment/biofilm phenotype of the Δ*nagC* mutant to the parental phenotype at 37ºC, 1 mM GlcNAc was added and incubated as described above. Figure 5.23 shows the attachment of GFP-labelled *Y. pseudotuberculosis* (and SYTO-9 stained complemented Δ*nagC* mutant) as

the sum of the mean GFP intensity. Exogenous GlcNAc restored the Δ*nagC* mutant phenotype to that of the parental strain.

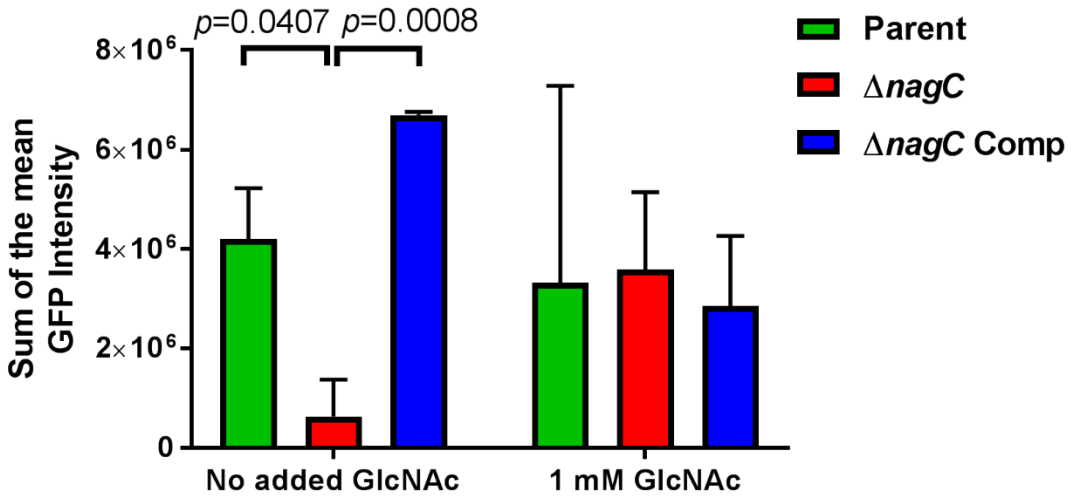

Figure 5.23. Exogenous GlcNAc restored the attachment phenotype of the *Y. pseudotuberculosis* Δ*nagC* mutant to that of the parent strain at 37ºC. The sample size for each was n=3, *P*-values were calculated using two-way ANOVA and Tukey's multiple comparison test.

5.3.3 Impact of NagC on *Y. pseudotuberculosis* infection of *P. corporis*

Despite the close genetic relationship between *Y. pestis* and *Y. pseudotuberculosis*, and the ability of *P. corporis* to harbour and experimentally transmit plague, further work on *Y. pseudotuberculosis* infection of *P. corporis* appears to have halted many decades ago (Krynski and Becla, 1965). As *Y. pseudotuberculosis* is often used as a model for *Y. pestis* in other areas of research (Hares *et al.*, 2008; Gengler *et al.*, 2015), it would seem an oversight not to explore *P. corporis* as a model for experimental *Yersinia* infections. To explore the possibility of a *Y. pseudotuberculosis* – *P. corporis* experimental infection model, *P. corporis* were fed defibrinated human

blood inoculated with the *Y. pseudotuberculosis* YPIII parent, Δ*nagC* and complemented Δ*nagC* mutant.

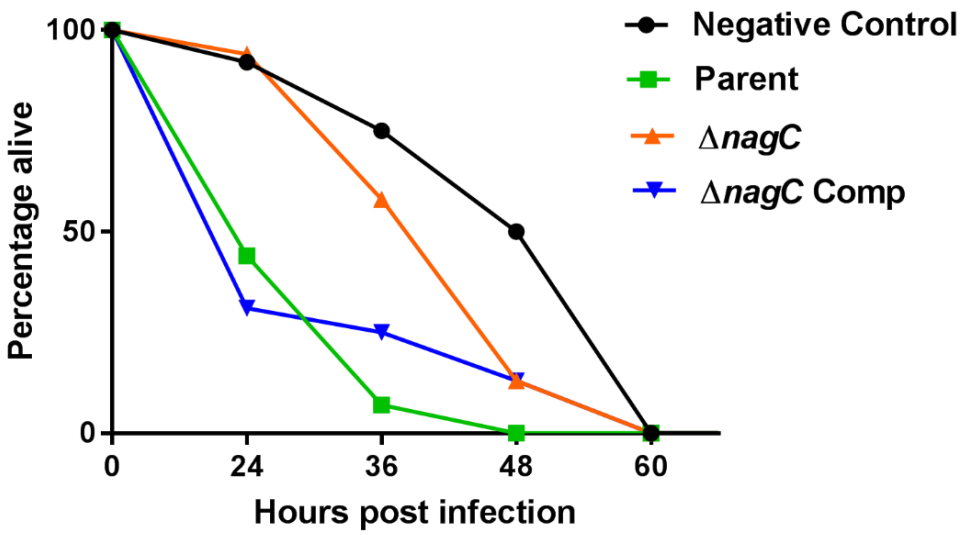

Figure 5.24. Survival rates of *P. corporis* fed *Y. pseudotuberculosis* parent and *ΔnagC*. The insects fed blood containing the *Y. pseudotuberculosis* parent and genetically complemented Δ*nagC* mutant died much faster than those fed blood containing Δ*nagC*.

The survival of *P. corporis* was measured and results shown in Figure 5.24. Lice fed blood containing *Y. pseudotuberculosis* parent and the complemented Δ*nagC* mutant died faster than those fed the Δ*nagC* mutant, which showed a similar survival rate to the negative control lice, fed only blood. At 24 h, less than 50% of insects fed parent and complemented Δ*nagC Y. pseudotuberculosis* were alive, compared to almost 100% of the negative control insects and those fed the Δ*nagC* mutant. This trend was also observed at 36 h, however, by 48 h, the percentage of live insects fed Δ*nagC* was similar to those fed blood containing the *Y. pseudotuberculosis* parent or the complemented Δ*nagC* mutant (10% alive) compared to 50% of the negative control insects. By 60 h post infection, all insects had died.

Insects were imaged using a Zeiss Elyra PS.1 super resolution confocal microscope and the sum of the mean fluorescence intensity analysed. As insects auto-fluoresce, only the gut area was included in the measurement (this accounts for the negative control insects also having low levels of background fluorescence). Due to the loss of GFP in the complemented *ΔnagC Y. pseudotuberculosis* strain, it was only possible to detect very low levels of fluorescence in those lice (see section 4.3.3). Immediately after feeding, all lice were engorged with fresh blood meals. No GFP could be detected in the lice, as shown in Figure 5.25, due to their abdominal cavities being filled with fresh blood and a low bacteraemia (approximately 32,0000 bacteria in 16 µl of blood) (as calculated from Waniek 2009). The auto-fluorescence of some lice was not as bright as others, making them appear redder when the two channels were combined using Zen software.

By 24 h post infection, there were no significant differences in GFP fluorescence detected in the abdomens of *P. corporis* that had fed on both the parent and *ΔnagC* strain of *Y. pseudotuberculosis*, as shown in Figure 5.26. In some of the lice fed on the complemented Δ*nagC* strain which had lost most of its GFP, low levels of GFP could be seen in the gut, indicating that the bacteria were present, some of which had maintained their fluorescence.

At 36 h post infection, GFP fluorescence could be detected in lice fed with blood containing all strains of *Y. pseudotuberculosis*, as shown in Figure 5.27. In the lice fed with parent *Y. pseudotuberculosis*, GFP fluorescence was 12 times higher than those fed the Δ*nagC* mutant, and bacteria were generally spread throughout the gut. The majority of the GFP-labelled bacteria were seen in the hind gut of insects fed blood containing the *ΔnagC* mutant, with

fewer bacteria found in the first two thirds of the intestinal tract, suggesting that the Δ*nagC* mutant was being passed through the lice's guts. The guts of those lice fed parental *Y. pseudotuberculosis* were physically larger than those fed the Δ*nagC* mutant, suggesting a blockage in those insects fed with the parent strain. Although it was very faint, the complemented Δ*nagC* bacteria could be seen within some parts of the louse gut, which was of a similar size to the parent strain, suggesting a potentially similar effect on the lice as the parent *Y. pseudotuberculosis*. At 48 h post infection, GFP fluorescence could still be seen in lice fed with blood containing parental and Δ*nagC Y. pseudotuberculosis*, in similar positions in the gut as at 36 h, as shown in Figure 5.28. There was no significant difference, as the fluorescence levels of the lice fed the parental strain had decreased to that of the other lice. The sum of the mean GFP intensity for lice fed each *Y. pseudotuberculosis* strain per time point is shown in Figure 5.29. GFP is degraded over time and affected by oxygen levels, which may account for the reduction of fluorescence found in lice fed the parental strain as all lice had died by this time.

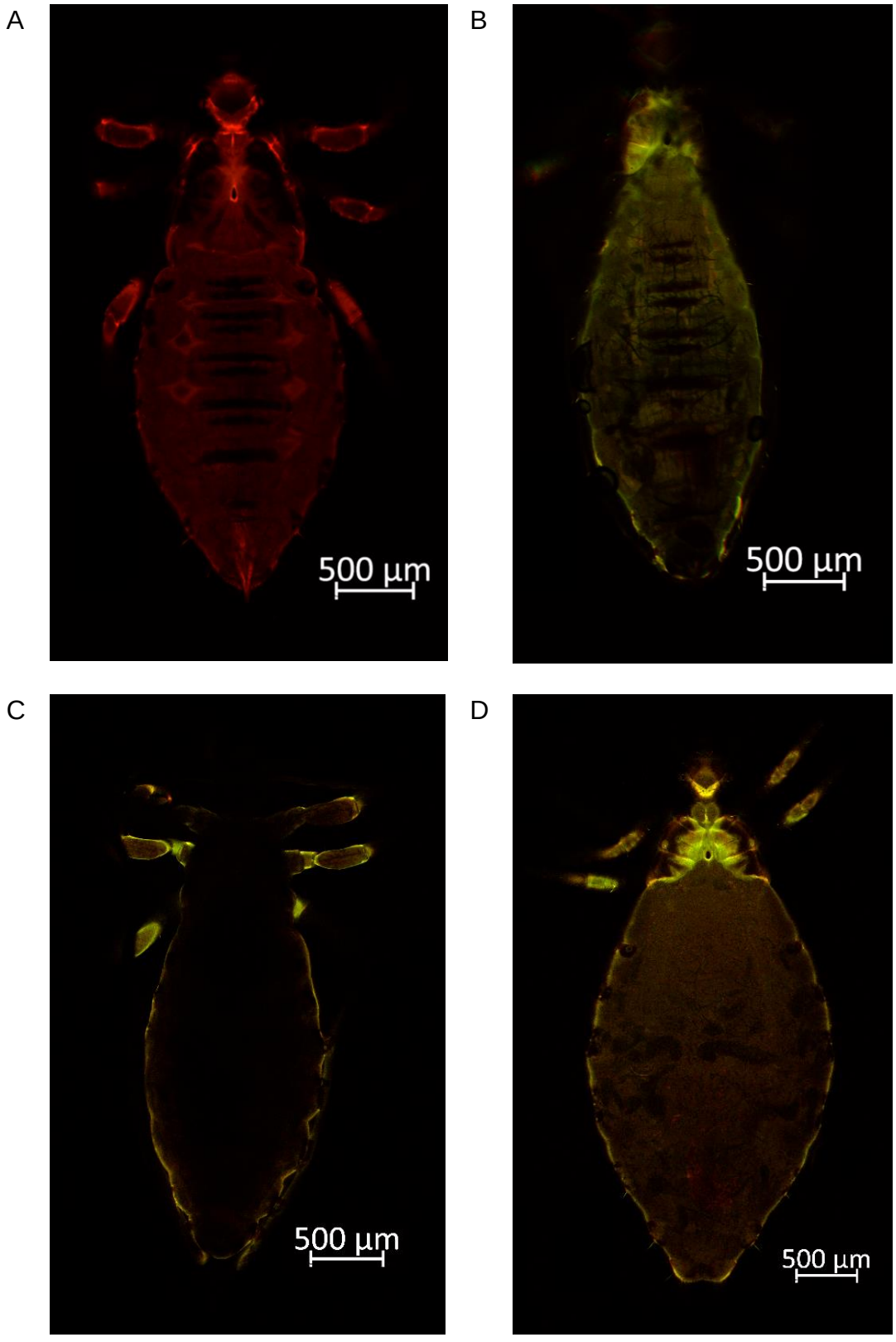

Figure 5.25. Confocal images of *P. corporis* 0 h post infection. No GFP can be seen due to the low numbers of bacteria and a high volume of blood. (A) negative control insect, fed sterile blood. (B) louse fed with parent *Y. pseudotuberculosis*, (C) louse fed with Δ*nagC* infected blood and (D) louse fed with the complemented Δ*nagC* lacking GFP.

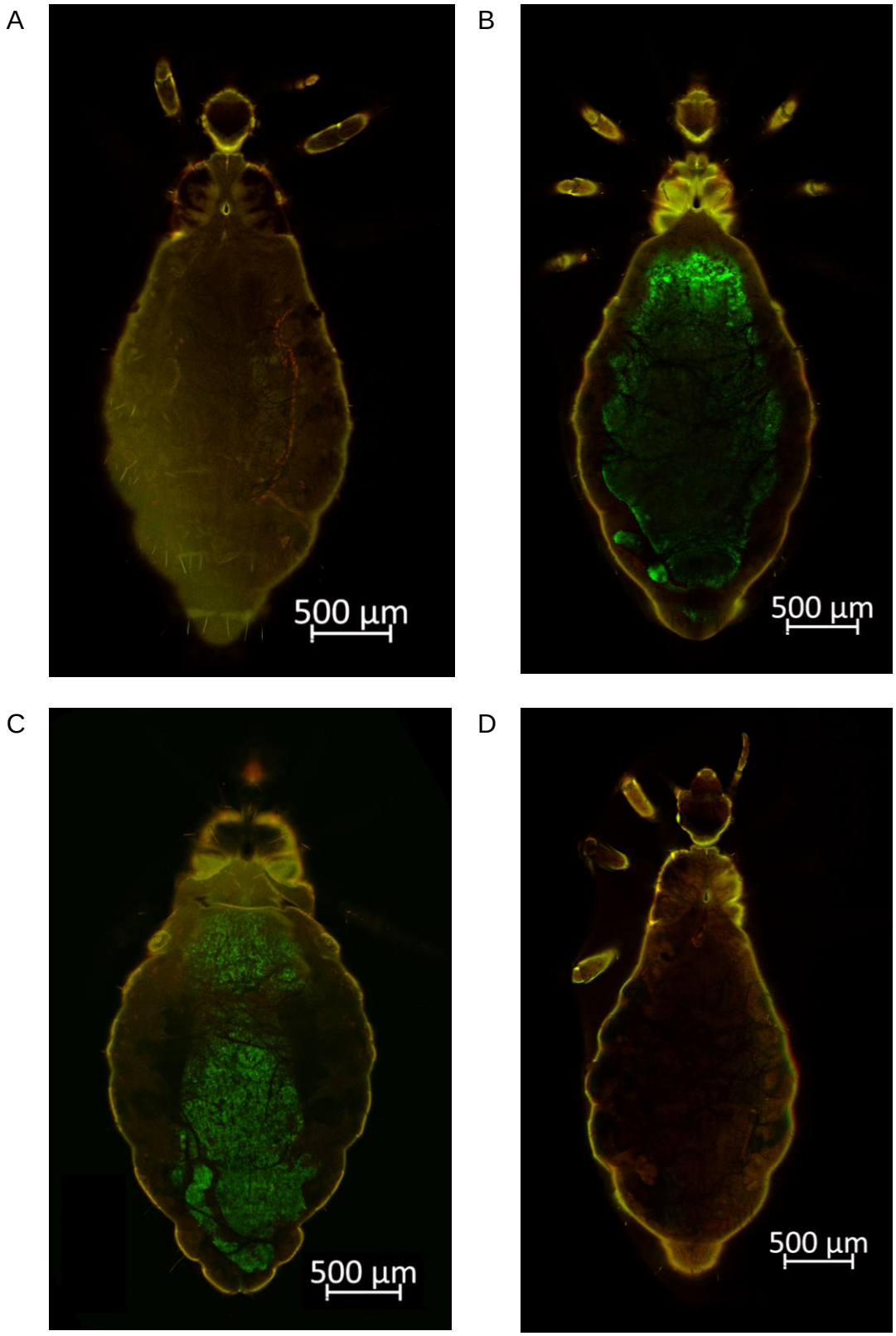

Figure 5.26. Confocal images of *P. corporis* 24 h post infection. (A) negative control insect, fed sterile blood. (B) louse fed with the GFP-labelled parent *Y. pseudotuberculosis*, with large amounts of GFP present in the distended gut (C) louse fed with the GFP-labelled Δ*nagC* mutant infected blood, also with large amounts of GFP and (D) louse fed with the complemented Δ*nagC* lacking GFP.

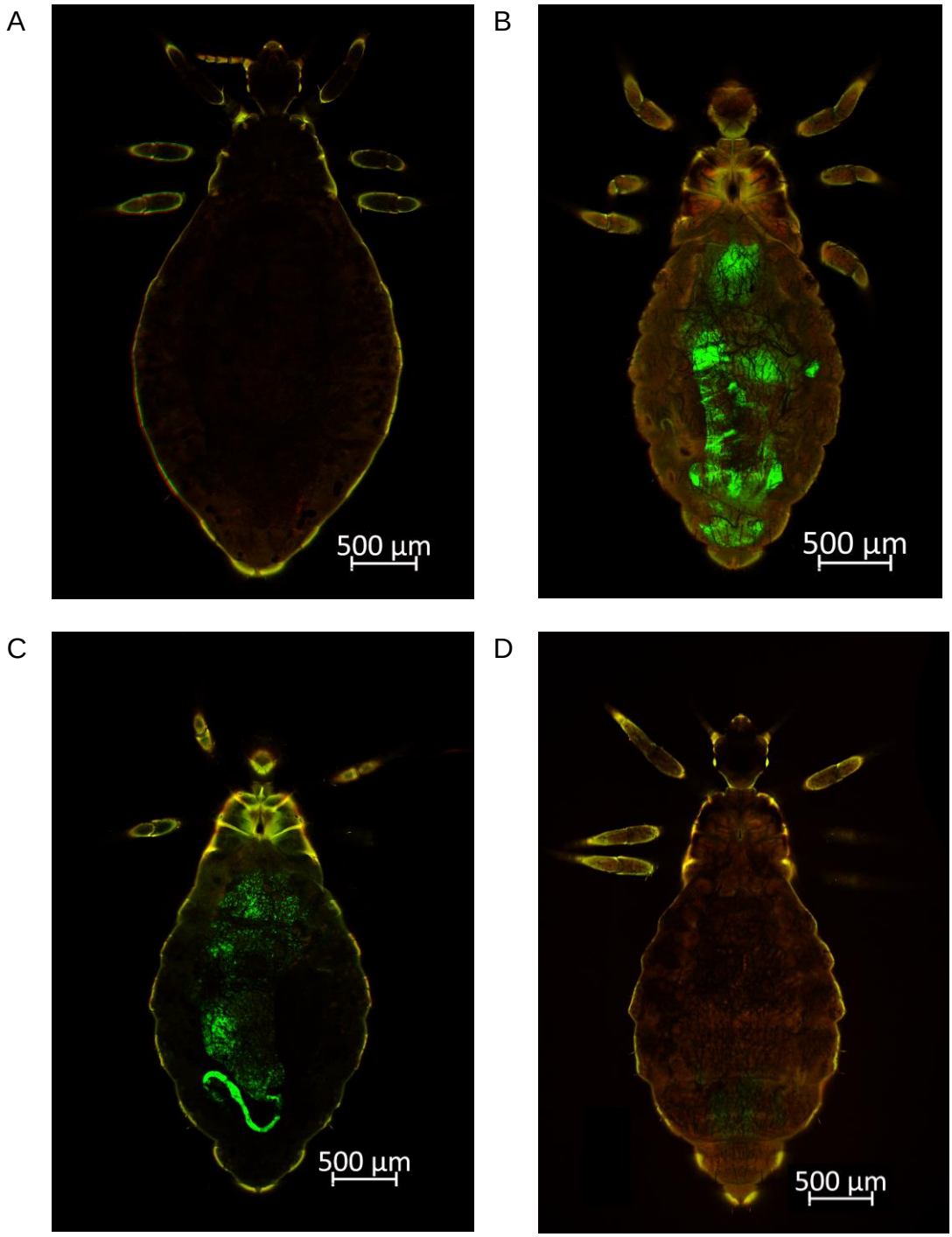

Figure 5.27. Confocal images of *P. corporis* 36 h post infection. (A) negative control insect, fed sterile blood. (B) louse fed with GFP-labelled parent *Y. pseudotuberculosis*, with large amounts of GFP still present in the still distended gut (C) louse fed with GFP-labelled Δ*nagC* mutant infected blood, with strongest fluorescence intensity in the hind gut, which has decreased in size and (D) louse fed with complemented Δ*nagC* that loses GFP.

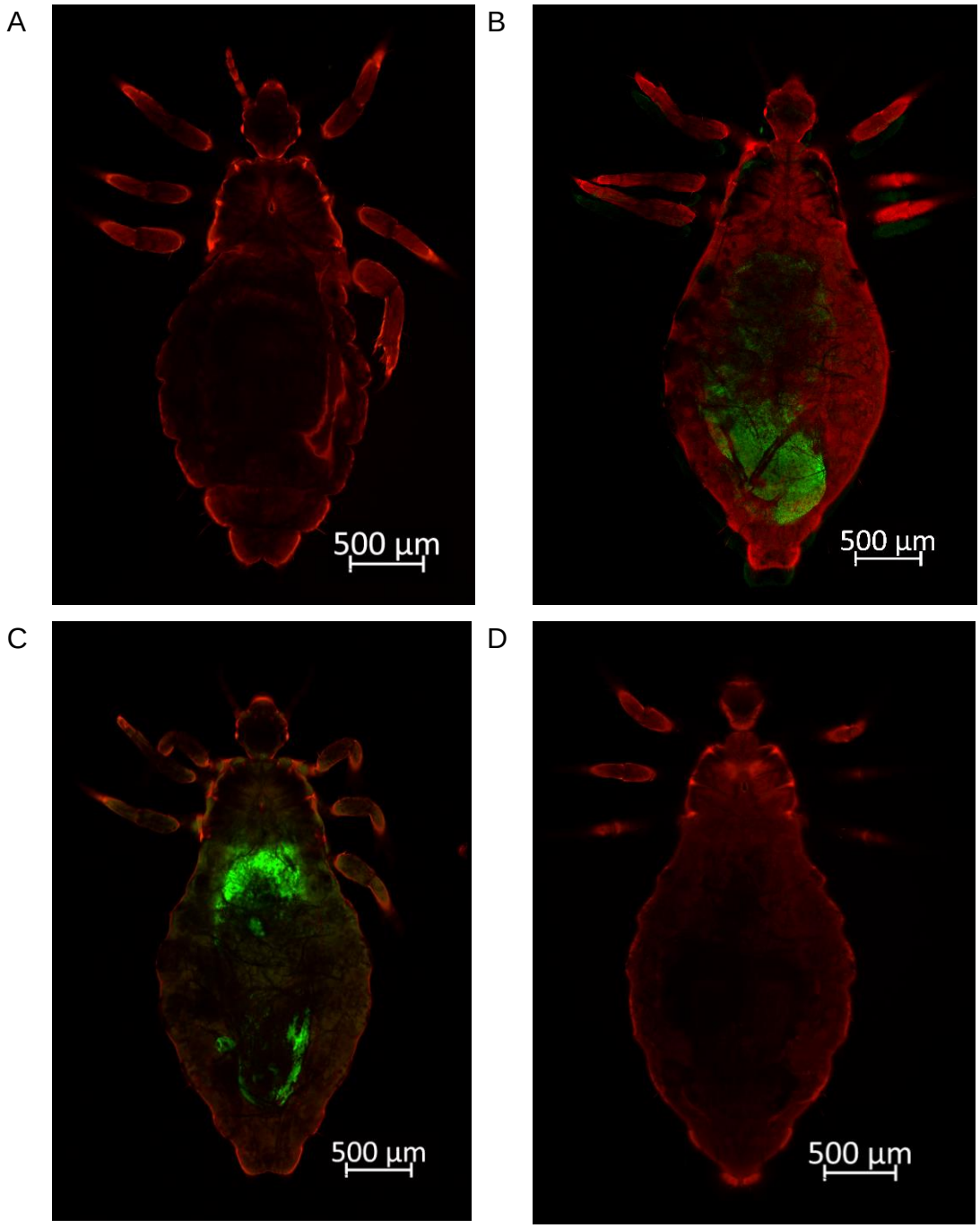

Figure 5.28. Confocal images of *P. corporis* 48 h post infection. (A) negative control insect, fed sterile blood. (B) louse fed with GFP-labelled parent *Y. pseudotuberculosis*, with large amounts of GFP present in the still swollen gut (C) louse fed with GFP-labelled Δ*nagC* infected blood with lower fluorescence intensity and a narrower gut and (D) louse fed with complemented Δ*nagC* that loses GFP.

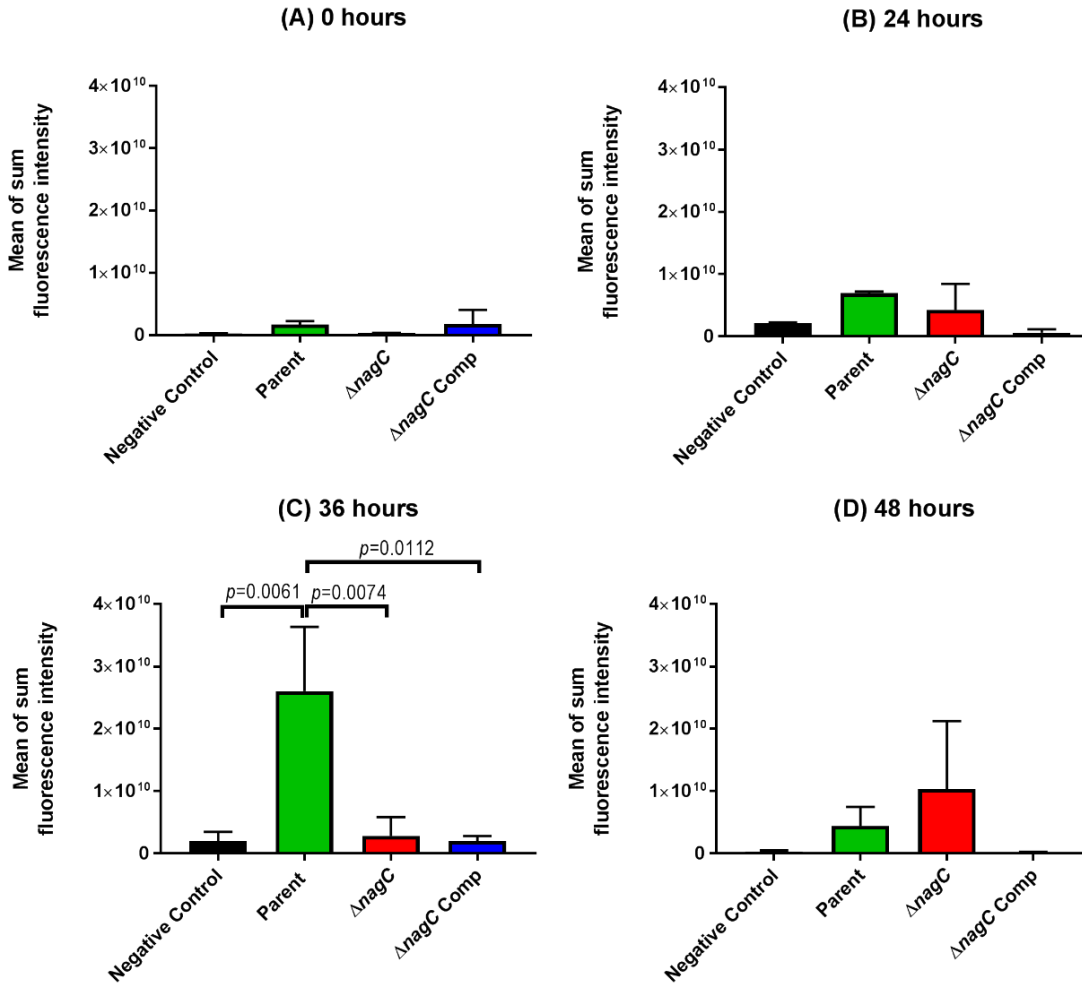

Figure 5.29. Fluorescence intensity over time for *P. corporis* fed *Y. pseudotuberculosis* parent and Δ*nagC* mutant. (A) very little fluorescence detected in lice killed at 0 h post infection, (B) slight increase in fluorescence, especially for those lice fed parent and *ΔnagC* strains. (C) significant increase in fluorescence detected in lice fed parent *Y. pseudotuberculosis* and (D) reduction of fluorescence in lice fed parent *Y. pseudotuberculosis*, to the same level as those lice fed Δ*nagC*. The sample size for each was n=20, *P*-values were calculated using one-way ANOVA and Tukey's multiple comparison test.

Although rhodamine-labelled WGA was added to the blood meals of all insects, little rhodamine fluorescence was detected in any of the lice apart from the auto fluorescence of the exoskeleton. Only 4 lice were seen to have red fluorescent patches within their guts, an example of which is shown in Figure 5.30. This was observed in lice fed both the parental and the Δ*nagC* mutant

strains of *Y. pseudotuberculosis*. Although the red stained areas did co-localise with the GFP-labelled bacteria in some cases, it was unclear whether this was poly-GlcNAc produced by the bacteria, or staining of louse or blood-based particulates.

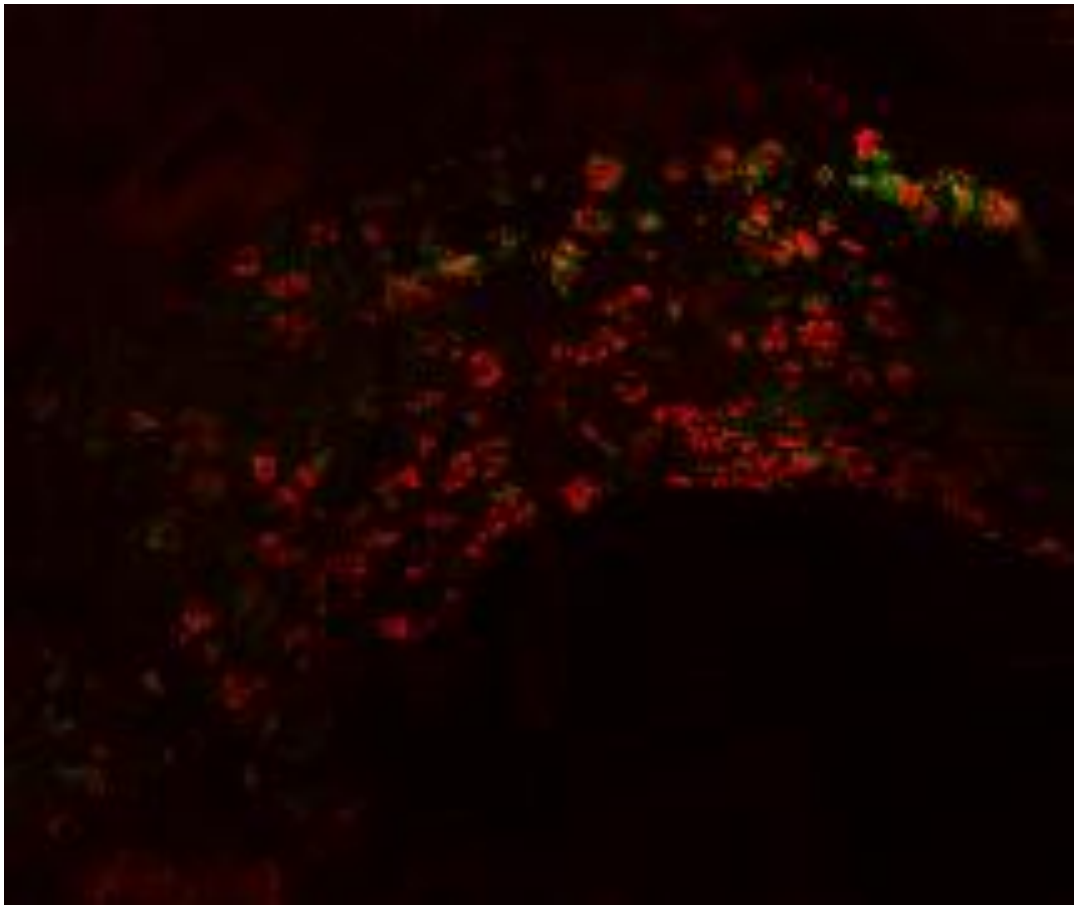

Figure 5.30. Confocal image showing an example of a louse gut with WGA-rhodamine red staining. Low levels of GFP fluorescence, indicating GFP-labelled *Y. pseudotuberculosis*, can be seen along the gut tract alongside patches of WGA staining. Only four lice showed this WGA staining within the gut. Taken at 10x magnification.

5.3.3.1 Deletion of NagC Enables *P. corporis* to Expel *Y. pseudotuberculosis* During Defaecation

After 24 h, insects fed with parent *Y. pseudotuberculosis* strain had produced twice as many faecal deposits as those fed the *ΔnagC* mutant or those not fed bacteria, as shown in Figure 5.31. Insects fed the complemented Δ*nagC* mutant were approximately half way between the two. After 36 h the rate of defaecation had slowed for all strains tested and approximate to that of the negative control insects.

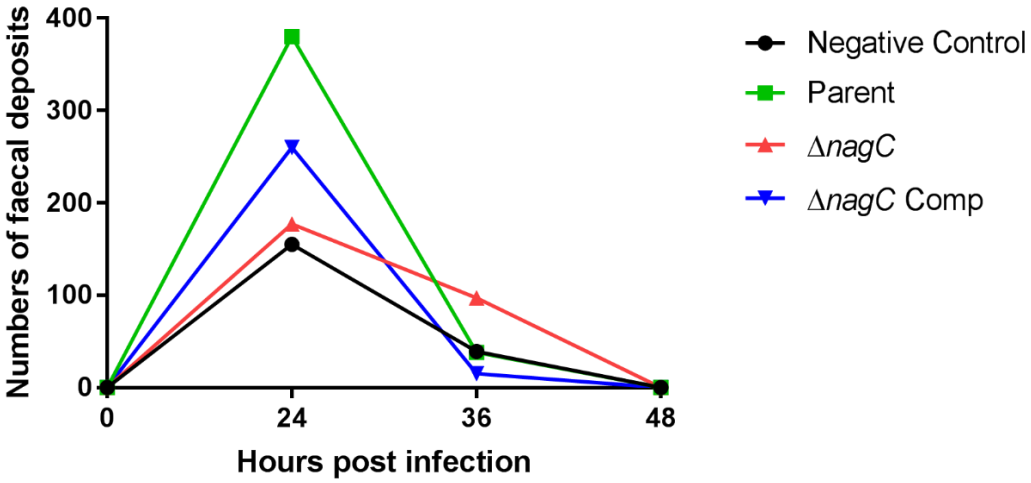

Figure 5.31. Number of faecal deposits produced by *P. corporis* fed *Y. pseudotuberculosis*. Insects fed parent and complemented Δ*nagC* strains produced more faecal deposits than those fed blood containing Δ*nagC*, which produced a similar number of deposits to those insects fed sterile blood.

GFP fluorescence was detected in individual faecal deposits for both the parental strain and the Δ*nagC* mutant. At both 24 and 36 h, the faecal deposits from insects fed parent *Y. pseudotuberculosis* had low levels of GFP, and individual cells could be counted. In comparison, the faecal deposits produced

by those insects fed on the Δ*nagC* mutant had much higher levels of GFP, to the point where some deposits were almost completely green. No GFP was detected in the faecal deposits of lice fed with the complemented Δ*nagC* mutant. Confocal images of individual faecal deposits are shown in Figure 5.32.

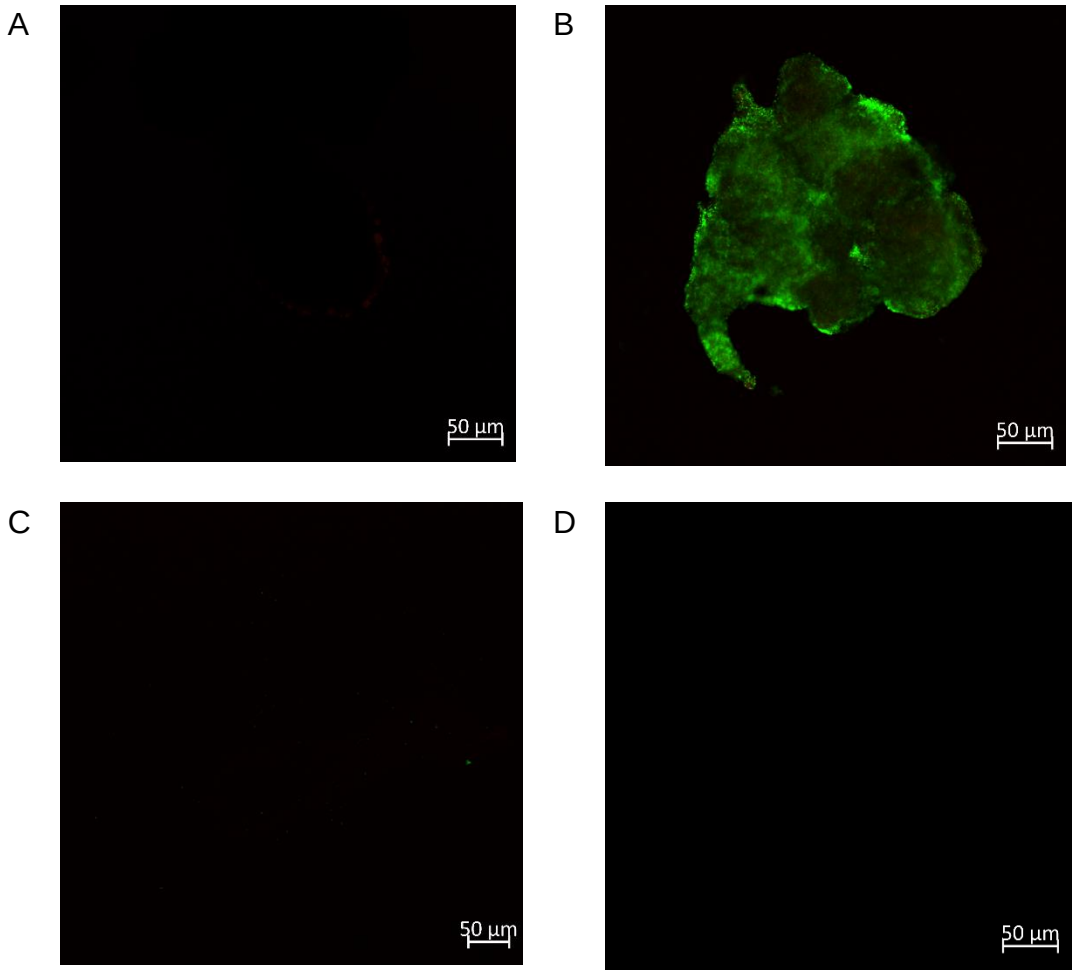

Figure 5.32. Confocal images showing GFP-labelled *Y. pseudotuberculosis* content of faecal deposits after 24 h produced by (A) negative control *P. corporis* (B) *P. corporis* fed the parent strain (C) insects fed the *ΔnagC* mutant and (D) insects fed the complemented *ΔnagC* strain.

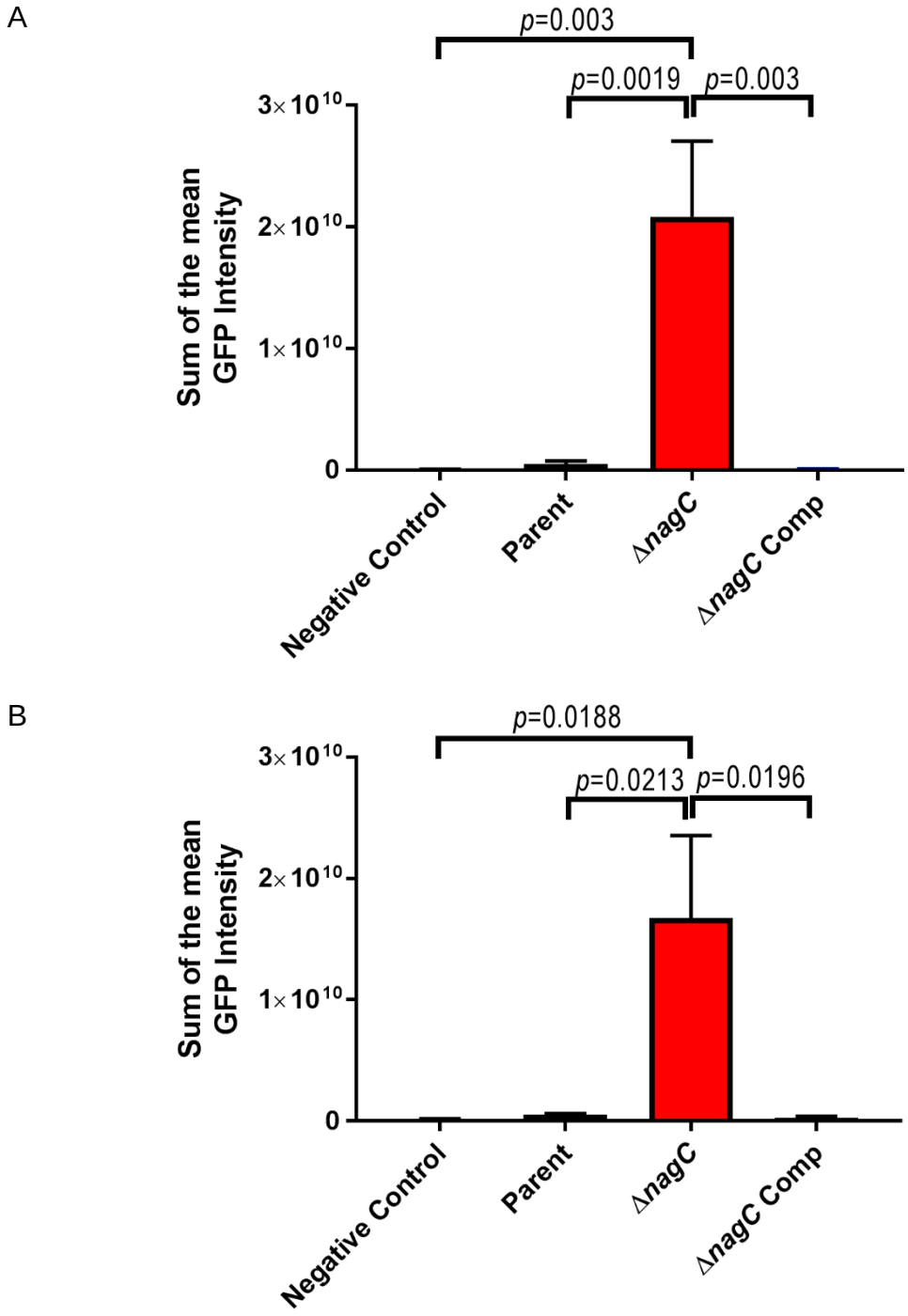

Figure 5.33. GFP fluorescence intensity detected in the faecal deposits of *P. corporis* at (A) 24 h and (B) 36 h. At both time points, the fluorescence intensity for insects fed Δ*nagC* was significantly higher than for those fed parent *Y. pseudotuberculosis*. The sample size for each was n=20, *P*-values were calculated using one-way ANOVA and Tukey's multiple comparison test.

When the GFP fluorescence of the faecal deposits was quantified, the lice fed blood containing the Δ*nagC* mutant were shown to have expelled significantly

more bacteria than those fed the parental strain. At 24 h post infection, those lice fed the *ΔnagC* mutant expelled 44 times more bacteria than those fed the parent strain and after 36 h they were still expelling 33 times more. This is shown in Figure 5.33.

5.4 Discussion

Chapter 4 described experiments that demonstrate a role for NagC in poly-GlcNAc production in *Y. pseudotuberculosis* and established that NagC binds to the promoter regions of the GlcNAc metabolism operons *nagE-nagBACD* and *glmUS* and the poly-GlcNAc biosynthesis operon *hmsHFRS* from *Y. pestis.* Given that poly-GlcNAc is the significant constituent of *Yersinia* biofilm ECM and Wiechmann (Ph.D. Thesis, 2015) showed that the *Y. pseudotuberculosis* Δ*nagC* mutant produces no biofilm on *C. elegans*, it was important to investigate the impact of the Δ*nagC* mutant on biofilm formation for both *Y. pestis* and *Y. pseudotuberculosis*.

When compared to *Y. pseudotuberculosis*, *Y. pestis* forms far more severe biofilms on the surface of *C. elegans*. BSI scores for *Y. pseudotuberculosis* were around 20%, whereas worms grown on *Y. pestis* plates scored four times higher. This suggests that large biofilms are important to *Y. pestis*, most likely when it needs to block the proventriculus of fleas (Hinnebusch, 2005). The more biofilm it can produce, the more likely the flea is to become fully 'blocked', thus the more likely it will be to pass on the bacteria to a new host. *Y. pseudotuberculosis* creates more biofilm at 37ºC than at 22ºC and whilst *Y. pestis* is likely to produce more biofilm at 22ºC, Yoong *et al.* (2012) have shown

that fully virulent KIM and CO92 strains of *Y. pestis* produce more poly-GlcNAc at mammalian temperatures, suggesting that the regulation of biofilm formation is a complex, multifaceted system.

These results correlate with the hypothesis put forward by Anja Wiechmann (Ph.D. Thesis, 2015), that the difference in biofilm formation between the *Y. pseudotuberculosis* parent and Δ*nagC* mutant strains on *C. elegans* could be a response to changes in the GlcNAc metabolism, caused by the up-regulation of the *nagE-nagBACD* operon and the lack of activation of the *glmUS* and *hmsHFRS* operons due to the absence of NagC. This leads to a reduction of poly-GlcNAc production, as there is no NagC to drive *hmsHFRS* expression.

C. elegans infected with the parental strain of *Y. pseudotuberculosis* exhibit exaggerated body bending, although Wiechmann (Ph.D. Thesis, 2015) showed that those worms fed with the Δ*nagC* mutant did not show this phenotype. In this study, worms infected with the parental, Δ*nagC* mutant and complemented Δ*nagC* strain of *Y. pestis* all showed exaggerated body bends and did not move well across the agar surface. This is likely due to the much higher levels of biofilm on *C. elegans* observed on all three strains, as even the *Y. pestis* Δ*nagC* mutant produced more biofilm than *Y. pseudotuberculosis*, which produced very little, allowing the worm to behave as if uninfected.

As presented in Chapter 4, the absence of NagC in *Y. pseudotuberculosis* results in lower levels of poly-GlcNAc and slower auto-aggregation, which may explain in part the reduction in biofilm formation observed for the *Y. pseudotuberculosis* and potentially the *Y. pestis* Δ*nagC* mutant. Auto-aggregation has been shown in some cases to be a precursor to biofilm

formation (Sorroche *et al.*, 2012; Trunk, S. Khalil and C. Leo, 2018). Auto-aggregation is also influenced by the T3SS and production of YOPs, so the degradation of virulence factors shown in Chapter 4 may affect the auto-aggregation for *Y. pestis in vitro* (Anja Wiechmann, Ph.D. Thesis, 2015, Natalie Barrett, Ph.D. Thesis, 2018).

Also shown in Chapter 4, NagC plays an important role in the production of poly-GlcNAc, the major component of *Yersinia* ECM and biofilm on *C. elegans* in this chapter (Wiechmann Ph.D. Thesis, 2015). Evaluating the Δ*nagC Y. pseudotuberculosis* and *Y. pestis* mutant in insect models was the next logical step. As biofilm is important for plague transmission in insects, the deletion of *nagC* could have important implications for the spread of *Y. pestis*. Due to practical constraints around using live insects in a CL3 environment, however, the 'fake flea' *in vitro* model was developed. This study found that dissolved chitin coated onto poly-L-lysine treated glass coverslips was the best chitin substrate for *Y. pseudotuberculosis* attachment. Although bacteria did attach to chitin flakes from shrimp shells, the uneven surface of the flakes made it difficult to obtain reproducible data. 48 h appeared to be the optimal length of time for incubation of *Y. pseudotuberculosis* with the chitin-coated coverslips. Shorter time intervals and the bacteria failed to form large aggregations and longer incubation periods resulted in a decrease in mean fluorescence intensity, suggesting that the bacteria began to lyse or detach from chitin surface.

The *Yersiniae* produce greater amounts of biofilm in low nutrient conditions to protect themselves from outside stresses (Petrova and Sauer, 2012). Despite the nutrients in the digested blood meal, the flea gut is thought to be a low

nutrient environment for *Y. pestis* (Willias *et al.*, 2015; Hinnebusch, Jarrett and Bland, 2017). Although there were no significant differences in the mean fluorescence intensity of bacteria on the coverslips when incubated in different media, YDMM, the lowest nutrient medium tested, showed a slight increase in attachment, which agrees with the literature (Petrova and Sauer, 2012; Willias *et al.*, 2015). Adding heat-inactivated bovine serum slightly increased attachment of *Y. pseudotuberculosis* to the chitin coverslips (Gallardo-Moreno *et al.*, 2002).

Once the optimal conditions for the 'fake flea' proventriculus model were ascertained, the *Y. pseudotuberculosis* Δ*nagC* mutant was tested, to see whether the deletion of *nagC* affected biofilm formation on a chitin surface. The Δ*nagC* mutant demonstrated a decreased fluorescence intensity and therefore attachment at 37ºC, but not at 22ºC. This was not unexpected for *Y. pseudotuberculosis*, as biofilm formation is part of its virulence response at mammalian temperatures. When conducted using *Y. pestis*, biofilm production is likely to be higher at flea temperatures (Hinnebusch and Erickson, 2008) although poly-GlcNAc expression is higher for *Y. pestis* at mammalian temperatures (Yoong, Cywes-Bentley and Pier, 2012). The presence of biofilm for the parental and complemented Δ*nagC* strains was confirmed using SEM, as it was not possible to identify poly-GlcNAc on a chitin surface with WGA because of the auto-fluorescence of the chitin. SEM images showed large aggregations of bacteria embedded within the ECM (Branda *et al.*, 2005; Annous, Fratamico and Smith, 2009; Joshua, Atkinson, Robert J Goldstone, *et al.*, 2015; Zhao *et al.*, 2017).

Having produced a working *in vitro* model for *Yersinia*-proventriculus biofilm interactions which helped elucidate the role of NagC in biofilm formation, it was important to ascertain whether NagC had a role *in vivo*. The results of this study's *P. corporis* infection assays are consistent with the limited literature on *Y. pseudotuberculosis* insect infection studies. *Y. pseudotuberculosis* has previously been reported to cause severe diarrhoea in both *X. cheopis* and *P. corporis*, leading to a reduced insect lifespan of 48 h or less (Krynski and Becla, 1965; Erickson *et al.*, 2007). The present study showed that the parental strain of *Y. pseudotuberculosis* persisted and proliferated in the lice, despite the large quantities of faecal deposits produced. Although there is little current literature on *Y. pseudotuberculosis* infection of *P. corporis*, Erickson *et al.* (2008) proposed that when fed to fleas, *Y. pseudotuberculosis* expresses the poly-GlcNAc hydrolase *nghA* gene that is absent from *Y. pestis*, which was suggested may interfere with biofilm formation and colonisation in insect vectors. While this study is consistent with the finding that insects fed parental *Y. pseudotuberculosis* do produce large volumes of faecal matter and have shorter lifespans, it is clear that the parental strain could remain and proliferate within the gut. This suggests that *Y. pseudotuberculosis* YPIII is capable of insect colonisation, albeit perhaps not as effectively as *Y. pestis*, as this is not a natural life stage for *Y. pseudotuberculosis*. Whilst functional insecticidal toxin complexes (Tcs) are found in *Y. pseudotuberculosis*, *Y. pestis* does not have Tcs, the loss of which is likely to have been due to the jump from enteric pathogen to insect-vector mediated pathogen (Pinheiro and Ellar, 2007; Gengler *et al.*, 2015).

This study extended this research to investigate the impact of NagC on the ability of *P. corporis* to clear a *Y. pseudotuberculosis* infection and whether biofilms may potentially play a role in insect colonisation. The lice fed parent and complemented Δ*nagC* strains had diarrhoea in the first 24 h, then appeared to become 'blocked up', producing no more faeces. There was little GFP signal in these faeces but when imaged, lice fed the parental strain showed high GFP intensities in their gastrointestinal tracts, suggesting the bacteria had remained and proliferated within the louse, rather than being expelled in the faeces. In comparison, lice fed the Δ*nagC* mutant produced similar amounts of faecal deposits to the negative control lice but when imaged, showed high numbers of bacteria, suggesting that NagC is likely to play a role in allowing *Y. pseudotuberculosis* to establish itself in the louse gut. As the lice fed the complemented Δ*nagC* strain showed similar survival and faecal deposit patterns to those fed parental *Y. pseudotuberculosis*, it is likely that the complemented strain restored the phenotype back to the parental one, but due to the failure of the GFP plasmid, this couldn't be confirmed using fluorescence microscopy.

Despite the addition of WGA to the bloodmeals of each louse, rhodamine fluorescence was only detected in the guts of four lice. These intestinal WGA patches were found in lice fed both parent and Δ*nagC Y. pseudotuberculosis* infected blood. Though the outline of the louse was apparent, the rhodamine channel failed to detect the intestinal tract, apart from a few small, red patches which may be derived from the ingestion of human cellular or louse cuticular debris (Osaki *et al.*, 2015).

If large amount of GlcNAc was present in the louse gut, lice fed the Δ*nagC* mutant are likely to have shown the same infection pattern as those fed the parental strain. This would be consistent with previous work (Wiechmann, Ph.D. Thesis, 2015), as well as this study, where exogenous GlcNAc restored biofilm formation for both *Y. pseudotuberculosis* and *Y. pestis* Δ*nagC* mutants on the 'fake flea' and *C. elegans* models.

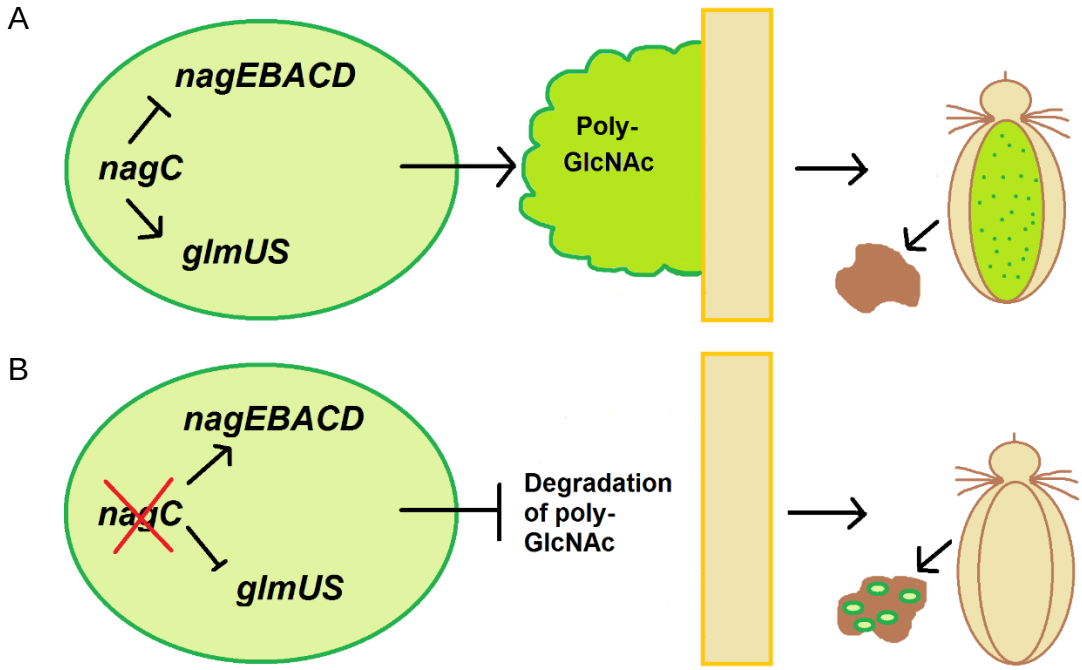

Figure 5.34. Proposed role of NagC in biofilm production in insect vectors of the *Yersiniae*. In the parent strain (A) of *Y. pseudotuberculosis* (depicted as a green circle in this figure), NagC represses the *nagE-nagBACD* operon (which degrades GlcNAc) and activates the *glmUS* operon, which produces GlcNAc. *Y. pseudotuberculosis* may form biofilms within the insect gut employing poly-GlcNAc as part of its ECM. This production of biofilm causes the insect gut to become blocked and therefore allows *Yersinia* transmission. In the Δ*nagC* mutant (B), the *nagE-nagBACD* operon remains de-repressed, thus degrading GlcNAc, and the *glmUS* operon is not activated, so no GlcNAc is produced. This means no biofilm can be produced and the insect is able to pass the bacteria out of the gut, reducing transmission likelihood.

Lice fed the parent and complemented Δ*nagC* strains produced twice as many faecal deposits within the first 24 h as those fed the *Y. pseudotuberculosis* Δ*nagC* mutant, which did not affect the rate of faecal production. However, the faecal deposits produced by Δ*nagC* mutant-fed lice exhibited high levels of GFP fluorescence. Given that the insects did not have significantly different amounts of GFP fluorescence compared with the negative controls, this provides further evidence of a role for NagC in the colonisation of the *P. corporis'* gut by *Y. pseudotuberculosis*. The larger quantities of faecal deposits produced by lice infected with the parent and complemented Δ*nagC* mutant is likely the cause of the shorter insect lifespans, as *P. corporis* are highly susceptible to desiccation (Waniek, 2009). These results are consistent with previous studies, that indicate that an infection with *Enterobacteriaceae* usually cause the death of a louse within 48 h when infected intrarectally (Krynski 1965).

This study proposes that as the louse gut is relatively nutrient-poor (Hinnebusch, Jarrett and Bland, 2017), when lice are infected, *Y. pseudotuberculosis* (and likely *Y. pestis*) will repress the GlcNAc-degrading operon *nagE-nagBACD* and activate the *glmUS* operon in the presence of NagC, allowing the production of poly-GlcNAc which enables the bacteria to form aggregations, potentially incorporating proteins from the gut, to stop the louse from passing the bacteria out in the faeces. Conversely, if NagC is not present, the opposite occurs and poly-GlcNAc is not produced, making it easier for the louse to pass individual bacteria out in its faeces. A schematic of the proposed effects of NagC on the retention of *Y. pseudotuberculosis* in insects is shown in Figure 5.34.

5.4.1 Summary

After studying the effects of NagC on biofilm formation in *Y. pseudotuberculosis* and *Y. pestis*, it can be proposed that:

- NagC controls the ability of *Y. pestis* to form biofilms on the surface of *C. elegans*
- The 'Fake flea' proventriculus model can be used as an *in vitro* model for studying chitin-bacterial interactions
- On a chitinous surface, the *Y. pseudotuberculosis* Δ*nagC* mutant produces less biofilm than the parental strain
- The parental phenotype can be restored with the addition of exogenous GlcNAc
- NagC plays an important role in the colonisation of *P. corporis*

6 Conclusions and Future Directions

6.1 Conclusions and Future Directions

Plague, or the black death, still kills numerous people across the world each year, prompting the World Health Organisation to class *Y. pestis* as a (re)emerging dangerous pathogen of epidemic potential (Galimand *et al.*, 1997; WHO, 2015). Previous research dating back to the turn of the 20th century has shown that *Y. pestis* is transmitted by fleas and produces a biofilm, which adheres to the proventriculus in the digestive system of fleas causing a blockage of the insect and spreading disease to mammalian hosts (Bacot, 1914b; Hinnebusch, Jarrett and Bland, 2017). Poly-GlcNAc is known to be the predominant component of the biofilm ECM of the *Yersiniae* and without it, *Y. pestis* is unable to form a biofilm and block the digestive system of the fleas, rendering the insects unable to transmit plague (Hinnebusch, 2005). GlcNAc metabolism is controlled by NagC in other bacterial species, such as *E. coli* (Plumbridge, 1990) and as shown in this study, also in *Y. pestis*. While the role of NagC has been studied extensively in *E. coli* (Plumbridge 1996; Le Bihan *et al.* 2017) and *V. fischeri* (Miyashiro *et al.* 2012), its functions were less well understood in *Y. pseudotuberculosis* (Wiechmann, Ph.D. Thesis, 2015) and not at all in *Y. pestis*. The contribution of NagC to the regulation of poly-GlcNAc in any bacterium was not known.

The use of vector insects in transmission and infection studies often relies upon the use of mammalian hosts, such as rabbits and guinea pigs to maintain colonies (Takano-Lee, Yoon, *et al.*, 2003; Hinnebusch, 2007; Mumcuoglu *et al.*, 2011; Chouikha and Hinnebusch, 2012). Whilst these systems are successful, the health, safety and ethical implications of the use of animals in

experiments made the development of artificial feeding systems an inviting prospect.

This study set out to establish artificially fed colonies of the Oriental rat flea, *X. cheopis* and the human body louse, *P. corporis*, using the Hemotek feeding system, rather than the conventional rabbit or neonatal mouse-based systems currently used. Whilst this research ultimately failed to maintain either of these colonies for use in experimentation, much useful information was ascertained. This study showed that environmental conditions are vital to the success of insect colonies, especially to *P. corporis*, which are highly sensitive to desiccation (Waniek, 2009). Further research into dual feeding to wean insects slowly onto an artificial feeding system may be the best way to successfully maintain these haematophagous insect colonies.

The most important environmental conditions for both *X. cheopis* and *P. corporis* were humidity and temperature. Humidity plays a key role, especially when considering the decrease in insect feeds per day using the artificial system compared to in the wild (Waniek, 2009). This is more important for lice, which feed up to five times per day on a human host, but is difficult and time consuming to replicate with a mammalian lab host, let alone an artificial feeding system (Bonilla *et al.*, 2009). Having had feeding success with both the lice and the fleas, it is likely that the environmental conditions are of paramount importance for the survival of both colonies. Acquisition of a specially adapted incubator to control both temperature and humidity is likely to provide greater success, especially for the more fragile *P. corporis*.

Both *X. cheopis* and *P. corporis* preferred defibrinated human blood compared to sheep and rabbit blood. Whilst this is closest to the human blood naturally

consumed by *P. corporis* and therefore unsurprising, the fact that *X. cheopis*, naturally a parasite of rats and rodents rather than people, preferred it, suggests that freshness of the blood also played a role (Service, 2008b, 2008a). The fact that the rabbit blood contained antibiotics may also point to why it was not favoured by either insect species and caused the lice to die more quickly. The use of different blood types and ways to process them, such as the use of anticoagulants versus defibrination is likely to be an important aspect of artificially rearing insect colonies and thus is a key area for future research consideration.

Both insect species preferred the collagen membrane over Parafilm or mouse skins. This is in contrast with reports from the keepers of the original flea colony, who suggested their fleas preferred mouse skins to collagen when fed artificially (Florent Sebbane, Institut Pasteur, Lille, France, personal communication).

While the results of the artificially fed colony maintenance did not provide *X. cheopis* and *P. corporis* for insect vector experiments, it was important to characterise the regulatory role of NagC in *Y. pestis*, as it has been shown to play an important role in biofilm formation in *V. fischeri* to aid colonisation of the Hawaiian squid *Euprymna scolopes* by repressing the *nagE-nagBAC* catabolism operon (Miyashiro *et al.*, 2011) as well as in *Y. pseudotuberculosis* and therefore may play an important role in the blockage of the guts of insect vectors of *Y. pestis* (Sun *et al.* 2015; Wiechmann, Ph.D. Thesis, 2015). Elucidating how plague is transmitted and the genes involved in transmission is important from a disease control perspective and may lead to potential prevention strategies.

By successfully constructing a *Y. pestis* Δ*nagC* mutant, this study has shown that NagC does influence AHL production and the *Y. pestis* QS phenotype of YOP production, although not auto-aggregation, under the environmental conditions tested. QS enables pathogenic bacteria to coordinate protective or virulent actions. Whilst NagC was not shown to influence *Y. pestis* auto-aggregation, it was shown to reduce auto-aggregation in *Y. pseudotuberculosis* at 37ºC, suggesting that it may play a role in the mammalian infection strategy of *Y. pseudotuberculosis*, as it uses auto-aggregation and biofilm formation to attach to and colonise host epithelial gut cells (Hares *et al.*, 2008). As auto-aggregation can be either T3SS-dependent or independent and therefore can be influenced by YOPs, preventing YOP cleavage by the plasminogen activator protease PI so ensuring a full YOP profile would be a useful next step further elucidating auto-aggregation of *Y. pestis* (Anja Wiechmann, Ph.D. Thesis, 2015, Natalie Barrett, Ph.D. Thesis, 2018). Given that blood products have also been implicated in *Y. pestis* auto-aggregation at 22ºC, the addition of blood serum may also be of interest (Hinnebusch, Jarrett and Bland, 2017).

Chapter 4 describes the elucidation of a role for NagC in the regulation of the GlcNAc pathway in the *Yersiniae*, given that it is known to regulate the GlcNAc degradation operon *nagE-nagBACD* and production operon *glmUS* in *E. coli* (Plumbridge, 1990). This study also set out to identify whether NagC directly regulates the *hmsHFRS* operon in *Y. pestis*, which is required for poly-GlcNAc in flea temperature biofilms (Bobrov *et al.*, 2008), although this is contradicted by Yoong *et al.* (2012) who suggest poly-GlcNAc production is maximal at 37ºC. Licencing and health and safety requirements meant that *Y.*

pseudotuberculosis was used to identify the influence of NagC on poly-GlcNAc production and this study showed that the Δ*nagC* mutant produced significantly less poly-GlcNAc at 37ºC compared to the parental strain and production could be restored by the introduction of 1 mM exogenous GlcNAc. Once it was ascertained that NagC plays a role in the production of poly-GlcNAc in *Y. pseudotuberculosis*, its role as a DNA binding protein was explored in *Y. pestis,* as CL3 conditions were not needed for this experiment. NagC in *Y. pseudotuberculosis* and *Y. pestis* has 99% sequence identity across the whole protein and thus the results obtained in this study potentially apply to both species. This study showed that recombinant NagC binds to the promoter region of the GlcNAc metabolic operons *nagE-nagBACD*, *glmUS* and the poly-GlcNAc biosynthesis operon *hmsHFRS*, indicating a role as a regulator of this pathway. The addition of GlcNAc-6-P, but not GlcNAc, enhanced the binding of recombinant NagC to *nagE-nagBACD* and inhibited the binding of NagC to *hmsHFRS*, suggesting that the GlcNAc pathway controls both GlcNAc and poly-GlcNAc biosynthesis. Interestingly, this is different from the literature, which has focused on *E. coli*, suggesting that there may be other factors involved in the *Yersiniae* GlcNAc metabolism. To elucidate how gene transcription is controlled and understand this highly complex system, further work, such as promoter fusions, is needed to establish the whole picture.

Although a NagC DNA binding site was predicted for *hmsHFRS*, further experimental work will be required to test this. It would also be interesting to further study the interaction of NagC with the GlcNAc metabolic operons, using additional *in silico* analysis, DNA foot printing, promoter fusions and confirming

by mutating residues in NagC binding sites to identify the role of NagC as a repressor or activator at each target promoter. Identifying NagC boxes in the other *hms* operons and T3SS promoters such as *virF* would also be of interest, as GlcNAc influences QS expression (Wiechmann, Ph.D. Thesis, 2015).

Whilst poly-GlcNAc production has previously been investigated in *Y. pestis* using WGA staining of cultures, and *hmsT* and *hmsP* positively and negatively regulate poly-GlcNAc production respectively (Bobrov *et al.*, 2008), the role of NagC in poly-GlcNAc production is yet to be identified. Given the role of NagC in regulating the GlcNAc metabolism elucidated in Chapter 4, creating a CL3 protocol to investigate poly-GlcNAc production in the Δ*nagC* mutant in *Y. pestis* would be the next logical step.

Having shown that NagC plays a role in the production of poly-GlcNAc in the *Yersiniae*, this study sought to understand the role of NagC in biofilm formation within *in vitro* and *in vivo* insect models. Previous research had used the model organism *C. elegans* to establish a role for NagC in biofilm formation in *Y. pseudotuberculosis* (Wiechmann, Ph.D. Thesis, 2015) and *C. elegans* has been used as a model for *Y. pestis* biofilm formation in fleas (Joshua *et al.*, 2003; Tan and Darby, 2006). This study showed that the *Y. pestis* Δ*nagC* mutant produced less biofilm than the parental strain on *C. elegans*. A diagram of the phenotypic roles for NagC identified in this study is presented in Figure 6.1.

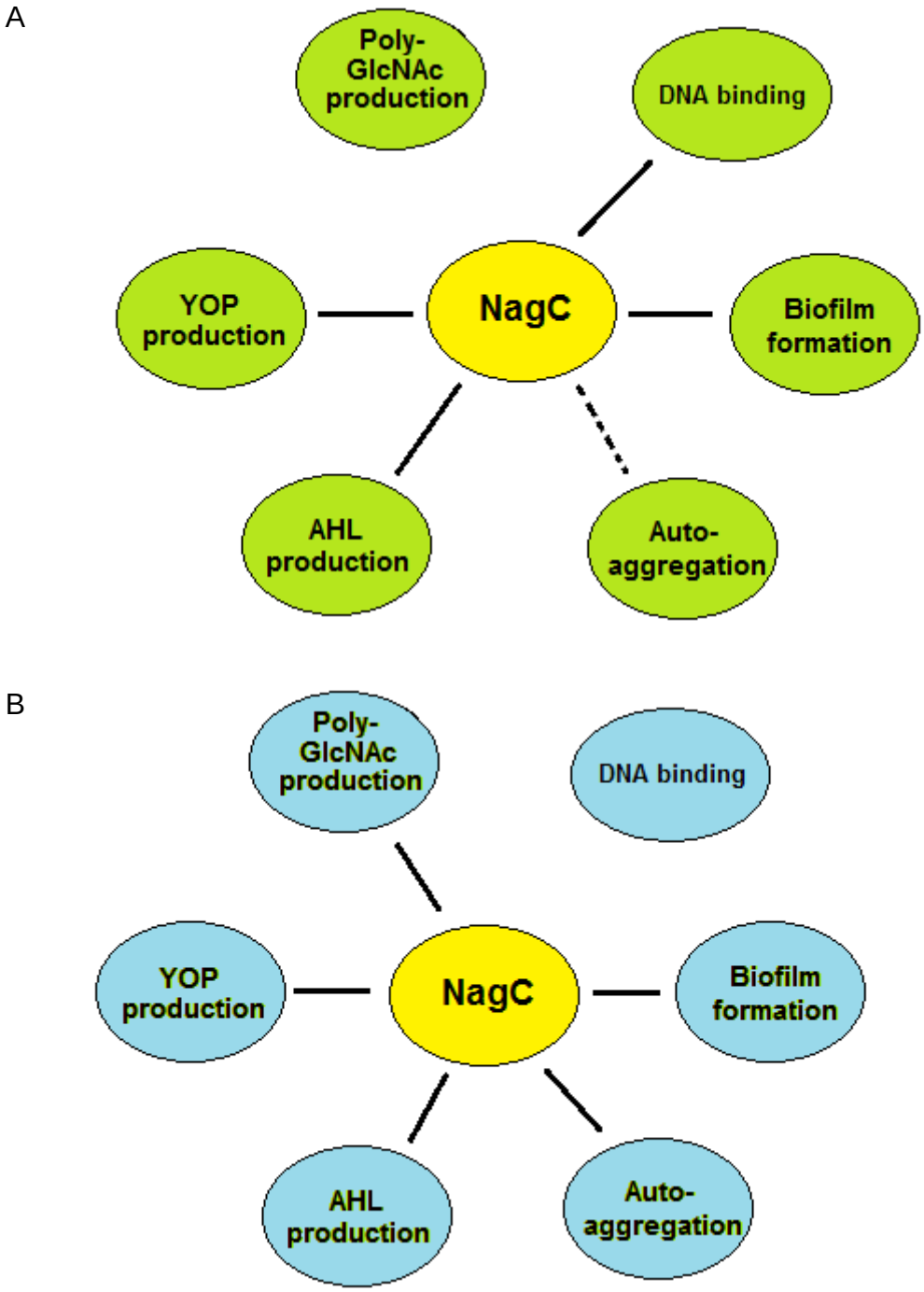

Figure 6.1 Schematic of the roles for NagC identified for (A) *Y. pestis* (represented in green) and (B) *Y. pseudotuberculosis* (represented in blue) in this study. Solid lines indicate that NagC has been shown to influence that phenotype. Dotted lines indicate that the relationship has been examined, but not relationship was found. No line indicated that a phenotype was not examined for that species in this study. The interactions between NagC, GlcNAc and QS in *Y. pestis* and *Y. pseudotuberculosis* is likely to be complex.

The Δ*nagC* mutant was found to influence QS phenotypes in *Y. pestis* and *Y. pseudotuberculosis* in this study, which further strengthens the model put forward by Wiechmann (Ph.D. Thesis, 2015), that NagC has a role to play in the control of QS in the *Yersiniae* due to its influence on the QS regulatory genes. That NagC controls GlcNAc biosynthesis, which has also been shown to influence QS, at a genetic level, suggests a complex regulatory network between NagC, GlcNAc and QS. This is backed up by research in other organisms showing that GlcNAc is associated with virulence, host colonisation and biofilm formation in *E. coli* (Chang et. al. 2004), *P. aeruginosa* (Korgaonkar et. al. 2013) and *V. cholerae* (Ghosh et. al. 2011).

Once it was established that the *Y. pestis* Δ*nagC* mutant produced reduced biofilm on *C. elegans*, this study aimed to test the mutant in insect models. Due to licensing issues and time constraints, this work was unable to be completed using *Y. pestis*. Consequently, the genetically similar *Y. pseudotuberculosis* was used to develop *in vitro* and *in vivo* models, the foundation for subsequent NagC work in *Y. pestis*. Given both the practical and legislative difficulties of using live insects within a CL3 laboratory, a ‘fake flea’ proventriculus model was developed to explore bacterial attachment and biofilm production on a chitinous surface. Aiming to mimic the flea gut as closely as possible, environmental conditions were tested until optimal bacterial attachment occurred. This involved coating a coverslip with dissolved chitin to obtain a reproducible surface (Moustafa *et al.*, 2007), the use of a low nutrient medium to mimic the flea gut environment (Willias *et al.*, 2015; Hinnebusch, Jarrett and Bland, 2017) and a 48 h incubation period (Eisen, Dennis and Gage, 2015). The addition of bovine serum did not appear to significantly influence bacterial

attachment (Gallardo-Moreno *et al.*, 2002). The 'fake flea' model was a simple and practical method to identify bacterial attachment to chitin and many adjustments and additions could be made to suit it to different scientific questions, such as the role of chitinases in the *Yersiniae*.

Once the optimal conditions for the 'fake flea' model had been established, it was used to ascertain that the *Y. pseudotuberculosis* Δ*nagC* mutant was not capable of as much attachment as the parental strain. The Δ*nagC* mutant showed mainly individual cells attaching, whereas the parent developed large surface aggregations of bacteria, of a substantial thickness at 37ºC. Since the biofilm being made is predominantly of poly-GlcNAc, and GlcNAc is the monomeric component of chitin, it was impossible to ascertain whether the parental strain aggregation showed biofilm properties using WGA stain. The ability of the parental strain and the inability of the Δ*nagC* mutant to form biofilms on the surface of the 'fake flea' was instead confirmed using SEM. This was further supported when 1 mM exogenous GlcNAc was added to restore the Δ*nagC* mutant to the parental phenotype at 37ºC. Whilst it is to be expected that *Y. pseudotuberculosis* would form more biofilm at 37ºC, it is likely that *Y. pestis* would form more at flea body temperature. Since more poly-GlcNAc was reported to be produced at mammalian rather than flea body temperatures, it will be interesting to extend this research to identify the optimum temperature for *Y. pestis* poly-GlcNAc production and biofilm formation (Yoong *et al.* 2012; Wiechmann, Ph.D. Thesis, 2015).

Given that the 'fake flea' model was successful, this study investigated whether NagC played a role in the colonisation of insect vectors *in vivo*. Owing to its more successful feeding rates, as identified in Chapter 3, *P. corporis* was

infected with *Y. pseudotuberculosis*. Very little research has been done on the infection of *P. corporis* with *Y. pestis* and even less with *Y. pseudotuberculosis* (Krynski and Becla, 1965; Houhamdi *et al.*, 2006). This study showed that lice fed the parental strain of *Y. pseudotuberculosis* experienced a much shorter life span and exhibited severe diarrhoea, which agrees with the previous literature (Krynski and Becla, 1965). Whilst the addition of WGA did not demonstrate the presence of *Y. pseudotuberculosis* mediated poly-GlcNAc or biofilm in the guts of the lice, the proliferation of GFP-labelled bacteria over time suggests that *Y. pseudotuberculosis* can in fact colonise the louse gut.

Given that the parental strain of *Y. pseudotuberculosis* appeared to cause pathology and early mortality in *P. corporis*, it was interesting to note that those lice fed with the Δ*nagC* mutant showed no signs of infection, with survival and faecal deposition rates similar to negative control lice fed uninfected blood. This would suggest that NagC and possibly the ability to produce poly-GlcNAc and therefore biofilm, does play a role in the colonisation of *P. corporis*. Owing to time and insect acquisition constraints, this experiment could not be expanded upon, so it would be of great interest to use this model with the *Y. pestis* Δ*nagC* mutant, to see whether it has the same effect. Identifying potential sources of exogenous GlcNAc within insect guts may also shed light on the metabolism of this polysaccharide in relation to *Y. pestis* colonisation.

6.2 Concluding Remarks

This study has shown that NagC plays a role in the QS phenotypes of the *Yersiniae*. NagC has an important role in the production of poly-GlcNAc and

biofilm and it has, for the first time, been shown that recombinant NagC binds to the promoter regions of the *nagE-nagBACD*, *hmsHFRS* and *glmUS* operons in *Y. pestis* and potentially, *Y. pseudotuberculosis* too. It has also been demonstrated that NagC controls the ability of *Y. pseudotuberculosis* to produce poly-GlcNAc and the ability of both *Y. pestis* and *Y. pseudotuberculosis* to produce biofilms in *in vitro* and *in vivo* insect vector models.

Although at times answering *Y. pestis*-insect interaction questions proved challenging, the development of an artificial 'fake flea' model paves the way for a range of further model bacteria-flea interaction studies and can be modified to suit many research questions. Due to the apparent difficulties of artificially maintaining haematophagous insect colonies and the health and safety implications of using live insects in a CL3 laboratory, this model may make research on fully virulent strains much more practical.

7 References

Achtman, M., Zurth, K., Morelli, G., Torrea, G., Guiyoule, A. and Carniel, E. (1999) '*Yersinia pestis*, the Cause of Plague, is a Recently Emerged Clone of *Yersinia pseudotuberculosis*', *Proceedings of the National Academy of Sciences of the United States of America*, 96(24), pp. 14043–8

Annous, B. A., Fratamico, P. M. and Smith, J. L. (2009) 'Quorum Sensing in Biofilms: Why Bacteria Behave the Way They Do', *Journal of Food Science*, 74(1)

Atkinson, S., Chang, C., Sockett, R. E., Ca, M., Williams, P. and Acteriol, J. B. (2006) 'Quorum Sensing in *Yersinia enterocolitica* Controls Swimming and Swarming Motility', *Journal of Bacteriology*, 188(4), pp. 1451–1461

Atkinson, S., Chang, C. Y., Patrick, H. L., Buckley, C. M. F., Wang, Y., Sockett, R. E., Cámara, M. and Williams, P. (2008) 'Functional Interplay Between the *Yersinia pseudotuberculosis* YpsRI and YtbRI Quorum Sensing Systems Modulates Swimming Motility by Controlling Expression of *flhDC* and *fliA*', *Molecular Microbiology*, 69(1), pp. 137–151

Atkinson, S., Goldstone, R. J., Joshua, G. W. P., Chang, C. Y., Patrick, H. L., Cámara, M., Wren, B. W. and Williams, P. (2011) 'Biofilm development on *Caenorhabditis elegans* by *Yersinia* is facilitated by quorum sensing-dependent repression of type III secretion', *PLoS Pathogens*, 7(1)

Atkinson, S., Throup, J. P., Stewart, G. S. A. B. and Williams, P. (1999) 'A Hierarchical Quorum-Sensing System in *Yersinia pseudotuberculosis* is Involved in the Regulation of Motility and Clumping', *Molecular Microbiology*, 33(6), pp. 1267–1277

Atkinson, S. and Williams, P. (2009) 'Quorum sensing and social networking in the microbial world', *Journal of the Royal Society, Interface / the Royal Society*, 6(40), pp. 959–978

Bacot, A. W. (1914a) 'Further Notes on the Mechanism of the Transmission of Plague by Fleas', *Journal of Hygiene*, pp. 774–778.

Bacot, A. W. (1914b) 'Observations on the Length of Time that fleas (*Ceratophyllus fasciatus*) Carrying *Bacillus pestis* in their Alimentary Canals are able to Survive in the Absence of a Host and Retain the Power to Re-infect with Plague', *Journal of Hygiene*, pp. 770–773

Bacot, A. W. and Martin, C. J. (1915) 'Observations on the Mechanism of the Transmission of Plague by Fleas', *Journal of Hygiene*, pp. 423–439.
Baker, D. G. (2008) *Flynn's Parasites of Laboratory Animals*

Barratt, N. A. (2018) *The Type III Secretion System and its Role in the Multicellular Behaviour of Yersinia Species*

Bearden, S. W., Sexton, C., Pare, J., Fowler, J. M., Arvidson, C. G., Yerman, L., Viola, R. E. and Brubaker, R. R. (2009) 'Attenuated Enzootic (*Pestoides*)

Isolates of *Yersinia pestis* Express Active Aspartase', *Microbiology*, 155(1), pp. 198–209

Bhaduri, S. and Smith, J. L. (2011) 'Virulence Plasmid (pYV)-Associated Expression of Phenotypic Virulent Determinants in Pathogenic *Yersinia* Species: A Convenient Method for Monitoring the Presence of pYV under Culture Conditions and Its Application for Isolation/Detection of *Yersinia pestis*', *Journal of Pathogens*, pp. 1–9

Bland, D. M. and Hinnebusch, B. J. (2016) 'Feeding Behavior Modulates Biofilm-Mediated Transmission of *Yersinia pestis* by the Cat Flea, *Ctenocephalides felis*', *PLOS Neglected Tropical Diseases*, 10(2), p. e0004413

Bobrov, A. G., Bearden, S. W., Fetherston, J. D., Khweek, A. A., Parrish, K. D. and Perry, R. D. (2007) 'Functional Quorum Sensing Systems Affect Biofilm Formation and Protein Expression in *Yersinia pestis*', *Advances in Experimental Medicine and Biology*, 603, pp. 178–191

Bobrov, A. G., Kirillina, O., Forman, S., Mack, D. and Perry, R. D. (2008) 'Insights into *Yersinia pestis* Biofilm Development: Topology and Co-Interaction of Hms Inner Membrane Proteins Involved in Exopolysaccharide Production', *Environmental Microbiology*, 10(6), pp. 1419–1432

Bobrov, A. G., Kirillina, O., Vadyvaloo, V., Koestler, B. J., Hinz, A. K., Mack, D., Waters, C. M. and Perry, R. D. (2014) 'The *Yersinia pestis* HmsCDE regulatory system is essential for blockage of the oriental rat flea (*Xenopsylla cheopis*), a classic plague vector', *Environmental Microbiology*, 17, pp. 947–959

Bonilla, D. L., Kabeya, H., Henn, J., Kramer, V. L. and Kosoy, M. Y. (2009) '*Bartonella quintana* in Body Lice and Head Lice from Homeless Persons, San Francisco, California, USA', *Emerging Infectious Diseases*, 15(6), pp. 912–915

Branda, S. S., Vik, Å., Friedman, L. and Kolter, R. (2005) 'Biofilms: The matrix revisited', *Trends in Microbiology*, 13(1), pp. 20–26

Brubaker, R. R. (1991) 'Factors Promoting Acute and Chronic Diseases Caused by *Yersiniae*', *Microbiology*, 4(3), pp. 309–324

Brubaker, R. R., Beesley, E. D. and Surgalla, M. J. (1965) '*Pasteurella pestis*: Role of Pesticin I and Iron in Experimental Plague', *Science*, 149(3682), pp. 422–424.

Bryers, J. D. (2008) 'Medical biofilms', *Biotechnology and Bioengineering*, 100(1), pp. 1–18

Busby, J. N., Landsberg, M. J., Simpson, R. M., Jones, S. A., Hankamer, B., Hurst, M. R. H. and Lott, J. S. (2012) 'Structural Analysis of Chi1 Chitinase

from Yen-Tc: The Multisubunit Insecticidal ABC Toxin Complex of *Yersinia entomophaga*', *Journal of Molecular Biology*. Elsevier Ltd, 415(2), pp. 359–371

Butler, T. (1994) '*Yersinia* Infections: Centennial of the Discovery of the Plague Bacillus', *Clinical Infectious Diseases*, 19(4), pp. 655–663

Butler, T. (2013) 'Review article: Plague gives surprises in the first decade of the 21st century in the United States and worldwide', *American Journal of Tropical Medicine and Hygiene*, 89(4), pp. 788–793

Buxton, P. a. (1940) 'The biology of the body louse (*Pediculus humanus corporis: Anoplura*) under experimental conditions', *Parasitology*, 32(03), p. 303

Cavanaugh, D. C., Wheeler, C. M., Suyemoto, W., Shimada, T. and Yamakawa, Y. (1956) 'Studies on *Pasteurella pestis* in Various Flea Species I. Infection of Flea Species with Avirulent Strains of *Pasteurella pestis*', *The Journal of Infectious Diseases*, 98(1), pp. 103–106

Chang, D., Smalley, D. J., Tucker, D. L., Leatham, M. P., Norris, W. E., Stevenson, S. J., Anderson, A. B., Grissom, J. E., Laux, D. C., Cohen, P. S. and Conway, T. (2004) 'Carbon Nutrition of *Escherichia coli* in The Mouse Intestine', *PNAS*, 101(19), pp. 7427–7432

Chouikha, I. and Hinnebusch, B. J. (2012) '*Yersinia*-flea interactions and the evolution of the arthropod-borne transmission route of plague', *Current Opinion in Microbiology*. Elsevier Ltd, 15(3), pp. 239–246

Cole, M. M. (1966) 'Body Lice', in Smith, C. N. (ed.) *Insect Colonization and Mass Production*. New York: Academic Press Inc., pp. 15–24

Cornelis, G. R. (2002) 'The *Yersinia* Ysc-Yop "type III" weaponry', *Nature reviews. Molecular cell biology*, 3(October), pp. 742–752

Cornelis, G. R. (2006) 'The type III secretion injectisome', *Nature reviews. Microbiology*, 4(November), pp. 811–825

Cowan, C., Jones, H. A., Kaya, Y. H., Perry, R. D. and Straley, S. C. (2000) 'Invasion of Epithelial Cells by *Yersinia pestis*: Evidence for a *Y. pestis*-Specific Invasin', *Infection and immunity*, 68(8), pp. 4523–4530

Culpepper, G. H. (1946) 'Factors Influencing the Rearing and Maintenance of a Laboratory Colony of the Body Louse', *Journal of Economic Entomology*, 39(4), pp. 472–474

Darby, C., Hsu, J. W., Ghori, N. and Falkow, S. (2002) '*Caenorhabditis elegans*: Plague Bacteria Biofilm Blocks Food Intake', *Nature*, 417(6886), pp. 243–244

Dean, K. R., Stenseth, N. C., Walløe, L., Lingærde, O. C., Bramanti, B. and Schmid, B. V (2018) 'Human Ectoparasites spread Plague during the Black Death and Second Pandemic', *Proceedings of the National Acadamy of Sciences*, pp. 1–6

Deng, W., Burland, V., Plunkett, G. I., Boutin, A., Mayhew, G. F., Liss, P., Perna, N. T., Rose, D. J., Mau, B., Zhou, S., Schwartz, D. C., Fetherston, J. D., Lindler, L. E., Brubaker, R. R., Plano, G. V, Straley, S. C., McDonough, K. A., Nilles, M. L., Matson, J. S., Blattner, F. R. and Perry, R. D. (2002) 'Genome Sequence of *Yersinia pestis* KIM', *American Society for Microbiology*, 184(16), pp. 4601–4611

Dennis, D. T., Gage, K. L., Gratz, N., Poland, J. D. and Tikhomirov, E. (1999) *Plague Manual: Epidemiology, Distribution, Surveillance and Control*, *World Health Organization*

Derbise, A., Chenal-Francisque, V., Huon, C., Fayolle, C., Demeure, C. E., Chane-Woon-Ming, B., Médigue, C., Hinnebusch, B. J. and Carniel, E. (2010) 'Delineation and Analysis of Chromosomal Regions Specifying *Yersinia pestis*', *Infection and Immunity*, 78(9), pp. 3930–3941

Doll, J. M., Zeitz, P. S., Ettestad, P., Bucholtz, a. L., Davis, T. and Gage, K. (1994) 'Cat-transmitted fatal pneumonic plague in a person who traveled from Colorado to Arizona', *American Journal of Tropical Medicine and Hygiene*, 51(1), pp. 109–114

Donlan, R. M. (2002) 'Biofilms: Microbial Life on Surfaces', *Emerging Infectious Diseases*, 8(9), pp. 881–890

Drali, R., Shako, J. C., Davoust, B., Diatta, G. and Raoult, D. (2015) 'A New Clade of African Body and Head Lice Infected by *Bartonella quintana* and *Yersinia pestis* - Democratic Republic of the Congo', *American Journal of Tropical Medicine and Hygiene*, 93(5), pp. 990–993

Du, Y., Rosqvist, R. and Forsberg, Å. (2002) 'Role of Fraction 1 Antigen of *Yersinia pestis* in Inhibition of Phagocytosis', *Infection and Immunity*, 70(3), pp. 1453–1460

Eisen, R. J., Dennis, D. T. and Gage, K. L. (2015) 'The Role of Early-Phase Transmission in the Spread of *Yersinia pestis*', *Journal of Medical Entomology*, 52(6), pp. 1183–1192

Eitel, J., Eitel, J., Dersch, P. and Dersch, P. (2002) 'The YadA Protein of *Yersinia pseudotuberculosis* Mediates High-Efficiency Uptake into Human Cells under Environmental Conditions in Which Invasin is Repressed', *Infection and Immunity*, 70(9), pp. 4880–4891

Engebrecht, J. and Silverman, M. (1984) 'Identification of Genes and Gene Products Necessary for Bacterial Bioluminescence', *Proceedings of the National Academy of Sciences of the United States of America*, 81(13), pp.

4154–4158

Epstein, H. F. and Shakes, D. C. (1995) '*Caenorhabditis elegans*: Modern Biological Analysis of an Organism', in *Methods in Cell Biology*, pp. 1–654

Erickson, D. L., Jarrett, C. O., Callison, J. A., Fischer, E. R. and Hinnebusch, B. J. (2008) 'Loss of a Biofilm-Inhibiting Glycosyl Hydrolase During the Emergence of *Yersinia pestis*', *Journal of Bacteriology*, 190(24), pp. 8163–8170

Erickson, D. L., Jarrett, C. O., Wren, B. W. and Hinnebusch, B. J. (2006) 'Serotype Differences and Lack of Biofilm Formation Characterize *Yersinia pseudotuberculosis* Infection of the *Xenopsylla cheopis* Flea Vector of *Yersinia pestis*', *Journal of Bacteriology*, 188(3), pp. 1113–1119

Erickson, D. L., Waterfield, N. R., Vadyvaloo, V., Long, D., Fischer, E. R., Ffrench-constant, R. and Hinnebusch, B. J. (2007) 'Acute Oral Toxicity of *Yersinia pseudotuberculosis* to Fleas: Implications for the Evolution of Vector-Borne Transmission of Plague', *Cellular Microbiology*, 9(11), pp. 2658–2666

Ewing, W. H., Ross, A. J., Brenner, D. O. N. J., Fanning, G. R., Biochemistry, D. and Reed, W. (1978) '*Yersinia ruckeri* sp. nov., the Redmouth (RM) Bacterium', *International Journal of Systematic Bacteriology*, 28(1), pp. 37–44

Fahlgren, A., Avican, K., Westermark, L., Nordfelth, R. and Fällman, M. (2014) 'Colonization of cecum is important for development of persistent infection by *Yersinia pseudotuberculosis*', *Infection and Immunity*, 82(8), pp. 3471–3482

Fang, N., Qu, S., Yang, H., Fang, H., Liu, L., Zhang, Y., Wang, L., Han, Y., Zhou, D. and Yang, R. (2014) 'HmsB enhances biofilm formation in *Yersinia pestis*', *Frontiers in Microbiology*, 5(December), pp. 1–8

Fang, N., Yang, H., Fang, H., Liu, L., Zhang, Y., Wang, L., Han, Y., Zhou, D. and Yang, R. (2015) 'RcsAB is a Major Repressor of *Yersinia* Biofilm Development Through Directly Acting on *hmsCDE, hmsT*, and *hmsHFRS*', *Scientific Reports*, 5, pp. 1–8

Felek, S., Muszyński, A., Carlson, R. W., Tsang, T. M., Hinnebusch, B. J. and Krukonis, E. S. (2010) 'Phosphoglucomutase of *Yersinia pestis* is Required for Autoaggregation and Polymyxin B Resistance', *Infection and Immunity*, 78(3), pp. 1163–1175

Frederiksen, R. F., Paspaliari, D. K., Larsen, T., Storgaard, B. G., Larsen, M. H., Ingmer, H., Palcic, M. M. and Leisner, J. J. (2013) 'Bacterial Chitinases and Chitin-Binding Proteins as Virulence Factors', *Microbiology (United Kingdom)*, 159(PART 5), pp. 833–847

Fukuto, H. S., Vadyvaloo, V., McPhee, J. B., Poinar, H. N., Holmes, E. C. and Bliska, J. B. (2018) 'A Single Amino Acid Change in the Response Regulator PhoP Acquired During *Yersinia pestis* Evolution Affects PhoP Target Gene Transcription and Polymyxin B Susceptibility', *Journal of Bacteriology*, (February), p. JB.00050-18

Fuqua, C. and Winans, S. C. (1996) 'Conserved cis-Acting Promoter Elements Are Required for Density-Dependent Transcription of *Agrobacterium tumefaciens* Conjugal Transfer Genes', *Journal of Bacteriology*, 178(2), pp. 435–440

Gage, K. L. and Kosoy, M. Y. (2005) 'Natural history of plague: perspectives from more than a century of research', *Annual review of entomology*, 50(70), pp. 505–528

Galimand, M., Guiyoule, A., Gerbaud, G., Rasoamanana, B. W., Chanteau, S., Carniel, E. and Courvalin, P. (1997) 'Multidrug Resistance in *Yersinia Pestis* Mediated by a Transferable Plasmid', *The New England Journal of Medicine*, 337(10), pp. 677–680

Gallardo-Moreno, A. M., Gonza, M. L., Pe, C., Bruque, M., Go, A. C. and Ru, W. (2002) 'Serum as a Factor Influencing Adhesion of *Enterococcus faecalis* to Glass and Silicone', *Applied and Environmental Microbiology*, 68(11), pp. 5784–5787

Gelhaus, H. C., Rozak, D. A., Nierman, W. C., Chen, D., Mojgan Zadeh, J. J. V., Ulrich, R. L. and Adamovicz, J. J. (2009) 'Exogenous *Yersinia pestis* Quorum Sensing Molecules N-octanoyl-homoserine lactone and N-(3-oxooctanoyl)-homoserine lactone Regulate the LcrV Virulence Factor', *Microbial Pathogenesis*. Elsevier Ltd, 46(5), pp. 283–287

Gengler, S., Laudisoit, A., Batoko, H. and Wattiau, P. (2015) 'Long-Term Persistence of *Yersinia pseudotuberculosis* in Entomopathogenic Nematodes', *PLoS ONE*, 10(1), pp. 1–17

Georgi, J. R. (1996) 'Artificial System and Method for Breeding Hematophagous Insects'. USA

Georgi, J. R. and Wade, S. E. (1989) 'Artificial System and Method for Breeding Fleas'. USA

Ghosh, S., Rao, K. H., Sengupta, M., Bhattacharya, S. K. and Datta, A. (2011) 'Two Gene Clusters Co-ordinate for a Functional N-acetylglucosamine Catabolic Pathway in *Vibrio cholerae*', *Molecular Microbiology*, 80(6), pp. 1549–1560

Götz-Rösch, C., Sieper, T., Fekete, A., Schmitt-Kopplin, P., Hartmann, A. and Schröder, P. (2015) 'Influence of Bacterial N-acyl-Homoserine Lactones on Growth Parameters, Pigments, Antioxidative Capacities and the Xenobiotic Phase II Detoxification Enzymes in Barley and Yam Bean',

Frontiers in Plant Science, 6(April), pp. 1–13

Guo, X.-P., Ren, G.-X., Zhu, H., Mao, X.-J. and Sun, Y.-C. (2015) 'Differential regulation of the *hmsCDE* operon in *Yersinia pestis* and *Yersinia pseudotuberculosis* by the Rcs phosphorelay system', *Scientific Reports*, 5, p. 8412

Habedank, B., Schrader, G., Scheurer, S., Schein, E., Robinson, W., Rettich, F. and Rambo, G. (1999) 'Investigations on the *in Vitro* Feeding and *in Vitro* Breeding of the Human Body Louse *Pediculus humanus corporis* (Anoplura: *Pediculidae*)', *Proceedings of the 3rd International Conference on Urban Pests Prague*, (1949), pp. 241–248

Hares, M. C., Hinchliffe, S. J., Strong, P. C. R., Eleftherianos, I., Dowling, A. J., Ffrench-Constant, R. H. and Waterfield, N. (2008) 'The *Yersinia pseudotuberculosis* and *Yersinia pestis* Toxin Complex is Active Against Cultured Mammalian Cells', *Microbiology*, 154(11), pp. 3503–3517

Heise, T. and Dersch, P. (2006) 'Identification of a Domain in *Yersinia* Virulence Factor YadA that is Crucial for Extracellular Matrix-specific Cell Adhesion and Uptake', *Proceedings of the National Academy of Sciences of the United States of America*, 103(9), pp. 3375–80

Hellman, L. and Fried, M. (2007) 'Electrophoretic Mobility Shift Assay (EMSA) for Detecting Protein-Nucleic Acid Interactions', *Nature protocols*, 2(8), pp. 1849–1861
.
Heroven, A. K. and Dersch, P. (2014) 'Coregulation of Host-Adapted Metabolism and Virulence by Pathogenic *Yersiniae*', *Frontiers in Cellular and Infection Microbiology*, 4(October), p. 146

Hill, J., Leiker, T., Sitterly, A., Tirrell, I., Nguyen, A. T., Mentz, R. and Slivka, E. (2007) 'NagD UMPase from *Escherichia coli* and virulence factor "NagD" phosphoglycolate phosphatase from *Staphylococcus aureus*, two distinct members of the nitrophenyl phosphatase family of the HAD superfamily', *Journal of the Federation of American Societies for Experimental Biology*, 21(792.2)

Hinnebusch, B. J. (1997) 'Bubonic plague: A molecular genetic case history of the emergence of an infectious disease', *Journal of Molecular Medicine*, 75(9), pp. 645–652

Hinnebusch, B. J. (2002) 'Role of *Yersinia* Murine Toxin in Survival of *Yersinia pestis* in the Midgut of the Flea Vector', *Science*, 296(5568), pp. 733–735

Hinnebusch, B. J. (2005) 'The Evolution of Flea-Borne Transmission in *Yersinia pestis*', *Current Issues in Molecular Biology*, 7(2), pp. 197–212

Hinnebusch, B. J. (2007) 'Flea Bedding for *X. cheopis*'

Hinnebusch, B. J., Bland, D. M., Bosio, C. F. and Jarrett, C. O. (2017) 'Comparative Ability of *Oropsylla montana* and *Xenopsylla cheopis* Fleas to Transmit *Yersinia pestis* by Two Different Mechanisms', *PLoS Neglected Tropical Diseases*, 11(1), pp. 1–15

Hinnebusch, B. J. and Erickson, D. L. (2008) '*Yersinia pestis* Biofilm in the Flea Vector and its Role in the Transmission of Plague', *Current Topics in Microbiology and Immunology*, 322, pp. 229–248

Hinnebusch, B. J., Fischer, E. R. and Schwan, T. G. (1998) 'Evaluation of the Role of the *Yersinia pestis* Plasminogen Activator and Other Plasmid-Encoded Factors in Temperature-Dependent Blockage of the Flea', *The Journal of Infectious Diseases*, 178, pp. 1406–1415
.
Hinnebusch, B. J., Jarrett, C. O. and Bland, D. M. (2017) '"Fleaing" the Plague: Adaptations of *Yersinia pestis* to its Insect Vector that Lead to Transmission', *Annual Review of Microbiology*, 71, pp. 215–232

Hinnebusch, B. J., Perry, R. D. and Schwan, T. G. (1996) 'Role of the *Yersinia pestis* hemin storage (*hms*) locus in the transmission of plague by fleas', *Science (New York, N.Y.)*, 273(5273), pp. 367–370

Hoang, T. T., Karkhoff-Schweizer, R. R., Kutchma, A. J. and Schweizer, H. P. (1998) 'A Broad-Host-Range F1p-FRT Recombination System for Site-Specific Excision of Chromosomally-Located DNA Sequences: Application for Isolation of Unmarked *Pseudomonas aeruginosa* Mutants', *Gene*, 212(1), pp. 77–86

Horisberger, M. and Rosset, J. (1977) 'Colloidal Gold, a Useful Marker for Transmission and Scanning Electron Microscopy', *The Journal of Histochemistry and Cytochemistry*, 25(5), pp. 295–305

Houhamdi, L., Fournier, P., Fang, R., Lepidi, H. and Raoult, D. (2002) 'An Experimental Model of Human Body Louse Infection with *Rickettsia prowazekii*', *The Journal of Infectious Diseases*, 186(11), pp. 1639–1646

Houhamdi, L., Lepidi, H., Drancourt, M. and Raoult, D. (2006) 'Experimental Model to Evaluate the Human Body Louse as a Vector of Plague', *The Journal of Infectious Diseases*, 194(11), pp. 1589–1596

Hurst, M. R. H., Jones, S. A., Binglin, T., Harper, L. A., Jackson, T. A. and Glare, T. R. (2011) 'The Main Virulence Determinant of *Yersinia entomophaga* MH96 is a Broad-Host-Range Toxin Complex Active Against Insects', *Journal of Bacteriology*, 193(8), pp. 1966–1980

Inglesby, T. V., Dennis, D. T., Henderson, D. A., Bartlett, J. G., Ascher, M. S., Eitzen, E., Fine, A. D., Friedlander, A. M., Hauer, J., Koerner, J. F., Layton, M., McDade, J., Osterholm, M. T., O'Toole, T., Parker, G., Perl, T. M., Russell, P. K., Schoch-Spana, M. and Tonat, K. (2000) 'Plague as a

Biological Weapon', *Journal of the American Medical Association*, 283(17), pp. 2281–2290

Jarrett, C. O., Deak, E., Isherwood, K. E., Oyston, P. C., Fischer, E. R., Whitney, A. R., Kobayashi, S. D., DeLeo, F. R. and Hinnebusch, B. J. (2004) 'Transmission of *Yersinia pestis* From an Infectious Biofilm in the Flea Vector', *The Journal of Infectious Diseases*, 190(4), pp. 783–792

Jarrett, C. O., Sebbane, F., Adamovicz, J. J., Andrews, G. P. and Hinnebusch, B. J. (2004) 'Flea-Borne Transmission Model To Evaluate Vaccine Efficacy against Naturally Acquired Bubonic Plague', *Infection and Immunity*, 72(4), pp. 2052–2056

Jones, D. (1998) 'The Neglected Saliva: Medically Important Toxins in the Saliva of Human Lice', *Parasitology*, 116 Suppl(1994), pp. S73-81

Joshua, G. W. P., Atkinson, S., Goldstone, R. J., Patrick, H. L., Stabler, R. A., Purves, J., Cámara, M., Williams, P. and Wren, B. W. (2015) 'Genome-Wide Evaluation of the Interplay Between *Caenorhabditis elegans* and *Yersinia pseudotuberculosis* During *in vivo* Biofilm Formation', *Infection and Immunity*, 83(1), pp. 17–27

Joshua, G. W. P., Karlyshev, A. V., Smith, M. P., Isherwood, K. E., Titball, R. W. and Wren, B. W. (2003) 'A *Caenorhabditis elegans* Model of *Yersinia* infection: Biofilm Formation on a Biotic Surface', *Microbiology*, 149(11), pp. 3221–3229

Kawada-Matsuo, M., Mazda, Y., Oogai, Y., Kajiya, M. and Kawai, T. (2012) 'GlmS and NagB Regulate Amino Sugar Metabolism in Opposing Directions and Affect *Streptococcus mutans* Virulence', *PLoS ONE*, 7(3), p. e33382

Kernif, T., Stafford, K., Coles, G. C., Bitam, I., Papa, K., Chiaroni, J., Raoult, D. and Parola, P. (2015) 'Responses of Artificially Reared Cat Fleas *Ctenocephalides felis felis* (Bouché, 1835) to Different Mammalian Bloods', *Medical and Veterinary Entomology*, 29(2), pp. 171–177

Kimyon, O., Uluturk, Z. I., Nizalapur, S., Lee, M., Kutty, S. K., Beckmann, S., Kumar, N. and Manefield, M. (2016) 'N-Acetylglucosamine Inhibits LuxR, LasR and CviR Based Quorum Sensing Regulated Gene Expression Levels', *Frontiers in Microbiology*, 7(August), pp. 1–14

Kimyon, Ö., Ulutürk, Z. İ., Nizalapur, S., Lee, M., Kutty, S. K., Beckmann, S., Kumar, N. and Manefield, M. (2016) 'N-Acetylglucosamine Inhibits LuxR, LasR and CviR Based Quorum Sensing Regulated Gene Expression Levels', *Frontiers in Microbiology*, 7(August), pp. 1–14

Kirn, T. J., Jude, B. A. and Taylor, R. K. (2005) 'A Colonization Factor Links *Vibrio cholerae* Environmental Survival and Human Infection', *Nature*, 438(8), pp. 863–866

Kirwan, J. P., Gould, T. a, Schweizer, H. P., Bearden, S. W., Murphy, R. C. and Churchill, M. E. a (2006) 'Quorum-Sensing Signal Synthesis by the *Yersinia pestis* Acyl-Homoserine Lactone Synthase YspI', *Journal of Bacteriology*, 188(2), pp. 784–788

Kolodziejek, A. M., Sinclair, D. J., Seo, K. S., Schnider, D. R., Deobald, C. F., Rohde, H. N., Viall, A. K., Minnich, S. S., Hovde, C. J., Minnich, S. A. and Bohach, G. A. (2007) 'Phenotypic Characterization of OmpX, an Ail Homologue of *Yersinia pestis* KIM', *Microbiology*, 153(9), pp. 2941–2951

Konopka, J. B. (2012) 'N-acetylglucosamine (GlcNAc) functions in cell signaling', *Scientifica*, 2012, pp. 631–632

Koornhof, H. J., Smego, R. a. and Nicol, M. (1999) 'Yersiniosis II: The pathogenesis of *Yersinia* infections', *European Journal of Clinical Microbiology and Infectious Diseases*, 18, pp. 87–112

Korgaonkar, A. K. and Whiteley, M. (2011) '*Pseudomonas aeruginosa* enhances production of an antimicrobial in response to N-acetylglucosamine and peptidoglycan', *Journal of Bacteriology*, 193(4), pp. 909–917

Krasnov, B. R. (2008) *Functional and Evolutionary Ecology of Fleas*. Cambridge University Press

Krishnamurthy, B. S. (1966) 'Rat Fleas', in Smith, C. N. (ed.) *Insect Colonization and Mass Production*. New York: Academic Press Inc., pp. 73–83

Krynski, S. and Becla, E. (1965) 'Infection of the Body Louse with *Pasteurella pseudotuberculosis* after Intrarectal Inoculation', *Journal of Infectious Diseases*, 114(5), pp. 379–385

LaRock, C. N., Yu, J., Horswill, A. R., Parsek, M. R. and Minion, F. C. (2013) 'Transcriptome Analysis of Acetyl-Homoserine Lactone-Based Quorum Sensing Regulation in *Yersinia pestis*', *PLoS ONE*, 8(4), pp. 1–8

Lavander, M., Ericsson, S. K., Bröms, J. E. and Bro, J. E. (2006) 'The Twin Arginine Translocation System Is Essential for Virulence of *Yersinia pseudotuberculosis* The Twin Arginine Translocation System Is Essential for Virulence of *Yersinia pseudotuberculosis*', *Infection and Immunity*, 74(3), pp. 1768–1776

Leino, R. and Kalliomaki, J. L. (1974) 'Yersiniosis as an Internal Disease', *Annals of Internal Medicine*, 81(4), pp. 458–461

Lillard, J. W., Fetherston, J. D., Pedersen, L., Pendrak, M. L. and Perry, R. D. (1997) 'Sequence and genetic analysis of the hemin storage (*hms*) system of *Yersinia pestis*', *Gene*, 193(1), pp. 13–21

Liu, L., Fang, H., Yang, H., Zhang, Y., Han, Y., Zhou, D. and Yang, R. (2016)

‘Reciprocal Regulation of *Yersinia pestis* Biofilm Formation and Virulence by RovM and RovA’, *Open Biology*, 6(3), p. 150198

Lorange, E. A, Race, B. L., Sebbane, F. and Joseph Hinnebusch, B. (2005) ‘Poor vector competence of fleas and the evolution of hypervirulence in *Yersinia pestis*’, *The Journal of Infectious Diseases*, 191(11), pp. 1907–1912

Losada, L., Varga, J. J., Hostetler, J., Radune, D., Kim, M., Durkin, S., Schneewind, O. and Nierman, W. C. (2011) ‘Genome Sequencing and Analysis of *Yersinia pestis* KIM D27, an Avirulent Strain Exempt from Select Agent Regulation’, *PLoS ONE*, 6(4), pp. 1–8

Luo, Y. (2014) ‘A Novel Multiple Membrane Blood-Feeding System for Investigating and Maintaining *Aedes aegypti* and *Aedes albopictus* mosquitoes’, *Journal of Vector Biology*, 39(2), pp. 271–277

Luria, S. E. and Delbrück, M. (1943) ‘Mutations of Bacteria From Virus Sensitivity to Virus Resistance’, *Genetics*, 28, pp. 491–511

McClean, K. H., Winson, M. K., Fish, L., Taylor, A., Chhabra, S. R., Camara, M., Daykin, M., John, H., Swift, S., Bycroft, B. W., Stewart, G. S. a B. and Williams, P. (1997) ‘Quorum Sensing and *Chromobacterium violaceum*: Exploitation of Violacein Production and Inhibition for the detection of N-acyl homoserine lactones’, *Microbiology*, 143, pp. 3703–3711

Mehigh, R. J., Sample, A. K. and Brubaker, R. R. (1989) ‘Expression of the low calcium response in *Yersinia pestis*’, *Microb Pathog*, 6(3), pp. 203–217

Milton, D. L., Toole, R. O. and Horstedt, P. (1996) ‘Flagellin A is Essential for the Virulence of *Vibrio anguillarum*’, *Microbiology*, 178(5), pp. 1310–1319

Miyashiro, T., Klein, W., Oehlert, D., Cao, X., Schwartzman, J. and Ruby, E. G. (2011) ‘The N-acetyl-d-glucosamine repressor NagC of *Vibrio fischeri* facilitates colonization of *Euprymna scolopes*’, *Molecular Microbiology*, 82(4), pp. 894–903

Morelli, G., Song, Y., Mazzoni, C. J., Eppinger, M., Roumagnac, P., Wagner, D. M., Feldkamp, M., Kusecek, B., Vogler, A. J., Li, Y., Cui, Y., Thomson, N. R., Jombart, T., Leblois, R., Lichtner, P., Rahalison, L., Petersen, J. M., Balloux, F., Keim, P., Wirth, T., Ravel, J., Yang, R., Carniel, E. and Achtman, M. (2010) ‘*Yersinia pestis* Genome Sequencing Identifies Patterns of Global Phylogenetic Diversity’, *Nature genetics*. Nature Publishing Group, 42(12), pp. 1140–1143

Moustafa, S. A., Kamil, Z., Rizk, M., Saleh, M. and Moustafa, S. (2007) ‘Isolation and Identification of Rhizosphere Soil Chitinolytic Bacteria and their Potential in Antifungal Biocontrol’, *Global Journal of Molecular Sciences*, 2(2), pp. 57–66

Mumcuoglu, K. Y., Danilevich, M., Zelig, O., Grinbaum, H., Friger, M. and

Meinking, T. L. (2011) ‘Effects of blood type and blood handling on feeding success, longevity and egg production in the body louse, *Pediculus humanus humanus*’, *Medical and Veterinary Entomology*, 25(1), pp. 12–16

Naseem, S. and Konopka, J. B. (2015) ‘N-acetylglucosamine Regulates Virulence Properties in Microbial Pathogens’, *PLoS Pathogens*, 11(7), pp. 6–11

Neyt, C., Iriarte, M., Thi, V. H. and Cornelis, G. R. (1997) ‘Virulence and arsenic resistance in *Yersiniae*’, *Journal of Bacteriology*, 179(3), pp. 612–619

Ng, Y.-K., Grasso, M., Wright, V., Garcia, V., Williams, P. and Atkinson, S. (2018) ‘The Quorum Sensing System of *Yersinia enterocolitica* 8081 Regulates Swimming Motility, Host Cell Attachment, and Virulence Plasmid Maintenance’, *Genes*, 9(6), p. 307

Nichols, M. C., Ettestad, P. J., Vinhatton, E. S., Melman, S. D., Onischuk, L., Pierce, E. a and Aragon, A. S. (2014) ‘*Yersinia pestis* infection in dogs: 62 cases (2003-2011)’, *Journal of the American Veterinary Medicine Association*, 244(10), pp. 1176–1180

Nishimura, A., Morita, M., Nishimura, Y. and Sugino, Y. (1990) ‘A Rapid and Highly Efficient Method for Preparation of Competent *Escherichia coli* Cells’, *Nucleic Acids Research*, 18(20), p. 6169

Novichkov, P. S., Kazakov, A. E., Ravcheev, D. A., Leyn, S. A., Kovaleva, G. Y., Sutormin, R. A., Kazanov, M. D., Riehl, W., Arkin, A. P., Dubchak, I. and Rodionov, D. A. (2013) ‘RegPrecise 3.0 - A Resource for Genome-Scale Exploration of Transcriptional Regulation in Bacteria’, *BMC Genomics*, 14(1)

Obrist, M. W. and Miller, V. L. (2012) ‘Low Copy Expression Vectors for Use in *Yersinia* sp. and Related Organisms’, *Plasmid*. Elsevier Inc., 68(1), pp. 33–42

Ortori, C. A., Atkinson, S., Chhabra, S. R., Cámara, M., Williams, P. and Barrett, D. A. (2007) ‘Comprehensive Profiling of N-acylhomoserine lactones Produced by *Yersinia pseudotuberculosis* Using Liquid Chromatography Coupled to Hybrid Quadrupole-Linear Ion Trap Mass Spectrometry’, *Analytical and Bioanalytical Chemistry*, 387(2), pp. 497–511

Osaki, T., Kurozumi, S., Sato, K., Terashi, T., Azuma, K., Murahata, Y., Tsuka, T., Ito, N., Imagawa, T., Minami, S. and Okamoto, Y. (2015) ‘Metabolomic Analysis of Blood Plasma after Oral Administration of N-acetyl-D-Glucosamine in Dogs’, *Marine Drugs*, 13, pp. 5007–5015

Paerregaard, A., Espersen, F., Jensen, O. M. and Skurnik, M. (1991) ‘Interactions Between *Yersinia enterocolitica* and Rabbit Ileal Mucus: Growth, Adhesion, Penetration, and Subsequent Changes in Surface Hydrophobicity and Ability to Adhere to Ileal Brush Border Membrane Vesicles’, *Infection and Immunity*, 59(1), pp. 253–260

Parkhill, J., Wren, B. W., Thomson, N. R., Titball, R. W., Holden, M. T., Prentice, M. B., Sebaihia, M., James, K. D., Churcher, C., Mungall, K. L., Baker, S., Basham, D., Bentley, S. D., Brooks, K., Cerdeño-Tárraga, a M., Chillingworth, T., Cronin, A., Davies, R. M., Davis, P., Dougan, G., Feltwell, T., Hamlin, N., Holroyd, S., Jagels, K., Karlyshev, a V, Leather, S., Moule, S., Oyston, P. C., Quail, M., Rutherford, K., Simmonds, M., Skelton, J., Stevens, K., Whitehead, S. and Barrell, B. G. (2001) 'Genome sequence of *Yersinia pestis*, the causative agent of plague', *Nature*, 413(6855), pp. 523–527

Parsek, M. R. and Greenberg, E. P. (2005) 'Sociomicrobiology: The Connections Between Quorum Sensing and Biofilms', *Trends in Microbiology*, 13(1), pp. 27–33

Patel, C. N., Wortham, B. W., Lines, J. L., Fetherston, J. D., Perry, R. D. and Oliveira, M. a. (2006) 'Polyamines are essential for the formation of plague biofilm', *Journal of Bacteriology*, 188(7), pp. 2355–2363

Pendrak, M. L. and Perry, R. D. (1993) 'Proteins Essential for Expression of the Hms+ phenotype of *Yersinia pestis*', *Molecular Microbiology*, 8(5), pp. 857–864

Pennetier, C., Domínguez-Ramírez, L. and Plumbridge, J. (2008) 'Different Regions of Mlc and NagC, Homologous Transcriptional Repressors Controlling Expression of the Glucose and N-Acetylglucosamine Phosphotransferase Systems in *Escherichia coli,* are Required for Inducer Signal Recognition', *Molecular Microbiology*, 67(2), pp. 364–377

Perry, R. D. (2003) 'A Plague of Fleas - Survival and Transmission of *Yersinia pestis*', *American Society for Microbiology News*, 69(7), pp. 336–340

Perry, R. D. and Brubaker, R. R. (1987) 'Transport of Ca2+ by *Yersinia pestis*', *Journal of Bacteriology*, 169(10), pp. 4861–4864

Perry, R. D. and Fetherston, J. D. (1997) '*Yersinia pestis* - Etiologic agent of plague', *Microbiology Reviews*, 10(1)(1), pp. 35–66

Perry, R. D., Pendrak, M. L. and Schuetze, P. (1990) 'Identification and cloning of a hemin storage locus involved in the pigementation phenotype of *Yersinia pestis*', *Journal of Bacteriology*, 172(10), pp. 5929–5937

Petrova, O. E. and Sauer, K. (2012) 'Sticky Situations: Key Components that Control Bacterial Surface Attachment', *Journal of Bacteriology*, 194(10), pp. 2413–2425

Piarroux, R., Abedi, A. A., Shako, J. C., Kebela, B., Karhemere, S., Diatta, G., Davoust, B., Raoult, D. and Drancourt, M. (2013) 'Plague Epidemics and Lice, Democratic Republic of the Congo', *Emerging Infectious Diseases*, 19(3), pp. 505–506

Pinheiro, V. B. and Ellar, D. J. (2007) 'Expression and Insecticidal Activity of *Yersinia pseudotuberculosis* and *Photorhabdus luminescens* Toxin Complex Proteins', *Cellular Microbiology*, 9(10), pp. 2372–2380

Pisano, F., Heine, W., Rosenheinrich, M., Schweer, J., Nuss, A. M. and Dersch, P. (2014) 'Influence of PhoP and Intra-Species Variations on Virulence of *Yersinia pseudotuberculosis* during the Natural Oral Infection Route', *PLoS ONE*, 9(7), pp. 1–17

Plumbridge, J. (1995) 'Co-ordinated Regulation of Amino Sugar Biosynthesis and Degradation: the NagC Repressor acts as both an Activator and a Repressor for the Transcription of the *glmUS* Operon and Requires Two separated NagC Binding Sites', *The EMBO Journal*, 14(16), pp. 3958–3965

Plumbridge, J. A. (1990) 'Induction of the nag Regulon of *Escherichia coli* by N-Acetylglucosamine and Glucosamine: Role of the Cyclic AMP- Catabolite Activator Protein Complex in Expression of the Regulon', *Microbiology*, 172(5), pp. 2728–2735

Plumbridge, J. A. (1991) 'Repression and induction of the *nag* regulon of *Escherichia coli* K-12: the roles of *nagC* and *nagA* in maintenance of the uninduced state', *Molecular Microbiology*, 5(8), pp. 2053–2062

Plumbridge, J. A. (1992) 'A dominant mutation in the gene for the Nag repressor of *Escherichia coli* that renders the *nag* regulon uninducible', *Journal of general microbiology*, 138(5), pp. 1011–1017

Pollitzer, R. (1954) *Plague*

Prentice, M. B. and Rahalison, L. (2007) 'Plague', *Lancet*, 369(1474–547X (Electronic)), pp. 1196–1207

Pullen, S. R. and Meola, R. W. (1995) 'Survival and Reproduction of the Cat Flea (*Siphonaptera: Pulicidae*) Fed Human Blood on an Artificial Membrane System', *Journal of Medical Entomology*, 32(4), pp. 467–470

Qi, Z., Zhou, L., Zhang, Q., Ren, L., Dai, R., Wu, B., Wang, T., Zhu, Z., Yang, Y., Cui, B., Wang, Z., Wang, H., Qiu, Y., Guo, Z., Yang, R. and Wang, X. (2010) 'Comparison of Mouse, Guinea Pig and Rabbit Models for Evaluation of Plague Subunit Vaccine F1 + rV270', *Vaccine*, 28(6), pp. 1655–1660

Qing, G., Ma, L., Khorchid, A., Swapna, G. V. T., Mal, T. K., Takayama, M. M., Xia, B., Phadtare, S., Ke, H., Acton, T., Montelione, G. T., Ikura, M. and Inouye, M. (2004) 'Cold-Shock Induced High-Yield Protein Production in *Escherichia coli*', *Nature Biotechnology*, 22(7), pp. 877–882

Riley, G. and Toma, S. (1989) 'Detection of Pathogenic *Yersinia enterocolitica* by Using Congo Red-Magnesium Oxalate agar medium', *Journal of Clinical Microbiology*, 27(1), pp. 213–214

Roberts, L. S. and Janovy, J. J. (2009) *Foundations of Parasitology*. 8th edn. New York: McGraw-Hill

Rodda, S. J. (1996) 'T-Cell Epitope Mapping with Synthetic Peptides and Peripheral Blood Mononuclear Cells', in Morris, G. E. (ed.) *Methods in Molecular Biology*. Humana Press Inc., Totowa, NJ, pp. 363–371

Rosqvist, R., Bolin, I. and Wolf-Watz, H. (1988) 'Inhibition of phagocytosis in *Yersinia pseudotuberculosis*: A virulence plasmid-encoded ability involving the Yop2b protein', *Infection and Immunity*, 56(8), pp. 2139–2143

Rosqvist, R., Skurnik, M. and Wolf-Watz, H. (1988) 'Increased Virulence of *Yersinia pseudotuberculosis* by Two Independent Mutations', *Nature*, 334(6182), pp. 522–4

Rothschild, M., Schlein, J., Parker, K., Sternberg, S. and Neville, C. (1973) 'The Flying Leap of the Flea', *Scientific American*, 229(5), pp. 92–100

Roy-Burman, A., Savel, R. H., Racine, S., Swanson, B. L., Revadigar, N. S., Fujimoto, J., Sawa, T. and Frank, D. W. (2001) 'Type III Protein Secretion Is Associated with Death in Lower Respiratory and Systemic *Pseudomonas aeruginosa* Infections', *The Journal of Infectious Diseases*, 183(12), pp. 1767–1774

Russell, H. (1868) *The Flea*. Cambridge University Press

Sadovskaya, I., Vinogradov, E., Flahaut, S., Kogan, G. and Jabbouri, S. (2005) 'Extracellular carbohydrate-containing polymers of a model biofilm-produring strain, *Staphylococcus epidermidis* RP62A', *Infection and Immunity*, 73(5), pp. 3007–3017

Sample, A. K., Fowler, J. M. and Brubaker, R. R. (1987) 'Modulation of the Low-Calcium Response in *Yersinia pestis via* Plasmid-Plasmid Interaction', *Microbial Pathogenesis*, 2(6), pp. 443–453

Sangaré, A. K., Rolain, J. M., Gaudart, J., Weber, P. and Raoult, D. (2016) 'Synergistic Activity of Antibiotics Combined with Ivermectin to Kill Body Lice', *International Journal of Antimicrobial Agents*. Elsevier B.V., 47(3), pp. 217–223

Sanger, F. and Coulson, A. R. (1975) 'A Rapid Method for Determining Sequences in DNA by Primed Synthesis with DNA Polymerase', *Journal of Molecular Biology*, 94(3), pp. 441–448

.

Sebbane, F., Gardner, D., Long, D., Gowen, B. B. and Hinnebusch, B. J. (2005) 'Kinetics of Disease Progression and Host Response in a Rat Model of Bubonic Plague', *The American Journal of Pathology*. American Society for Investigative Pathology, 166(5), pp. 1427–1439

Sebbane, F., Jarrett, C. O., Gardner, D., Long, D. and Hinnebusch, B. J. (2006) 'Role of the *Yersinia pestis* plasminogen activator in the incidence of distinct septicemic and bubonic forms of flea-borne plague', *Proceedings of the National Academy of Sciences of the United States of America*, 103(14), pp. 5526–5530

Service, M. (2008a) 'Fleas (Siphonaptera)', in *Medical Entomology for Students*. 4th edn. Cambridge, pp. 168–182

Service, M. (2008b) 'Sucking Lice (Anoplura)', in *Medical Entomology for Students*. 4th edn. Cambridge, pp. 183–194

Sicard, J.-F., Vogeleer, P., Le Bihan, G., Rodriguez Olivera, Y., Beaudry, F., Jacques, M. and Harel, J. (2018) 'N-Acetyl-glucosamine Influences the Biofilm Formation of *Escherichia coli*', *Gut Pathogens*. BioMed Central, 10(1), p. 26

Sikkema, D. J. and Brubaker, R. R. (1987) 'Resistance to Pesticin, Storage of Iron, and Invasion of HeLa cells by *Yersiniae*', *Infection and Immunity*, 55(3), pp. 572–578

Skurnik, M., Peippo, A. and Ervelä, E. (2000) 'Characterization of the O-antigen Gene Clusters of *Yersinia pseudotuberculosis* and the Cryptic O-antigen Gene Cluster of *Yersinia pestis* Shows that the Plague Bacillus is Most Closely Related to and has Evolved from *Y. pseudotuberculosis* Serotype O:1b', *Molecular Microbiology*, 37(2), pp. 316–330

Slater, A. (2017) *Identifying a relationship between QS and the T3SS through virulence regulators LcrF and YmoA in Y. pseudotuberculosis*

Sodeinde, O. A., Sample, A. K., Brubaker, R. R. and Coguen, J. D. (1988) 'Plasminogen activator/coagulase gene of *Yersinia pestis* is responsible for degradation of plasmid-encoded outer membrane proteins', *Infection and Immunity*, 56(10), pp. 2749–2752

Sodeinde, O. L. A. A. and Goguen, J. O. N. D. (1989) 'Nucleotide Sequence of the Plasminogen Activator Gene of *Yersinia pestis*: Relationship to *ompT* of *Escherichia coli* and Gene E of *Salmonella typhimurium*', *Infection and Immunity*, 57(5), pp. 1517–1523

Sorroche, F. G., Spesia, M. B., Zorreguieta, Á. and Giordano, W. (2012) 'A Positive Correlation Between Bacterial Autoaggregation and Biofilm Formation in Native *Sinorhizobium meliloti* Isolates from Argentina', *Applied and Environmental Microbiology*, 78(12), pp. 4092–4101

Stewart, G. S. A. B., Lubinsky-Mink, S., Jackson, C. G., Cassel, A. and Kuhn, J. (1986) 'pHG165: A pBR322 Copy Number Derivative of pUC8 for Cloning and Expression', *Plasmid*, 15, pp. 172–181

Straley, S. C. and Bowmer, W. S. (1986) 'Virulence Genes Regulated at the

Transcriptional Level by Ca2+ in *Yersinia pestis* Include Structural Genes for Outer Membrane Proteins', *Infection and Immunity*, 51(2), pp. 445–454

Streichsbier, F. (1983) 'Utilization of Chitin as Sole Carbon and Nitrogen Source by *Chromobacterium violaceum*', *FEMS Microbiology Letters*, 19, pp. 129–132

Styer, K. L., Hopkins, G. W., Bartra, S. S., Plano, G. V, Frothingham, R. and Aballay, A. (2005) '*Yersinia pestis* Kills *Caenorhabditis elegans* by a Biofilm-Independent Process that Involves Novel Virulence Factors', *EMBO Reports*, 6(10), pp. 992–997

Sun, Y. C., Jarrett, C. O., Bosio, C. F. and Hinnebusch, B. J. (2014) 'Retracing the Evolutionary Path that Led to Flea-Borne Transmission of *Yersinia pestis*', *Cell Host and Microbe*. Elsevier Inc., 15(5), pp. 578–586

Sun, Y., Verma, S. C., Bogale, H. and Miyashiro, T. (2015) 'NagC Represses N-acetyl-glucosamine Utilization Genes in *Vibrio fischeri* Within the Light Organ of *Euprymna scolopes*', *Frontiers in Microbiology*, 6(JUL), pp. 1–9

Surgalla, M. J. and Beesley, E. D. (1969) 'Congo Red-Agar Plating Medium for Detecting Pigmentation in *Pasteurella pestis*', *Applied Microbiology*, 18(5), pp. 834–837

Suyemoto, W., Wheeler, C. M., Cavanaugh, D. C., Yamakawa, Y. and Shimada, T. (1956) 'Studies on *Pasteurella pestis* in Various Flea Species III. Transmission of Avirulent Strains of *Pasteurella pestis* by *Xenopsylla cheopis*', *The Journal of Infectious Diseases*, 99(1), pp. 72–75

El Tahir, Y. and Skurnik, M. (2001) 'YadA, the Multifaceted *Yersinia* Adhesin', *International Journal of Medical Microbiology*, 291(3), pp. 209–218

Takano-Lee, M., Velten, R. K., Edman, J. D., Mullens, B. a and Clark, J. M. (2003) 'An automated feeding apparatus for *in vitro* maintenance of the human head louse, *Pediculus capitis* (*Anoplura: Pediculidae*)', *Journal of medical entomology*, 40(6), pp. 795–799

Takano-Lee, M., Yoon, K. S., Edman, J. D., Mullens, B. a and Clark, J. M. (2003) '*In vivo* and *in vitro* rearing of *Pediculus humanus capitis* (*Anoplura: Pediculidae*)', *Journal of medical entomology*, 40(5), pp. 628–635

Tan, L. and Darby, C. (2006) '*Yersinia pestis* YrbH is a Multifunctional Protein Required for Both 3-deoxy-D-manno-oct-2-ulosonic acid Biosynthesis and Biofilm Formation', *Molecular Microbiology*, 61(4), pp. 861–870

Thomas, R. E., Karstens, R. H. and Schwan, T. G. (1990) 'Experimental Infection of *Ornithodoros* spp. Ticks (*Acari: Argasidae*) with *Yersinia pestis*', *Journal of Medical Entomology*, 27(4), pp. 720–723

Throup, J. P., Camara, M., Briggs, G. S., Winson, M. K., Chhabra, S. R.,

Bycroft, B. W., Williams, P. and Stewart, G. S. (1995) 'Characterisation of the *yenI/yenR* Locus From *Yersinia* enterocolitica Mediating the Synthesis of Two N-acylhomoserine Lactone Signal Molecules', *Molecular Microbiology*, 17(2), pp. 345–56

Titgemeyer, F., Reizer, J., Reizer, a. and Saier, M. H. (1994) 'Evolutionary relationships between sugar kinases and transcriptional repressors in bacteria', *Microbiology*, 140(9), pp. 2349–2354

Torruellas, J., Jackson, M. W., Pennock, J. W. and Plano, G. V (2005) '*Yersinia pestis*', *Molecular Microbiology*, 57, pp. 1719–1733

Trosky, J. E., Liverman, A. D. B. and Orth, K. (2008) '*Yersinia* outer proteins: Yops', *Cellular Microbiology*, 10(January), pp. 557–565

Trunk, T., S. Khalil, H. and C. Leo, J. (2018) 'Bacterial Autoaggregation', *AIMS Microbiology*, 4(1), pp. 140–164

Veracx, A. and Raoult, D. (2012) 'Biology and genetics of human head and body lice', *Trends in Parasitology*, 28(12), pp. 563–571

Waniek, P. J. (2009) 'The Digestive System of Human Lice: Current Advances and Potential Applications', *Physiological Entomology*, 34(3), pp. 203–210

Whitehorn, C. (2010) 'Entomology Handbook'. The London School of Hygiene and Tropical Medicine

WHO (2015) *Emerging and Dangerous Pathogens Laboratory Network (EDPLN)*, *World Health Organization*. Available at: http://www.who.int/csr/disease/OP_EDPLN_FINAL.pdf?ua=1&ua=1

Wiechmann, A. (2015) *Quorum Sensing and the Regulation of Multicellular Behaviour in Yersinia pseudotuberculosis*

Williams, P. (2007) 'Quorum sensing, communication and cross-kingdom signalling in the bacterial world', *Microbiology*, 153, pp. 3923–3938

Willias, S. P., Chauhan, S., Lo, C. C., Chain, P. S. G. and Motin, V. L. (2015) 'CRP-Mediated Carbon Catabolite Regulation of *Yersinia pestis* Biofilm Formation is Enhanced by the Carbon Storage Regulator Protein, CsrA', *PLoS ONE*, 10(8), pp. 1–20

Wortham, B. W., Oliveira, M. A., Fetherston, J. D. and Perry, R. D. (2010) 'Polyamines are Required for the Expression of Key Hms Proteins Important for *Yersinia pestis* Biofilm Formation', *Environmental Microbiology*, 12(7), pp. 2034–2047

Wren, B. W. (2003) 'The *Yersiniae* - a Model Genus to Study the Rapid Evolution of Bacterial Pathogens', *Nature Reviews Microbiology*, 1(1), pp.

55–64

Yates, E. A., Philipp, B., Buckley, C., Atkinson, S., Chhabra, S. R., Sockett, R. E., Goldner, M. and Dessaux, Y. (2002) 'N-Acylhomoserine Lactones Undergo Lactonolysis in a pH- , Temperature- , and Acyl Chain Length-Dependent Manner during Growth of *Yersinia pseudotuberculosis* and *Pseudomonas aeruginosa*', *Infection and Immunity*, 70(10), pp. 5635–5646

Yoong, P., Cywes-Bentley, C. and Pier, G. B. (2012) 'Poly-N-acetylglucosamine Expression by Wild-Type *Yersinia pestis* is Maximal at Mammalian, not Flea, Temperatures', *mBio*, 3(4)

Yu, J., Madsen, M. L., Carruthers, M. D., Phillips, G. J., Kavanaugh, J. S., Boyd, J. M., Horswill, A. R. and Minion, C. F. (2013) 'Analysis of Autoinducer-2 Quorum Sensing in *Yersinia pestis*', *Infection and Immunity*, 81(11), pp. 4053–4062

Zarda, B., Hahn, D., Chatzinotas, A., Schonhuber, W., Neef, A., Amann, R. I., Zeyer, J. and Schönhuber, W. (1997) 'Analysis of Bacterial Community Structure in Bulk Soil by In Situ Hybridization', *Archives of Microbiology*, 168, pp. 185–192

Zhang, W., Xu, S., Li, J., Shen, X., Wang, Y. and Yuan, Z. (2011) 'Modulation of a thermoregulated type VI secretion system by AHL-dependent quorum sensing in *Yersinia pseudotuberculosis*', *Archives of Microbiology*, 193, pp. 351–363

Zhao, R., Song, Y., Dai, Q., Kang, Y., Pan, J., Zhu, L., Zhang, L., Wang, Y. and Shen, X. (2017) 'A starvation-Induced Regulator, RovM, acts as a Switch for Planktonic/Biofilm State Transition in *Yersinia pseudotuberculosis*', *Scientific Reports*. Springer US, 7(1), pp. 1–12

Zhou, D. and Yang, R. (2011) 'Formation and Regulation of *Yersinia* Biofilms', *Protein and Cell*, 2(3), pp. 173–179

Zietz, B. P. and Dunkelberg, H. (2004) 'The history of the plague and the research on the causative agent *Yersinia pestis*', *International Journal of Hygiene and Environmental Health*, 207(2), pp. 165–178

Zimbler, D. L., Schroeder, J. a., Eddy, J. L. and Lathem, W. W. (2015) 'Early emergence of *Yersinia pestis* as a severe respiratory pathogen', *Nature Communications*. Nature Publishing Group, 6(May), p. 7487

8 Appendix

8.1 Verification of *nagC* constructs in *E. coli* and confirmation of *nagC* transformants in *Y. pestis*

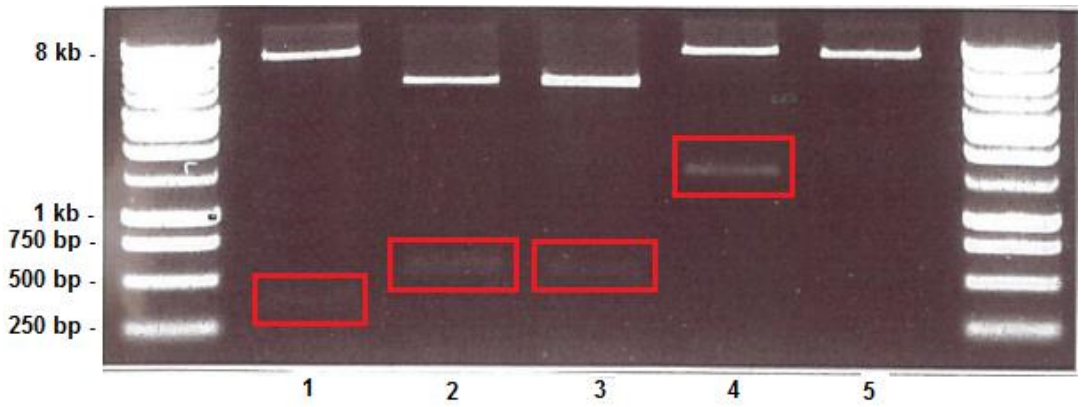

Figure 8.1 Agarose gel confirming the Δ*nagC* mutant in the suicide plasmid pDM4 in *E. coli* by restriction digest. Lane 1 shows pDM4 (~7 kb + 1068 bp) and the *nagC* upstream fragment (384 bp) cut with *XhoI* and *XbaI*. Lane 2 shows pDM4 (~7 kb + 888 bp) and the gentamicin cassette (564 bp) cut with *XbaI* and *KpnI.* Lane 3 shows pDM4 (~7 kb + 948 bp) and the *nagC* downstream fragment (504 bp) cut with *KpnI* and *SpeI*. Lane 4 shows pDM4 (~7 kb) and the *nagC* upstream::gentamicin::downstream cassette (1452 bp) cut with *XhoI* and *SpeI*. Lane 5 shows empty pDM4 (~7 kb) cut with *XhoI* as a control.

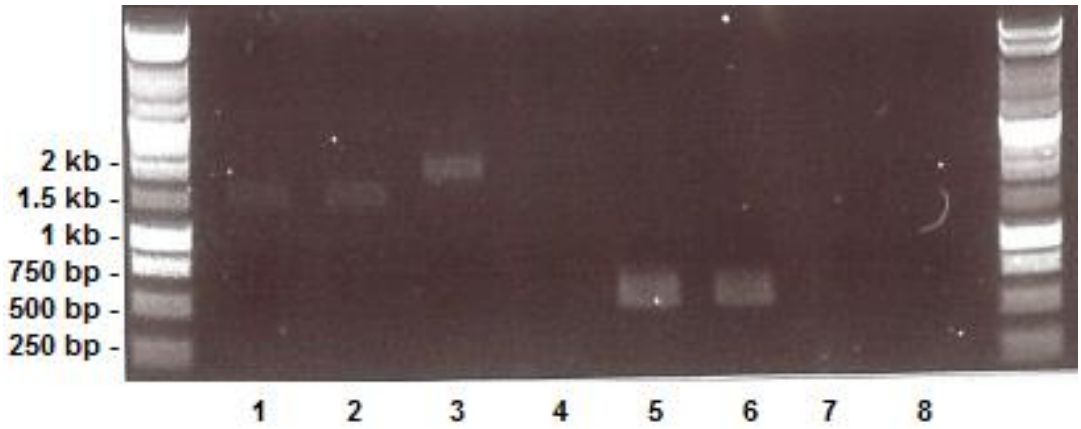

Figure 8.2 Agarose gel confirming the gentamicin cassette in *nagC* when transformed in *Y. pestis*. Lanes 1 and 2 indicate Δ*nagC* mutant colony 1 and 2 when amplified with *nagC*_ F and *nagC*_R primers (1394 bp). This can be compared to the parental strain *nagC* using the same primers in lane 3 (1999 bp). Lane 4 is the negative control with no DNA added to PCR reaction. Lanes 5 and 6 indicate Δ*nagC* mutant colony 1 and 2 when amplified with Gm_out_F and *nagC*_R primers (486 bp). The parental strain does not amplify, as the Gm_out_F primer is within the gentamicin cassette (lane 7). Lane 8 is the negative control with no DNA added to the PCR reaction.

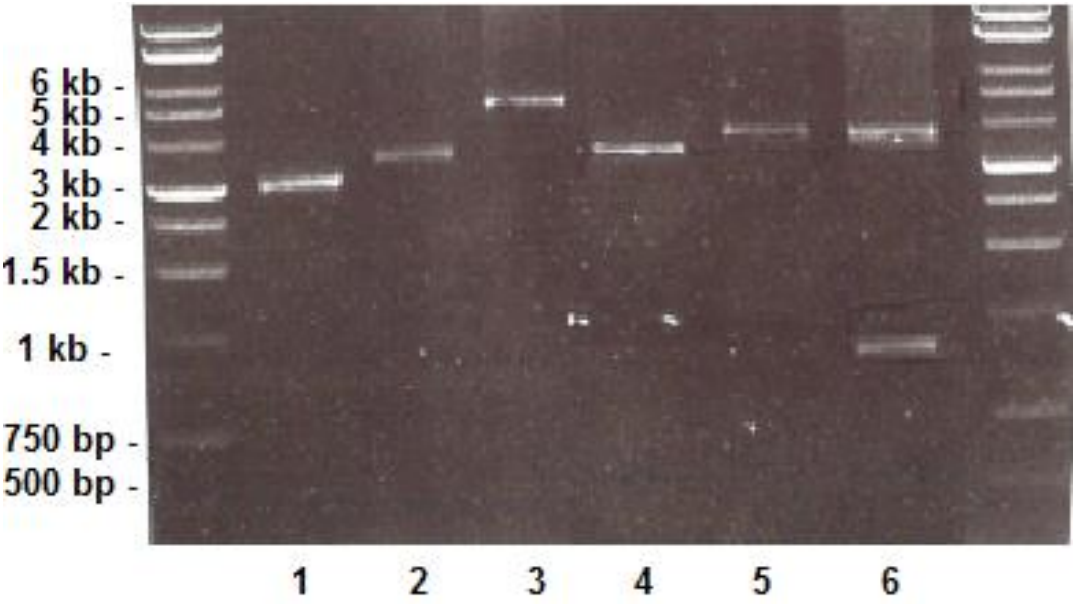

Figure 8.3 Agarose gel confirming *nagC* in the complement plasmid pHG327 and not in pGEM-T Easy in *E.coli* by restriction digest. Lane 1 shows pGEM-T Easy cut with *XbaI* (3014 bp), lane 2 shows pHG327 cut with *XbaI* (3374 bp), lane 3 shows pHG327::*nagC* cut with *XbaI* (4574 bp), lane 4 shows pGEM-T Easy cut with *XbaI* and *HindIII* (3014 bp), lane 6 shows pHG327 cut with *XbaI* and *HindIII* (3374 bp) and lane 6 shows pHG327::*nagC* cut with *XbaI* and *HindIII* (3374 + 1200 bp).

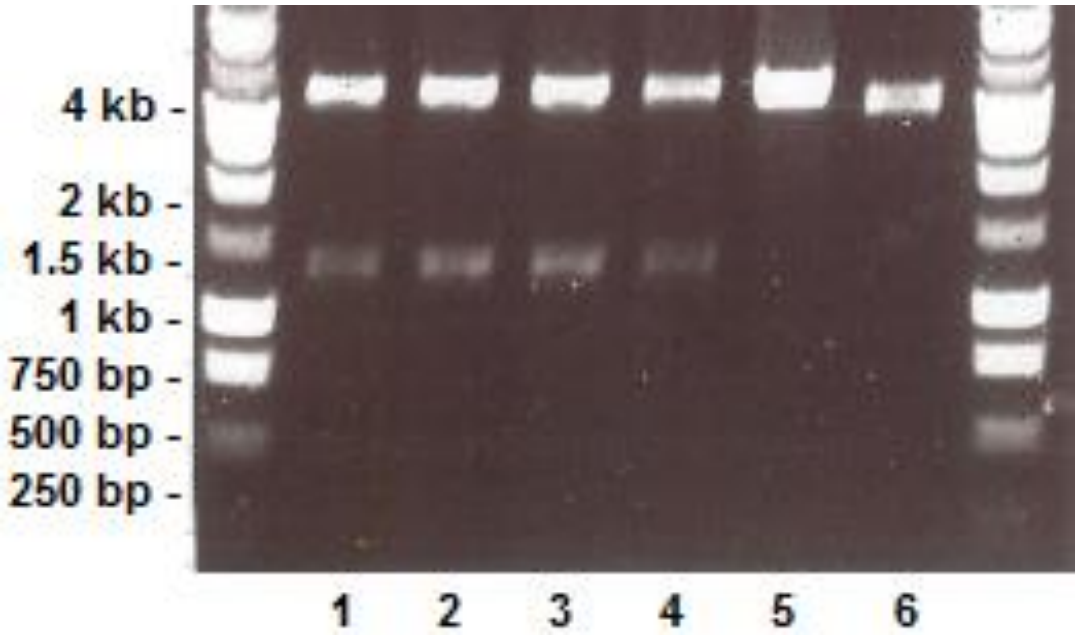

Figure 8.4 Agarose gel confirming *nagC* in the complement plasmid pHG327 when miniprepped from *Y. pestis* and digested with *HindII* and *XbaI* (enzymes used to ligate *nagC* into pHG327). Lanes 1, 2, 3 and 4 indicate that *nagC* (1200 bp) has been doubly digested out of pHG327 (3374 bp). Lane 5 is pHG327 without *nagC* as a control (3374 bp). Lane 6 is pGEM-T Easy (3000 bp) without *nagC*, indicating that *nagC* has been successfully transferred from pGEM-T easy to pHG327.

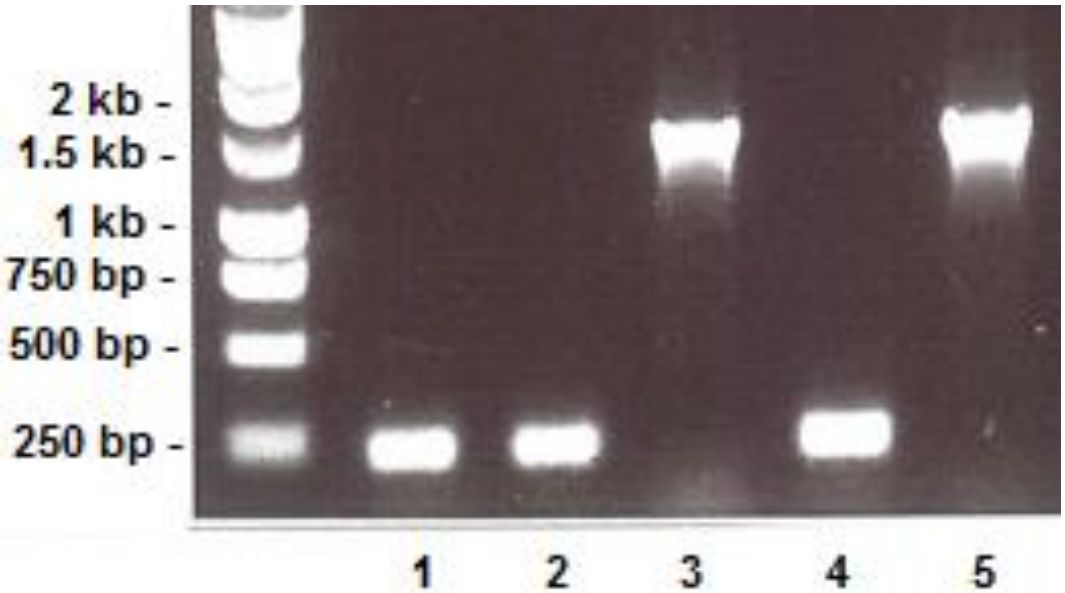

Figure 8.5 Agarose gel showing PCR confirmation, using M13_F and M13_R primers, of the NagC construct within pGEM-T Easy, which was transformed into pCOLD1 and NagC was expressed. Lanes 1,2 and 4 the empty M13 amplicon (250bp), lanes 3 and 5 show the M13 amplicon with the NagC gene inserted (1.5 kb).

8.2 Purity of NagC Protein Purification

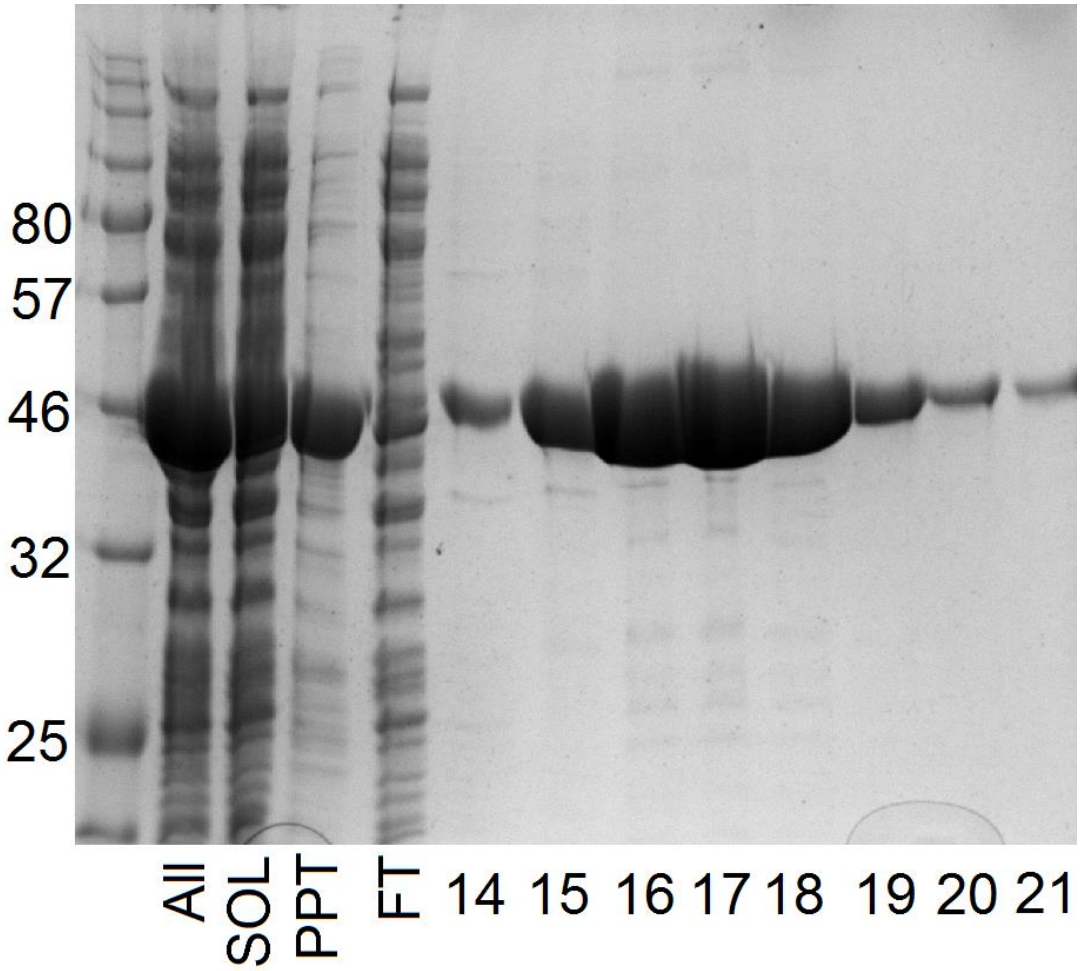

Figure 8.6 SDS-PAGE gel showing 60 µl samples from NagC (~46 kDa) purification process. 'All' indicates sonicated culture, 'SOL' indicates soluble material from the column, 'PPT' indicates the insoluble discard not added to the column and 'FT' indicates the non-bound column material. Numbers 14-21 indicate the fractions containing NagC obtained from the ÄKTA prime. The strong band at 46 kDa and otherwise clear lanes indicates very pure protein. Run alongside an NEB Prestained Broad Range Protein Ladder (11-245 kDa).

8.3 Homology Between *Y. pestis* and *Y. pseudotuberculosis*

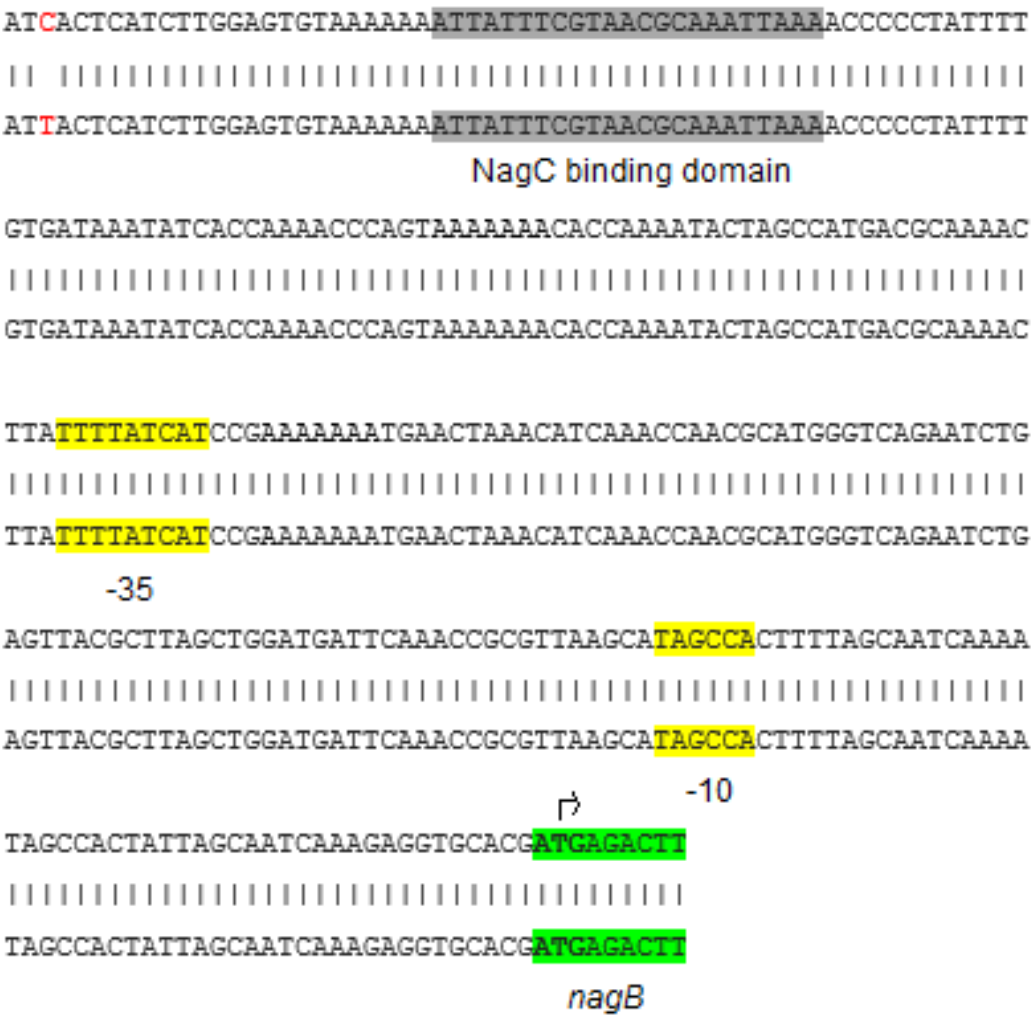

Figure 8.7. Homology between *Y. pestis* (top row) and *Y. pseudotuberculosis* (bottom row) for the *nagE-nagBACD* promoter region. Highlighted in red are base changes.

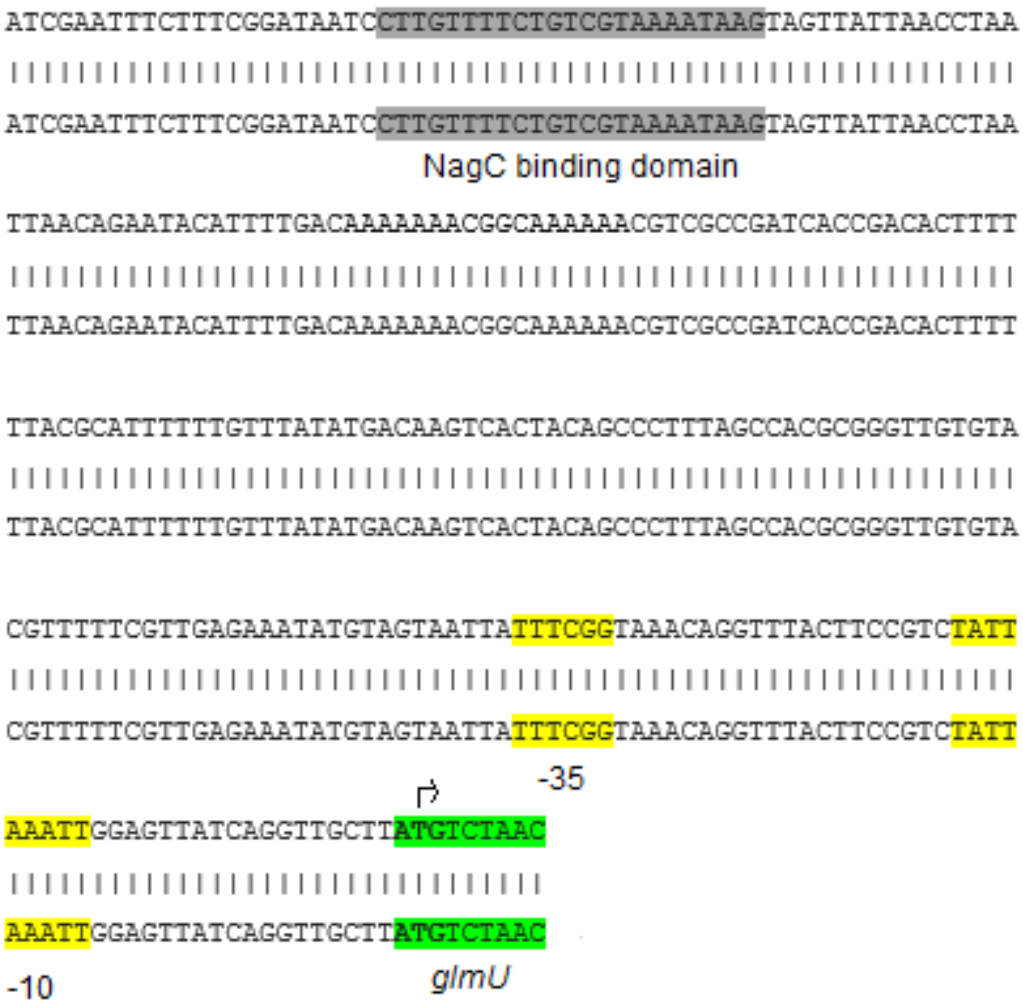

Figure 8.8. Homology between *Y. pestis* (top row) and *Y. pseudotuberculosis* (bottom row) for the *glmUS* promoter region. Highlighted in red are base changes.

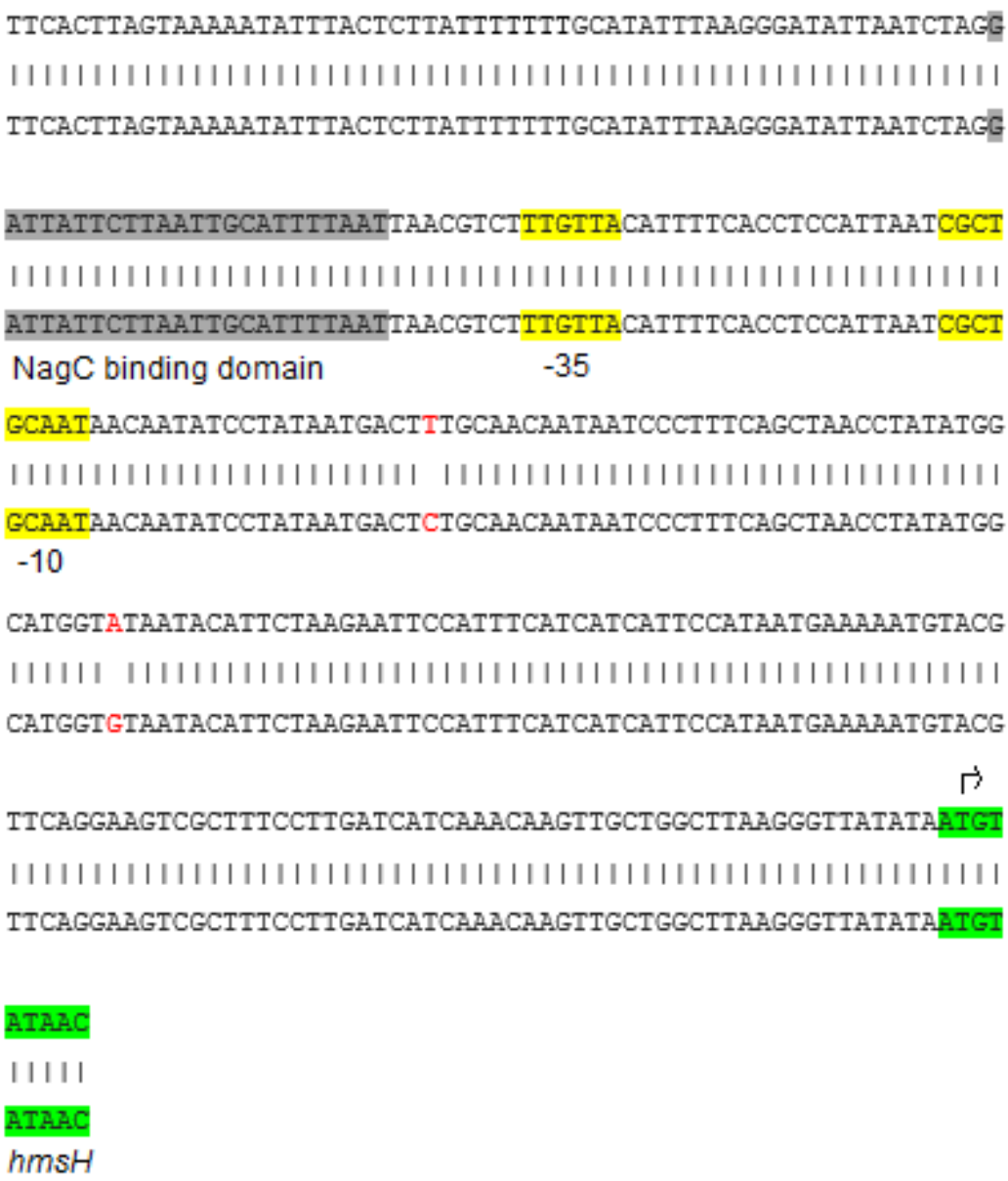

Figure 8.9. Homology between *Y. pestis* (top row) and *Y. pseudotuberculosis* (bottom row) for the *hmsHFRS* promoter region. Highlighted in red are base changes.

ATGAGCACCGGCGGACAAGCACAAATTGGTAACGTGGATCTGGTAAAACAACTCAATGGA

ATGAGCACCGGCGGACAAGCACAAATTGGTAACGTGGATCTGGTAAAACAACTCAATGGA

GCCGTGGTTTATCGGCTAATTGATCAGCAAGGCCCGATTTCTCGCATACAGATTGCCGAT

GCCGCGGTTTACCGGCTAATTGATCAGCAAGGCCCGATTTCTCGCATACAGATTGCCGAT

CTCAGCCAGCTAGCCCCCGCCAGTGTCACCAAAATCACCCGGCAATTGTTGGAGCGCGGG

CTCAGCCAGCTAGCCCCCGCCAGTGTCACCAAAATCACCCGGCAATTGTTGGAGCGCGGG

CTGATCAAAGAGGTCGATCAGCAAGCCTCCACCGGGGGGCGTCGCGCTATCTCTATCGTG

CTGATCAAAGAGGTCGATCAGCAAGCCTCCACCGGGGGGCGTCGCGCTATCTCTATCGTG

ACGGAAAACCGCCAATTCCATACCGTTGCAGTCCGTTTAGGTCGTAATGATGCCACGATC

ACGGAAAACCGCCAATTCCATACCGTTGCAGTCCGTTTAGGTCGTAATGATGCCACGATC

ACCCTCTTTGATATGAGCGGTAAATCGCTGGGTGAAGAGCACTATGCCCTGCCAGAACGA

ACCCTCTTTGACATGAGCGGTAAATCGCTGGGTGAAGAGCACTATGCCCTGCCAGAACGA

ACACAAGAAACGCTGGAACACGCCTTATTTAATATCATCAGTCAGTTTATTGACGCCTAT

ACACAAGAAACGCTGGAACACGCCTTATTTAATATCATCAGTCAGTTTATTGACGCCTAT

CAGCGTAAATTACGTGAACTGATTGCCATCGCGGTTATCCTGCCTGGGCTGGTTGAGCAA

CAGCGTAAATTACGTGAACTGATTGCCATCGCGGTTATCCTGCCTGGGCTGGTTGAGCAA

AGCAAAGGTATCGTGCGCTATATGCCGCATATCAGTGTCAGTAACTGGCCGTTAGTCGAT

AGCAAAGGTATCGTGCGCTATATGCCGCATATCAGTGTCAGTAACTGGCCGTTAGTCGAT

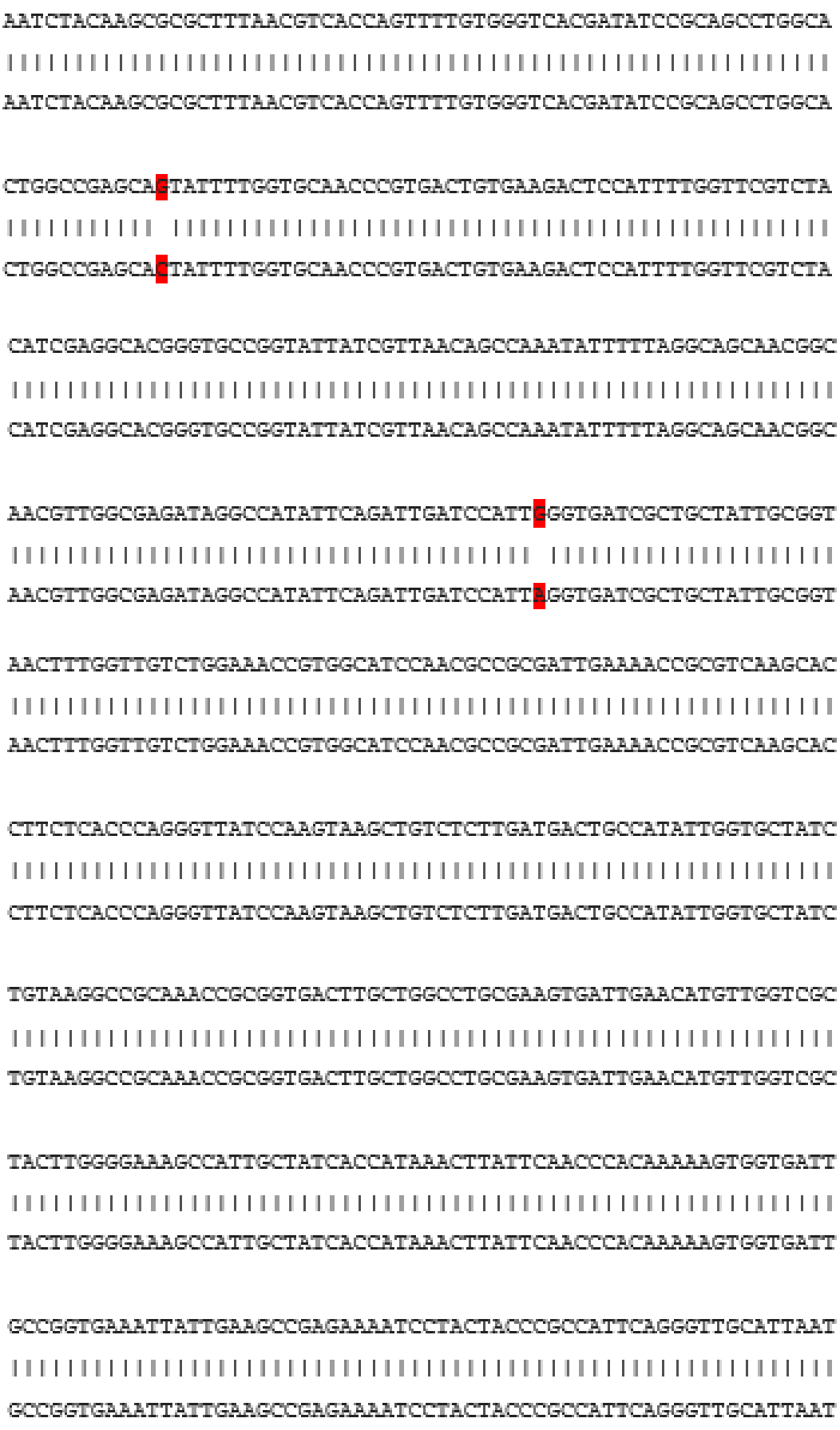
AATCTACAAGCGCGCTTTAACGTCACCAGTTTTGTGGGTCACGATATCCGCAGCCTGGCA
AATCTACAAGCGCGCTTTAACGTCACCAGTTTTGTGGGTCACGATATCCGCAGCCTGGCA
CTGGCCGAGCAGTATTTTGGTGCAACCCGTGACTGTGAAGACTCCATTTTGGTTCGTCTA
CTGGCCGAGCACTATTTTGGTGCAACCCGTGACTGTGAAGACTCCATTTTGGTTCGTCTA
CATCGAGGCACGGGTGCCGGTATTATCGTTAACAGCCAAATATTTTTAGGCAGCAACGGC
CATCGAGGCACGGGTGCCGGTATTATCGTTAACAGCCAAATATTTTTAGGCAGCAACGGC
AACGTTGGCGAGATAGGCCATATTCAGATTGATCCATTGGGTGATCGCTGCTATTGCGGT
AACGTTGGCGAGATAGGCCATATTCAGATTGATCCATTAGGTGATCGCTGCTATTGCGGT
AACTTTGGTTGTCTGGAAACCGTGGCATCCAACGCCGCGATTGAAAACCGCGTCAAGCAC
AACTTTGGTTGTCTGGAAACCGTGGCATCCAACGCCGCGATTGAAAACCGCGTCAAGCAC
CTTCTCACCCAGGGTTATCCAAGTAAGCTGTCTCTTGATGACTGCCATATTGGTGCTATC
CTTCTCACCCAGGGTTATCCAAGTAAGCTGTCTCTTGATGACTGCCATATTGGTGCTATC
TGTAAGGCCGCAAACCGCGGTGACTTGCTGGCCTGCGAAGTGATTGAACATGTTGGTCGC
TGTAAGGCCGCAAACCGCGGTGACTTGCTGGCCTGCGAAGTGATTGAACATGTTGGTCGC
TACTTGGGGAAAGCCATTGCTATCACCATAAACTTATTCAACCCACAAAAAGTGGTGATT
TACTTGGGGAAAGCCATTGCTATCACCATAAACTTATTCAACCCACAAAAAGTGGTGATT
GCCGGTGAAATTATTGAAGCCGAGAAAATCCTACTACCCGCCATTCAGGGTTGCATTAAT
GCCGGTGAAATTATTGAAGCCGAGAAAATCCTACTACCCGCCATTCAGGGTTGCATTAAT

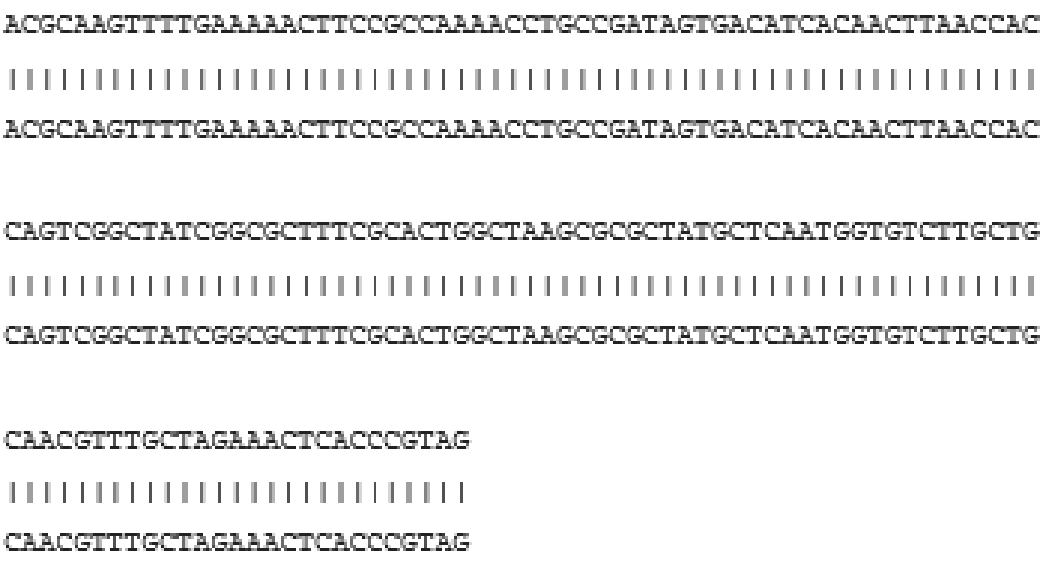

Figure 8.10. Homology of *Y. pestis* (top row) and *Y. pseudotuberculosis* (bottom row) for *nagC*. Highlighted in purple is the helix-turn-helix domain. Highlighted in red are base changes.

8.4 Professional Internships for PhD Students

Name of Organization

Schistosomiasis Control Initiative, based at Imperial College, London, UK and The Vector Control Division, Kampala, Uganda

Details of Placement

The first two weeks were spent in Nottingham doing a literature review on the snail research that has occurred in Uganda, as well as planning and preparing for the mapping in Uganda. The first week in Uganda I was based at the Ministry of Health's Vector Control Division in Kampala, helping the field teams to plan and prepare for the field work (e.g. logistics, purchasing etc.) The next 4 weeks were spent in the field with various different teams around the country, helping with the mapping. My responsibilities included handing out materials to pupils, processing samples and counting *Schistosoma mansoni* and other helminth eggs under the microscope. The rest of my placement was spent in London. I was given many tasks including learning the coding program 'R', cleaning up the coverage survey data for the Cote d'Ivoire (in French) and compiling a summary table for the 2016 Malawi and Zanzibar MDA (mass drug administration) programmes. I helped to test out new phone-based questionnaire software, for functionality and usability and I also planned out how I will analyse the Uganda data (working out variables and the code that I am likely to need to clean it up).

Placement Achievements

I believe I contributed a great deal to the reassessment mapping in Uganda, both with the logistics and the practical field work. I was involved in some of the larger decision-making meetings for the surveying planning both in the UK and in Uganda. I have also completed as fully as I can the report that describes the reassessment survey; describing the previous data, the need for the reassessment, the field methods and the outputs. I have contributed to a number of the other country programmes too, by assisting the programme managers with (for example) cleaning and analysing survey data for the Cote d'Ivoire, collating many reports into summary tables for Malawi and Zanzibar and testing new surveying software for use in the field. This re-mapping of schistosomiasis prevalence in Uganda should enable the SCI and the Ugandan Ministry of Health to better target areas with heavy helminth burdens and possibly identify previously unmapped areas.

Skill development

I personally felt that my analysis skills were the thing that improved the most. Whilst in London I learned how to use the coding program 'R' to clean and analyse large data sets, which I was not able to do before. This has given me a greater confidence in my statistical analysis skills. I also relearned how to use GIS mapping software (previously I had used ArcGIS, whereas for the SCI I learned QGIS) to create prevalence maps of schistosomiasis across the districts that were surveyed. I also feel that my field work skills have vastly improved. My ability to plan and implement large scale projects, including things such as logistics and data planning were focused in Uganda, as well as

refreshing my 'field laboratory' skills, such as Kato Katz and microscopy. My ability to work with groups of different people has also been strengthened, as has my knowledge of working in resource-poor rural settings.

Future Work

I have always wanted to work in the public health or tropical medicine sector, either in research or logistics, so I purposefully chose this placement to gain as much relevant experience as I could, having previously worked on mapping schistosomiasis in Zanzibar. I found that in terms of future career aspirations, this placement was excellent, as it gave me a greater insight into the logistical and planning side of public health programmes, which I felt has complimented my field research skills. It has also improved my data analysis skills, which will be helpful in many areas of research. I hope that it has also fostered connections with a number of people within the field that I can perhaps call upon for advice. Mostly, it has reminded me of how much I enjoy working in the field and has solidified my desire to pursue a career in this area, either in the UK or abroad.